Top copy to CUA

ProQuest LLC.
789 East Eisenhower Parkway
P.O. Box 1346
Ann Arbor, MI 48106 – 1346

THE INACTIVATION OF SINGLE STRANDED RNA VIRUSES BY ULTRA VIOLET LIGHT.

David Barrie Jones, M.I.Biol.

Thesis submitted as part of the requirement for the degree, Doctor of Philosophy, of the Council for National Academic Awards.

August 1977.

The experimental work was carried out in the Water Resources Unit of the Department of Life Sciences, Trent Polytechnic, Nottingham.

Acknowledgements.

The author would like to thank the following for their kind assistance in this project.

Mr. J.D.McIver, for his guidance and supervision of the work and in the preparation of this thesis.

Mr. J.D.Jepson, for his encouragement and interest.

Mrs. E.Boxhall, for her interest and advice.

Dr. T.Vickers, for his advice and suggestions.

Mr. W.Creswell, for help in constructing the UV equipment.

Osram G.E.C. Ltd. for the donation of much equipment and practical discussions.

British Rail Area Science Laboratories, Crewe, for the loan of the Mk I UV steriliser.

Miss M.Rae, for help in preparing some of the illustrations, and the staff (academic and technical) of the Department of Life Sciences for their co-operation.

CONTENTS.

	page
Introduction.	1
Ultra Violet and the Water Industry.	5
Properties of Ultra Violet Light.	10
Sources of Ultra Violet Light.	13
The Absorbance of UV in Water	16
The Structure of Single Stranded RNA Bacteriophages.	21
The Structure of Picorna Viruses.	31
The Effect of UV on Viruses.	39
1. Kinetics of Inactivation.	39
2. Photochemical Effects.	44
3. Reactivation of UV Irradiated Viruses.	50
Methods.	54
Ultra Violet Sources.	
i) Monochromatic UV light at 253.7nm	54
ii) British Rail Steriliser.	54
iii) Monochromator.	56
Calibration of UV Sources.	66
i) Dosiometer.	66
ii) Actinometry.	66
X-Ray Source.	70
X-Ray Actinometry.	70
Temperature Inactivation.	73
Production, Purification and Assay of Bacteriophage	74
A. Bacteriphage host.	
i) Culture and selection.	74

ii) Assay of viable bacteriophage. 75

B. Production of Bacteriphages MS2 and Qβ 76

i) Source and selection of bacteriophage. 76

ii) Production of bacteriophages. 77

iii) Large scale production of bacteriophage. 77

C. Concentration and Purification of MS2. 83

i) Concentration by ammonium sulphate precipitation. 83

ii) Acetone precipitation. 84

iii) Polyethylene glycol two phase concentration and purification. 84

iv) Sedimentation by ultracentrifugation. 85

v) Purification by Sephadex molecular sieve. 85

vi) Density gradient centrifugation. 86

vii) Separation by electrophoretic focusing. 87

Preparation of Glassware. 90

Aseptic Technique. 90

Production, Purification and Assay of Poliovirus. 94

Production of Host Cells.

i) Host. 94

ii) Growth of host. 95

iii) Suspension growth. 96

Growth of Poliovirus. 97

Purification of Poliovirus. 98

i) Polyethylene glycol two phase separation and concentration. 98

ii) Density gradient separation of poliovirus. 99

Assay of Poliovirus. 99

i) Monolayer assay. 99

ii) Suspended plaque assay. 101

iii) Most probable number method. 101

De-aggregation of Viruses. 103

Electron Microscopy. 104

Results and Discussion. 105

Calibration of sources.

i) Potassium ferrioxalate actinometry. 105

ii) Calibration of 254nm surface steriliser. 105

iii) Calibration of the British Rail UV steriliser. 107

iv) Inactivation of bacteriophage QB in the British Rail UV steriliser. 108

v) Calibration of the deuterium lamp output from the monochromator. 110

vi) Output of the 250w medium pressure mercury lamp. 111

vii) Output of the 250w very high pressure mercury lamp. 112

viii) Output of the 250w medium pressure lamp driven at 750w. 113

ix) Output of the 2 kw medium pressure lamp. 114

Production of Bacteriophage.

A. Selection of host. 118

B. Concentration by Ammonium Sulphate Precipitation. 119

C. Concentration of MS2 by Acetone Precipitation. 119

D. Polyethylene Glycol Concentration. 119

The Inactivation of MS2 by Ultra Violet Light. 120

A. Choice of Depth of Irradiation Suspension. 120

B. Effect of Aggregation. 125

C. Biphasic Inactivation of MS2. 138

a) Mutiplicity reactivation. 138

b) Accuracy of observations. 143

c) Attachment to vessel walls. 143

d) Effect of shielding. 146

e) Photoreversal. 146

i) Inactivation of MS2 by 222-300nm UV. 149

ii) Inactivation of MS2 by tandem irradiation at two wavelengths. 155

f) Selection of resistant strains. 155

g) X-ray inactivation of MS2. 161

i) Calibration of X-ray source. 164

ii) Inactivation of 'resistant' and 'sensitive' MS2 by X-rays. 164

h) Heat inactivation of MS2. 169

i) UV inactivation of H and L forms of MS2. 175

j) Separation of two iso-electric forms of MS2. 178

k) Inactivation of expanded particles of MS2. 188

Inactivation of Bacteriophage Qβ by Ultra Violet Light. 192

Inactivation of Poliovirus by Ultra Violet Light. 194

a) Dilution de-aggregation of polio. 194

b) UV inactivation of poliovirus. 195

c) Density Gradient separation of poliovirus. 197

Conclusions. 201

Summary. 202

INTRODUCTION.

There are several groups of single stranded RNA viruses:- the Rhabdovirales (naked, helical capsid, such as Tobacco Mosaic Virus), Sagovirales (enveloped helical capsid, such as Influenza Virus), and Gymnovirales (naked cubical capsid, such as Poliovirus). Another group, the male specific RNA bacteriophages with naked spherical capsids, such as MS2, may have a similar structure to enteroviruses, to which Polio belongs.

This thesis describes experiments carried out on MS2 and Poliovirus, two viruses on which a great deal of work has recently been undertaken. The sequencing of the genome of MS2 by Fiers et al (1,2, 3) makes this virus the first organism for which the primary structure of the genetic material is known, and will probably be the first for which the primary structure of the whole organism will be known.

Sequencing and structural studies of picorna viruses is at present proceeding in several laboratories throughout the world.

RNA phages and picornaviruses share many properties, but differ markedly in mode of replication. The picornavirus virion is composed of a molecule of single stranded RNA of 2.4-2.6 x 10^6 daltons and a protein coat to a total particle weight of 8.3-8.5 x 10^6 daltons. The particle diameter is between 27-28 nanometers (nm).RNA bacteriophages have an RNA of about 1.1 x 10^6 daltons, a total particle weight of about 3.9 x 10^6 daltons and a diameter of about 21nm.

Picornaviruses include many human pathogens, and one group, the enteroviruses, have been the subject of many investigations related to the water industry as they replicate in the gut and are therefore excreted in large numbers in the faeces. If, as a result of contamination, they enter a water course, they can persist

(4,5) and it has been suggested that ingestion of abstracted water containing viruses might cause infection (6). Table 1 shows the major enteroviruses and other important viruses that have been implicated for transmission of disease by the water route.

There has only been one case, an outbreak of infectious hepatitis affecting 29,000 people in Delhi 1956 (7), where water has been shown to be the sole vector, but water supplies have been implicated in outbreaks of polio (8) and illnesses caused by coxsackie viruses (9). An outbreak of polio in the vicinity of a sewage farm in Canada was thought to be caused by aerosol infection because the location of the outbreaks correlated with the wind direction (10). Indeed the effluent from all types of sewage treatment contain high numbers of pathogenic viruses, up to 400 ml^{-1} (11).

The importance of viruses in water supplies probably lies less in the possibility of large scale outbreaks of infection than in the infection of one person, from whom the infection can spread rapidly by direct contact. In view of the low incidence of viruses in potable water, the focus of fresh outbreaks might be caused by the isolated ingestion of one virus.

The low incidence of viral disease spread by water in this country is undoubtedly due to the care taken in the past over the selection of water sources of a high standard of purity and in ensuring proper treatment.

The conventional water resources of this country, already stretched, as the drought of 1976 has shown, are faced with an increasing demand, from both industry and the domestic consumer, for water of a potable standard. Between 1962 and 1972, average daily per capita consumption in England and Wales rose from 54 to

TABLE 1.

Pathogenic Viruses Commonly Found in Sewage.

Physical properties and associated diseases.

Virus (No of serotypes)	Type of nucleic acid Molecular Weight.	Associated Diseases
Poliovirus (3)	Single stranded RNA 2×10^6	Poliomyelitis, acute meningitis, herpangina
Coxsackievirus A (24)	"	common cold, myocarditis fever, rash, gastro-
Coxsackievirus B (6)	"	enteritis, Bornholm disease, mild respiritory
Echovirus (31)	"	diseases.
Reovirus (3)	Double stranded RNA 10×10^6	Ill defined upper and lower respiritory ills
Adenovirus (30)	Double stranded DNA 23×10^6	Minor respiritory ills pharangytis, follicular conjunctivitis, some types tumouregenic

Another important agent, not clearly understood, is that of infectious hepatitis. Most interest is directed at a 25nm single stranded RNA picorna virus.

63 gallons, and this annual 1.6% increase is likely to continue into the foreseeable future. The present resources, including reservoirs, artesian wells and unpolluted rivers however, can only be extended to a limited degree. Thus new sources will have to be brought into supply and these may well include barrage schemes, desalination of sea water and the recycling of polluted water.

Of these possibilities, recycling would appear to be the most attractive since the highest demand comes from cities already situated on rivers, albeit polluted. The high capital cost of pipes and pumping involved in transporting water would thus be avoided.

The recycling of polluted water however, poses new problems in its treatment, as, by definition, it contains high levels of chemical pollutants and/or large numbers of pathogenic organisms from sewage and agricultural run-off. We must also realise that traditional methods of water treatment (to a bacteriological standard) may not be satisfactory for the inactivation or removal of viruses. One such example is chlorination, the main method of biological control in this country. Poynter (4) has noted that in circumstances that reduce the concentration of the $HOCl^-$ ion (high organic content of the water, low pH, marginal chlorination) effective virucidal action does not occur, although bacteria, more sensitive to chlorination than viruses are still inactivated to an acceptable degree. The presence of organic materials during the chlorination process can also lead to the formation of chlorinated hydrocarbons which are thought to be carcinogenic (12). Their formation in treated water is another reason to look for an alternative to chlorination. One of these alternatives is the use of ultra violet light.

Ultra Violet and the Water Industry.

Ultra violet light is a water treatment for which there are indications of an effective virucidal action (13-21,48). The data presented in these reports (some of which are presented in Figure 1 and in Table 2) while showing this, also shows considerable disagreement as to the resistance of enteric viruses to UV. The figures for Poliovirus vary by as much as 1.6 times. It is therefore essential that in the application of UV to the treatment of water there should be a full understanding of its effects on viruses, which can be quantitated.

UV is at present used by several regional water authorities (e.g. the Seven-Trent Water Authority (22)) for treating small (105 m^3 day^{-1}) sources of relatively clean water. British Rail uses a 15 watt UV steriliser for water sterilisation in its restaurant cars. The food industry is another large scale user of UV sterilisers for controlling contamination and there are many other sterilisers employed where a safe supply of potable water is required. The USSR has recently installed many large UV sterilisers to overcome the uneconomic transport of chlorine over large distances (22).

The water industry has often examined UV as a means of biological control and concluded that it is a good method for treating clear water sources. Jepson (22) has tabled the relative advantages of UV for such a purpose, and this is paraphrased in Table 3. One of the demerits mentioned 'no residual germicidal effect' is no longer believed to be strictly true since some types of UV source (ones producing short wavelengths of UV) produce a small amount of ozone. As ozone is an effective viricide this should impart some residual activity, although in practice this is short lived (23).

FIGURE 1.

The Inactivation of various enteric viruses by 254nm UV.

Values published in the literature have been plotted to a common origin

Key.

a)	Poliovirus 1	Dulbecco and Vogt
b)	Poliovirus 1	Norman
c)	Poliovirus 1	Taylor et al
d)	Poliovirus 1	Fogh
e)	Poliovirus 1	Hill et all
f)	Bacteriophage MS2	Rauth

FIGURE 1.

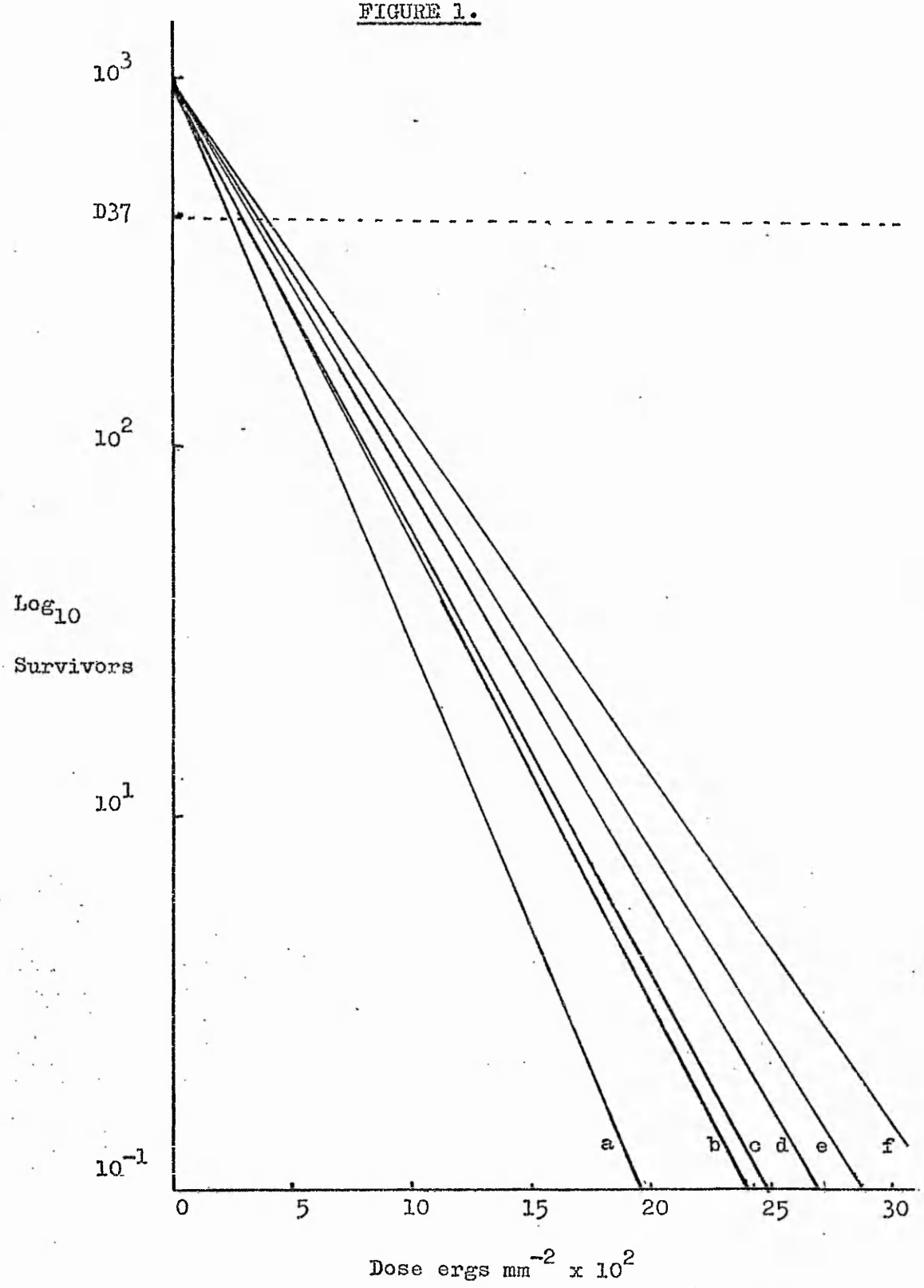
10^3
D37
10^2
Log_{10}
Survivors
10^1
10^{-1}
a
b
c
d
e
f
0
5
10
15
20
25
30
Dose ergs mm^{-2} x 10^2

TABLE 2

COMPUTED D37 VALUES OF ENTERIC VIRUSES FROM DATA PUBLISHED IN THE LITERATURE.

VIRUS	D37 (ergs mm^{-2})	REFERENCE
Poliovirus 1	406	Hill et al 1970 (13)
Poliovirus 2	445	Hill et al 1970
Poliovirus 3	380	Hill et al 1970
Coxsackievirus A9	441	Hill et al 1970
Coxsackievirus B1	577	Hill et al 1970
Echovirus 1	400	Hill et al 1970
Echovirus 2	449	Hill et al 1970
Poliovirus 1	365	Dulbecco and Vogt (124)
Poliovirus 1	500	Fogh (39)
Poliovirus 2	560	Fogh
Poliovirus 2	740	Taylor et al (20)
Poliovirus 2	314	Norman (154)
Poliovirus 3	650	Fogh
Poliovirus 3	760	Taylor et al
Poliovirus 1	580	Taylor et al
Reovirus 1	570	Hill et al 1970

Table 3.

Relative Advantages and Disadvantages of Ultraviolet as a Water Treatment Process. (Paraphrased from Jepson,22).

Merits	Demerits
1. The water does not change in chemical composition and taste is not affected.	1. The process is generally more expensive than chemical treatment.
2. The equipment requires little attention and is easily automated.	2. There is no long term germicidal effect.
3. An overdose of UV presents no danger, and is usually contrived to ensure adequate treatment.	3. The treated water must exhibit good UV transmission, otherwise the process is drastically affected. Pre-treatment may be required.
4. Varying the treatment rates is not a problem and can be achieved quickly.	
5. Viruses can be effectively inactivated.	
6. The destructive effect is rapid	
7. There is no handling of toxic chemicals.	

Properties of Ultra Violet Light.

Ultra violet light is part of the electromagnetic wave spectrum (reproduced in Figures 2 and 3) whose wavelengths and associated energies impart their specific characteristics. It will be noted that there is an overlap in the catagories since this classification is purely artificial, for instance a 10^9 photon can be used as a radio wave or a radar frequency.

UV may be defined as that part of the electromagnetic spectrum beyond visible light that is non-ionising, i.e. between 100 and 380 nm. Within this region three bands can be distinguished, vacuum UV, far UV and near UV (Figure 3). The first of these extends from 100 to 190nm and as these wavelengths are readily absorbed by air, experiments in this region have to be carried out in a vacuum. Far UV lies between 190 and 300nm. Artificial sources are needed to produce light in this region as the ozone in the upper atmosphere absorbs the sun's output below 300nm.

Electromagnetic radiation is made up of quantum particles, called photons, which travel at the speed of light and possess energy but no mass. The relationship between wavelength and energy can be expressed in the following equation:-

$$E(ev) = \frac{1240}{\lambda nm}$$

Where:-

E(ev) is the energy in electron volts

(one electron volt = 1.602×10^{12} ergs)

and nm is the wavelength expressed in nanometers.

The electrons of atoms and molecules are arranged in discrete quantum shells around the nucleus from which they can move to other

Figure 2.

The Electromagnetic Wave Spectrum. (logarithmic scale)

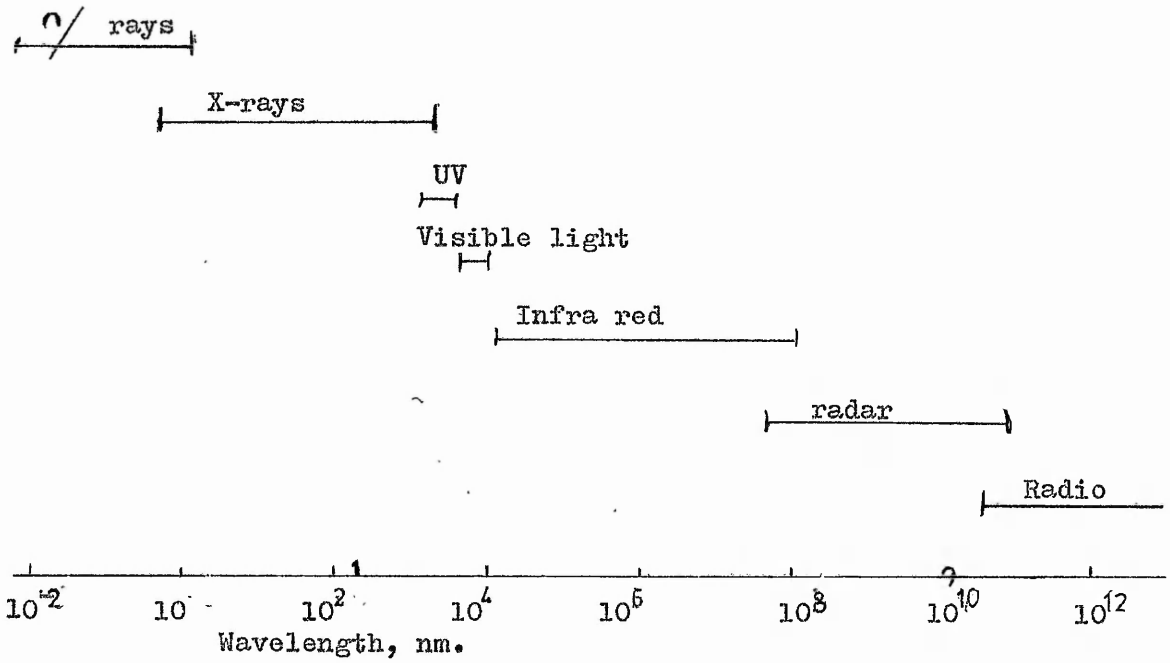

Figure 3.

Spectrum of UV and Visible Light. (Arithmetic scale)

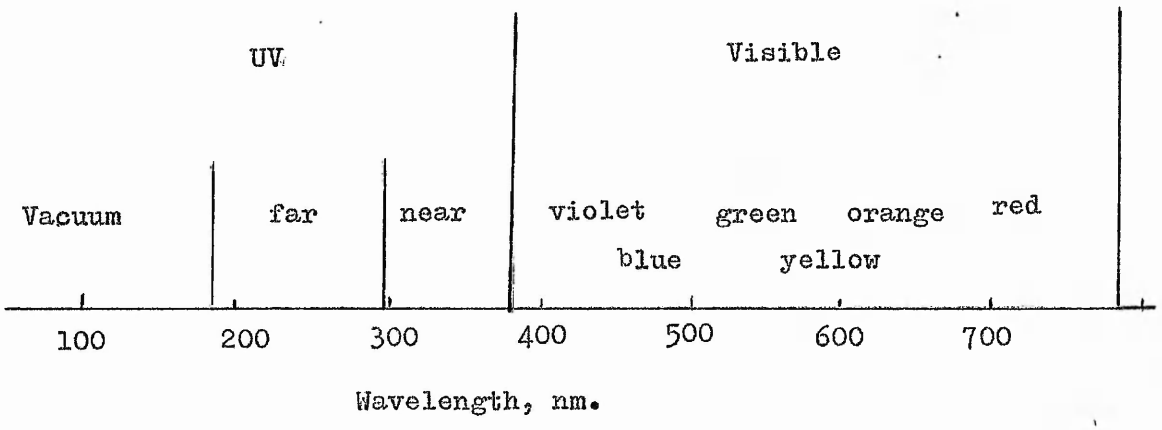

quantum levels, the change being associated with an input or output of energy. Only two electrons can occupy the same level at the same time, but because they both cannot possess the same energy (Pauli principle) they have opposite spins. The electron which spins in the same direction as its direction of rotation has a greater energy of momentum than the other with opposite spin. When energy is absorbed by a molecule some can be transferred to an electron which can then jump to a higher quantum level. It is more likely that the energy will be absorbed if it is exactly that of the energy needed to raise an electron to a higher state; this accounts for the discrete absorption spectra of many atoms and molecules. When an electron absorbs energy its spin can be reversed and a meta-stable state reached, which can last for several milliseconds. While in this state the surplus energy can be used to drive chemical reactions that would normally be energetically unfavourable.

The most important UV absorbers are molecules containing conjugated bonds, especially ring structures. Nucleic acids are rich in such compounds and, to a lesser degree, so are proteins. On a per weight basis nucleic acids absorb twenty times as much UV as proteins but although there is about three times as much protein in an enterovirus than nucleic acid, damage to the nucleic acid is thought to account for all the inactivation at 254nm (44). Figure 4 shows a typical absorption spectrum of a nucleic acid (single stranded RNA) and shows the peak of absorbance (260nm) which is also the most efficient wavelength in inactivating most viruses (31,32,33,34,35, 45,46).

FIGURE 4.

Absorption spectrum of single stranded RNA.

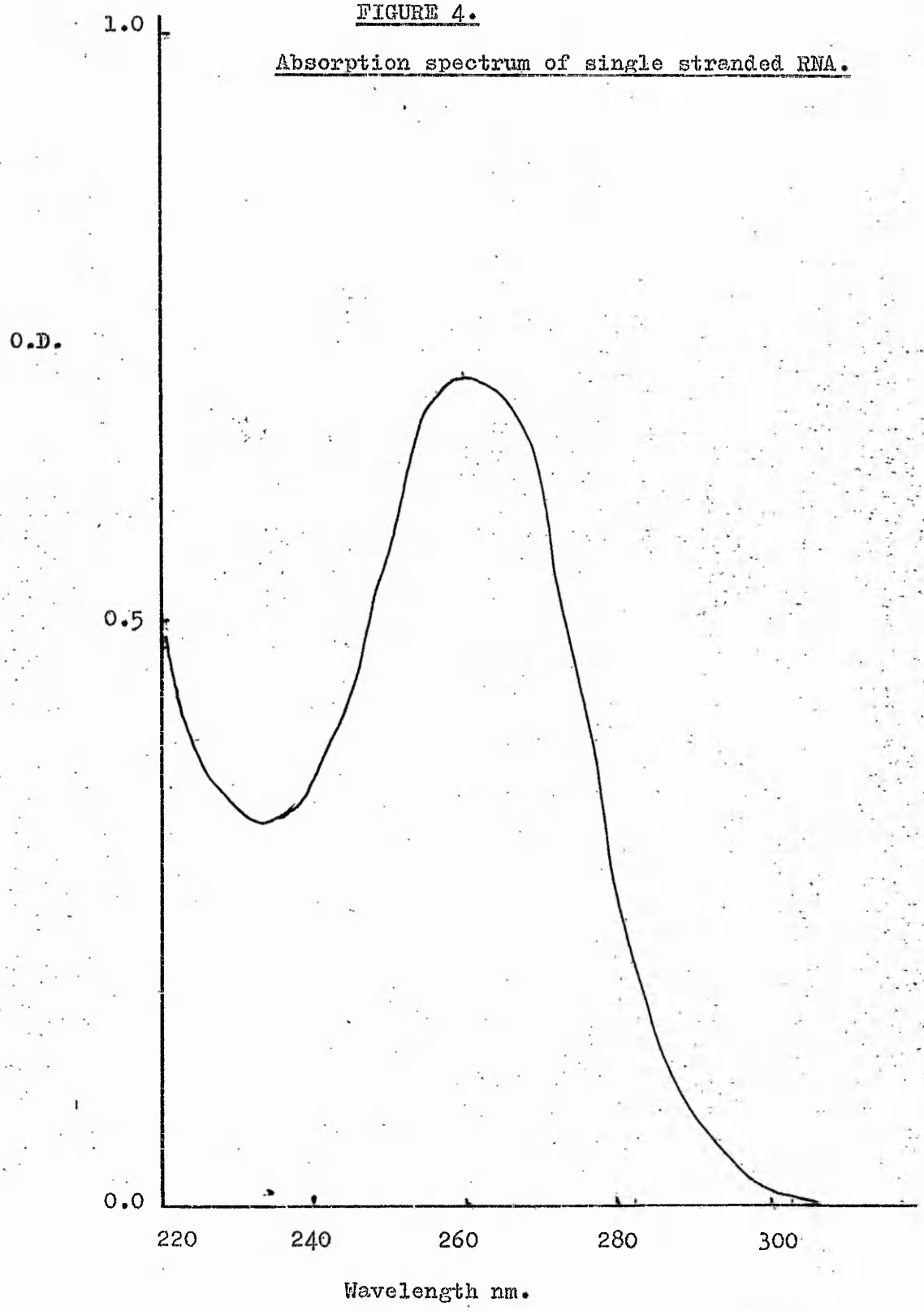

Sources of Ultra Violet Light.

There are many different sources of UV with different intensities and spectral emissions. The most common source is the mercury vapour lamp. The spectral and power output of UV from such a source depends on the nature of the envelope, the pressure of the mercury vapour, the electrical loading and the type of ballast gas. The pressure of the vapour when working determines which emission lines occur. At low pressures only one line of the mercury spectrum is present, that at 253.7 nm. Higher pressures lead to an increasing number of lines appearing until at very high pressures the lines run together into a continuum. Table 4 lists the major UV emission lines of the mercury spectrum. Three types of mercury source may be distinguished on the basis of the spectral output caused by working at different pressures, low, medium and high pressure lamps.

Low pressure lamps are the flourescent lamps of every day use, stripped of the phosphorescent coating on the inside of the tube and housed in a special envelope that is transparent to UV. Such lamps emit 99% of their light output at 253.7nm. Tube life is usually about 7,000 hrs and the UV energy output is between 1/7 and 1/15 of the electrical input power. Lamps of 15 watts consumption are in common use for sterilisation in laboratories, hospitals and factories or wherever airborne and surface contamination needs to be controlled.

If the pressure of the vapour is increased, more and more lines of the mercury spectrum appear until at a few atmospheres of pressure all the major emission lines are present. These lamps are termed polykymatic and are suitable for water treatment because of their higher output. Sources of up to 15 kilowatts have been manufactured.

The output from these lamps is, however, rarely better than 1/15

TABLE 4.

The Major Emission Lines of the Mercury Spectrum below 500nm.

185*	222.5	302.2	404.7*
194.2*	237.8	313*(3)	407.8
	239.9	334.1	435*(3)
	248.3	365.6*(4)	491.6
	253.7*	390.6	496
	265.2	398.4	
	269.9		
	275.3		
	280.4		
	289.4		
	296.7		

Relative intensities are not given because they depend on the nature of the source.

*Indicates a very strong line. At very high pressures the line at 253.7 completely disappears. Numbers in parenthesis indicate the number of very close lines of which the indicated line is the intensity-weighted average.

the input power, and the average life is about 7,000 hours or less for the more powerful types.

The continuous spectrum is produced by very high pressure lamps of 100 atmospheres, which are very useful laboratory lamps, but their short life of 50 to 500 hours makes replacement too costly for their consideration in water treatment.

Discharge lamps filled with xenon also give a component of UV, and high pressure lamps, used in photography, have a continuous output from 200nm to 900nm. Very little of the input energy appears as UV however, and this makes their use as industrial sources of UV uneconomic. Several workers have used xenon lamps in conjunction with a monochromator to study the inactivation of viruses by different UV wavelengths (e.g. Sime and Bedson, 35).

Deuterium lamps have most of their output as a continuous emission between 190nm and 400nm, but because the most powerful commercially available are less than 3 watts capacity, in total UV output, their use is restricted to laboratory work.

Other metallic sources, such as lead, copper, zinc, cadmium and thallium have rich emission lines in the UV region. However difficulties in the construction and use of lamps made from these materials have limited their availability.

The advent of powerful, tunable, continuous UV lasers has opened up possibilities in the use of these sources for experimental work. One of the greatest shortcomings in the present source/monochromator equipment is in the production of high power in the short UV wavelengths. UV lasers tunable to $\pm$ 1nm or less with a power of many watts will enable photoproducts to be produced in assessable quantities and enable action spectra to be constructed very accurately.

The Absorbance of UV in Water.

Absorption of UV by substances present in the water will reduce the amount of UV available for inactivating the virus and thus reduce the efficiency of the treatment. Hoather (24) and Kleczkowski (25) have reviewed these effects in relation to water treatment and the inactivation of viruses. It is obvious that water of high absorbance will be very difficult to treat economically and that pre-treatment clarification is needed on some water supplies.

Turbidity will also reduce the amount of UV available for inactivation although the situation is not straightforward since some particles, such as silicates,will reflect UV internally and the treatment is much more effective than would be indicated by the amount of absorbance of the water.

When a monochromatic radiation passes through an absorbing medium of thickness dl, the decrease in intensity is proportional to the concentration of the absorbing material, its absorbance (a constant) and the thickness of the liquid, as in :-

$$-dI = kcIdl \qquad (1)$$

Where

I = intensity of radiation

k = absorption coefficient

l = thickness of solution

Integrating (1), we get

$$-\ln I/Io = kcl \qquad (2)$$

or

$$I = Ioe^{-kcl} \qquad (3)$$

Where

Io = intensity of the incident radiation

I = radiation transmitted by the solution.

This is known as the Beer-Lambert law.

The ratio I/Io is called transmittance (T). Using T and $\log_{10}$ equation (2) can be written:-

$$-\log T = Kcl \qquad (4)$$

where K is another constant and equals 0.4343k.

Optical density, or absorbance, D, is defined as:-

$$D = \log 1/T = \log Io/I \qquad (5)$$

Equation 4 can therefore be rewritten

$$D = \log Io/I = Kcl \qquad (6)$$

Optical density is therefore directly proportional to the concentration of absorbing material and to the length of the light path.

When c is given in terms of grams per litre, and the light path l, in centimetres, the constant K becomes the 'extinction coefficient' α. When c is given in terms of molarity, and l in centimetres, K becomes the 'molecular extinction coefficient', ε.

$$\varepsilon = M\alpha \quad (M = \text{molecular weight}).$$

The amount of radiant energy (the dose) applied to a surface perpendicular to the direction of the radiation is

IoAt

where

A = area of the surface in square centimetres

t = time of irradiation

Again Io is the intensity of irradiation.

When there is negligable absorbance, or when the irradiated layer is extremely thin, the amount of energy absorbed per unit mass of the solute is given by :-

$$Eab = IabAt = IoAt\ (1-e^{-kcl}) = Eo(1-e^{-kcl}) \qquad (7)$$

Where

$$Eo = IoAt$$

Eab = Absorbed energy

Since D= 0.4343 kcl tends towards zero, then $(1-e^{-kcl}) \rightarrow kcl$, therefore:-

$$Eab = Eokcl = 2.3\ EoKcl \qquad (8)$$

Since Al is the volume of irradiated solution in cubic centimetres the mass of irradiated material in grams or moles is :-

$$m = cAl \times 10^{-3} \qquad (9)$$

Thus the amount of energy absorbed per unit mass is :-

$$Eab/m = 2.3(Eo/A)K \times 10^{3} \qquad (10)$$

Many types of UV steriliser use a high pressure mercury lamp as a source of UV and give out many wavelengths. Kleczkowski (25) gives a method for calculating absorbance for many wavelengths:-

$$I = {}^{1}I + {}^{2}I = {}^{1}Io\ \exp(-k_1 cl) + {}^{2}Io\ \exp(-k_2 cl) \qquad (11)$$

and optical density:-

$$D = \log Io/I = \log({}^{1}Io + {}^{2}Io)/({}^{1}Ice^{-k_1 cl} + {}^{2}Ice^{-k_2 cl}) \qquad (12)$$

As k_1 and k_2 differ, D is a curvilinear function of c and l, and the Beer-Lambert law does not apply. The amount of absorbed energy per unit weight of a dilute solution exposed to polychromatic radiation can therefore only be calculated by measuring the absorption at different wavelengths, finding the spectral distribution of the radiant energy (and, to compute expected inactivation, calculate the expected death at each wavelength) and integrating it for the whole of the spectrum. This is so complex that it would be best approached with the use of a computer.

The usual situation in water to be treated is that it contains

several solutes. In this case the optical density of the mixture is additive:-

$$D = D_1 + D_2 + D_3 + D_4 + \ldots\ldots\ldots \quad (13)$$

However the presence of one absorber will decrease the amount of energy available to be absorbed by the second, the 'inner filter effect'. The energy is divided between the solutes so that the energy absorbed by solute 1 is :-

$$E_1 = E_o(1-\exp-(k_1c_1 + k_2c_2 + k_3c_3 \ldots) 1)$$
$$k_1c_1/k_1c_1 + k_2c_2 \ldots \quad (14)$$

If solute 1 were alone the amount of energy absorbed would be:-

$$E'_1 = E_o(1-\exp-k_1c_1 1) \quad (15)$$

Therefore $E_1 < E'_1$.

This again results in a very complex solution for which there is no easy answer. The most practical way of assessing absorbance in this situation would of course be to try to measure it directly over the total path length.

Other features to be considered in trying to understand the dynamics of UV sterilisation in UV reactors are reflection from reactor walls and stratification of the water as it flows through. Hiatt and Morowitz (26,27) have derived equations to take these features into account.

For mixed liquids with reflectance:-

$$\frac{N}{No} = e^{-AEo}\ \frac{1-e^{-\alpha L} + Re^{-2\alpha L}(e^{\alpha L}-1)}{\alpha L} \quad (16)$$

And for unmixed liquids:-

$$\frac{N}{No} = \frac{1}{\alpha L}\int_{e^{-\alpha L}}^{1} \frac{e^{-AEo\left(u + \frac{Re^{-2\alpha L}}{u}\right)}}{u}\, du$$

Where:-

N = number of organisms surviving

No = number of organisms initially

Re is the reflectance of the reactor wall

In a short path length reactor, reflectance from the wall is quite a significant factor and the choice of wall material is quite important. Stainless steel is suprisingly a poor reflector of 254nm UV, only reflecting about 25% of the incident radiation. Polished aluminium on the other hand has a very high reflectance, about 85%. Using aluminium instead of stainless steel would mean a higher efficiency and less operating costs.

The Structure of Single Stranded RNA Bacteriophages.

MS2 is one of a group of related single stranded RNA viruses that infect male strains (F^+ and Hfr) of Escherichia coli. It has been determined that the specific attachment site of all these viruses (and some filamentous DNA ones) is the F pilus, the structure concerned with the exchange of genetic material between donor and recipient bacteria (66). The other viruses include R17,fr,f2,fcan,R23,ZR GA,SD,β,VK,M12 and Qβ. They can be classified into three groups, serologically:- ZR,f2,MS2,R17,fr and fcan all have close similarity of coat protein amino acid sequence (67,68,69,70,71,72). GA and SD form a second group and Qβ, M12 and VK are typical of the third group.

The sizes range from 20nm for f2,21nm for Qβ to 27nm for M12 (73, 74) as measured by electron microscopy. X-ray studies in solution give a minimum size for f2 of 26nm (75). Since there is at least 1gm of water per gm of dried phage (76) it may be that drying viruses down on EM grids removes this water and shrinks the particles.

Infectious viruses are composed of 180 molecules of coat protein (M.W. 13,700), one molecule of A or maturation protein (M.W. 40,000) and one molecule of single stranded RNA (M.W. 1.1-1.3 x 10^6). This RNA molecule has recently been completely sequenced (1,2,3) making MS2 the first organism for which the primary sequence of its genetic material is known and from which the primary sequence of the entire organism can be deduced.

Qβ has in addition to the above mentioned components, a variable amount of another protein of molecular weight 36,000. This protein arises from read through of the coat protein gene into the intercistronic region, between the coat and replicase genes. It behaves

as a fully functional coat protein and does not appear to interfere with function in any way.

Infection of a bacterial cell with a phage leads to the replication of virus within the cell under the direction of a virus specified RNA dependant RNA polymerase. About 2,000 infectious particles per cell are released, which represent about about 10% of the total particles that are produced.

There are at least four separate types of particles:-

I Infectious particles, absorb effeciently to F^+ pili. The A protein and entire RNA genome is transferred to the host cell during the RNA ejection reaction. These account for approximately 10% of total production.

II Non-infectious, particles absorb to F^+ pili about a third as efficiently as class I particles. The ejection reaction results in transfer of A protein to host cell, but only partial RNA ejection. These particles account for 80% of the total particles.

III Non-infectious, lack A protein and do not absorb to the F^+ pili or undergo RNA ejection reaction. The RNA is resistant to pancreatic ribonuclease. About 10% of the particles are produced like this.

IV Non-infectious, lack RNA, seen as empty capsids. In a new burst they account for less than 1% of the total population but loss of RNA from the other classes increases the proportions with time.

It is clear that class III particles have the RNA tightly bound within the capsid and that the A protein is not necessary for wrapping the RNA inside the coat.

Mutants of phage that have defective A protein, 'A class mutants' contain RNA, but the RNA is sensitive to RNAse so that under normal conditions of growth only RNA deficient particles are found (77). If the particles are grown on an RNase I^- host, particles can be obtained that contain infectious RNA, but they are not themselves infectious. These particles look larger under the electron microscope and sediment at 70s instead of 80s. 30% of the RNA is sensitive to RNAse, and when treated the particle then sediments at 74s, indicating that part of the RNA was protruding from the capsid (78). This suggests that the RNA, normally bound to the A protein, is not bound correctly to defective A protein and the RNA 'flops out' of the capsid and is susceptable to the action of RNAse. The interaction of the A protein with the RNA and the capsid protein is obviously complex as particles lacking A protein are a normal diameter while those with defective A protein and 'floppy'RNA are larger.

Defective A protein also prevents the phage from absorbing to F^+ pili. The normal function of the A protein is probably to attach to the F^+ pilus and to carry the RNA with it when it penetrates the cell. This process involves the splitting of the A protein into two fragments, 15,000 and 24,000 M.W. and it might be that this cleavage mechanism acts in a key role in the triggering mechanism for the ejection process. Reynolds and Paranchych (80) noted that the A protein was attached to the RNA near the 3' end (the 3' end entering the host first and containing the code for the replicase gene). It may be worth noting that Fiers et al (1,2,3) noticed that the region 2352-2367 in the phage RNA (near the 3' end) was exceptionally rich in adenine residues and had unusual properties, sticking to cellulose acetate and DEAE paper. Perhaps it is this region that binds the A

protein?

Expanded particles of phage can be made by heating viruses at 46°C in 0.15 M NaCl, which converts them from 80s to 45-50s. These particles still have the normal components of RNA, coat protein and A protein and retain 30-50% of their infectivity (81). The RNA within these particles is sensitive to RNase, which indicates a structural or spatial re-arrangement of phage components. When suspended in 0.015 M NaCl, the heated phage still sediment at 45-50s, but if the salinity is increased to 0.15 M NaCl, the sedimentation velocity increases to 65s, indicating that the particles can be made more compact again, but not back to their original sedimentation coefficient.

Normal, unheated,phage do not change sedimentation rate under this treatment. This suggests that some permanent structural change has taken place, either the loss of a hitherto unsuspected component or a change in structure. Since the expansion takes place in a narrow temperature range, reminiscent of melting of structural nucleic acids, and is prevented by the inclusion of low concentrations of magnesium ions (just as magnesium stabilises nucleic acids against denaturation), this indicates that the major change is in the secondary structure of the RNA. Jacobsen (82) has reported structural changes in MS2 RNA, viewed under the electron microscope, when in different concentrations of magnesium ions.

Rohrmann and Krueger (83) have found a light component of MS2 which has a density of 1.44 gm cm^{-3} in $CsCl_2$, as opposed to the major particles' 1.46 gm cm^{-3}, yet has the same amount of RNA, coat protein and A protein. The absorption spectrum shows that the light particles absorb slightly more UV than heavy. They are slightly less infectious but don't differ in antigenic properties. The

significance of these particles is not understood.

The coat protein of MS2 is made up of 129 amino acids, and does not contain histidine. Matthews and Cole (84) have proposed a structure of the coat protein in which the basic amino acids are in the interior of the shell, neutralising the RNA phosphate groups or interacting with counterions. The acidic amino acids are on the outside of the coat, interacting with the solvent. The hydrophobic apolar regions are in the middle, holding the protein subunits in place. A diagram of their proposed structure is shown in Figure 5. RNA seems to have a role in the nucleation of the particle as experiments in assembling capsids have shown (85). In the absence of RNA higher concentrations of capsid proteins are necessary to produce shells, but once a shell has formed it is stable, independant of the presence of RNA. Phage, defective particles and empty shells all 'melt' at the same temperature and show the same degree of resistance to other denaturing conditions. The forces holding the capsid together must lie largely in protein-protein interactions.

The RNA molecule is 3,569 nucleotides long and codes for three genes. Starting from the 5' end the cistron specifying the A protein begins with a GUG codon at nucleotide 129. It codes for 394 amino acids. An intercistronic region of 23 nucleotides is followed by the AUG initiation of the coat protein gene. (The non-translated region of 23 nucleotides does not preserve the reading frame, the coat protein gene being read separately and re-initiated). An intercistronic space of 33 nucleotides is followed at nucleotide 1760 by the AUG initiation site of the replicase gene. The replicase gene is 1632 nucleotides long and is followed by 171 untranslated nucleotides to the 3' end (1,2,3).

Figure 5.

Structure of MS2 Capsid, as Proposed by Matthews and Cole (84).

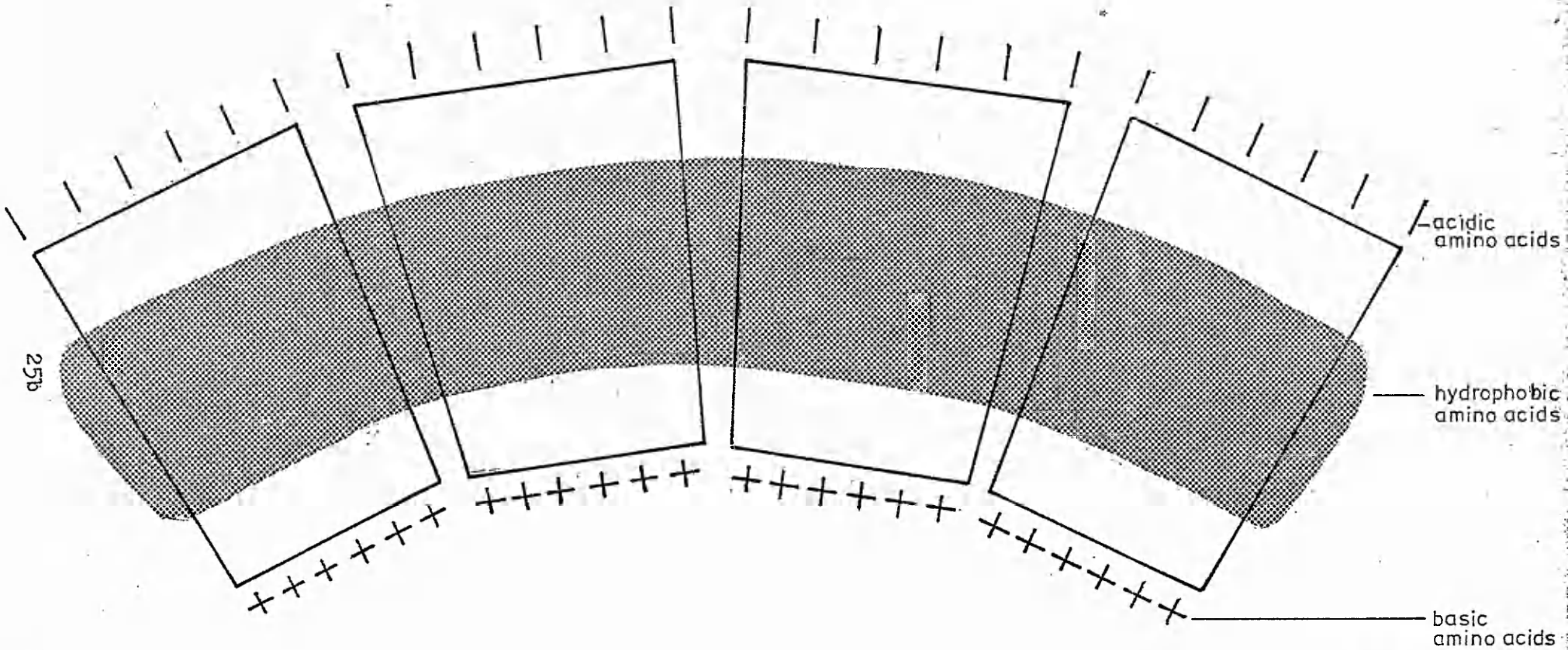
acidic
amino acids
hydrophobic
amino acids
basic
amino acids

25b

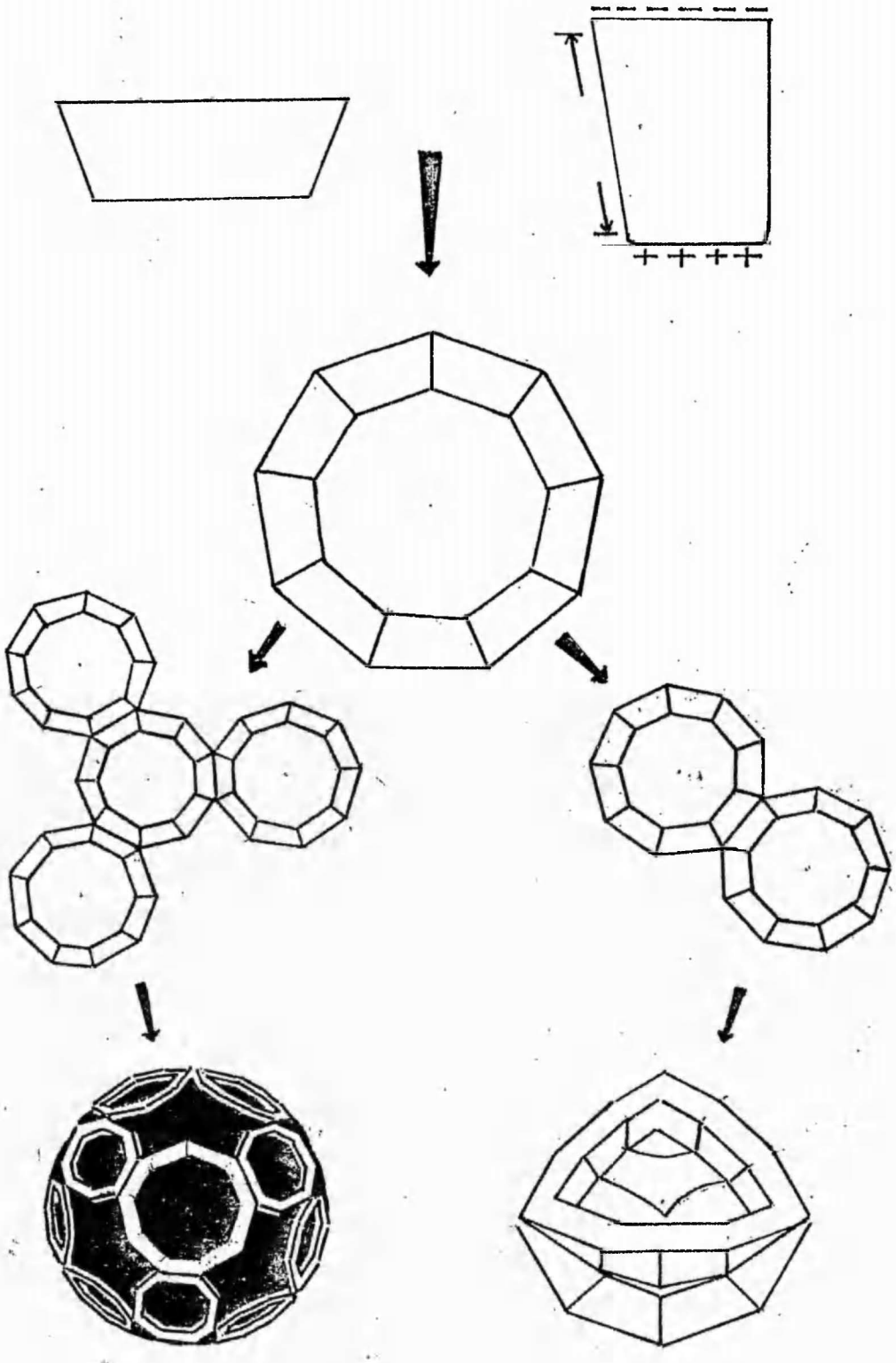

The existence of a fourth gene, a small polypeptide, has recently been proposed (86). In a search for opal (UGA) mutants of bacteriophage f2, a mutant, op3, was isolated that did not lyse a nonpermissive host (Su^-), but does lyse UGA suppressor strains. The mutant makes a normal amount of phage but has to be lysed from without with lysozyme and EDTA. The mutant complements mutants in the other three complementation groups, which is good evidence for being a separate structural peptide. In view of the recent reports on the genes of ϕX174, where the single stranded DNA phage was thought to have only three genes but made nine peptides,(This was achieved by reading the same stretch of DNA more than once in a different frame and also reading into the 'intercistronic spaces') it is tempting to wonder if the same phenomenon might not be happening in MS2 and related phages. The Qβ read through protein is perhaps an instance of this.

Based on the primary structure and mutagenic and biochemical evidence Fiers et al (1,2,3) have proposed a secondary structure for the RNA of MS2. This is reproduced in Figure 6 . They propose that the RNA of MS2 is 80% paired with many loops. Thomas and Prescott (87) in a study of the structure of MS2 by laser-Raman spectroscopy, concluded that about 85% of the bases were either paired or stacked (or stacked and paired). The RNA backbone assumes an 'A' geometry. Cerutti et al (88) investigating the photohydration of R17 RNA concluded that in a low ionic strength medium at 25°C most of the uridine residues are not paired or stacked but in 0.15 M NaCl a substantial proportion do pair or stack. Direct electron microscopic examination of MS2 RNA (82) shows a linear molecule which has one loop in low salt and which increases in complexity in higher concentra-

Figure 6.

Part of the Ribonucleic Acid Genome of MS2: The Replicase Gene. (from W.Fiers et al, 2,).

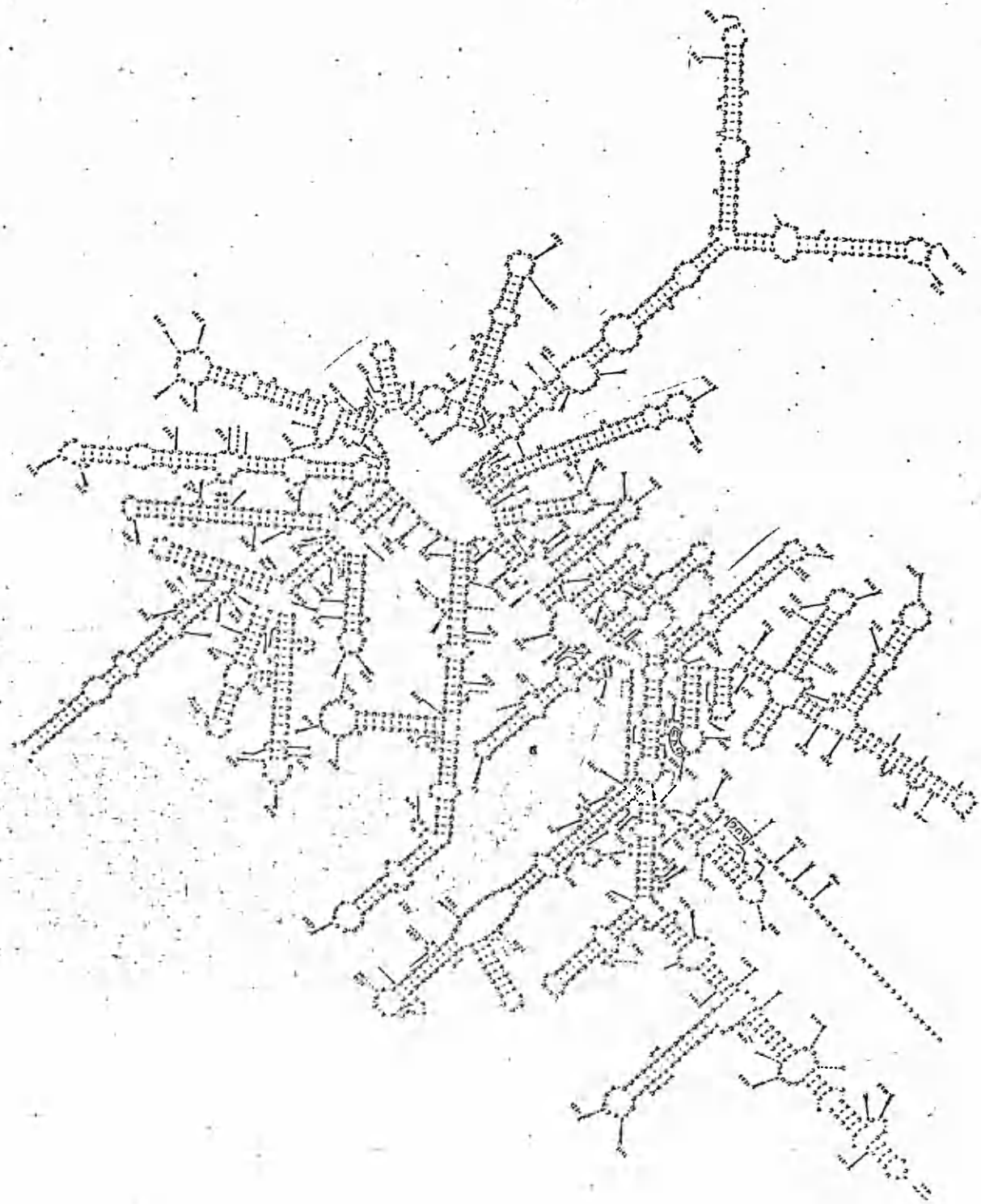

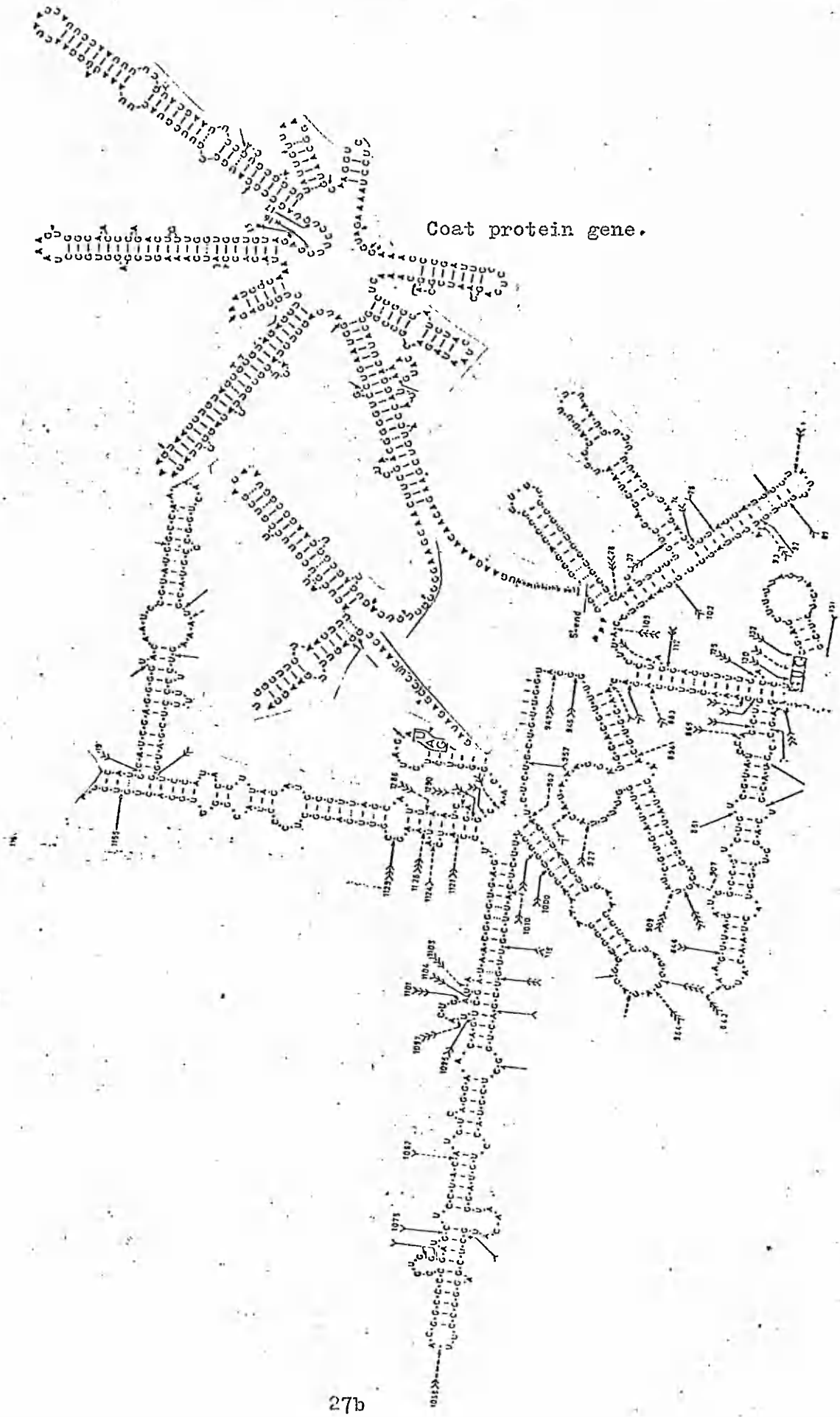
Coat protein gene.

Figure 6.

The A Protein Gene and the Coat Protein Gene of MS2, (from W.Min Jou et al,1, and W.Fiers et al,3.)

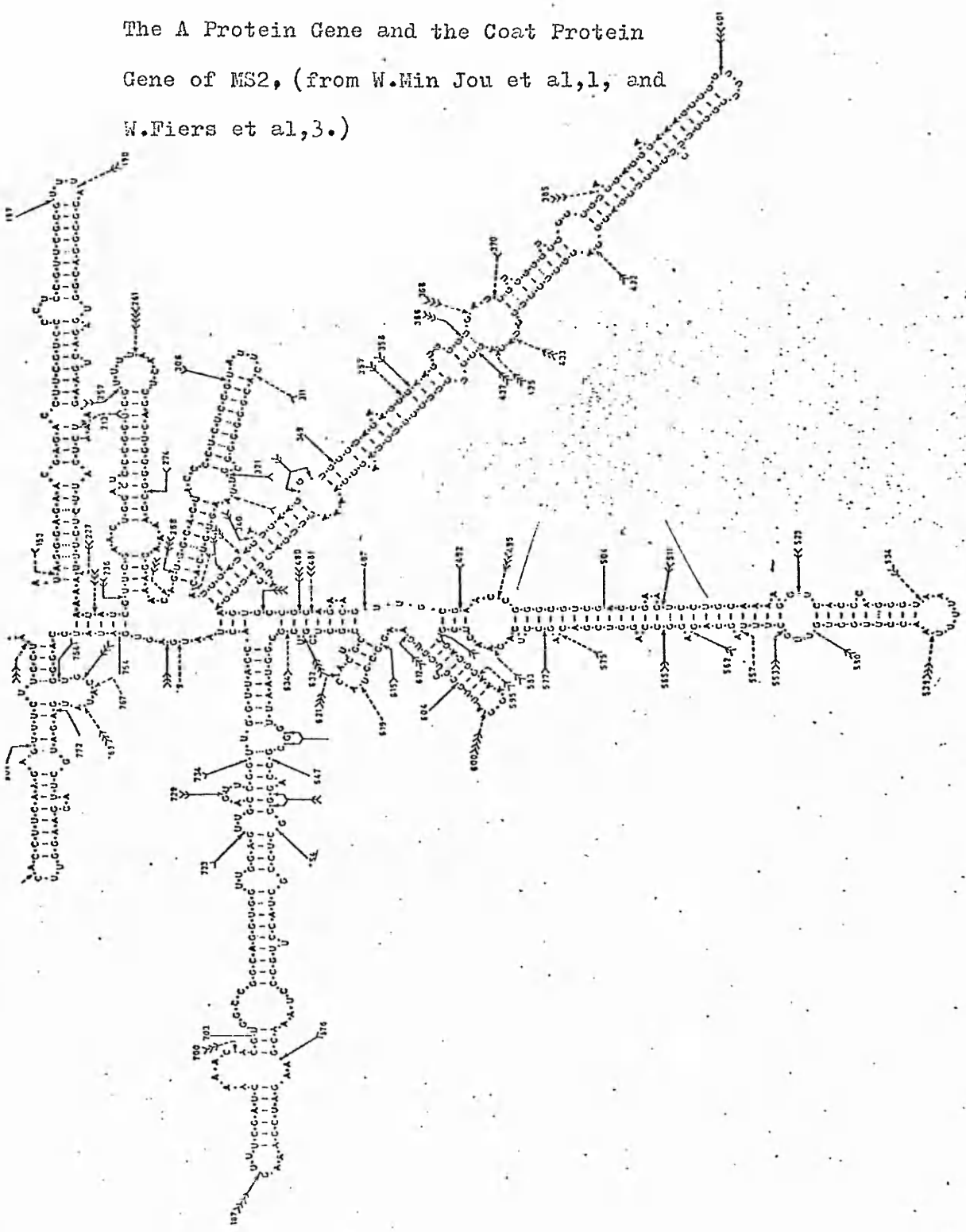

tions of magnesium ions.

It is possible that the secondary structure of RNA within the phage is determined partly by its primary structure and partly by interaction with the coat protein and with the A protein. Whether the RNA is paired or stacked will make a deal of difference in the response of the virus to the inactivating effect of UV light.

The RNA enters the host cell with the A protein by the 3' end. One possible mechanism of RNA penetration is that once the replicase gene has entered, replication 'winds' in the rest. It is known from in vivo and in vitro experiments that part of the coat cistron has to be 'opened up' before the replicase gene can be transcribed (89), the 'polarity' effect: so it is more probable that the mechanism that transports bacterial DNA during mating is involved in the penetration of phage RNA.

The phage RNA that is injected is the strand that encodes the information for the viral proteins; i.e. it is the plus strand rather than the anti codon 'minus' strand. Robertson (90) and Lodish (91) have recently reviewed the mechanism of the replication of the viral RNA and its control during synthesis.

The first product to be transcribed is the replicase gene, which reaches a peak of production 10-20 minutes after infection. The replicase protein uses three host specified proteins to form the replication complex, as well as other co-factors. Two of these are Tu and Ts, host elongation factors. The other protein, central to the replicase reaction seems to be a host polymerase.

The replicative structure does not appear to be a conventional double stranded RNA species. The host RNAse III is efficient in destroying such RNA and the phage has appeared to avoid using struc-

tures and sequences that would attract nuclease activity. Robertson (90) has proposed a model of RNA synthesis in phage, the butterfly model, to take account of most of the features noted. The enzyme complex binds onto the 3' end of the viral 'plus' strand, and as synthesis proceeds two of the subunits bind onto the 3' end and the growing 5' end. Two large loops are formed as the complex is attached to each end of the newly synthetised RNA as well as to one end and the middle of the template strand. Figure 7 shows a diagram of this model. When RNA synthesis reaches the end of the 'plus' strand template, the 3' end of the plus strand is replaced by the 3' end of the newly made minus strand. It is postulated that the complex has a high affinity for the 3' end of the minus strand rather than the plus strand. The attachment of the replicase to the complex is thought to be permanent to the 3' end of the minus strand and so will survive through many rounds of plus strand production.

The replicase protein must be translated from the original viral RNA in order to initiate RNA synthesis. The control of translation during and following RNA synthesis is brought about by interaction between the gene products and the RNA and between the RNA with itself.

When many replicases have been transcibed (the replicase gene is opened up for translation by ribosomes translating the coat gene) the build up of coat protein reaches a level where interaction with a site at the beginning of the replicase cistron becomes favourable. A coat protein molecule sitting on the RNA blocks further transcription of the replicase and thus turns it off. It is about this time that coat protein is aggregating and the RNA being packaged. While nascent strands of the RNA are being produced, the A proteins

Figure 7.

Model of RNA Synthesis in Bacteriophage MS2. (After Robinson,90).

Explanation in text.

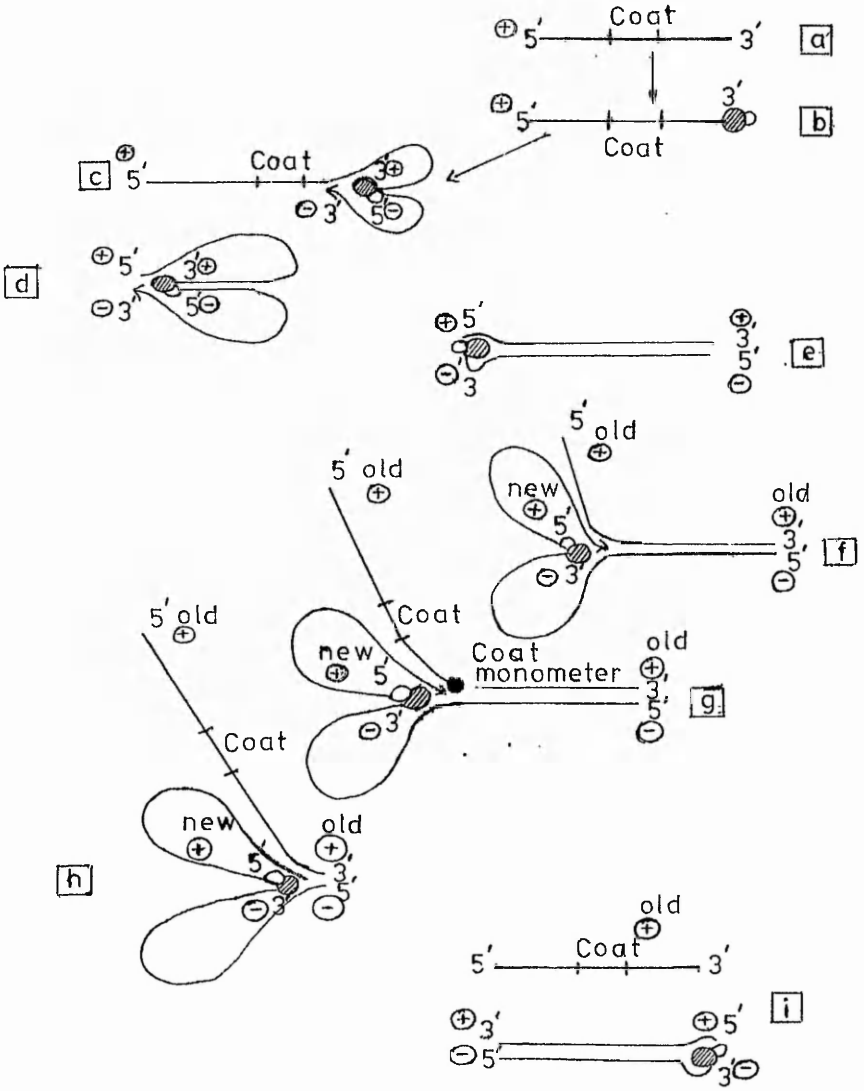
a
Coat
5′
3′
b
Coat
c
d
e
f
old
new
g
Coat monometer
h
i

transcription is initiated. When the nascent strands are a certain length the RNA interacts with itself by pairing and thus effectively stops A protein transcription. Many A proteins are initiated, but only those initiated when a nascent plus strand is relatively short complete transcription. The initiation sites are thought to be specified by the secondary structure and surrounding codons of the RNA. Fiers has proposed that initiating codons appear at the summit of loops in the secondary structure (see Figure 6). It is clear that the structure of the virus, and the structure of the RNA packaged within the virus and the structure of the RNA within the host all play an important active role in the replication of the virus and each component has evolved several important roles to play.

The RNA plays a part in the structure of the particle, has a function in its own control, provides the genetic information for the other components and several genes may be derived from the same stretch of genome. The coat protein has to interact with itself and the RNA to provide a stable particle and also plays a part in the control of transcription. The A protein provides attachment to the pilus, probably some energy for the ejection process and also leads the RNA into the host.

The Structure of Picorna Viruses.

Poliovirus is one of a group of related single stranded RNA viruses, the enteroviruses, which in turn are related in structure to other members of the picornaviridae (e.g. the napoviridae). In comparison with the RNA phages, not as much is known about enteroviruses. This is due in part to the difficulty of obtaining large amounts of material to work with and the relative difficulty in assessing experiments.

The picorna virus is composed of a molecule of single stranded RNA of molecular weight 2.4-2.6 x 10^6 daltons (30% by weight of the total particle) enclosed in a shell of protein (70% by weight). The particle diameter under the electron microscope is 27-28nm and the total M.W. is about 8.3-8.5 x 10^6 daltons. There are four major polypeptide species in the coat, designated VP (for viral protein) 1-VP4. The average molecular weights for these proteins are :- VP1, 35,000, VP2 28,000, VP3 24,000 and VP4 5,500. There is in addition a larger peptide, designated VP0 present in small amounts in some viruses (92,93).

When a cell is infected with poliovirus, 14 different virus specified protein are detectable (94). Four of these correspond to the capsid proteins VP1-4. The others were designated NCVP 1-10. It was demonstrated that NCVP6 was the same as VP0, and that in turn VP0 was a precursor of VP2 and VP4. NCVP1 was shown to be a precursor of all the capsid viral proteins. A scheme of proteolytic cleavages has been worked out by Butterworth et al (95,96) in EMC infected cells Work by others has enabled a scheme of the infectious process to be partially understood.

The viral RNA forms a double stranded RNA replicating complex

from which the entire genome is translated as one giant polypeptide (97,98).(Although sequential control of transcription and translation has been demonstrated, and that NCVP4*, part of the replication complex, is only synthetised during early infection, little more is known about the details.) The giant polypeptide is then cleaved into three large gene products, designated A,F and C. F is a stable end product of M.W. 38,000. Two smaller non-capsid viral polypeptides, G and I (16,000 and 11,000 M.W.) are also primary cleavage products. Product C (the 3' end of the viral RNA) undergoes further cleavage to produce the stable, non-capsid polypeptides E (56,000 M.W.) and H (12,000 M.W.). Product A is the precursor of the capsid polypeptides and is split first into product B (97,000 M.W.) which is further split into D2 (58,000 M.W.) and VP0 (40,000 M.W.). D2 is then split into VP1 and VP3 and VP0 into VP2 and VP4.

Ziola and Scraba (152) suggest that a viral coded protease participates in this action, probably recognising structures in the peptide to initiate cleavage. This is supported by the fact that picorna viruses have similar amino acid sequences at the cleavage sites. Figure 8 shows a diagram of the scheme of cleavage.

It is suggested (99) that VPs 1-3 exist as single interwoven trimeric complexes, with VP4 attached to the vertices. As some authors find eveidence for an external site for VP4 (99) and others an internal one (100), perhaps, as in the A protein of MS2, the VP4 is incontact with the RNA on the inside and 'pokes through' the coat. Breindl (101) has shown that VP4 is readily lost when the particle is heated and that this occurs at the same time as loss of the RNA. This argues for some link between VP4 and the RNA.

There are many viral specified products of infection, and the

Figure 8.

Cleavage of Poliovirus Giant Polypeptide.

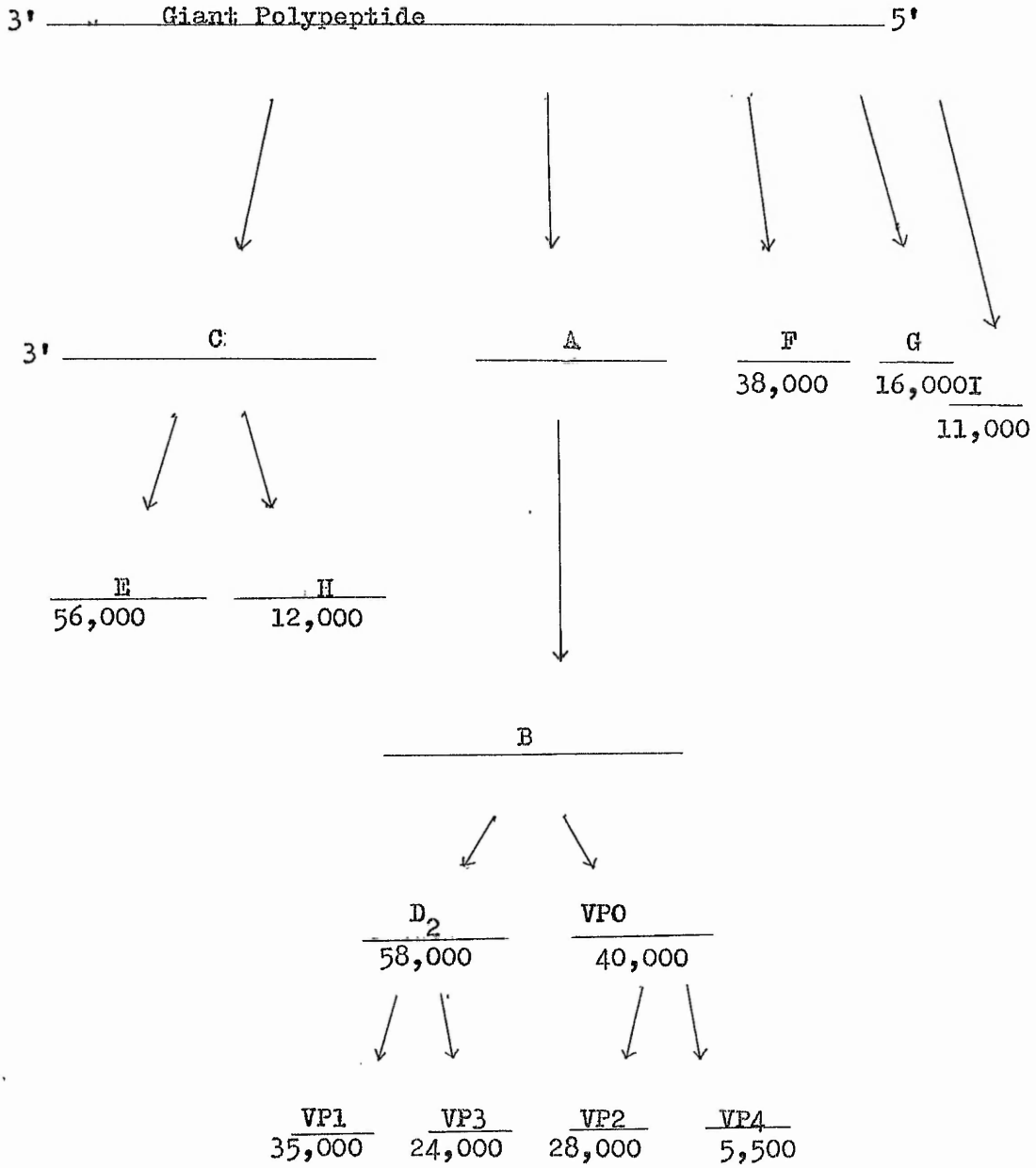

yield of infectious particles to non-infectious particles is low.5s 14s 73s and 155s particles occur in polio infections, while 5s,14s,45s 80s,130s and 160s particles occur in bovine enterovirus infections (102). Baltimore (103) has proposed a scheme for the assembly sequence of the poliovirion, which is shown in Figure 9. This assembly sequence might be common to all mammalian picornaviruses.

Mandel (104) demonstrated that the normal poliovirus exists in two forms, characterised by their mobility in electrophoresis. The major form has an isoelectric point of pH 7.1 and the minor at pH 4.5. The two forms were interconvertable by various treatments, while some treatments, such as heat or large doses of UV would turn the pH 4.5 form into a stable 7.1 form. Since large UV doses have been shown to release VP4 and RNA from the capsid (105,101) , this change is probably related to this loss.

The isolation of a 'heavy' particle of poliovirus (106,107) and of several vertebrate enteroviruses (108) has demonstrated a further complication in the structure of picornaviruses. The dense forms (1.44 gm cc^{-3}) are infectious but have a lower infectivity than the light. They have a normal distribution of viral capsid polypeptides and single stranded RNA of normal size. Boublik and Drzeniek (107) suggest that the dense particles have a more open structure than light that can be penetrated by the caesium chloride used in the centrifugal separation, making them more dense. (A comparison may be drawn here between the heavy and light forms of MS2 and these two components of polio, exept that the light fraction of MS2 compares to the heavy of polio). The dense structure of polio is therefore in reality a less dense form that appears denser due to the artifact of caesium chloride penetration.

Figure 9.

Assembly Sequence of the Poliovirion.

(After Baltimore,103).

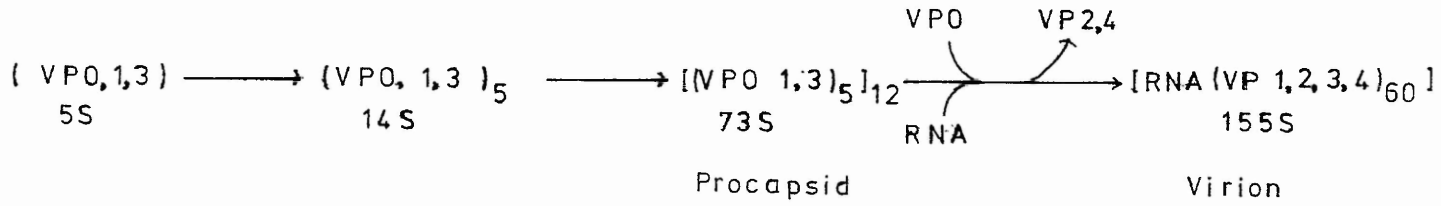
(VPO,1,3)
5S
(VPO, 1,3)5
14S
[(VPO 1,3)5]12
73S
Procapsid
VPO
VP2,4
RNA
[RNA (VP 1,2,3,4)60]
155S
Virion

Su and Taylor (102) report the transforming of 130s Bovine enterovirus into a 160s form under high ionic strength. Perhaps this phenomenon has something in common with the change of sedimentation rates reported in RNA phages with heat and 0.15 M NaCl?

The nucleotide sequence of poliovirus RNA has not yet been elucidated. Yogo and Wimmer (109) have reported that the 3' terminal end of poliovirus type 1 is ....GpGp$(Ap)_{89}$A-OH. It has been recently shown that the defective interfering particles of poliovirus (Huang and Baltimore, 153) are deletion mutants involving this segment. The poliovirion RNA contains 7,700 nucleotides while defective interfering particle, DI 1 was shown to be 6,900 nucleotides long (110). The functional purpose of the poly A segment is unclear, but might be related to the same function of the poly A segments found in heterogenous nuclear RNAs found in Hela cells (111).

Apart from the effect of UV on poliovirus described elsewhere in this introduction, investigations on the effect of UV on the viral RNA have been carried out. Norman (154) looking at the difference in senstivity between the free RNA and the sensitivity of the entire virus (the virus is three times more sensitive than the free RNA) suggested that a low water concentration within the virus results in the formation of more lethal photoproducts than photohydrations of the bases. Bishop et al (112) investigated the resistance of polio virus double stranded RNA and found it more resistant than single stranded RNA and found that some uracil dimers were formed.

Very little is known of the replication of poliovirus within the host, the structure is poorly understood and the significance of the variety of infective forms is unknown. A better understanding of the inter-relationships between the coat proteins, the coat proteins with

the RNA and the RNA with itself might help us to understand the biology of these viruses a great deal more.

The Effect of Ultraviolet Light on Viruses.

(1) Kinetics of Inactivation.

When exposed to UV the virion is inactivated, as defined by its inability to reproduce. Finsen and Dryer (47) were the first to realise this, and since then the mechanism and the kinetics of death by UV have been extensively studied. It has been determined that the rate of inactivation depends on the dose rate (the amount of UV received per unit time) and the extent of death on the integral dose (total amount of UV), Hiatt (49, but see Kleczkowski, 36). The reduction in numbers of survivors is an exponential function, and can be expressed mathematically as:-

$$\frac{N}{No} = e^{-kIt} \qquad (1)$$

Where,

N is the number surviving at time t

No is the number originally present

t is the time of exposure

I is the intensity of irradiation (e.g. ergs mm^{-2} sec^{-1})

k is a constant expressing resistance

e is the base of natural logarithms

Since the amount of reduction depends on the integral dose,D, any combination of I and t can be used as long as it produces the same integral dose. Equation (1) can therefore be simplified by replacing It by D, as in equation (2):-

$$\frac{N}{No} = e^{-kD} \qquad (2)$$

These equations imply that the degree of reduction in number of survivors is proportional only to the number originally present, and is independant of any dose previously absorbed. Inactivation there-

fore depends on one event and not a sequence of events, this being termed 'one hit kinetics' (49,50,51).

The converse, 'multi-hit kinetics', implies that more than one event was required for inactivation (as in the case of an organism carrying more than one gene with the same information, destruction of one would not be sufficient to inactivate the organism) and would result in a lag before exponential death occurs. During this phase the photons would be absorbed by each target; inactivation only occuring when the last was hit. The diagram in Figure 10 compares the two types of inactivation curve, organism survival being plotted on a logarithmic ordinate. When the straight line of the multi-hit curve is extrapolated back to the ordinate, a number is obtained (b on the diagram), which, if No is subtracted from it and the antilogarithm found, gives the extrapolation number, the average number of targets within each unit of the population. It should be noted that viruses will give this type of response when aggregated, and this number is not then a diagnosis of the number of targets within one virus, but rather a measure of the degree of aggregation.

The exponent $^{-kD}$, from equation (2), can be substituted by other dose related expressions (since the dose required to hit a particle is always the same under similar conditions). The expression D can be replaced by H, for hits cm^{-2}, as in equation (3):-

$$\frac{N}{No} = e^{-kH} \qquad (3)$$

k can therefore be considered to be a number expressing the inactivation area of the particle, cm^2 hit^{-1}, or σ. It is evident that the greater the area, the less resistant is the organism. Substituting σ into (3) we have :-

Figure 10.

Comparison of 'one hit' and 'multiple hit' survival curves.

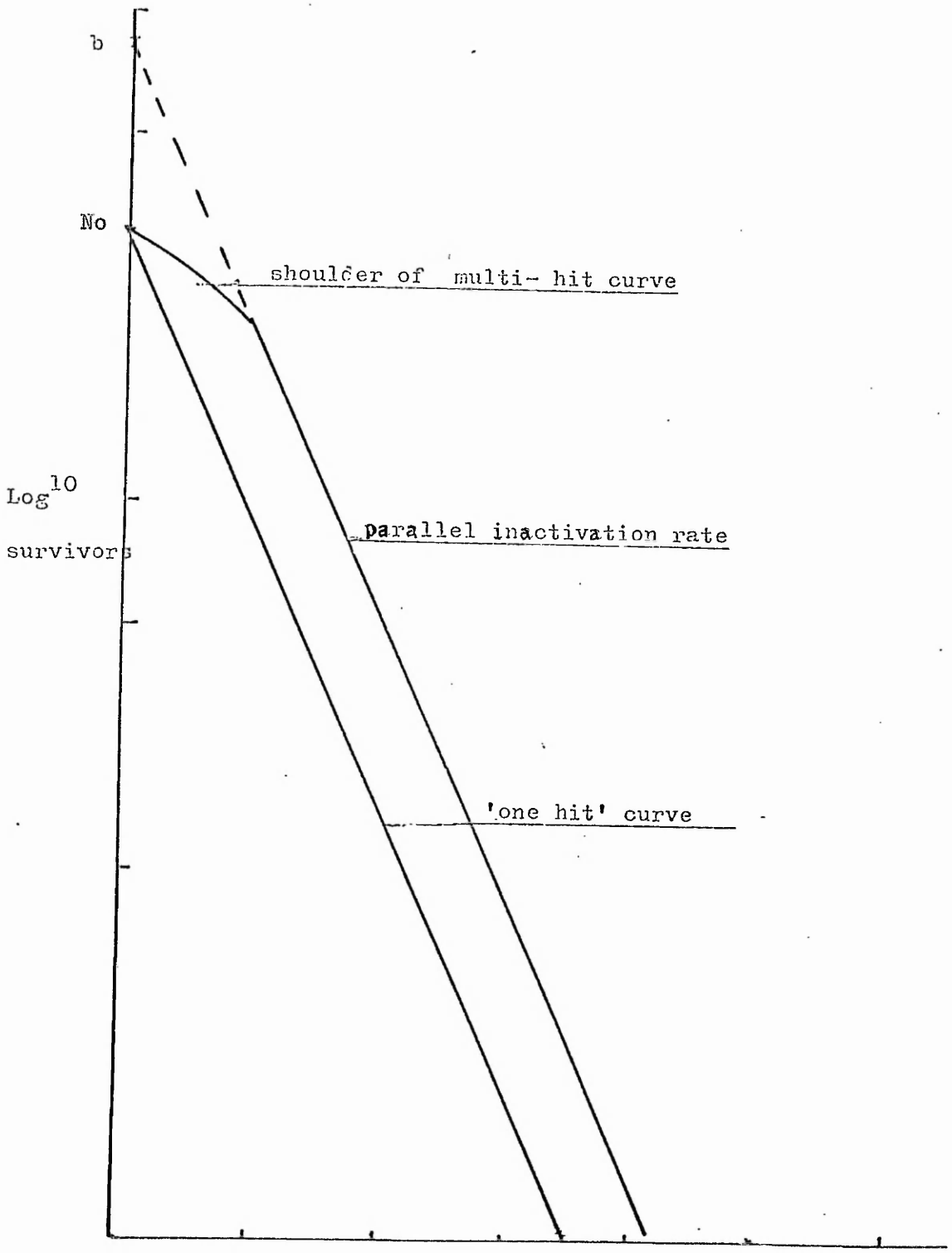

$$\frac{N}{No} = e^{-\sigma H} \qquad (4)$$

The product σH is the 'hits per particle', and for one hit per particle:-

$$\sigma H = 1 \qquad (5)$$

Therefore for a one hit curve:-

$$\frac{N}{No} = e^{-1} \qquad (6)$$

Now as

$$e^{-1} = 0.37 \qquad (7)$$

Then at 37% survival there has been an average of one hit per particle, and this quantity, termed the D37, is a useful mathematical factor. The dose required to produce a 63% inactivation has been termed a Lethe.

σ from equation (4) is also termed the inactivation cross-section and is the relative probability that a photon will be incident and cause inactivation. The relative probability that an incident photon will be absorbed (number of photons absorbed/the number of photons incident) is termed the absorption cross-section.

Figure 11 shows the relationship between these two quantities in diagrammatical form. Their ratio, $\frac{\sigma}{s}$ is known as the quantum yield,

$$\frac{\sigma}{s} = \phi = \frac{\text{Number of particles altered}}{\text{Number of photons absorbed}} \qquad (8)$$

From equation (5) at 37% survival, $\sigma H = 1$, or :-

$$\sigma = \frac{1}{D37} \qquad (9)$$

Substituting (9) into (8), we get:-

$$\phi = \frac{1}{s\ D37} \qquad (10)$$

Therefore knowing the D37 and the absorption cross-section , the quantum yield can be calculated. Since the amount of UV reaching the organism can be measured, the decrease in survivors after a

Figure 11.

Diagrammatical Representation of Absorption Cross Section and Inactivation Cross Section.

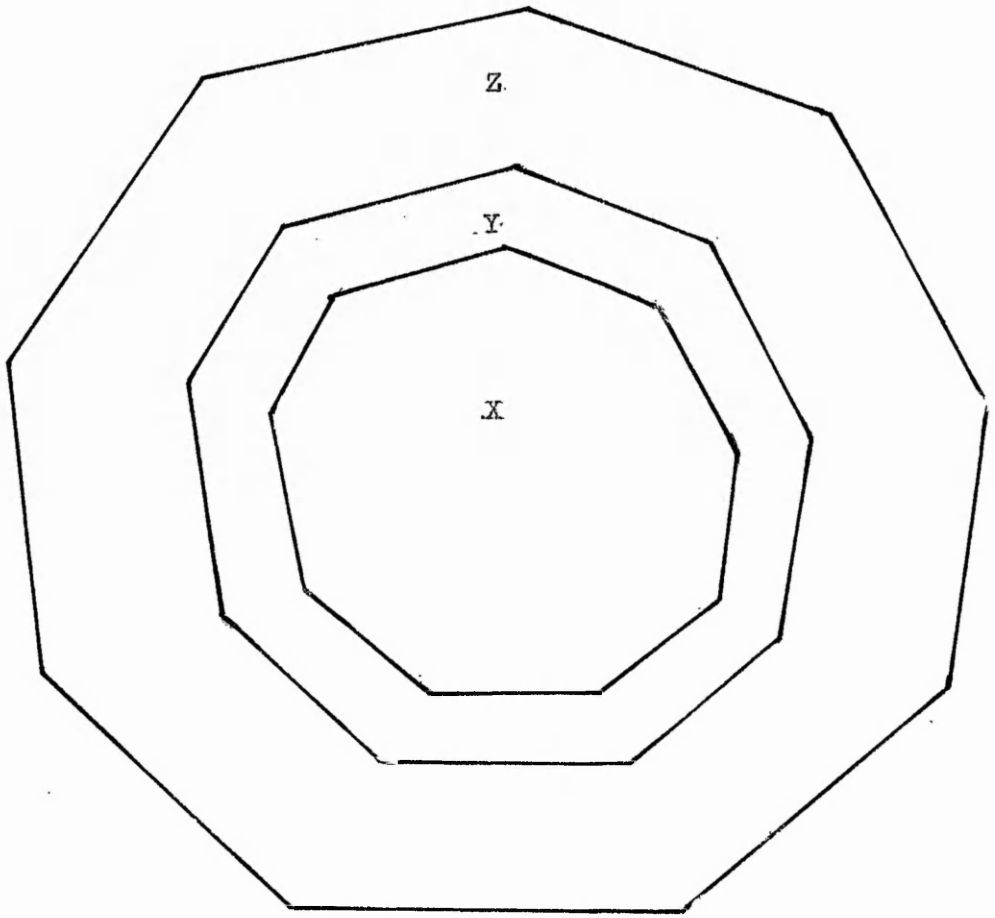

The area within 'Z' is the physical cross sectional area

The area within 'Y' is the cross sectional area of absorption

The area within 'X' is the cross sectional area of inactivation

certain dose should be predictable. Table 5 shows the relative quantum yields of various biological objects and illustrates that the smaller the object the more difficult it is to alter.

(2) Photochemical Effects.

Ultra violet inactivates viruses by causing chemical reactions in the nucleic acid genome, which interferes with its functioning, leading to a failure to reproduce. Other photochemical effects which do not lead to inactivation also take place, e.g. changes in the nucleic acid causing mutations, and photochemical damage to the capsid protein (some of which may lead to changes in the immunological activity of the virus).

Of these photochemical events, Setlow and Setlow (44) have shown that pyrimidine dimers, thymine-thymine, cytosine-cytosine and cytosine-thymine are the main photoproducts causing inactivation in bacteria. UV in the region 240nm-300nm are the main wavelengths involved in dimerisation. The formation of a thymine dimer (depicted in Figure 12) is favoured by 280nm photons in vitro, with the reverse reaction being favoured by 240nm photons. However, the most efficient wavelength for inactivation of most viruses is 265nm. This does not necessarily mean that dimers are formed directly at this wavelength in vivo, but rather that transfer of UV energy by resonance along the nucleic acid chain might be taking place (51). In RNA uracil dimerises similarly to thymine.

Rather suprisingly, Setlow (52) and Miller et al (53) suggest that a number of dimers (6 in T2 and 1.7 in Mengovirus) are required per lethal event. As each show a 'one hit' inactivation, either more than one dimer is formed per hit or not all dimers are lethal. It is probable that only 1/6 of the dimers are lethal in T2 and

TABLE 5.

The Relative Quantum Yields of Various Biological Objects.

Object	Quantum Yield (ϕ)
Thymine dimer	1
Enzyme	10^{-2}
Virus	10^{-4}
Bacterium	10^{-6}
Diploid yeast	10^{-8}
Amoeba	10^{-12}

Figure 12.

Formation of a Thymine Dimer by Ultra Violet Light at 280nm and Photoreversal by 240nm Ultra Violet Light.

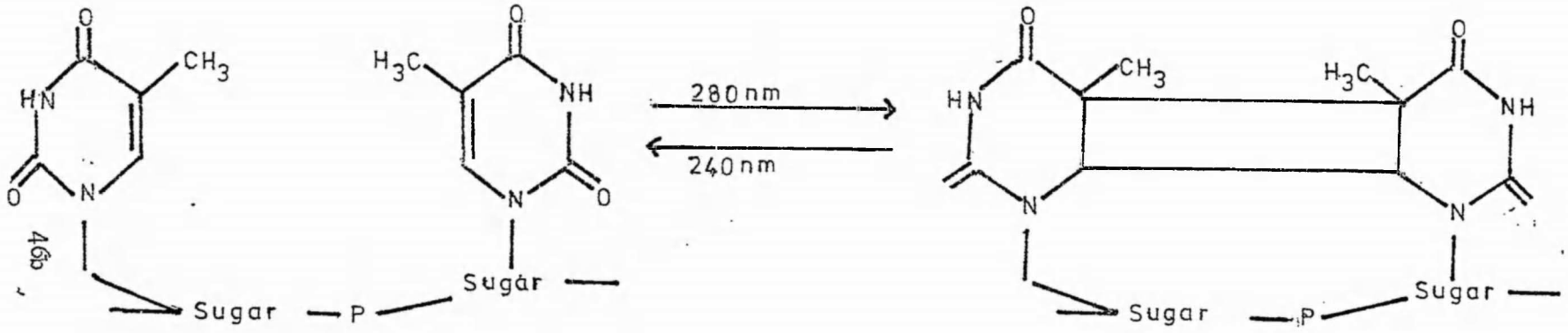

Adjacent thymines

Thymine dimer

1/1.7 in mengovirus. Although UV is a mutagenic agent and the reactivation of dimers can cause transitions and transvertions (see later), it is probably not through the accumulation of mutations that death occurs, but poosibly through inhibition of polymerases and transcriptases. In explanation of their results, it is plausable to assume that dimerisations occur randomly throughout the chain. Since only one in six dimers are lethal in T phage, it might be that dimers in the translated portion of the chain do not cause any effects, only dimers in control regions, blocking initiation of transcription.

The formation of 1.7 dimers per lethal event in mengovirus is probably a reflection of the different way in which this virus replicates. The infectious RNA strand is replicated along its entire length into an mRNA strand, which is translated into a giant polypeptide. Because of this single initiation and translation, a dimer anywhere on the infectious RNA would be more likely to completely block replication and transcription and hence inactivate.

It should be noted that the poliovirus genome of 2.4×10^6 daltons only produces active peptides from a genome length of 2.2×10^5 daltons, 9/10ths of the genome presumably being 'redundant' (although these sequences probably have some function in regulation). This virus is more sensitive to UV than MS2,which means that hits on non-translated genome is just as lethal as a hit on translated nucleic acid.

Evidence from action spectra show that after a peak of inactivation at 265nm, efficiency falls to a low level at 240nm, and then rises again below 220nm. This suggests that pyrimidine dimers are not the major inactivating mechanism at these short wavelengths, but

that a protein-nucleic acid link may be forming. This phenomenon is best shown in Tobacco Mosaic Virus, an unusual virus in that its single stranded RNA is intercalated in the capsid protein; some strains not showing a peak of inactivation at 260nm but being five times more susceptable at 200nm. The virus still shows a peak of absorbance at 260nm but Kleczkowski (50) has shown that uracil dimers are not formed in the virus following irradiation by UV and Goddard et al (37) have demonstrated that inactivation is due to the binding of protein to the nucleic acid, approximately one sub-unit bound per lethal hit. Since there is no transfer of energy between the two macromolecules (55) a likely explanation is that UV is absorbed by the protein capsid causing it to react with the nucleic acid, rather than vice versa. This protein-nucleic acid reaction may occur in other viruses (56).

Other photochemical effects that have been noted include:-

a) Cross linking of nucleic acid strands, shown in several viruses, (57,53,58,56,59) but this is only detected at very high doses of UV and cannot contribute very much to inactivation.

b) Mutation, an effect of low doses of UV, is caused by photochemical alteration of the nucleic acid bases, causing transitions, or during reactivation of UV damage, causing transversions (Howard-Flanders, personal communication). This effect may also cause an expression of the oncopotential of the virus following irradiation (61).

c) Nucleic acid-protein links. Rather than the protein absorbing UV as above, the nucleic acid absorbs the energy and reacts with the coat protein. Budowsky et al (63) have suggested that at least 50% of the inactivating photoproducts formed in MS2 at 254nm are

nucleic acid-protein bonds , due to the close contact of the RNA with the capsid.

d) Irradiation effects on proteins. These are not normally important for inactivation (with the exception of the above)and can cause immunological changes at high doses in several viruses, due, for example to the loss of the D antigen in poliovirus (62).

Table 6 shows the main photoproducts formed in vitro by UV irradiation of nucleic acid bases and macromolecules.

TABLE 6

The Main Photoproducts of UV Irradiation of Nucleic Acids. (from Jagger 1967).

Maximum percentage production at 254nm.

Molecule	Hydration products (aqueous solution)	Dimers (frozen)
uracil	50	70
uridine	95	20
uridylic acid	95	40
cytosine	60-90	0
cytidilic acid	100	0
thymine	0	85
thymidine	0	50
thymidilic acid	0	40
poly rU	65	15
poly dT	0	35
DNA (double stranded)	0	6.5

(3) Reactivation of UV Irradiated Viruses.

After a virus has been irradiated with a dose of UV there are several phenomena which can cause the virus to regain infectivity, and these are known collectively as reactivation. Reactivation will be discussed under four main headings:-

A. Fortuitous recovery.

B. Reversal in situ.

C. Reconstruction of damage in the host.

D. Damage ignored or bypassed

A. Fortuitous recovery.

This covers a number of separate effects.

i) The damage may be biologically undetectable, e.g. a UV damaged cytosine may behave as a uracil during replication (leading to the presence of adenine in the opposite strand), but, depending on the position in the codon, may not result in a change of amino acid in the protein,(which in most cases might not be important).

ii) There may be more than one copy of the damaged region, as in polyploidy, leading to no loss in function.

iii) Multiplicity reactivation, the co-operative effect of mutually inactive virus when multiply infecting a cell. It operates through pooling undamaged genetic material through recombination. The effect may occur either when several attached (aggregated) viruses or independant viruses infect a cell.

iv) Cross reactivation is similar to multiplicity reactivation, but involves the co-operation of two independant genomes, one irradiated and the other not. Genetic markers from the un-irradiated virus can be used to repair the defective genome of the irradiated virus (as in the case of an attenuated poliovirus donating genes

to an inactivated wild type poliovirus which then becomes infectious) or genetic markers from an irradiated virus being incorporated into an unirradiated virus and donating virulence.

B. Reversal of damage in situ.

i) Decay of photoproducts. Some photoproducts have very short half lives while others can revert spontaneously, especially under favourable enviromental conditions.

ii) Direct photoreversal of pyrimidine dimers by shorter wavelengths of UV. This is not a significant repair process in living systems, but is probably the only type of reactivation in single stranded mammalian viruses (64).

iii) Photoreactivation (PR) is an enzymic process taking place in the host cell and uses 3eV photons to repair damage promoted by 5eV photons. The PR enzyme binds to UV irradiated DNA and splits pyrimidine dimers in the light (300nm to 500nm).

C. Reconstruction of damaged DNA.

Excision repair may proceed by the two slightly different paths 'cut and patch' or 'patch and cut', illustrated in Figure 13.

Steps in repair process:-

a) Recognition. A variety of defects can be recognised which require repairing before DNA can be replicated.

b) Incision. Endonucleases have been isolated from Escherichia coli that cut UV irradiated,but not normal DNA (65).

c) Excision and repair replication. Pyrimidine dimers and nucleotides are released as tri- and tetra- nucleotides. The known specificities of exonuclease III and DNA polymerase from E. coli make them suitable candidates for the excision and polymerisation steps.

Figure 13.

Possible Pathways of the Excision Repair Process.

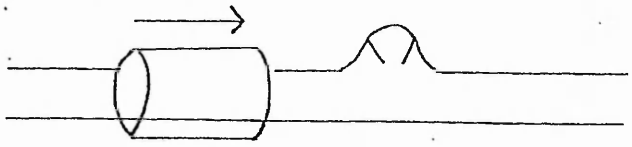

i. Recognition.

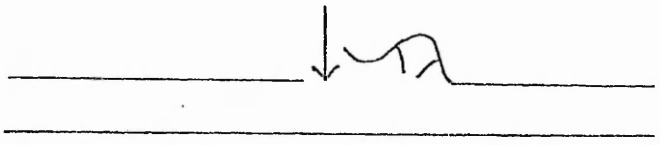

ii. Incision.

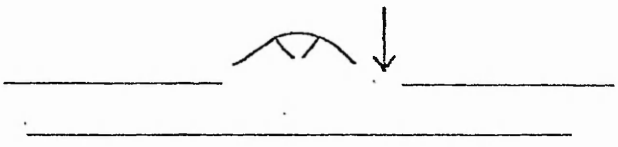

iii. Excision

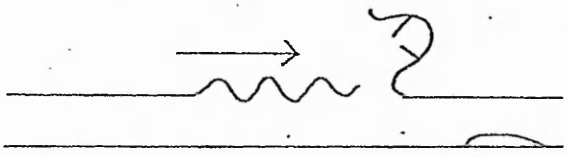

iii. Repair replication

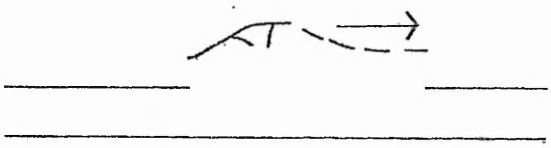

iv. Degradation

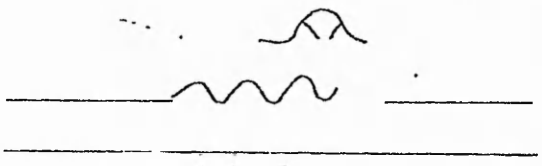

iv Excision

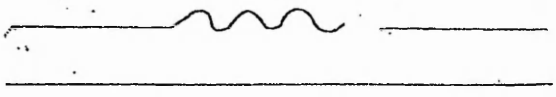

v. Repair replication

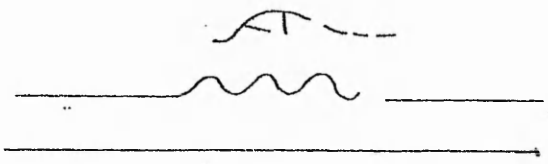

v. Degradation

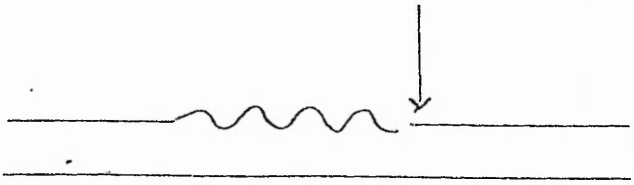

vi. Rejoining

d) Rejoining. Continuity in base sequence must be ensured by joins being made only while both fragments are hydrogen bonded to the template with their ends in juxtaposition, the enzyme responsible being probably DNA polynucleotide ligase.

D. DNA synthesis on unrepaired templates.

Pyrimidine dimers may not completely stop DNA synthesis but may leave gaps in the daughter strand which are subsequently eliminated by a recombinational event between sister strands (post replication recombinational repair).

Conclusion.

There are several aspects of the effects of Ultra Violet light on viruses which are not very clear, the reason why UV inactivates and the exact susceptability of many viruses to UV. This last is very important to know if UV is to be used in inactivating viruses present in water supplies.

The use of UV as an analytical tool in understanding the structure of viruses is also important, as in Mayo et al (58) in showing the presence of several species of RNA in different particles.

This thesis will attempt to resolve some of the questions that arise in the effect of UV on single stranded RNA bacteriophages and on poliovirus.

METHODS

Ultraviolet Sources

i) Monochromatic UV light of 254nm wavelength was obtained from two units, both based on 18'', 15 watt low pressure mercury discharge tubes, emitting between 87-95% of the light output at 253.7nm.

In the surface steriliser (built and designed by the researcher) two tubes were housed within a shield to minimise UV being directed towards the eyes. This shield was mounted on a rod allowing adjustment of the distance between the lamp and the target. The UV lamps (donated by Osram G.E.C. Ltd.) were wired to separate switches allowing further control over irradiation intensity by operating the equipment with one or both lamps. The shield was also designed to fit flush with the base at its lowest elevation so that when used for sterilising small pieces of equipment (such as plastic petri plates used for exposing viruses) no stray UV could escape from the unit. The electrical control gear was mounted in a unit integral with the base (a separate circuit for each lamp) and was well ventilated. Construction was of plywood, for electrical insulation, painted with polyurethane gloss, for ease of cleaning. Figure 14 shows a scale drawing of this unit.

ii) The other source of 254nm monochromatic UV light was a flow through UV steriliser (kindly loaned by the British Rail Area Science Laboratory, Crewe), the 'British Rail UV Steriliser Mk I'. (This unit differed from subsequent production sterilisers which had a smaller diameter and were made from polished stainless steel. It is likely that the effective sterilising power of the new steriliser is less than that of the prototype because stainless steel will reflect less UV back into the unit than the aluminium

Figure 14.

Diagram of 254nm UV Surface Steriliser.

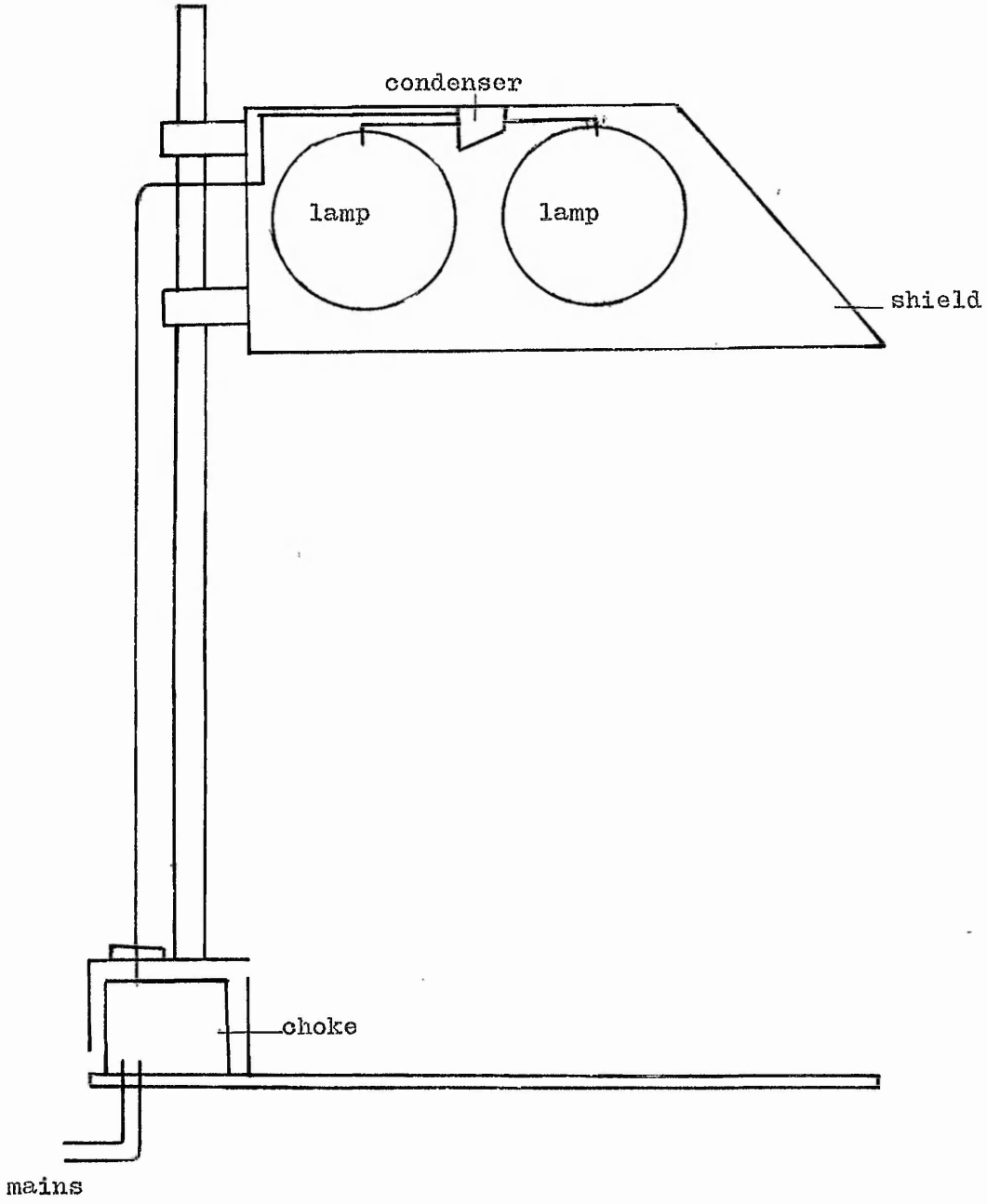

of the prototype).

A diagram of this unit is shown in Figure 15. The 18'' lamp is mounted inside a quartz thimble which is sealed at the top by a neoprene collar. Electrical connections were run to the lamp from the top of the thimble. The raw input water was fed by gravity to the bottom of the unit and the treated effluent overflowed from the top and collected by pipe.

iii) A monochromator unit was used to provide monochromatic light between 200nm and 300nm. The unit was composed of four parts, the source, the condenser, the monochromator and the shaking platform.

a. The source.

Several sources of UV light were used, a deuterium lamp (Cathodeon Ltd. C70-3V-H,),a 250 watt high pressure mercury discharge lamp (Osram G.E.C.Ltd., MBF/U),a 250 watt very high pressure mercury discharge lamp (Osram G.E.C.Ltd., MED/D) and a 2 kilowatt high pressure mercury discharge lamp (Osram G.E.C Ltd., MBI).

The deuterium source gave a continuous spectrum of UV from 190nm to 400nm, but because of its low output, was abandoned in favour of higher power sources.

Osram G.E.C.Ltd., provided several high powered mercury lamps and their control gear. The 250 watt and 2 kilowatt lamps were specially adapted for this work by Osram G.E.C. Instead of the normal quartz envelope, a quartz with a better UV transmission characteristic in the shorter wavelengths was used. These envelopes were then provided with porcelain insulators and connectors that would accept 'bullet' connecting leads. The lamp was provided without the normal glass outer envelope. The wiring to the electrical control gear was of asbestos covered copper wire (heat resistant). The wiring diagrams

Figure 15.

Diagram of British Rail UV Steriliser Mk I.

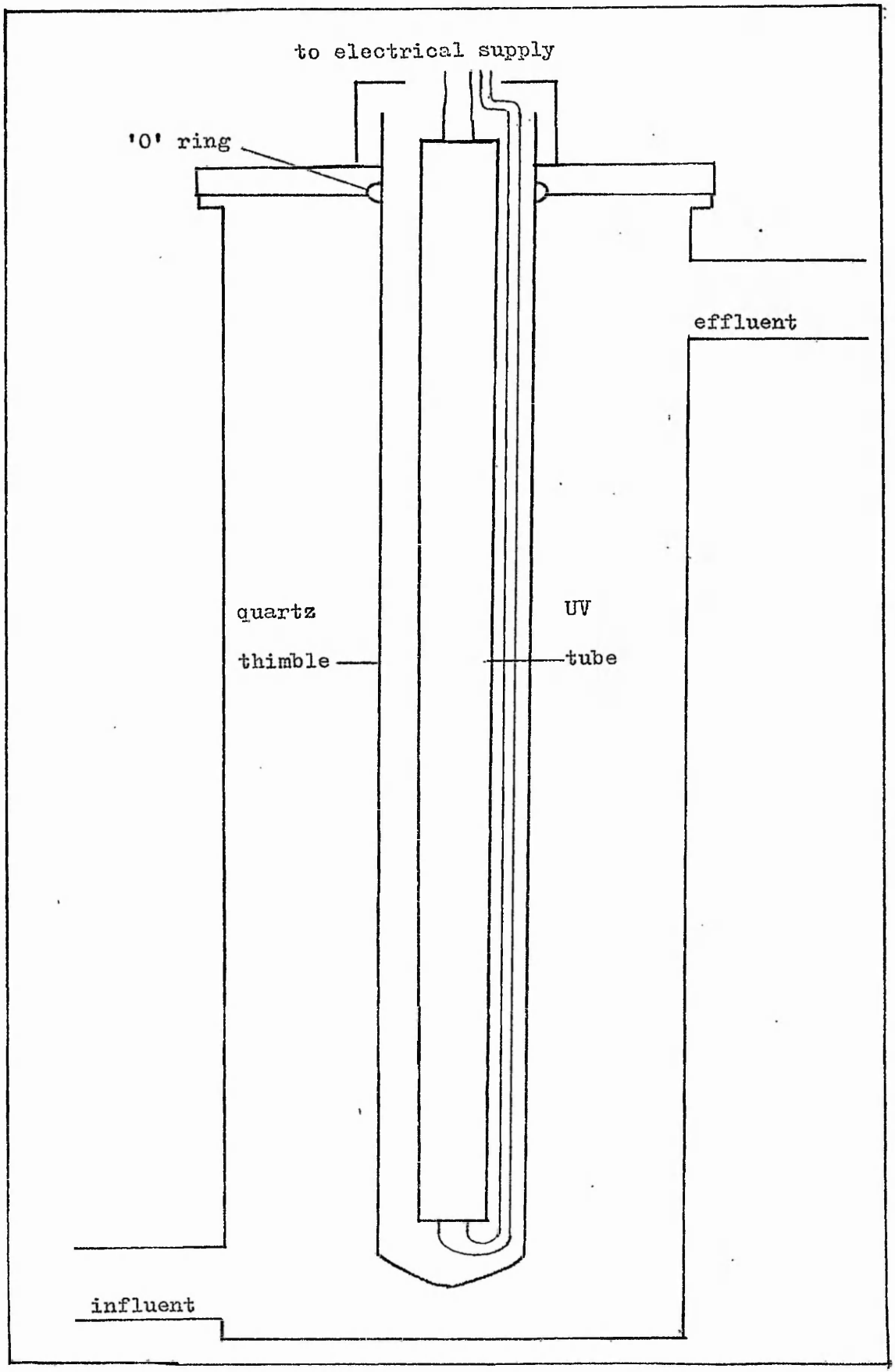
to electrical supply
'O' ring
effluent
quartz
thimble
UV
tube
influent

of these lamps are shown in Figures 16a and 16b.

To achieve greater UV output, a 250 watt lamp (MBF/U) was run with three times as much current as normal, by connecting three chokes and capacitors in parallel. It was reasoned that the output from this lamp per steradian should exceed that of the 2 kilowatt lamp because of its more compact size (the 2 kilowatt lamp being 3.5 x longer than the 250 watt lamp and had a greater diameter). The output in the wavelengths between the major emission lines should also have been higher because the increased temperature of operation would increase the pressure of the mercury vapour.

A 250 watt high pressure mercury lamp was used for a few experiments. The casing around the lamp was modified for mounting the lamp in the lamp housing and the thick glass safety window removed to allow transmission of the UV. These lamps operated at high pressure and represent an explosion hazard.

All the lamps had a very high output of UV and represented serious hazards to the eye and could cause severe burning. UV will also cause skin cancers. The lamp housing was designed to keep hazards to a minimum by making sure that no direct or reflected UV could strike the eye.

The mercury vapour lamps were provided with a polished aluminium reflector to increase the amount of UV entering the condenser lens.

b. The Condenser.

The lamps were housed in a lamp/condenser unit, a diagram of which is shown in Figure 17. The unit was built by the researcher for use in connection with the monochromator. The lamps were held by 'U' clips in alignment with the entrance slit of the monochromator and with the optical axis of the monochromator.

Figure 16a.

Wiring Diagram of 250w Mercury Lamp.

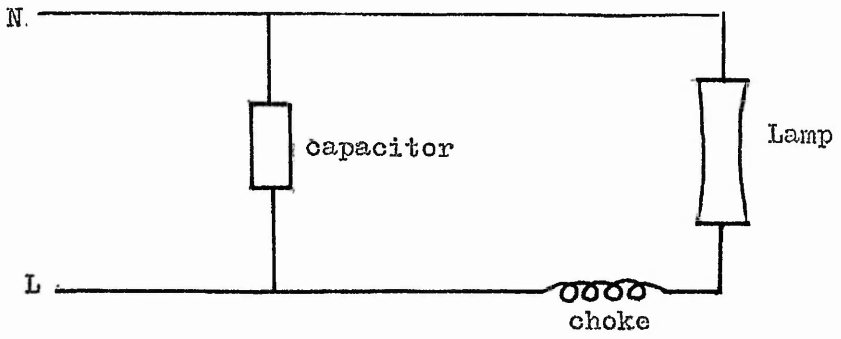

Figure 16b.

Wiring Diagram of 2kw Mercury Lamp.

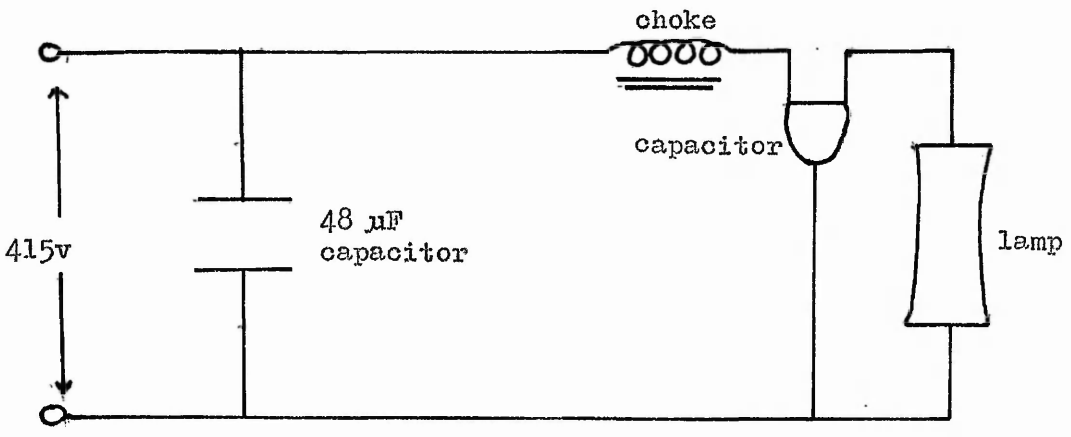

Figure 17.

Diagram of Monochromator Source and Condenser Unit.

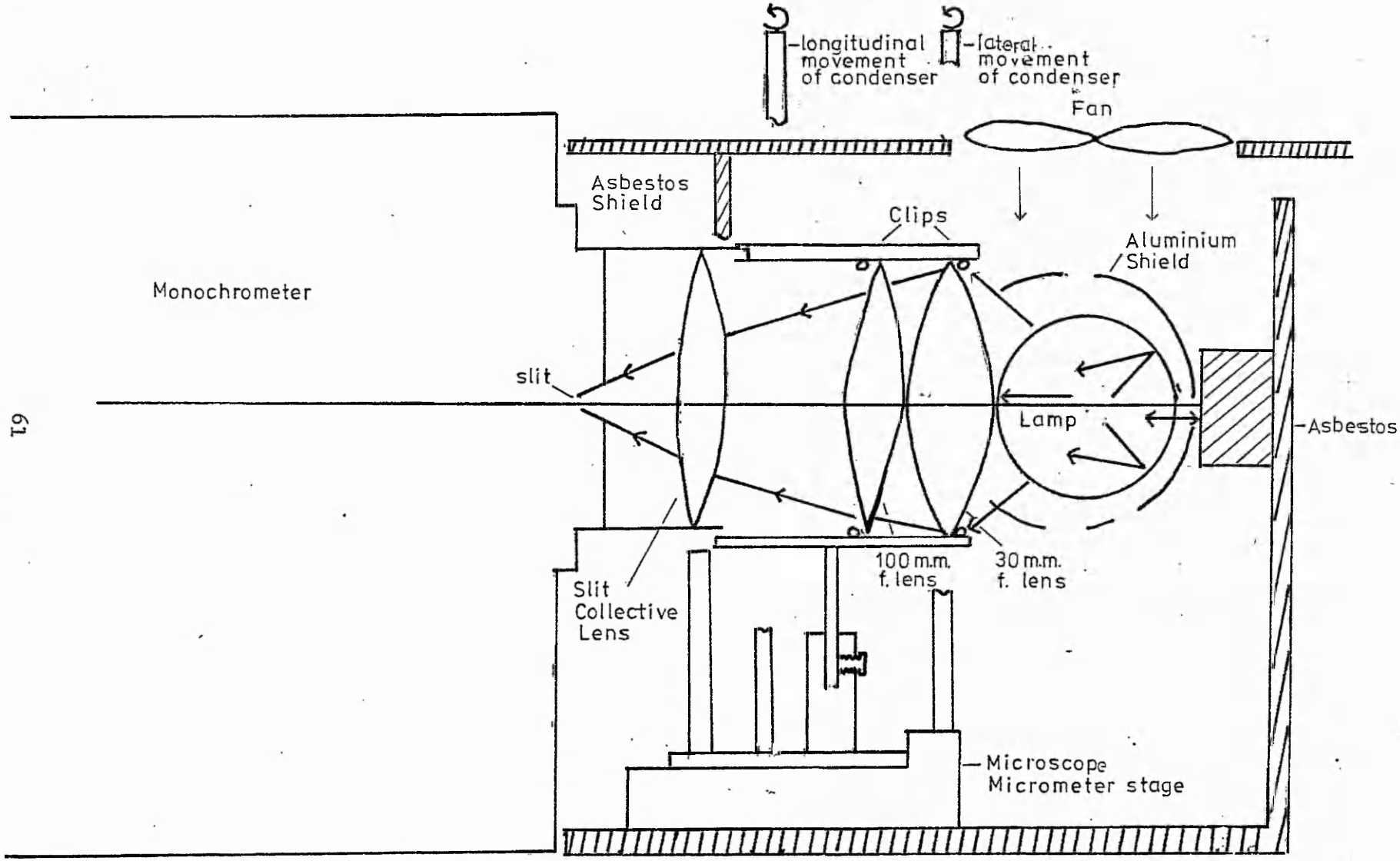
longitudinal movement of condenser
lateral movement of condenser
Fan
Asbestos Shield
Clips
Aluminium Shield
Monochrometer
slit
Lamp
Asbestos
100 m.m. f. lens
30 m.m. f. lens
Slit Collective Lens
Microscope Micrometer stage

Because the lamps were so powerful, a great deal of heat was radiated by them. Shielding of the lamps made this heat build up until the temperature of the lamp rose above 1,050°C, which was the melting point of the quartz. Therefore heat shielding had to be provided for the bench and the surrounding equipment. Cooling was achieved using a cold air fan blowing directly onto the surface of the lamp, hot air being vented through holes in the side of the unit.

The housing was constucted of a wood skeleton, lined with 3mm asbestos sheet attached by 'Araldite' epoxy resin. A sheet metal box covered the whole unit to act as a UV shield.

An asbestos shield was placed between the source and the condenser lens mounting (a cut out was provided for the lens to collect as much UV as possible) and between the condenser lens and the monochromator. The condenser lens assembly was mounted on an adapted microscope stage (see Figure 17) which could be adjusted for vertical, lateral and longitudinal movement from outside the shield.

A lens holder (an aluminium tube machined to size) was mounted on the stage and held the 50mm diameter quartz lenses.

Two lenses, made from spectrosil B by the Thermal Syndicate Ltd., of focal lengths 30mm and 100mm, were held in the lens holder by circlips. By having a short focal length the lenses could be moved to within a few mm of the source to trap a large proportion of the UV emitted and to focus it onto the entrance slit of the monochromator. A lens with a short focal length is thicker than one with a long focal length, and the thicker a lens is the more UV it will absorb. It is estimated that the 30mm f lens absorbed about 50% of the incident UV.

The focal lengths of these lenses were chosen so that, in conj-

unction with the entrance slit collector lens, the UV from the source would be focused, in a narrow beam, onto the diffraction grating in the monochromator, 200mm away from the centre of the lens. The focal lengths were calculated using the following equation:-

$$\frac{1}{f} = \frac{1}{a} = \frac{1}{b}$$

Where,

a is the distance between the image and the lens

b is the distance between the source and the lens

f is the focal length of the lens.

The reciprocals of the focal lengths of the lenses were added together to calculate the focal length of the whole system:-

$$\frac{1}{30} + \frac{1}{100} + \frac{1}{200} = \frac{1}{20.7}$$

To achieve focus at 200mm, the lens unit was moved to within 0.5mm of the source.

c. The monochromator.

The monochromator was a Bausch and Lomb High Intensity Monochromator (Cat 33-86-75) with a UV grating blazed at 2,700 lines mm^{-1}, selecting UV wavelengths between 200nm and 400nm. A diagram of the light paths in the source-monochromator-platform is shown in Figure 18.

Light emitted by the source (A) is focused by quartz condenser lenses (B) and collected by the quartz collective lens (C) in front of the monochromator entrance slit (D). This creates a uniformally illuminating bundle of light incident on a plane diffraction grating (E) where it is angularly dispersed according to wavelength. The grating can be rotated about an axis perpendicular to the plane of incidence of the light to permit selection of any wavelength for

Figure 18.

Diagram of The Monochromator Unit, Showing Light Paths.

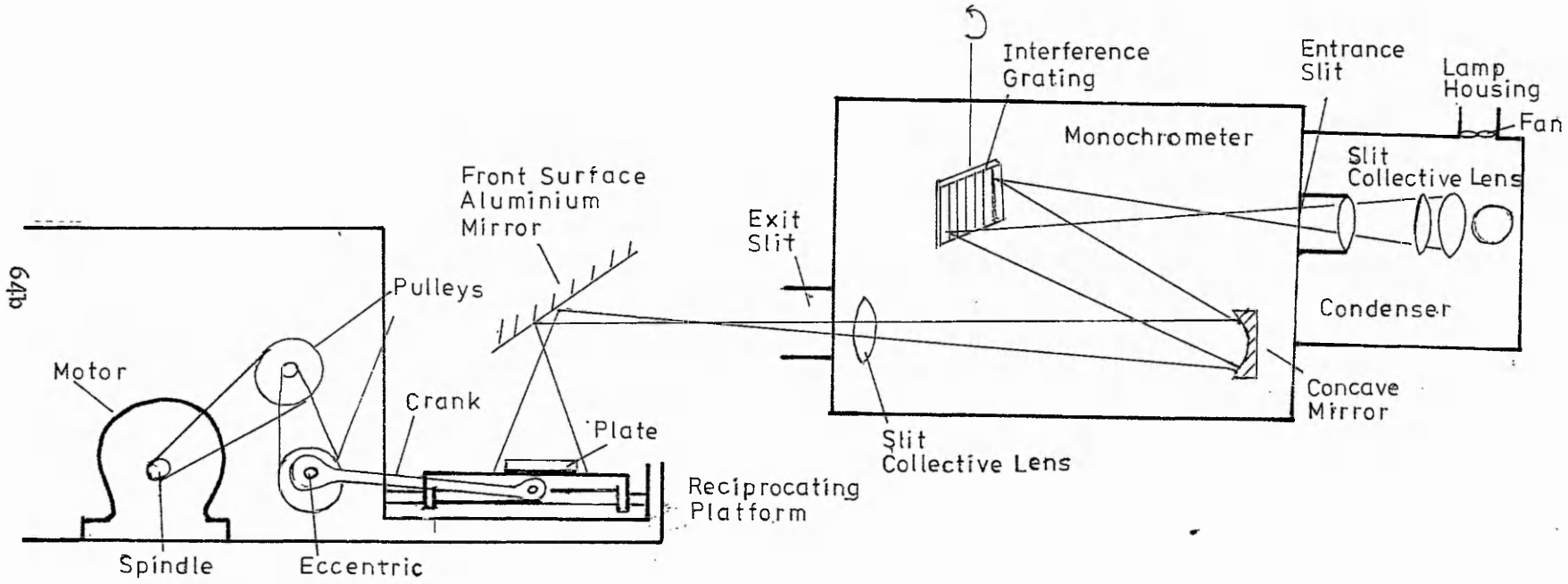
Interference Grating
Entrance Slit
Lamp Housing
Fan
Monochrometer
Slit Collective Lens
Front Surface Aluminium Mirror
Exit Slit
Pulleys
Condenser
Motor
Crank
Plate
Concave Mirror
Slit Collective Lens
Reciprocating Platform
Spindle
Eccentric

64b

reflection at the mirror (F) and hence the slit collective lens (G) where it is focused onto slit (H). Only the wavelength striking the exact centre of the concave mirror is imaged at the exit slit, other wavelengths producing images on either side. The lateral dispersion of these images is a measure of the purity of the emergent wavelength (for this monochromator the dispersion is 3.2nm mm^{-1}). The exit slit width and the dispersion determine the bandpass of the system; in this case a slit width of 3mm gives a bandpass of 9.6nm.

The monochromator and source-condenser units were aligned by the mating of the two units. Final alignment took place with the source switched on and the monochromator adjusted to pass 254nm UV. A sheet of white paper (which flouresces under UV) was held to the exit slit. The condenser lens was adjusted for height and other alignments until the brightest spot of flourescence was obtained on the paper (it was considered that the brighter the flourescence, the higher the output).

The beam of UV leaving the monochromator was reflected through 90 degrees onto the plate containing the virus suspension by a front surface aluminium mirror. The silvering of this mirror was carried out in a Nanotech coating unit. 0.5 g of aluminium wire was wound on to a tungsten shadowing basket (Polaron Ltd.) which was suspended between two high tension terminals of the unit. A glass plate, washed with acid and dried with acetone was placed 6 cm away from the basket. The unit was then evacuated and at 10^{-5} torr, a 10 amp current was passed through the basket and the aluminium was vapour - ised onto the glass. This resulted in the glass plate being coated with a thin layer of very reflective aluminium- a front surface mirror. Comparing flourescence of <u>reflected</u> and <u>non-reflected</u> light on a piece of white paper, a subjective estimate of reflectance

of 80-90% was made, a figure in agreement with Jagger (51).

d. The Shaking platform.

The UV was reflected onto 1,000 mm^2 plastic or glass petri plates capable of holding up to 6 ml of liquid. The plate and its contents were held within a shaking platform with a reciprocal throw of 2-5mm (depending on the eccentric drive used).The UV beam was just wider than the travel of the plate, so that the suspension was always fully in the beam. A two speed linear induction motor powered the shaking platform, the shaking rate of 70 rpm being achieved by gearing down the motor through a system of pulleys.

The platform reciprocated on two 3mm diameter silver steel runners passing through 13mm PTFE block (as a bearing surface) on the base of the platform.

Calibration of UV Sources.

i) The output of the monochromatic surface steriliser was measured with a 'Paragerm Pocket Dosiometer' supplied by F.R.Stiff and Associates. This meter only measures 254nm UV. It was calibrated in mWatts cm^{-2}. Since 1 Watt = 10^7 ergs sec^{-1}, 1 mWatt = 10^4 ergs sec^{-1}. 1mWatt cm^{-2} = 10^4 ergs sec^{-1} cm^{-2} = $\underline{10^2 \text{ ergs } sec^{-1} \ mm^{-2}}$

The meter could be read to the nearest 0.2 mWatt cm^{-2}. All readings were converted to ergs sec^{-1} mm^{-2}.

The meter was cross checked with a chemical method known as actinometry, first described by Hatchard and Parker (115). Actinometry was then used to calibrate the output of the British Rail steriliser and the monochromator.

ii) Potasium ferrioxalate actinometry.

6mM potassium ferrioxalate was prepared by mixing 1 part of 1.5 M analar ferric chloride with three parts of 1.5 M analar potassium

oxalate. After mixing thouroughly the solution was evaporated in a dish at 70°C, in the dark, until three quarters had evaporated. Cooling at room temperature for two hours resulted in the formation of potassium ferrioxalate crystals. These crystals were resuspended in distilled water and re-crystallised as before. The crystals were dried with a hair dryer and 2.947 g suspended in 800 ml of distilled water. 100 ml of 1 N H_2SO_4 was then added and the whole solution brought up to 1 litre with distilled water. The actinometer was then poured into a brown glass winchester and stored in the dark for up to four months until required.

5 ml of the actinometer was irradiated in 1,000 mm^2 glass petri plates (plastic petri plates were found to interfere with the assay by reducing the ferric ion in the absence of light). Wavelengths sho shorter than 550nm promote electron transfer from an oxalate ligand to the central ferric ion, reducing it to the ferrous state:-

$$Fe^{3+}(C_2O_4)^{2-} \xrightarrow{h\nu} Fe^{2+} + (C_2O_4)^{-}$$

$$(C_2O_4)^{-} + Fe^{3+}(C_2O_4)^{2-} \longrightarrow 2CO_2 + Fe^{2+} + (C_2O_4)^{2-}$$

After irradiation, the yield of ferrous ions was determined by measuring the optical density of the red complex formed on addition of 1:10 phenanthroline monohydrate (0.1% aqueous solution), buffered at pH 3.5 by acetate buffer (600 ml N sodium acetate plus 360 ml N H_2SO_4 made up to 1 litre with distilled water). In a typical experiment, 5 ml of irradiated actinometer was pipetted by an ARH automatic pipette into 5 ml of 0.1 N H_2SO_4, 8 ml of buffer and 2 ml of phenanthroline, making a total of 20 ml. The amount of actinometer added to the assay was varied depending on the amount

of ferrous ions produced in the actinometer. If a large dose of radiation was received, less actinometer would be assayed to prevent the optical density of the complex from being outside the range of the spectrophotometer. More actinometer would be used if the dose were weak.

The optical density of the complex was measured at 510nm, and the amount of ferrous ions produced determined by interpolating the O.D. into a calibration curve made from 0.0.2 μM Fe^{2+} (see results).

Below 360nm, the quantum yield of ferrous ions (the number of ferrous ions produced per quantum) is 1.26 moles $einstein^{-1}$. The number of moles is therefore related to the number of einsteins (or the number of quanta) by dividing by 1.26.

Different wavelengths have different energies, (Table 7 shows the energies of UV photons between 200nm and 300nm) and to find the total amount of energy the number of quanta is multiplied by the amount of energy (in ergs) per quanta. At 254nm this is 4.71×10^{12} ergs $einstein^{-1}$. Multiplying the number of quanta by the energy gives the total amount of energy striking the plate (the integral dose). Dividing this energy by the area (in mm^2) gives the dose. The dose rate is the dose divided by the time of exposure, in this case to give the dose rate in ergs sec^{-1} mm^{-2}.

According to Jagger (113), the results should be significant to two significant figures.

Both the surface steriliser and the monochromator were calibrated by exposing actinometer on the shaking platform.

iii) Calibration of the British Rail UV Steriliser Mk I.

The British Rail UV steriliser was also calibrated using actinometry. 60 litres of 6 mM potassium ferrioxalate were used in cont-

Table 7.

Energies of Photons of Wavelengths Between 200nm and 300nm.

Wavelength	Energy
200nm	9.93×10^{-12} ergs
210	9.46
222.5	8.93
230	8.64
238	8.35
250	7.95
253.7	7.83
265	7.5
270	7.36
275	7.22
280	7.1
289	6.87
300	6.62

inuous flow equipment. The actinometer was placed in a marriotti bottle (a device that ensures a continuous hydrostatic head). Figure 19 shows a diagram of the equipment used. The actinometer was led into the UV steriliser via a flow meter and regulator. The irradiated actinometer was collected from the top of the steriliser and led into a waste container. 5 ml samples were taken from the effluent mixed with 5 ml of 0.1 N H_2SO_4, 2 ml phenanthroline solution and 8 ml of acetate buffer. After 30 min, the optical density at 510nm was measured and the amount of ferrous ions (and hence the dose) determined from the calibration curve.

When the flow rate was changed (from faster to slower), time was allowed for at least three volumes of solution to pass through to ensure that a representative sample at the new flow rate could be taken.

X-Ray Source.

Bacteriophage was exposed to X-rays emitted from an Andrex Portable Lightweight X-ray machine, fitted with a 200 kV tube. Bacteriophage were exposed in 1,000 mm^2 glass dishes, 8 cm from the source, at a flux of 30,000 rad min^{-1}.

X-ray actinometry.

The method used (114) measured spectrophotometrically the amount of oxidation of ferrous ions induced by radiation, mediated by free radicals produced in the water, as in the equations below:-

$$Fe^{2+} + H^+ + {}^*HO_2 \longrightarrow Fe^{3+} + H_2O_2$$

$$Fe^{2+} + H_2O_2 \longrightarrow Fe^{3+} + OH^- + {}^*OH$$

$$Fe^{2+} + {}^*OH \longrightarrow Fe^{3+} + OH^-$$

Figure 19.

Flow Through Equipment Used With B.R. UV Steriliser.

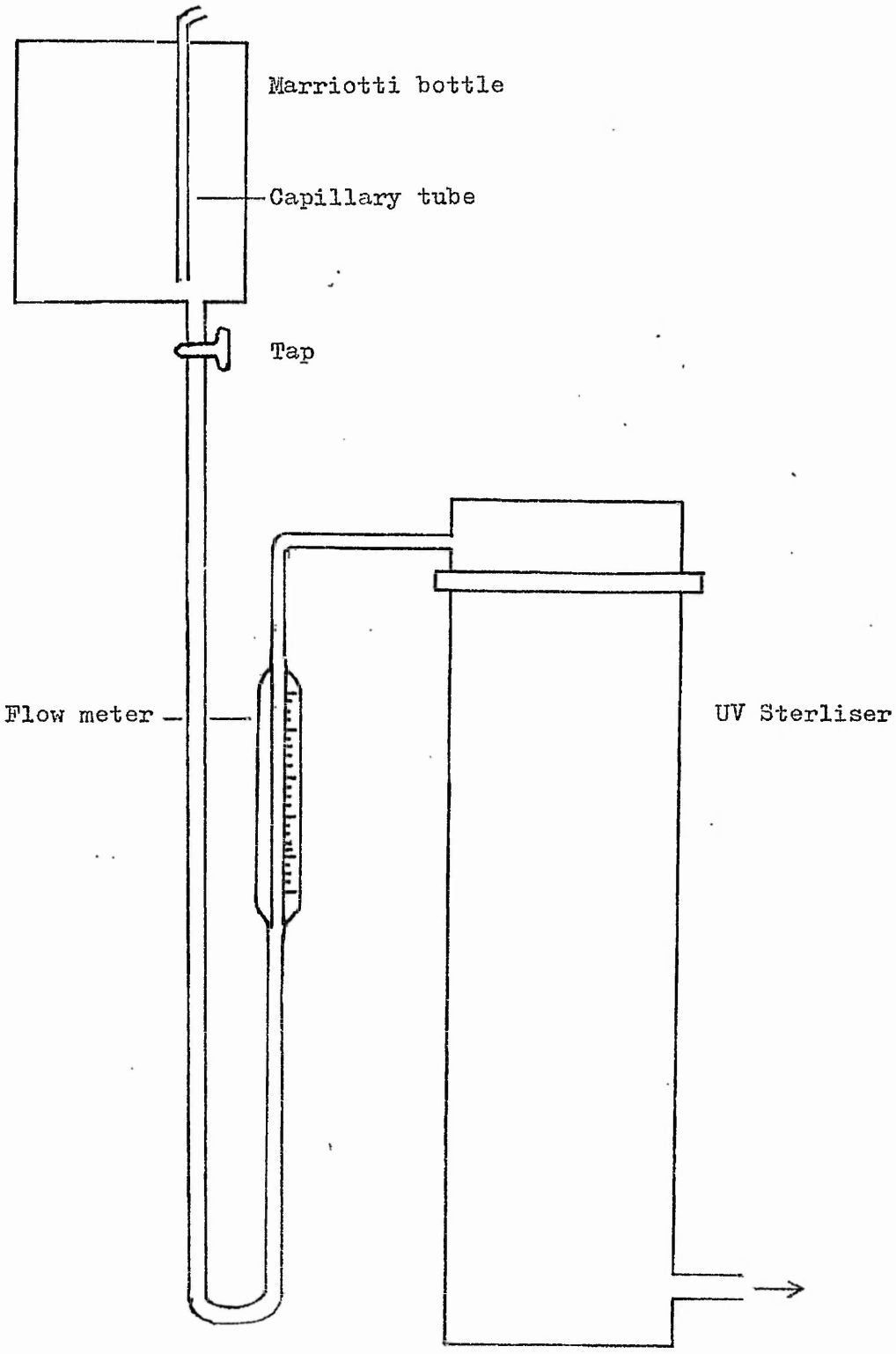

The tendancy of a compound or ion to undergo a radiation induced reaction is measured by its G value (the number of molecules produced or destroyed for each 100 ev absorbed). The value of G for the oxidation of ferrous ions is 15.5, i.e. 6.5 ev per ion oxidised. The energy required to cause the reaction of one mole of ions or molecules is :-

$$(100/G)(6.02 \times 10^{23}) = 6.02 \times 10^{25}/G \text{ electron volts.}$$

And the energy for one micromole:-

$$6.02 \times 10^{13}/G \text{ Mev.}$$

Since 1 Mev = 1.6×10^{-6} ergs, this is equivalent to $9.6 \times 10^{7}/G$ ergs

As 1 rad = 100 erg/g, then

$$1 \text{ micromole/G} = 9.6 \times 10^{5}/\text{g rad.}$$

For ferrous ions this is 6.2×10^{4} rads.

Determination of the yield of ferric ions was carried out as follows:-

20 ml of a 2×10^{-3} M ferrous ammonium sulphate (in 1.6 N sulphuric acid) solution was saturated before use with oxygen, by bubbling air through it with a pipette. The solution was exposed to X-rays in a 1,000 mm^2 glass dish for multiples of 9 minutes (the maximum time that could be set on the machine). The concentration of ferric ions was then measured spectrophotometrically at 305nm (maximum absorption of ferric ions occurs at this wavelength, while the absorbance of ferric ions is negligable). Ferric ions (as ferric sulphate) from 0.1 mM to 1 mM in 0.5 M sulphuric acid were prepared to calibrate the spectrophotometer.

5 ml of virus suspension were exposed to X-rays in 1,000 mm^2 glass dishes for multiples of 2.5 minutes.

Temperature Inactivation.

Bacteriophage, in distilled water, were exposed to heat in 1 x 6 cm glass tubes in a Techne SB-4 shaking water bath. The temperature was set with the thermostat and checked with a thermometer (accurate to $\pm$ 0.1^{o}C). The thermostat did not need adjusting to reach the required temperature. After the tube containing 5 ml of virus suspension was put into the water bath, 10 seconds were allowed for the contents to rise to the temperature of the water before 0.1 ml aliquots were removed, for dilution and plating out, with a Sigma 100 µl automatic pipette.

Production, Purification and Assay of Bacteriophages.

A.Bacteriophage Host.

i) Culture and selection.

A strain of bacteria, selected from Escherichia coli K12 Hfr Hayes λ^- (NCIB strain 10235) was used throughout for the assay of MS2 and QB.

A replica plaque technique was used to select stable expression of the F^+ factor, and thus stable expression of the pili necessary for the attachment of the male specific phages.

A suspension of host was diluted to 200 cells ml^{-1} in nutrient broth, 0.1 ml of this being spread with a sterile glass spreader over a pre-poured petri plate containing 10 ml of Oxoid blood agar base. Several plates were prepared in the same way and incubated overnight, inverted, at 37°C. Several plates containing agar were then spread with o.1 ml of a 10^{11} pfu ml^{-1} virus suspension. A felt pad, sterilised by 1 hour exposure to UV at 100 ergs sec^{-1} mm^{-2}, was aseptically placed over a rubber block (of slightly smaller diameter than a petri plate) and retained with a rubber band. The pad was then inverted gently over the colonies on the first plate (orientation marks on the plate and the rubber block being aligned) removing some of the bacteria from the plate. These bacteria were then transfered to a virus plate, which was then incubated, inverted, at 37°C overnight. Colonies that grew on the virus plate, it was reasoned, arose from bacteria not expressing the sex pilus, these in turn arose from a colony that did not have 100% expression of the F^+ factor, which was probably lost. As only one cell in a colony needed to have lost the F^+ factor for a colony to arise on the virus plate, the regression rate of a colony not appearing on a virus rate must be very low.

Reference to the original colony plate was made and a colony that did not have any progeny on the virus plate (and thus had a very stable F^+ factor) was selected. A sterile wire loop was used to transfer the colony into 10 ml of sterile nutrient broth and the culture was incubated at 37°C overnight. By comparing the numbers of plaques formed from a dilution of stock virus against the original host, it was shown that the new host supported the production of more plaques (see results).

Host for stock was grown in 20 ml and 100 ml nutrient broth at 37°C in 25 ml universals and 120 ml medical flats. They were not aerated or agitated and grew to about 10^9 cells ml^{-1}. Some of this host was streaked with a sterile wire loop onto 10 ml blood agar slopes in universals. These were grown overnight at 37°C or until a good growth was visible on the slope. These slopes were stored at 4°C as 'stock' for up to 2 years. Other slopes were subcultured from these as the need arose.

Host was grown for assay by transferring a loopful of bacteria from a slope into 100 ml of sterile nutrient broth. This was then incubated, without shaking, at 37°C overnight. This suspension could then be stored at 4°C for up to 3 months before being used in the assay.

The Oxoid nutrient broth and blood agar base (0.6% in distilled water) media were autoclaved at 121°C for 15 minutes.

ii) Assay of viable bacteriophage.

Bacteriophage were enumerated by their ability to form plaques on a lawn of host.

Clean 10 ml glass tubes, capped with 'Cap O'Test' aluminium caps were sterilised with dry heat at 160°C for 2 hours.

1% peptone (B.D.H.) in distilled water was adjusted to pH 7.0 by the dropwise addition of conc. NaOH, pH being measured with an EIL 7030 pH meter. 0.6% Oxoid agar No 3 was then added to the peptone and the solution autoclaved at 121°C for 15 minutes. The soft agar was dispensed in 2.5 ml aliquots with an ARH automatic pipette. The tubes were placed in a water bath at 47°C in order to keep the agar liquid.

750 ml of 4% Oxoid blood agar base was autoclaved at 121°C for 15 minutes, and 10 ml aliquots poured into petri plates when cooled to 70°C. The plates were air dried overnight before use.

4 drops of the host suspension were added to the soft agar from a sterile pasteur pipette, 15 tubes being innoculated at one time. 0.1 ml of a virus dilution was then added to the tube, which was then shaken and poured over a prepoured plate. Three replicates of each dilution were plated out. The plates were allowed to set and then incubated overnight, inverted, at 37°C. Plaques per plate were counted the next day and the pfu ml^{-1} of the original virus suspension determined.

The virus was diluted and added to the assay with Sigma 100 µl automatic pipettes equipped with disposable plastic tips. After use these tips were discarded into alcohol and later boiled in distilled water and re-used, absolute guarantee of sterility not being required in the assay as the high level of host overgrew any contaminants.

B. Production of Bacteriophages MS2 and Qβ.

i) Source and selection of bacteriophage.

Qβ was donated by Dr. T.G.Vickers of Trent Polytechnic, being originally a strain used at Bristol University. MS2 was donated by Dr. P.A. Heacock of the Department of Genetics, University

of Leicester.

Clones of these viruses were selected from plaques on plates of virus dilutions and separate plaques were aseptically transferred to an exponentially growing suspension of host. (Exponentially growing host produce the highest titres of phage). Dilutions of the resultant lysate were re-plated and new plaques selected and re-innoculated into the host. This process was repeated once more and the resultant clone chosen was viewed under the electron microscope to confirm that the clone chosen was a male specific bacteriophage and of the same morphology as that published for these viruses.

ii) Production of bacteriophages.

The selected MS2 or QB suspensions or lysates were titred by the assay method above and then diluted to about 3×10^4 pfu ml^{-1}. 0.1 ml of this was added to soft agar and poured (with 8 drops of host) onto a blood agar plate. After overnight incubation the soft agar overlay containing the resultant confluent lysis was scraped off with a scalpel blade and agitated with 10 ml of distilled water. The soft agar from several plates were combined in the 10 ml and also agitated. Thirty other plates were treated in the same way to produce a total of 75 ml of distilled water plus soft agar.
5 ml of chloroform was added and the lysate shaken for a minute to kill the host bacteria. The lysate was then centrifuged at 3,000 rpm in a Janetzki T32b centrifuge to separate the chloroform and bacterial debris. The supernatant was decanted and stored until required at $4^{o}C$. Titres of phage obtained by this method ranged from 1×10^{11} to 1×10^{13} pfu ml^{-1}.

iii) Large scale production of bacteriophage.

Yield of bacteriophage depends on the physiological state

of the cell, a high metabolic rate leading to higher production of virus particles as well as 100% production of pili which means a high level of infectivity. Previous work (117) has shown that the maximum yield of phage was obtained when the host was exponentially growing in the last third of the growth cycle, were well aerated and infected with high multiplication of phage.

Three methods were used to achieve large scale production of bacteriophage.

(a) 3 litres of Oxoid nutrient broth + 2 % glucose were sterilised by autoclaving, in a 5 litre aspirator, for 25 minutes at 121°C. A diagram of the culture vessel is shown in Figure 20.When cooled, the vessel was placed in a 37°C incubator on a magnetic stirrer. A compressed air cylinder was attached to the sterile Microflow miniature line filters and an air flow of 500 c.c. min^{-1} passed through the medium. 100 ml of 1 x 10^9 cells ml^{-1} host were added as an inoculum and the culture agitated by a magnetic follower.

During the course of growth, samples of suspension were withdrawn by air pressure through the sample arm. The samples were measured with a spectrophotometer (Pye Unicam SP500) at 650nm. At an O.D. of 0.34, equivalent to 7 x 10^8 cells ml^{-1} (118), phage was added at a multiplicity of 20 pfu $cell^{-1}$, to ensure that all susceptable cells were infected. After a further three hours of incubation, stirred and agitated, the lysate was taken from the incubator and 300 ml of lysing medium added.

Figure 20.

Batch Culture Equipment Used for the Production of Bacteriophage.

Key.

A. Medium inflow line.

B. Sterile joint. (Male and female 'Quickfit' joints.)

C. Air filter.

D. Magnetic follower.

E. Air outlet.

F. Sampling arm.

G. Sterile sampling bottle.

H. Sterile joint.

I. Harvesting flask.

J. Magnetic stirrer

K. Culture harvesting line.

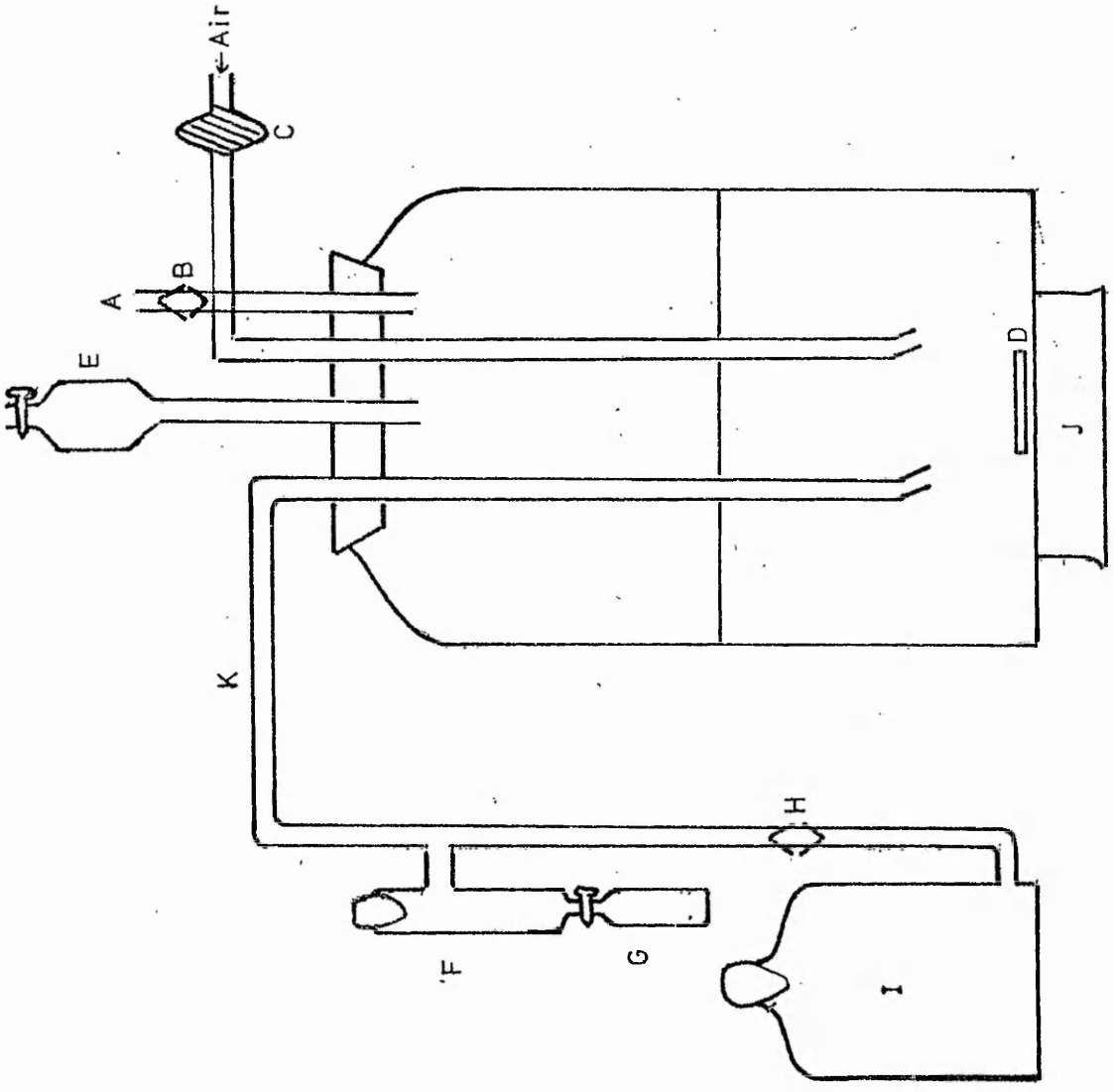
Air
C
A
B
E
D
J
K
H
F
G
I

Lysing medium.

Lysozyme (dried protein, B.D.H.)	10mg
1 M EDTA pH 8.0 (B.D.H.)	1ml
1 M Trizma base pH 8.0 (B.D.H.)	96.5ml
Distilled water to	100ml

After the suspension was kept overnight at $4^{o}C$, 100 ml of chloro form was shaken into the lysate for 5 minutes to lyse any remaining host or bacterial contaminants. The lysate was decanted to separate it from the chloroform and spun in the 6 x 250 ml rotor of the M.S.E 18 centrifuge at 10,000 rpm for 15 minutes to remove bacterial debris. This method gave a yield of about 10^{11} pfu ml^{-1}.

(b) 2 litres of Oxoid nutrient broth + 2% glucose were sterilised in an LHE batch vessel. Temperature, dissolved oxygen and pH probes were inserted to monitor the culture. 100 ml of 2 x 10^{9} cells ml^{-1} were inoculated through a port and growth at $37^{o}C$ was followed spectrophotometrically by removing 10 ml aliquots through the sampling arm. Air was sterilised by a Microflow filter and was passed from a compressed air cylinder into the culture at a rate of 350 cc min^{-1} through a sparger. At an O.D. of 0.35 at 650nm (about 7 x 10^{8} cells ml^{-1}) 50 pfu $cell^{-1}$ of phage were added. Incubation continued for a further three hours when 300 ml of lysing medium were added. The yield of phage was about 5 x 10^{8} pfu ml^{-1}, which was very low.

Osborn et al (156)from whom this method was adapted, reached a titre of 10^{13} pfu ml^{-1}. It is assumed that the amount of agitation used was too much for the fragile pili in this system and they were probably sheared off.

(c) 250 ml Erlenmeyer flasks were sterilised by dry heat at $160^{o}C$ for two hours. 3 litres of medium A salts were sterilised in a 5

litre flask for 30 minutes at 121°C in an autoclave. When the medium had cooled to room temperature, the glycerol and calcium chloride components (filter sterilised through a 0.22 micron Millipore cellulose nitrate filter) were added slowly with stirring.

Medium A.

Na_2HPO_4	7g
KH_2PO_4	3g
NH_4Cl	0.5g
Distilled water	1 litre
30% glycerol in 0.5 M $MgSO_4$	10 ml
12% casamino acids	50 ml
0.5 M $CaCl_2$	2 ml

The medium was then dispensed into the conical flasks, 75 ml per flask, using a measuring cylinder. 2 ml of host bacteria at 5 x 10^9 cells ml^{-1} were added to each flask with an ARH automatic pipetting system and the flasks covered with aluminium foil. No special precautions were taken to ensure asepsis at this stage, other than rinsing the equipment with boiling water to kill any contaminating phages, as the large innoculum of host outgrew any bacterial contaminants.

The flasks were placed in a Gallenkamp orbital incubator and shaken at 150 rpm at 37°C. Growth was measured in a spectrophotometer at 650nm and at an O.D. of 0.38 the shaking rate was cut to 75 rpm for ten minutes. (Pili are very fragile and this was done to ensure that pili wern't sheared off, ten minutes being adjudged time for pili to lengthen). The cells were then infected with 100 pfu $cell^{-1}$ of phage and ten minutes later the shaking rate increased to 150 rpm for a further two hours. At the end of this period the lysate was

pooled and 100 ml of lysing medium per litre of lysate added. A typical lysate contained 10^{12} - 10^{13} pfu ml^{-1}.

The lysate plus lysing medium was cooled to 4°C and left overnight in a refrigerator. All subsequent methods were carried out at 4°C.

C. Concentration and Purification of MS2.

i) Concentration by ammonium sulphate precipitation.

The concentration by ammonium sulphate technique was adapted from a method used by T.Vickers (118). 280 grams of ammonium sulphate per litre of lysate were added over three hours with constant stirring on a magnetic stirrer. The lysate was left overnight at 4°C, when the precipitate was collected in a Sharples centrifuge at 12,000 rpm. The precipitate was suspended in 250 ml of buffer A (0.01 M EDTA, adjusted to pH 7.6 with conc. HCl, 0.05 M tris (hydroxymethyl) aminomethane, 0.1 M sodium chloride). This was then centrifuged in the 6 x 250 ml rotor of the M.S.E. High Speed 18 centrifuge at 10,000 rpm for 15 minutes and the precipitate discarded. Ammonium sulphate at 300 g $litre^{-1}$ of supernatant was then added and the resultant precipitate collected by another 10,000 rpm centrifugation. The pellet was re-suspended in 50 ml of buffer A and an equal volume of freon (trichloroflouromethane) was added. Vigorous shaking by hand in a stoppered flask yielded an emulsion which was broken by centrifugation at 20,000 rpm for 15 minutes. The upper layer was decanted to leave behind the denatured proteins visible at the interface. The lower layer was removed by pipette and re-extracted with half its volume of buffer A and the aqueous layer combined with the aqueous layer from the centrifugation. This method was found to recover 1-10% of the original viable virus, giving a concentration of only 10 times, at maximum.

ii) Acetone precipitation.

This method was adapted from a technique used by W.Carlile (119) to precipitate enzymes extracted from fungi so that a high degree of activity was preserved. It was reasoned that this method should therefore not inactivate any viruses.

The overnight lysate + lysing medium was shaken with 100 ml of chloroform litre^{-1} of lysate, to lyse any remaining cells and to kill any contaminating bacteria. The aqueous layer was decanted and centrifuged in the 6 x 250 ml rotor of the M.S.E. 18 centrifuge at 15,000 rpm for 20 minutes to sediment cell debris. An equal volume of analar acetone at -10^{o}C was then mixed with the supernatant and left to stand at 4^{o}C. After 1 hour the resultant precipitate was collected in the Sharples centrifuge, operating at 12,000 rpm. The precipitate was taken up into 50 ml of a 1:10 dilution of buffer A and left at 4^{o}C overnight.

Although the method recovered 95-99% of the viable virus (see results), the large volumes of lysate + acetone were difficult to handle. Small volumes had to be fed through the Sharples to prevent the lysate warming up and the Sharples tended to overheat through prolonged use.

iii) Polyethylene glycol two phase concentrarion and purification.

This method by Albertsson (120) was employed to overcome the difficulties found in the other methods.

130 g of polyethylene glycol (PEG) (average molecular weight 6,000) from Sigma Ltd. was ground in a pestle and mortar and added to 2 litres of lysate together with 33 g of NaCl and 4 g of sodium dextran 500 (Sigma Ltd.). The solution was allowed to stand in a separating funnel for 6 hours at 4^{o}C. The heavy turbid bottom layer

was collected in a 25 ml universal, which was spun at 2,000 rpm for 15 minutes in a Janetzki T32b centrifuge. The clear top layer and the bottom phase were collected with a wide bore pasteur pipette (the bottom layer was very viscous) and discarded. The heavy interface was suspended in 20 ml of a 1% w/w dextran sulphate solution and kept at 4°C for three hours. 3 ml of a 3 M KCl solution was then added to precipitate the dextran sulphate. After standing for two hours the mixture was centrifuged at 2,000 rpm for 10 minutes to deposit the dextran sulphate along with cellular debris and other impurities. The concentrated and partly purified viruses were stored at 4°C until required. This method gave 95% recovery of the viable viruses and a 100 fold volume concentration.

iv) Sedimentation by ultracentrifugation.

The concentrated viruses were then sedimented by centrifugation at 130,000 x g in the 8 x 25 ml angle rotor of the M.S.E. Super Speed 50 preparative ultracentrifuge for 3½ hours. The rotor was pre-cooled to 3°C and the centrifuge operated at this temperature. The rotor was allowed to decelerate without braking. The supernatant was removed with a pasteur pipette and 5 ml of a 1:10 dilution of buffer A in distilled water added to the pale yellow precipitate, which was taken up overnight at 4°C.

v) Purification by Sephadex molecular sieve.

Sephadex G50 (molecular cut off 1,500-30,000) was added to twice its own volume of distilled water and allowed to settle. After the gel had absorbed water and expanded, excess water was poured off and twice the slurry volume added to wash off any small particles of the gel and any impurities. The excess was poured off and the thick slurry then poured into an 800 x 20 mm ion exchange

column. The slurry was allowed to settle and the liquid level run off until the gel was just covered. 5 ml of a concentrated virus suspension was then added to the column and run into the top of the gel. The column was then placed in a cold room at 4°C and filled with a 1:10 dilution of buffer A.A 2 litre reservoir of diluted buffer A was gravity fed to the top of the column to create a pressure head and to ensure the column did not run dry. The bottom of the column was connected to a plastic tube which led through an LKB Uvicord to an LKB fraction collector. The Uvicord was connected to an LKB chart recorder and detected the passing of the virus front by the measurement of the optical density at 280nm. The fraction collector collected fractions every 10 minutes, which represented 5 ml samples, into clean 15 ml centrifuge tubes.

The fractions containing the virus were pooled and re-sedimented in the M.S.E. Super Speed 50. The virus was taken up in 5 ml of dilute buffer A and left overnight at 4°C.

vi) Density gradient centrifugation.

The partly purified and concentrated virus was further purified for use in some experiments by caesium chloride density gradient centrifugation. 0.55 g of caesium chloride were added to each gram of virus suspension. 25 ml of suspension were then put into a polypropylene centrifuge tube, which was then balanced against two other tubes containing 55% w/w $CsCl_2$, and placed in the 3 x 25 ml swing out rotor of the M.S.E. Super Speed 50. Centrifugation was carried out at 130,000 x g for 48 hours at 3°C. At the end of the run the centrifuge was allowed to decelerate without braking.

Centrifugation resulted in two bands of virus, one large straw coloured band a third of the way up the tube, and a smaller, white band, four fifths from the bottom of the tube.

Fractions were collected in the first instance from the bottom of the tube, being pierced with the M.S.E. tube piercer (cat. no. 59557) and the 5 drop fractions collected in sterile 10 ml test tubes.

Fractions were also collected from the top to avoid contamination from debris. The tube was pierced at the base, as before, but 65% $CsCl_2$ was pumped slowly by an LKB peristaltic pump (at a flow rate of about 0.5 ml min^{-1}). The sample was pushed through the capillary tube and collected in 5 drop fractions in sterile 10 ml glass tubes. The fractions from both methods of collection were made up to 2.5 ml with sterile distilled water. The viral titres of each fraction were determined by plating out dilutions of the virus suspensions in the plaque assay method. Peaks of infectivity were pooled and then dialysed against 1 litre of 0.1 M tris (pH 7.0) overnight at 4°C in Visking tubing. The dialysis tubing was prepared by boiling for 10 minutes in a solution of 2% sodium bicarbonate and 0.01 M EDTA, followed by boilings in two changes of distilled water. This procedure removes heavy metals, a green colour and corrects acidity in the tubing.

The dialysed samples were placed in sterile 25 ml universals and stored for use at 4°C.

vii) Separation by electrophoretic focusing.

Crude lysate, density gradient purified and partially purified virus were purified by electrophoretic focusing in Ampholine buffer.

A pH gradient was set up in 1, 2, and 3% acrylamide gels and agarose gels by passing a current through the gels loaded with 1.7% ampholine.

30 g acrylamide and 1 g of N N' -methylene-bisacrylamide was made up into 100 ml distilled water. 2.25 ml of this was added to 14.9 ml distilled water together with 0.45 ml ampholine (obtained as a 40% solution from L.K.B.) 10 ml of a fresh 1% solution taken up into a 20 ml disposable syringe. The end of the syringe was blocked off and the plunger pulled back to de-gas the solution. 2 ml of the solution was then discharged into gel tubes (made from plastic disposable 5 ml pipettes, cut into 5 cm lengths). One end was blocked off with plasticine until the gel had set. A 250 µl sample of virus preparation was injected into the top of the gel with a Hamilton microlitre syringe and the tubes transferred to a refigerator to set at 4°C. After the tubes had set they were transferred to a Shandon Disc Electrophoresis unit which was then loaded with electrolyte, 0.2% H_2SO_4 was placed in the anode and 0.4% ethanolamine in the cathode. A Vokam power pack was adjusted to pass a potential of 350 volts through the gels at a current of 1.5 ma per tube. Electrophoresis took place for three hours at 4°C.

At the end of the run the gels were carefully pushed from the tubes with a glass rod onto a sterile plastic petri plate and cut into 20 roughly equal slices with a sterile scalpel blade. Each fraction was transferred to a separate 25 ml universal and 2 ml of distilled water added. After 10 minutes the gel was mascerated with a sterile glass rod and the pH measured with an EIL 7030 pH meter, calibrated against a standard buffer.

3 ml of buffer A was then added to each fraction which was then left overnight at 4°C to elute the phage, the viable number of phage in each fraction being measured by plaque assay.

Acrylamide gels, apart from being highly toxic, also caused

Inactivation of the viruses. Reducing the concentration of acrylamide resulted in sloppy gels which meant that proper pH gradients did not form and cross contamination of the virus peaks occured when the gels were pushed from the tubes.

To overcome these difficulties, electrophoretic separations were carried out using 0.9% agarose in distilled water. Molten agarose (0.9%) at 40°C was mixed with ampholine (0.15 ml per 6 ml of agarose), persulphate (0.3 ml of a 2% solution) and 250 ul of phage preparation. The gels were loaded into the electrophoresis unit and run at 350 volts D.C. at 1.5 ma per tube. The gels were fractionated and assayed in the same manner as for the acrylamide gels mentioned above.

Preparation of Glassware.

All glassware was boiled in distilled water and Decon, rinsed three times in tap water and five times in distilled water before being dried in a warm air drying cabinet. Pipettes were boiled in distilled water and rinsed in a pipette washer connected to a tap before being rinsed in distilled water and dried.

Medical flats, used for the growth of mammalian cells, had the growth surfaces prepared by being autoclaved full of distilled water which was poured off when cool and replaced with x 1 growth salts to condition the glass for pH and attachment.

Pipette tips from the Sigma automatic pipettes used for bacteriophage dilutions were discarded into 100% ethanol and later boiled in distilled water, dried and re-used, but pipette tips used for poliovirus assay were discaded into Chloros (25% solution) and later autoclaved.

Pasteur pipettes used in bacteriophage assay were discarded into Chloros as were pasteurs used in the poliovirus assay. These were boiled in distilled water, dried, plugged with cotton wool, sterilised by dry heat sterilisation at 160°C for two hours and re-used.

Graduated glass pipettes were plugged with cotton wool, loaded into aluminium containers and sterilised by dry heat at 160°C for two hours.

Aseptic technique.

Techniques used in aseptic methods varied depending on the materials handled. When handling bacteriophage, priority was given to the prevention of phage contaminating other samples and the host. The handling of mammalian cells required strict asepsis to prevent bacterial, fungal, mycoplasmal and viral infections of the cell line.

The handling of potentially pathogenic virus strains required that there be no dispersal of virus in the laboratory.

To meet all of these requirements a suite of rooms had been adapted and equipped. Figure 21 shows a diagram of the layout of these rooms. A general work room was used for glassware prparation, dry heat sterilisation, weighing of chemicals and non-sterile experiments.

Entry to the virus room was restricted to those people working in the unit and special laboratory coats (surgeons gowns) were worn exclusively in the virus laboratory. Bacteriophage work and enteric virus work were carried out in this room. Virus equipment was autoclaved and washed in this room, only virus preparations that had been sterilised were carried out of this room. All enteric virus preparations were autoclaved immediately they were discarded.

The sterile room, off the virus laboratory, was used exclusively for tissue culture work, exept for the growing of virus cultures which were incubated in the virus room. A separate laboratory coat was used for this room.

The virus room, sterile room (and UV area) were kept free of contamination by several methods. Air from outside the building was blown by fan into the sterile room through an LKB ultra filter. Another ultra filter, in the virus lab, extracted air and passed it to the outside. This system ensured a circulation of sterile air through the rooms, created a positive pressure in the sterile room, to prevent contamination entering, and a negative pressure in the virus room, to prevent possible contamination escaping.

Dust was kept to a minimum by periodic washing of the walls and equipment with Chloros and quaternary ammonium detergents. Formalin (50 ml of 25%) was sprayed into the virus room and sterile room

every night to control airborne and surface contamination. Petri plates containing blood agar base were exposed in the laboratories to check on contamination from bacteria and fungi in the air at periodic intervals. In the sterile room less than one colony was found after three hours exposure, but the virus lab produced three in ½ hour.

Tissue culture work in the sterile room was carried out on the open bench or in a LEEC cabinet, The LEEC cabinet blew ultra-filtered air towards the worker so that contamination from the worker could not infect the cells.

Entero virus manipulations took place in the virus cabinet. Any virus aerosols produced inside the cabinet were contained inside by a curtain of ultra filtered air blown down the front of the cabinet as a curtain of air. The cabinet was equipped with UV tubes to decontaminate any aerosols or spillages. Spillages were immediately wiped with neat Chloros, the wipers being autoclaved.

Pipetting of enteroviruses was carried out either by using Sigma automatic pipettes (discarding the tip into Chloros) or by ARH adjustable automatic pipettes fitted with a sterile pasteur pipette on the end so that no virus entered the glass barrel of the syringe.

Bacteriophage work was carried out on the open bench, using normal microbiological techniques.

Figure 21.

Diagram of Virus Laboratories.

Key.

Inc.	Incubator.
W.A.	Washing up area
E.A.	Experimental area
R	Refrigerator
Aut area	Autoclave facilities
Filt	Ultra filter
V.C.	Virus cabinet
D H S	Dry heat steriliser
D C	Drying cabinet

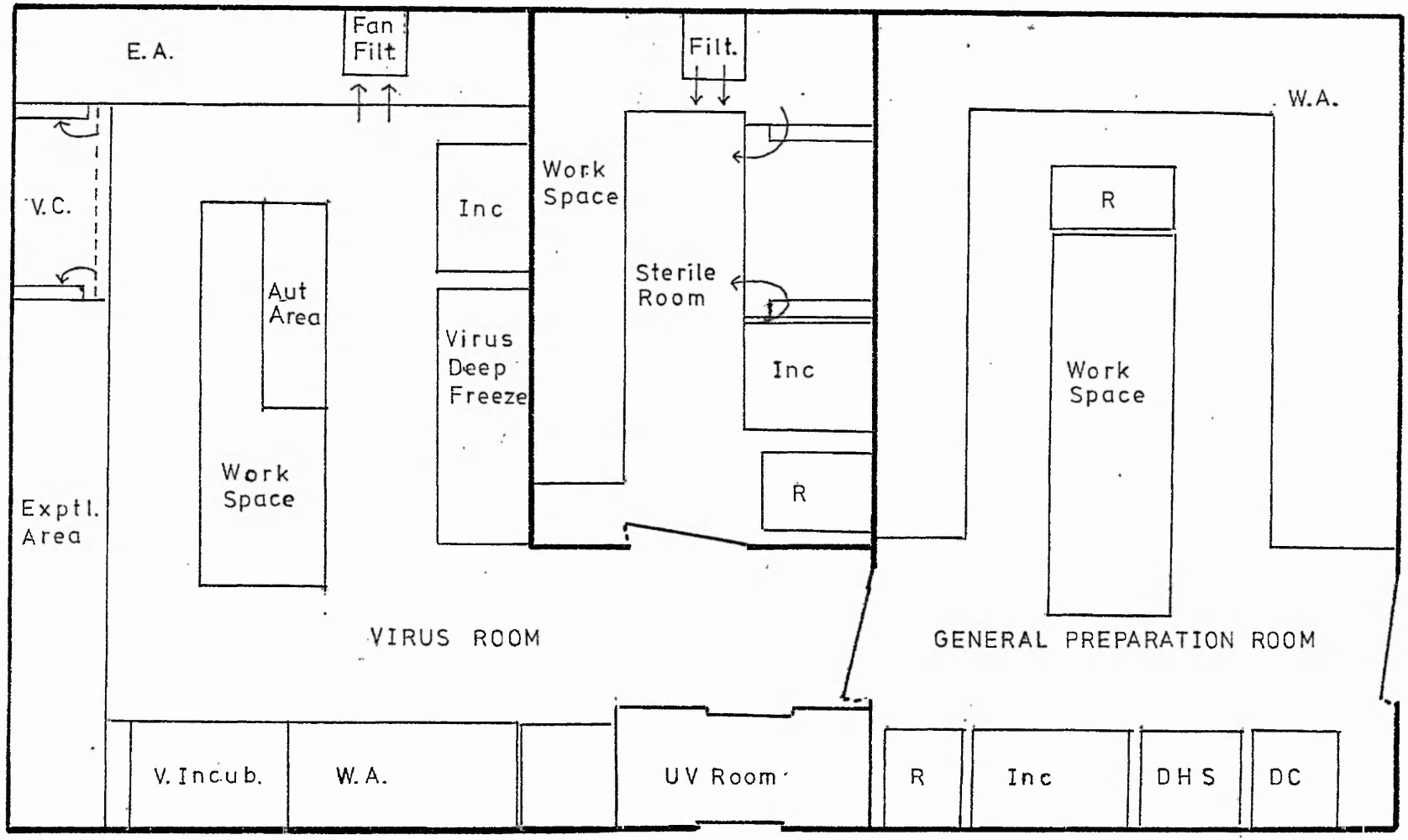
E. A.
Fan Filt
Filt.
W.A.
V.C.
Inc
Work Space
R
Aut Area
Sterile Room
Virus Deep Freeze
Inc
Work Space
Expt l. Area
Work Space
R
VIRUS ROOM
GENERAL PREPARATION ROOM
V. Incub.
W. A.
UV Room
R
Inc
DH S
DC

Production, Purification and Assay of Poliovirus.

A. Production of Host Cells.

i) Host.

The mammalian cells, Vero, Hela, Hela S3 (adapted for growth in suspension) and Hep 2, were grown routinely as monolayers in 4 oz medical flats, Roux bottles, Carrel flasks, and, in the case of Hela S3, in 250ml Erlenmeyer conical flasks as suspensions.

Host cells were bought as 100 cm^2 monolayers from GiBCo BioCult Ltd., Flow Laboratories Ltd., or were donated by the Public Health Laboratories, City Hospital, Nottingham.

Vero cell line is commonly used for virus isolation and plaque assays. It was initiated in 1962 from the kidney of a normal African Greem Monkey, Cercopithecus aethiops. The cells are a continous line, fibroblast like and exhibit rapid vigorous growth in 199 medium, tolerating a split ratio at passage of approximately 1:3, subculturing taking place between 5-7 days. The standard stock is held by the American Type Culture Collection.

Hela was the first aneuploid epithelial-like cell line to be derived from human tissue and maintained continuously by serial cell culture. It is probably the most widely used and best documented mammalian cell line available. It was isolated in 1951 from a cervical carcinoma of a negro female. When grown in minimal essential medium supplemented with 10% calf serum, they tolerate a split ratio of 1:7 - 1:10 every 5-7 days. Hela cells have been adapted to suspension culture, and one of the suspension adapted strains is Hela S3, isolated by Puck et al in 1956 (123). These cells may be grown as a monolayer but adhere loosely to the culture vessel surface.

Hep 2 cells were isolated from a carcinoma of the larynx and are a continuous cell line with similar properties to Hela. Some strains of Hela and Hep 2 do not support good growth of poliovirus until the virus has been adapted to the cell line by several passages.

ii) Growth of host.

Media for growth of the cells were obtained from GiBCo as x 10 concentrated salts. Foetal calf, newborn calf and calf serum were obtained from Flow Laboratories and from GiBCo.

Cells were incubated in growth medium at 37°C until they were confluent (usually 3-4 days), the growth medium being poured off and replaced with maintenance medium, incubation then continuing at 33°C until passage.

Vero growth medium:-

199 medium (modified) with Hank's salts x 1.

5% foetal calf serum.

50 units ml^{-1} penicillin G.

50 units ml^{-1} streptomycin.

Maintenance medium consisted of the same salts and antibiotics, but only 1% calf serum.

Hela growth medium:-

Minimal essential medium (Eagle) with Earle's salts x 1.

8% calf serum.

2% foetal calf serum.

1% 200 mM L-glutamine.

2% Non essential amino acids.

50 units ml^{-1} penicillin G.

50 units ml^{-1} streptomycin.

Hela maintenance medium had reduced (1%) calf serum. Both media were buffered with sodium bicarbonate at a final concentration of 2 g l^{-1}.

To passage the cells, media was decanted from the cell sheet and 10% trypsin (of a 2.5% trypsin in saline solution) in 199 salts pipetted on until it covered the cell sheet. The trypsin was absorbed onto the cells for 10 minutes at room temperature before being decanted and the cell sheet incubated at 37°C until the cells detached from the glass.

When the cell sheet was loosened, 8 ml of growth medium was pipetted onto the cells to completely detach them from the glass. Pipetting the cells twenty times dispersed the cell clumps. Aliquots of cells were distributed into sterile growth containers and fresh growth medium poured or pipetted to cover the cells with a few mm of medium. The bottles were shaken to disperse the cells and then incubated, on their side, at 37°C. The bottles were checked every day for growth and for possible contamination.

iii) Suspension growth.

Hela S3 cells were grown in MEM suspension medium in 250 ml Erlenmeyer conical flasks, 50 ml per flask.

MEM suspension medium:-

NaCl	68,000 mg l^{-1}
KCl	4,000 mg l^{-1}
$MgCl_2.6H_2O$	2,000 mg l^{-1}
$NaH_2PO_4.H_2O$	15,000 mg l^{-1}
Dextrose	10,000 mg l^{-1}
Phenol red	17 mg l^{-1}
Calf serum	10 %
200 mM L-glutamine	1 %
Non essential amino acids	2 %

50 units penicillin G ml^{-1}

50 units streptomycin ml^{-1}

Buffering was by sodium bicarbonate (2 g $litre^{-1}$) or by N-2-hyrdroxy-ethylpiperazine N'-2-ethanesulphonic acid (HEPES, 2%).

1ml suspension cells were taken aseptically from the growth flask, mixed with an equal volume of 1% nigrosin dye, and counted in a haemocytometer chamber. When the cell numbers had reached 1 x 10^7 cells ml^{-1}, 40 ml were withdrawn (for use in plaque assay or for seeding new flasks) and 40 ml of new growth medium added. The neck of the flask was flamed and a sterile cotton wool bung fitted every time a sample was taken or the cells passaged. The mouth was sealed with a double layer of Parafilm to provide a tight seal.

Growth of Poliovirus.

Attenuated Poliovirus type 1 (vaccine strain) was obtained from the public health laboratories, City Hospital, Nottingham.

Hela cells that had just reached confluency were seeded with 1 ml of crude lysate per medical flat. After three days, or when the cells showed marked cytopathetic effect (CPE) the bottles were removed from the incubator and the cells broken by alternatively freezing and thawing three times. The lysate was re-innoculated onto new cells and the process repeated twice to adapt the virus to the cell line.

The crude lysate was spun at 12,000 rpm in the 6 x 250 ml rotor of the M.S.E. Superspeed 18 centrifuge for 30 minutes at $4^{o}C$ to precipitate cell debris. The lysate was then assayed by the Dulbecco and Vogt plaque assay method (124) and stored at $-10^{o}C$ in 25 ml universals until required.

To grow large amounts of poliovirus, confluent Hela cells in Roux bottles were infected with virus at a multiplicity of 100 viruses per cell. After a day, or when C.P.E. was marked (shrinkage of the cell and granulation of the cytoplasm), the medium was decanted (The dicarded medium was autoclaved) and 20 ml distilled water added to the cells. The cells were frozen and thawed three times to disrupt them and the lysates from all the bottles pooled. Centrifugation at 12,000 rpm in the 6 x 250 ml rotor of the M.S.E. 18 for 20 minutes precipitated cell debris.

The lysate was stored at -10°C as 10 ml aliquots in 25 ml universals, or in 90 ml aliquots in 150 ml round screw topped bottles.

Purification of Poliovirus.

i) Polyethylene glycol two phase separation and purification.

The lysate was further purified by the polyethylene glycol dextran sulphate two phase separation method (120).

161 g of PEG 6,000 were ground in a pestle and mortar and added to 2.5 litres of lysate. 5 g of sodium dextran sulphate 500 and NaCl to a final concentration of 0.3 M (if medium lysate was used, the 0.15 M NaCl already in the medium was accounted for and added to the final concentration to make a total of 0.3 M). The lysate was then stored in a separating funnel overnight at 4°C to allow the phases to form. A bottom phase, with a volume 1/100th the original lysate was collected with the interface and the dextran sulphate removed by adding 0.7 ml of 3 M KCl g^{-1} of bottom phase. The precipitated dextran was removed by centrifugation at 2,000 rpm for 20 minutes, the viruses staying in suspension.

This supernatant was then spun in the 8 x 25 ml angle rotor of the M.S.E. Superspeed 50 at 130,000 x g for 3½ hours at 3°C to sedi-

ment the virus. The pale yellow precipitate was taken up in 20 ml of buffer A and left at 4°C until required.

ii) Density gradient separation of poliovirus I.

Purified and sedimented virus were spun in a caesium chloride density gradient to separate the different density forms (106).

0.5 g of caesium chloride were added to each gram of virus suspension. 25 ml of virus + $CsCl_2$ were balanced against two other tubes containing 50% w/w water and $CsCl_2$ and loaded into the 3 x 25 ml swing out rotor of the M.S.E. 50. Centrifugation was carried out at 125,000 x g for 48 hours at a temperature of 3°C. The rotor was allowed to decelerate without the brake and the virus tube fixed into the M.S.E. tube piercer. 60% $CsCl_2$ was pumped in from the bottom and displaced the 50% gradient which was collected from the top via a silicone rubber tube.

4 drop fractions were collected in sterile 10 ml test tubes, 5 ml sterile distilled water added to each fraction after collection. 0.1 ml aliquots were assayed for viable phage by a most probable number method. Peaks of infectivity were pooled and dialysed against 0.1 M tris at pH 7.0 The fractions were stored for further use at -10°C in 25 ml universals.

Assay of poliovirus.

Three methods of assessing the numbers of poliovirus were used, the Dulbecco and Vogt method (124), a suspended cell method adapted from Cooper (125) and a variation of the Most Probable Number method (MPN).

i) Monolayer assay.

A sample of a virus dilution in sample dilution medium was added to a confluent Hela monolayer in a 4 oz medical flat for 1 hour. Modified 199 medium or MEM plus 1.5% acetone washed agar was then

overlaid on the cell sheet and incubated for 3-4 days at 37°C. 5ml of a 20mg ml^{-1} neutral red stain was then poured over the surface of the agar and the bottles returned to the incubator (under a cloth to exclude light) for two hours. The dead, non-stained, virus infected cells were visualised as clear plaques. Each plaque, it was assumed arose from one virus.

Media preparation.

Difco Bacto agar was washed three times in distilled water, then twice with acetone. Following drying at 37°C, it was ground into a powder and made up to 3% agar in distilled water, distributed in 50ml aliquots and autoclaved at 121°C for 15 minutes. Just before use the agar was melted, cooled to 50°C in a water bath, and added to 55ml of overlay medium (at 50°C) to produce x1 concentrated overlay medium in 1.5% agar

Overlay medium.

199 salts x 10 (or MEM x 10)	10ml
Calf serum	1.5ml
Foetal calf serum	0.5ml
Sodium bicarbonate, 7.5% solution.	2ml
Pen and strep 2,500 units ml^{-1}	2ml
Distilled water	40ml

Sample dilution medium.

199 salts x 10	10ml
calf serum	1ml
Foetal calf serum	0.5ml
Pen and strep. 2,500 units ml^{-1}	2ml
Sodium bicarbonate, 7.5% solution	2ml
Distilled water	90ml
$CaCl_2.6H_2O$, 10% solution	10ml

Neutral red stain.

Distilled water	90ml
Hank's salts	10ml
Sodium bicarbonate	0.75ml
0.1% neutral red in distilled water (filter sterilised)	10ml

The neutral red stain was prepared one day before use and stored at $4^{\circ}C$ in the dark.

ii) Suspended plaque assay.

In this technique 2.5 ml of overlay medium plus 1.5% agar were poured into 1,000 mm^2 tissue culture grade plastic petri plates and allowed to solidify.

30 ml of Hela S3 suspension cells at 1 x 10^7 cells ml^{-1} were centrifuged in sterile universals in the Janetzki T32b centrifuge at 200 rpm for 5 minutes. The loosely packed cells were then made up to 3 ml with fresh suspension growth medium and incubated with 0.3 ml of a virus dilution for 30 minutes in a Techne water bath at $37^{\circ}C$, with gentle shaking. 1.5 ml of 1.5% agar (at $50^{\circ}C$) was then added, mixed with the cells and 1.6 ml aliquots quickly distributed to the pre-poured plates with an ARH automatic pipette equipped with a sterile disposable pasteur pipette fixed to the end.

The plates were then sealed with cellotape and incubated at $37^{\circ}C$ for three days before staining with neutral red stain.

iii) Most probable number method.

This method was used to judge the approximate number of viruses in a suspension.

Clean sterile 10 ml test tubes were seeded with 2 ml of mammalian cells (about 50,000 cells ml^{-1}), sealed with Parafilm and incubated at 10° to the horizontal at $37^{\circ}C$ until confluent. The growth medium

was then decanted and 2 ml of maintenance medium added together with 0.1 ml of a virus dilution. If the dilution had contained virus the cells would have become infected and showed a typical CPE (the medium would also have turned yellow with the acid products of metabolism of the normal cells, infected cells stay at pH 7.4). There would be a point at which dilution would lower the chances of viable products being added to the cells and thus an assessment to the nearest order of magnitude of virus particles could be made.

De-aggregation of Viruses.

Two methods of de-aggregation were employed, sonic vibration and dilution de-aggregation.

i) Sonic vibration.

10 ml of crude virus lysate in a universal were sonicated in an M.S.E. 100 watt ultrasonic disintegrator, the universal being immersed in crushed ice for the duration of the sonication as a precaution against heating.

A half inch probe was lowered onto the surface of the suspension and 2 mm into it. After warm up the probe was driven at 5 microns peak to peak at maximum amplitude. The drive was engaged for three periods of twenty seconds (with twenty seconds between each period of sonication), to prevent heat build up in the virus suspension.

ii) Dilution de-aggregation.

1 ml of crude or purified phage was pipetted into 99 ml of sterile distilled water and left for 12 hours at $4^{o}C$. This method was evolved from an observation by M.Hawkes (126 personal communication) that when bacteriophage lysate was pipetted into a large volume of tap water, the titre was higher than was expected, sometimes by a factor of two.

Distribution of aggregates were studied in the electron microscope and aggregated samples exposed to UV for target curve analysis.

Unless otherwise stated, all suspensions of virus used for irradiation by UV and other methods, were de-aggregated by 1/100 dilution in distilled water overnight at $4^{o}C$.

Electron Microscopy.

Viruses, on a carbon filmed G400 copper grid, negatively stained with 2% phosphotungstic acid, were viewed with an A.E.I. EM 802.

i) Preparation of carbon films.

Clean microscope slides were dipped into a 0.2% solution of Formvar (Polaron Ltd.) in chloroform. When dry the plastic film was cut with a razor and floated onto the surface of dust free distilled water. Copper G400 grids were placed dull side down onto the film which was then picked up with Parafilm. The grids were then placed in a Nanotech coating unit, after being picked off the Parafilm with forceps.

A piece of white tile with a drop of Piezzon oil on it was also placed in the coating unit near the grids. The unit was evacuated and at 10^{-5} torr, an arc was struck across two carbon electrodes, which evaporated carbon onto the grids. The oil prevented carbon sticking to the tile beneath it and gave a comparison to the build up of carbon on the rest of the tile. The arc was stopped when the carbon was a uniform silvery grey. The carbon/Formvar films were then placed on a steel mesh (film side up) and the Formvar dissolved with chloroform. The carbon film was left in contact with the copper grid.

ii) Preparation of specimens.

Virus suspensions were dried from a small drop on a carbon filmed grid. When just dry the grid was rinsed three times with distilled water to remove low atomic weight salts that would interfere with the stain. 2% phosphotungstic acid at pH 7.4 was applied as the stain, a small drop just wetting the surface. The stain was dried and the specimen loaded into the microscope. Viruses appeared white against a dark background.

Results and Discussion.

Calibration of Sources.

i) Potassium ferrioxalate actinometry.

The production of ferrous ions in the actinometer by UV was measured by the optical density of the phenanthroline complex at 510 nm. The value was compared to the optical density of known concentrations of ferrous ions, which were plotted on a graph. Fig. 22 shows this calibration curve from which all values were computed. Fresh calibration curves were completed from time to time during the experiments, but the values obtained did not deviate substantially from the values shown on the graph.

ii) Calibration of the 254 nm Surface Steriliser.

The actinometer method was compared to the value obtained by the Paragerm Pocket Dosiometer. Results of this comparison, reproduced in Table 8 below, show that the two methods gave the same result and that the production of ferrous ions in the actinometer solution was linear with time.

Table 8. Calibration of Surface Steriliser.

Secs.	OD 510nm	uM Fe^{++}	ergs	ergs mm^{-2} sec^{-1}
0	0.00	0	0.0	0
5	0.042	0.1	4.3×10^5	101
10	0.08	0.2	8.6×10^5	100
20	0.15	0.5	18.7×10^5	109
30	0.245	0.8	29.9×10^5	116
50	0.45	1.1	41.1×10^5	96
70	0.48	1.6	59.8×10^5	99
90	0.73	2.34	87.0×10^5	113

The meter reading throughout was 1mW cm^{-2} (100 ergs sec^{-1} mm^{-2})

Figure 22.

Calibration Curve, Actinometry. μMoles Fe^{++} Against O.D. 510nm.

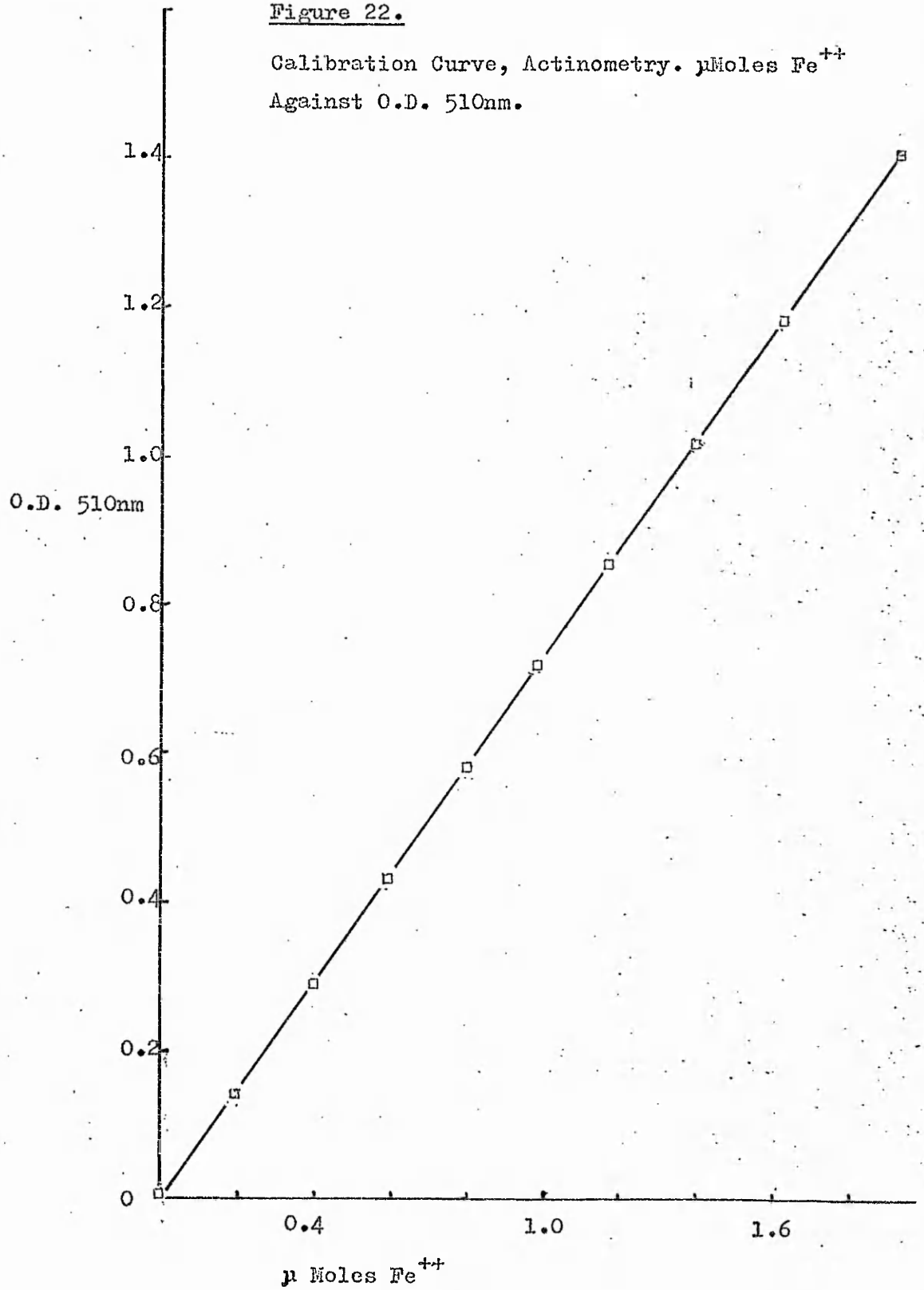

iii) Calibration of the British Rail UV Steriliser.

The output of the flow-through steriliser was determined by actinometry. Two flow rates were used, 1,400 ml min^{-1} and 700 ml min^{-1}. The results of this calibration are shown in Table 9, below.

Table 9. Calibration of UV Output of the British Rail Steriliser.

Flow rate ml min^{-1}	$\mu M\ Fe^{++}$ ml^{-1}	ergs ml^{-1}	Total output Watts
1,400	0.35	1.308×10^6	3.05
1,400	0.35	1.308×10^6	3.05
700	0.75	2.8×10^6	3.2
700	0.75	2.8×10^6	3.2

At a flow rate of 1,400 ml min^{-1}, 1.308×10^6 ergs were absorbed per ml of actinometer. There were 3,000 ml in total volume and each ml = 1 c.c = 100 mm^2 in cross section (assuming little absorbance).

$1.308 \times 10^6 \times 3{,}000 = 3.924 \times 10^9$ ergs.

These were produced over 2.14 min (the contact time of the actinometer in the steriliser), or 128.57 sec, so:-

3.924×10^9 ergs/128.57 sec = 3.05×10^7 ergs sec^{-1}

Since 1×10^7 ergs = 1 Watt,

3.05×10^7 ergs = 3.05 watts.

The total output of the lamp at 3.05 watts shows an output/input ratio of 1:5. The normal output of a 15 watt UV lamp is usually about 1/7 of the input energy, or about 2 watts. British Rail figures for the ageing of UV tubes (127) show that for the first 20 hours the output of the lamp is higher than the rest of the life of

the lamp. The output drops to 60% of the initial value after 48 hr and gradually falls off to 40% over 3-4,000 hr. The value obtained for this source is what one would expect for a new lamp.

iv) Inactivation of Bacteriophage QB in the British Rail UV Steriliser.

An experiment was carried out to determine the efficiency of the unit to inactivate viruses. The dose of 3.05×10^{7} ergs sec^{-1} is radiated over a surface area of 1,850 cm^{2}, and is therefore equal to 1.65×10^{4} ergs cm^{-2} sec^{-1}, or 1.65×10^{2} ergs mm^{-2} sec^{-1}. (Assuming no absorbance over the 4.75 cm path length between the lamp and the steriliser wall. Since in use the steriliser is filled with water taken from the public supply, little absorbance will occur).

Acceptable water treatment depends on the load of organisms present, but a general figure used in the water industry is a 99.9998% inactivation. As there is about 90% inactivation for every 1,300 ergs mm^{-2} (based on data given later in results) a contact time of 44 secs is needed, or a flow rate of 4,100 ml min^{-1}. Operation at a faster flow rate than this would not achieve what is normally regarded as an adequate treatment for a primary source. In the case of this steriliser the designed flow rate is about 6 litres a minute, which gives a contact time of 30 secs. While this is more than adequate to treat bacterial contamination, a reduction in the virus load of 99.99% would be expected.

20 litres of 1×10^{8} pfu ml^{-1} phage (the greatest amount that could be grown for the experiment) were irradiated in the steriliser at a flow rate of 1,400 ml min^{-1}. This is a contact time of 128.5 secs and a dose of 21,202 ergs mm^{-2}. A reduction of 10^{-16} could be expected from this dose. When 8 0.1 ml samples were assayed by the

plaque technique, no survivors were detected. A faster flow rate than 1,400 ml min^{-1} could not be achieved at the time of the experiment because a larger flow meter was not available. To fully test the efficiency of the steriliser a much faster flow rate of 4-6 litres a minute with 1 x 10^{8} pfu ml^{-1} should be used to get accurate figures of inactivation.

As previousely stated, operation at 6 litres a minute should result in the reduction of the virus population by 99.99%, only giving 10^{-4} reduction instead of the recommended 2 x 10^{-5} reduction.

This does not mean that the quality of the water from the unit is unsafe in any way - the unit is only giving secondary treatment to tap water which has already been treated and therefore does not represent any hazard, other than contamination occuring when the water is transferred to the reservoirs on the restuarant cars.

Other factors in this treatment should also be taken into account, the dose above does not include any correction for reflection from the steriliser walls, and if reflection does occur a higher dose would be given to the water. If the steriliser were painted with aluminium paint then there would be about 60% reflection from the walls and the dose would be 264 ergs mm^{-2} sec^{-1} (if the steriliser had polished aluminium walls the reflectance would be higher. In the case of the production model, made out of stainless steel, the reflectance would be 25% at maximum). Only 25 secs would be needed for 99.998% inactivation, or a flow rate of 7.5 litres per minute, which means that a satisfactory inactivation would be achieved.

It must be noted that even in sewage effluent there are only about 400 pfu ml^{-1} pathogenic viruses (128), and therefore given the most contaminated water, adequate treatment of the viruses would be

given by a flow rate of 5 litres min^{-1}. As bacteria are about ten times as sensitive to UV than viruses, a dose of 2,000 erg mm^{-2} (a flow rate of about 9 litres min^{-1}) would inactivate 10^{10} bacteria ml^{-1}. It is concluded that the British Rail steriliser is efficient in producing a microbiologically safe water supply.

v) Calibration of the deuterium lamp output from the monochromator.

The deuterium lamp gave a continuous spectral output of UV from 180nm to 450nm, most of the output being between 245nm and 300nm.

The source of UV was an arc 1 mm across. A short arc source is ideal for use in conjunction with a monochromator as the condenser lens can capture a lot of the output, and as the light originates over a small area, uniform illumination within the monochromator can be achieved.

The output from the monochromator at different wavelengths was measured by actinometry, as described in methods. Typical outputs are shown in Table 10, below.

Table 10. Output of the monochromator with the deuterium source.

Wavelength, nm.	ergs mm^{-2} sec^{-1}
200	0.000
210	0.001
220	0.005
230	0.007
240	0.015
250	0.018
260	0.023
270	0.014
280	0.015
290	0.009

These outputs were very low, and involved exposing the actinometer for periods of up to 24 hours. To achieve 99% inactivation with this source would involve exposures of up to 48 hours at the less efficient wavelengths as the output was so low. Because of the danger of leaving the equipment unattended, because of fire risks, this was considered impractical and a higher powered source chosen.

(99% inactivation was desired because it was thought that this gave readings over a sufficiently long inactivation to give accurate data. Any longer inactivation would run into the biphasic resistant part of the inactivation (see later in the results), which would give different values.)

vi) Output of the 250 watt medium pressure mercury lamp.

The 250 watt discharge lamp from Osram G.E.C. Ltd was used to achieve the required higher outputs of UV. The greatest outputs from this lamp were at the spectral emission lines of the mercury spectrum, although the 194.2 line was not seen, probably due to self absorption by the carrier gas in the lamp. Typical outputs are shown in Table 11, below.

Table 11 Output of the monochromator with the 250w mercury lamp.

Wavelength, nm	ergs mm^{-2} sec^{-1}
222.5	0.2
238.7	0.46
248.3	0.38
253.7	0.64
265.2	0.32
275.3	0.13
280.4	0.25

Table 11 cont.

289.4	0.16
296.7	0.54
313.0	0.79
367.0	0.63

These outputs were much higher than those of the deuterium lamp, but exposures of up to 4 hours were needed for 99% inactivation. It was felt that still shorter inactivation times would be advantageous to cut down temperature effects during exposure and also to study inactivation during the second, more resistant part of the curve, (see later).

vii) Output of the 250 watt very high pressure lamp.

The high pressure lamp, although having the same wattage as the medium pressure lamp had a short arc, which in theory should enable a larger amount of the output to be captured by the condenser lens and the arc should have been able to have been imaged within the monochromator. The outputs at different wavelengths were measured by actinometry and typical outputs are shown in Table 12, below.

Table 12. Output of the monochromator with the 250w high pressure mercury lamp.

Wavelength, nm.	ergs mm^{-2} sec^{-1}
200	0.00
222.5	0.08
230	0.05
238.7	0.2
248.3	0.24
253.7	0.12
265.2	0.31

Table 12 cont.

275.3	0.06
280.4	0.14
289.4	0.06
296.7	0.47

These outputs were lower than for the medium pressure lamp and the output of the intermediate outputs (between the peaks) were too low to be of practical use. The spectral lines had been flattened and more UV had appeared in the intermediate wavelengths, this had reduced the power at the peak wavelengths. Another source was needed to provide the necessary output of UV.

viii) Output of the 250 watt medium pressure lamp driven at 750 watts.

Increasing the power through the lamp increased the output of UV. The increased power also increased the amount of heat output, which without cooling could rapidly rise to above 1,200^{o}C and melt the quartz envelope. The aluminium reflector was melted too without a cold air fan. Cooling increased tube life to about twenty hours. Table 13 shows that the output from the monochromator using this lamp is about 2.5 times the output from the normal 250w lamp.

Table 13. Output of the monochromator with the 250w medium pressure lamp driven at 750w.

Wavelength, nm.	ergs mm^{-2} sec^{-1}
222.5	0.5
238.7	1.15
248.3	0.95
253.7	1.6
265.2	0.8

Table 13 contd.

275.3	0.32
280.4	0.6
289.4	0.4
296.7	1.3

This lamp was then used for a number of experiments.

One reason for building a powerful monochromator would be to study lethal photoproduct production formed at different wavelengths. For this one needs enough material for analysis. At the present time only those photoproducts formed at 254nm in vivo and vitro have been investigated thoroughly as powerful sources are available at this wavelength. An interesting region to study in terms of lethal photo-products would be between 180 and 210nm. It is usually assumed that inactivation at these wavelengths is caused by absorption and damage to protein, but the degree of inactivation and type of inactivation (one hit curves) argue that there is some involvment with the nucleic acid. The problem is to produce enough power at these short wavelengths The lamps used in this study do not produce significant amounts of UV in the short wavelengths, probably due to absorption of the short wavelengths by the carrier gas.

ix) Output of the 2 kilowatt medium pressure lamp.

A 2 kilowatt medium pressure lamp from Osram G.E.C. was tested to see if it gave any increase in power over the 250w, 750w driven lamp. Tests over a few wavelengths did not show much increase in output. This was probably due to the lamp being much larger than the 250w lamp and although the total flux was greater, the output per steradian was only a little higher.

Figure 24 shows the output characteristics of the sources used

with the monochromator. The spectral outputs come from data sheets published from Bausch and Lomb and Osram G.E.C. Ltd. The relative intensities of the sources have been plotted from the output data above.

Figure 24.

Spectral outputs of UV sources, deuterium, medium pressure mercury and high pressure mercury.

Values plotted Tables 10,11,12 and 13. Intermediate values interpolated from data published by Bausch and Lomb and Osram G.E.C. Ltd.

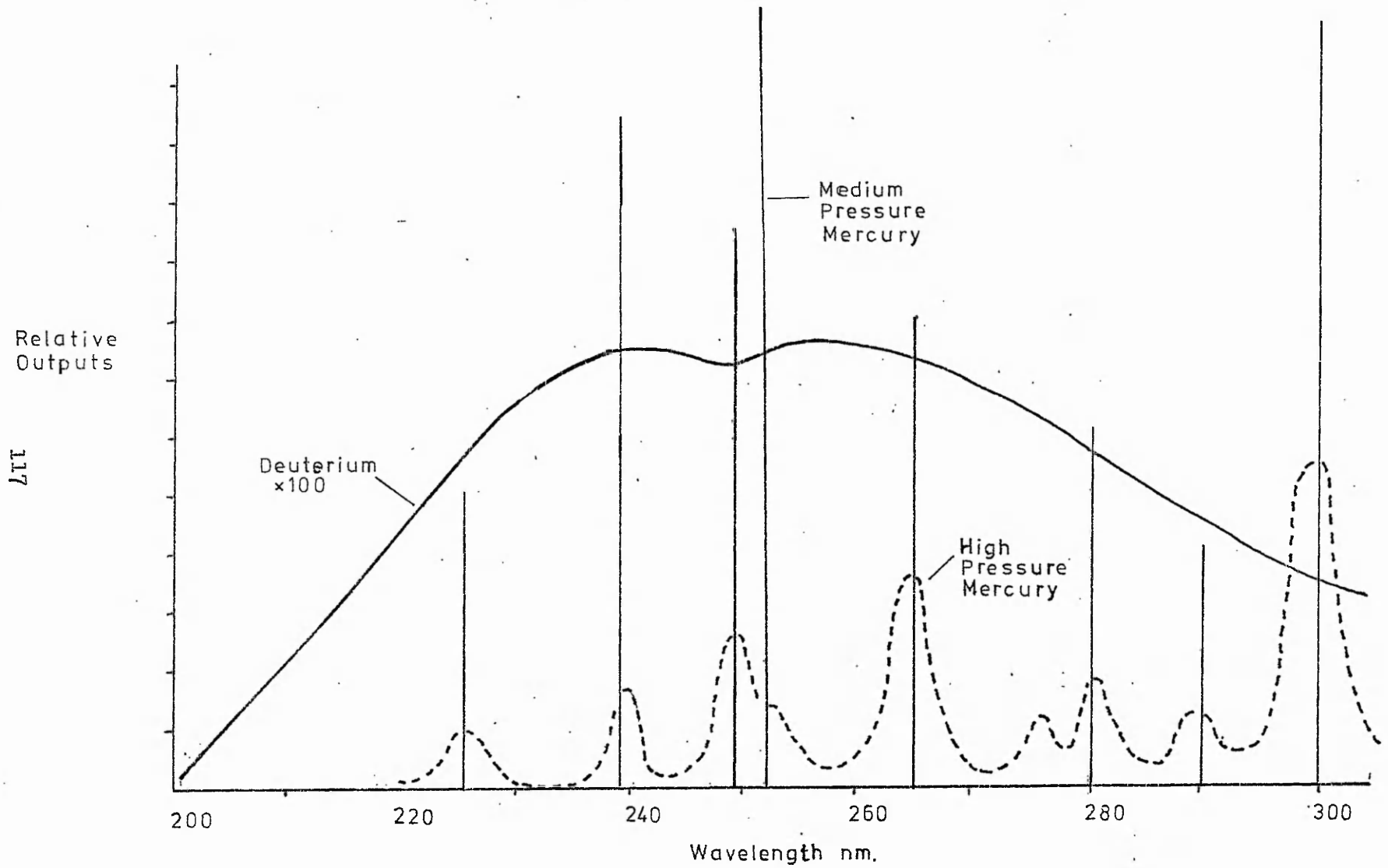
Relative
Outputs
Medium
Pressure
Mercury
Deuterium
×100
High
Pressure
Mercury
200
220
240
260
280
300
Wavelength nm.

Production of Bacteriophage.

A. Selection of Host.

Host, selected by the replica plaque technique described in methods, was tested for its ability to plate out phage plaques against the original culture. Six replicates for each host of the same 10^{-8} dilution of an MS2 lysate were plated out in the plaque assay system, the results of which are shown in Table 15 below, together with results from other lysates.

Table 15. Comparison of hosts' plaque forming ability.

plaques standard host			plaques selected host		
10^{-8} dilution lysate A					
30	31	33	37	36	38
35	29	33	39	37	36
Av.	31.8			37.1	
10^{-9} dilution lysate B.					
42	46	44	51	51	52
44	44	45	49	53	50
Av.	44.16			51	
10^{-5} dilution lysate C					
131	129	124	152	153	154
133	137	133	156	155	154
Av.	131.16			154	

These results show, rather suprisingly, that the selected host was, on average, 16% more efficient in plaqueing than the standard host. Perhaps because the selected host was selected on the basis of high stability of its F factor, it contained more than one F pilus (the loss of one F factor would still leave it susceptable to male

specific bacteriophages),the possession of two would increase the chances of attachment by increasing the surface area of sex pili.

B. The Concentration of MS2 by Ammonium Sulphate Precipitation.

3 litres of MS2 lysate were titred at 2 x 10^{11} pfu ml^{-1} before being precipitated by ammonium sulphate (6 x 10^{14} pfu in total). After precipitation 75 ml of virus were recovered at 1.2 x 10^{12} pfu ml^{-1} (9 x 10^{13} pfu)and therefore 83% of the viruses were not recovered. Other precipitations gave 1-10% recovery. This method, although it concentrates virus material, inactivates too many for it to be a useful technique in studies on active phage.

C. The Concentration of MS2 by Acetone Precipitation.

A pilot experiment was carried out to determine the efficiency of this technique. 10 ml of a 3.4 x 10^{9} pfu ml^{-1} lysate of MS2 was mixed with 10 ml of analar acetone at -10°C. The precipitate was collected by centrifugation at 5,000 rpm in a 25 ml universal and the supernatant pipetted off. The precipitate on the walls and at the bottom of the bottle was taken up into 1 ml of distilled water and assayed. 3.35 x 10^{10} pfu ml^{-1} were recovered, which represents 98% of the total number of active viruses.

Larger scale precipitation gave a recovery of 95% from 1 litre but the large volumes of suspensions were difficult to handle.

D. Polyethylene Glycol Two Phase Concentration and Purification of MS2.

2 litres of lysate containing 1.3 x 10^{13} pfu ml^{-1} MS2 were purified and concentrated by the polyethylene glycol two phase system. 20 ml of suspension was recovered and found to contain 1.23 x 10^{15} pfu ml^{-1}. This is a recovery of 95% and a volume concentration of x 100. This method was found to be ideal for the production of phage.

The Inactivation of MS2 by Ultra Violet Light.

A. Choice of Depth of Irradiation Suspension.

The absorbance of the medium which contains the viruses affects the amount of UV that reaches them and hence affects their susceptability. If the medium is highly absorbant and the path length of the UV is such that most of the UV is absorbed, viruses will not be inactivated. If the path length is very short, the absorbance of the medium will not be of great significance.

The lysates of bacteriophage were usually in nutrient broth, which because of its high protein content, had a high UV absorbance (O.D. 254nm 30) and would have affected death rates. Figure 25 shows the absorbance of a 10^8 pfu ml^{-1} lysate of MS2 in neat nutrient broth and in a 1/100 dilution of nutrient broth in distilled water, over wavelengths between 200nm and 300nm. There is little absorbance at 253.7nm by the 1/100 diluted nutrient broth, but absorbance rises sharply at 230nm. If the medium were absorbing enough UV to affect the death rates, differing depths of suspension would show different rates of inactivation, deeper suspensions being more resistant. The study of the effect of depth of suspension was also important to remove any bias in the system used for inactivating viruses that might affect inactivation rates.

Lysate volumes of 0.5,1,2,3,4 and 5 ml in 1,000 mm^2 plates were used (representing depths of 0.5-5 mm). Figure 26 shows the results of irradiating a virus suspension at these depths and shows that there is no difference in inactivation over these depths. It is concluded that in the system used, 1/100 dil lysate does not absorb significant amounts of UV to affect the rate of inactivation at 253.7nm.

Figure 25

Absorbance of nutient broth MS2 lysate and 1/100 lysate in distilled water over 200nm - 300nm. Optical density against wavelength.

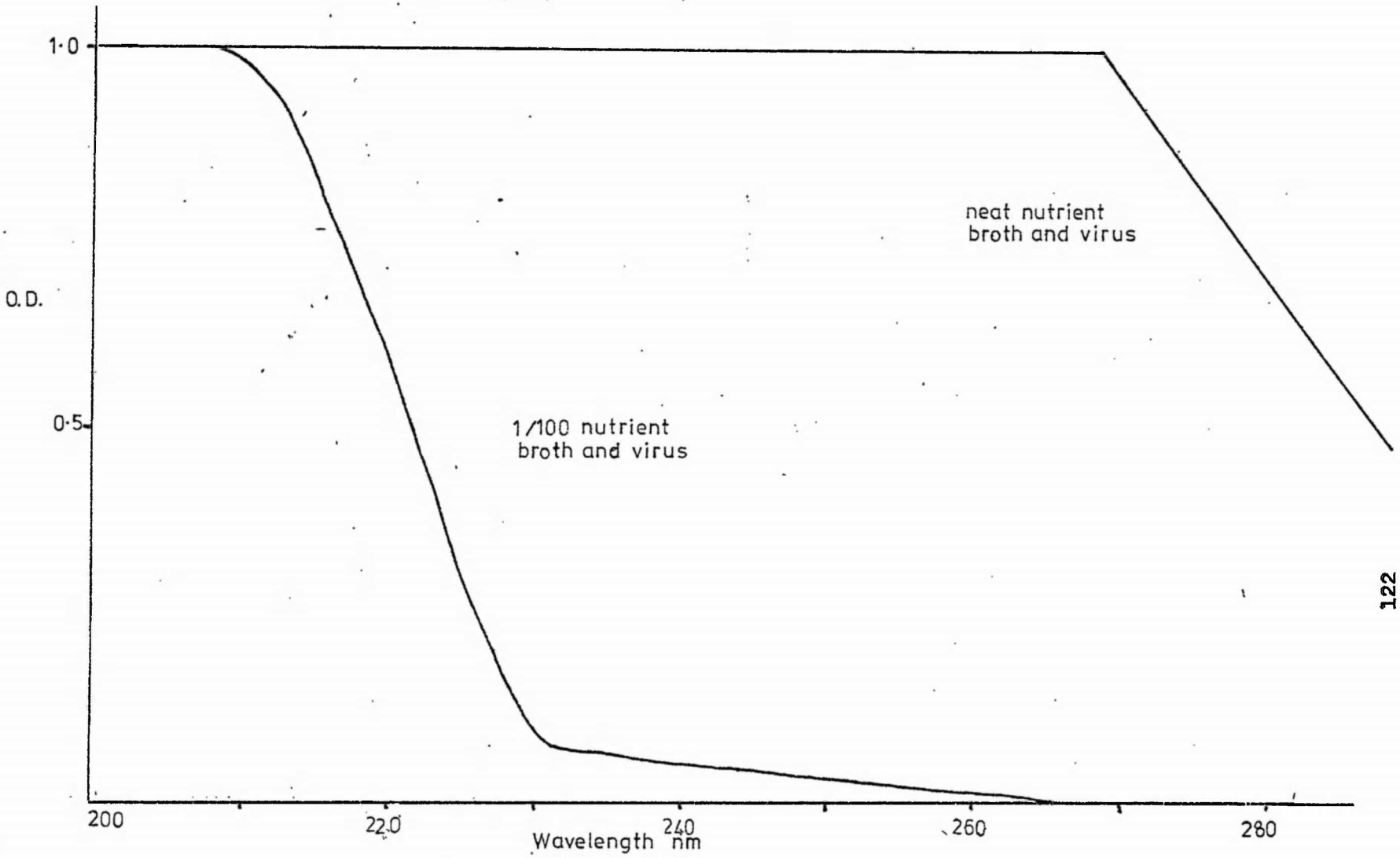
1·0
0·5
O.D.
neat nutrient
broth and virus
1/100 nutrient
broth and virus
200
220
240
260
280
Wavelength nm

Figure 26.

The effect of suspension depth on the inactivation rate of MS2 by 253.7nm Ultra Violet light.

0 0.5 mm

X 3.0 mm

□ 5.0 mm

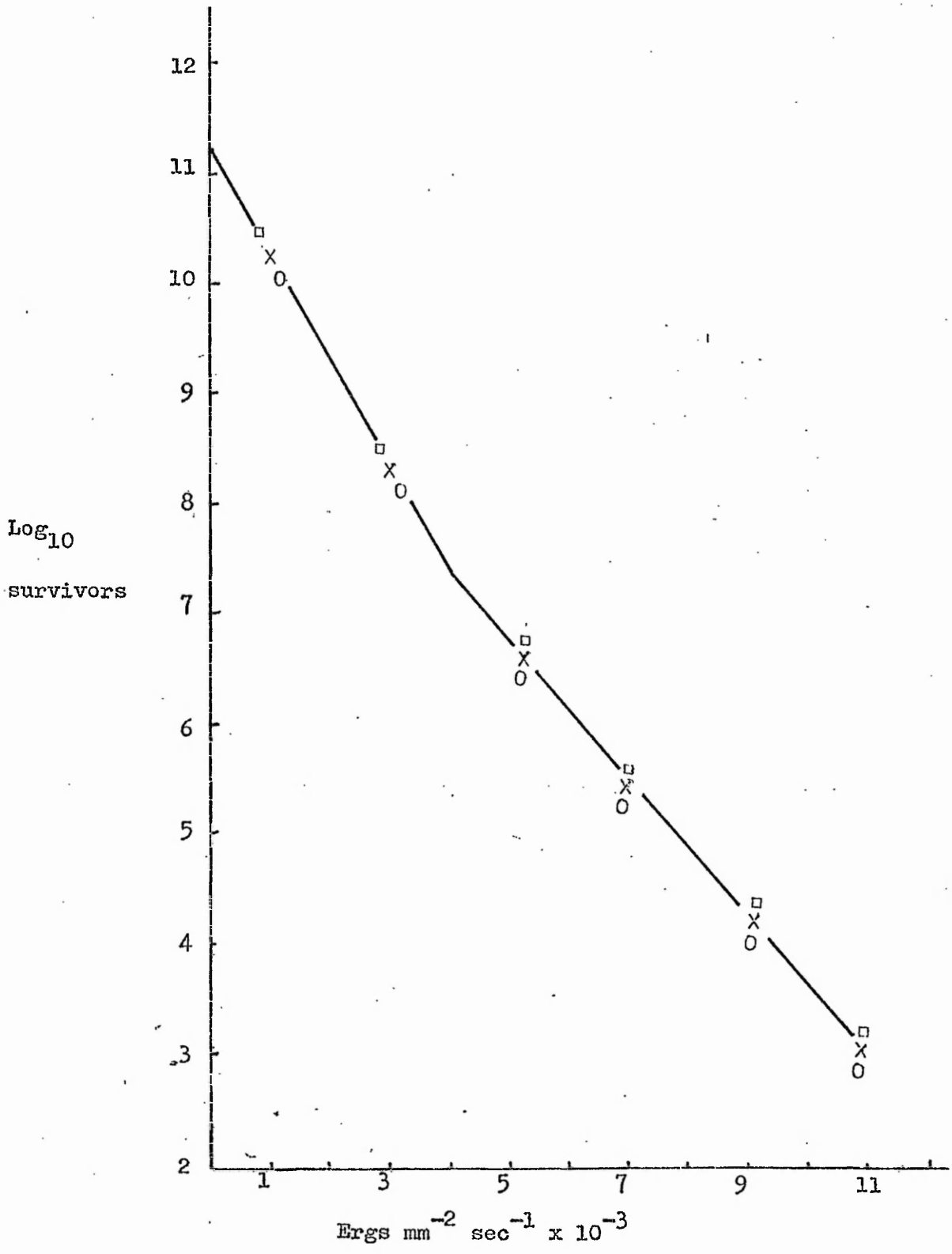
Log10
survivors
12
11
10
9
8
7
6
5
4
3
2
1
3
5
7
9
11
Ergs mm-2 sec-1 x 10-3

Since there is no difference between different depths of suspension between 0.5 mm and 5 mm, choice of a suspension depth depended on the amount of material needed for assay. It was decided that 0.1 ml samples were to be withdrawn from the suspension at various time intervals and that a sufficient volume of suspension should remain to ensure adequate coverage of the dish and efficient mixing of the remaining suspension. Ten samples were withdrawn from a 2 ml suspension as this reduced absorption if any should occur in later experiments and still gave a large enough volume for representative sampling.

B. Effect of Aggregation.

Aggregates of viruses can occur in crude preparations of virus stocks and highly purified and concentrated preparations, as in the sedimentation of viruses in the ultra centrifuge. Aggregation is known to affect the susceptability of viruses to UV (42,43) and has two effects on the UV sensitivity of viruses.

Firstly, several targets are presented, each of which needs to be inactivated before the complex as a whole is. This means that there will be a lag in inactivation, multi hit kinetics.

Secondly, when an aggregate enters a cell, this can, in some cases, lead to multiplicity of infection. If multiplicity reactivation operates the genomes can co-operate and recombine to synthesise fully active viruses.

This type of multiplicity reactivation is different in quality to the multiplicity reactivation described by Abel (42). In the system she worked on, reactivation depended on the size of the cell (if the virus replicates in the cytoplasm). In a small cell two independantly replicating viruses might set up foci near to one

another and take part in recombinational events. On the other hand in a large cell the foci might be too far apart for genetic material to come together. Therefore reactivation is dependant on the size of the cell and the number of infecting viruses per cell.

In an aggregative system reactivation is only dependant on the number of viral particles in each aggregate as they will automatically set up a common focus of infection.

Galasso and Sharp (43) demonstrated this phenomenon with Vaccinia when they showed that increasing aggregation led to an increasing resistance to UV. This resistance was combined with a shoulder on the curve to give'straight' exponential inactivations of differing slopes, as shown in Figure 27.

This distinction between MR caused by single and MR caused by aggregated viruses is important when considering the effects of UV on viruses. The researcher terms reactivation with aggregates 'aggregative multiplicity reactivation' to distinguish it from ordinary MR.

Since aggregates are important (because they affect response to UV), it is necessary to remove them or de-aggregate them. Many factors affect the degree of aggregation, amongst which are pH, the presence of particles (especially cell debris) and the concentration of salts.

Various methods of de-aggregation were tried with MS2, pH change (which probably alters the surface charge of the capsid), sonic vibration and dilution of the salts involved in aggregation.

a) Alteration of pH.

Virus stocks in nutient broth at pH 7.0 were brought to pH 4.0 by the dropwise addition of conc. HCl. Table 16 shows the results

Figure 27.

Effect of aggregation on UV inactivation of Vaccinia virus. (From Galasso and Sharp,43).

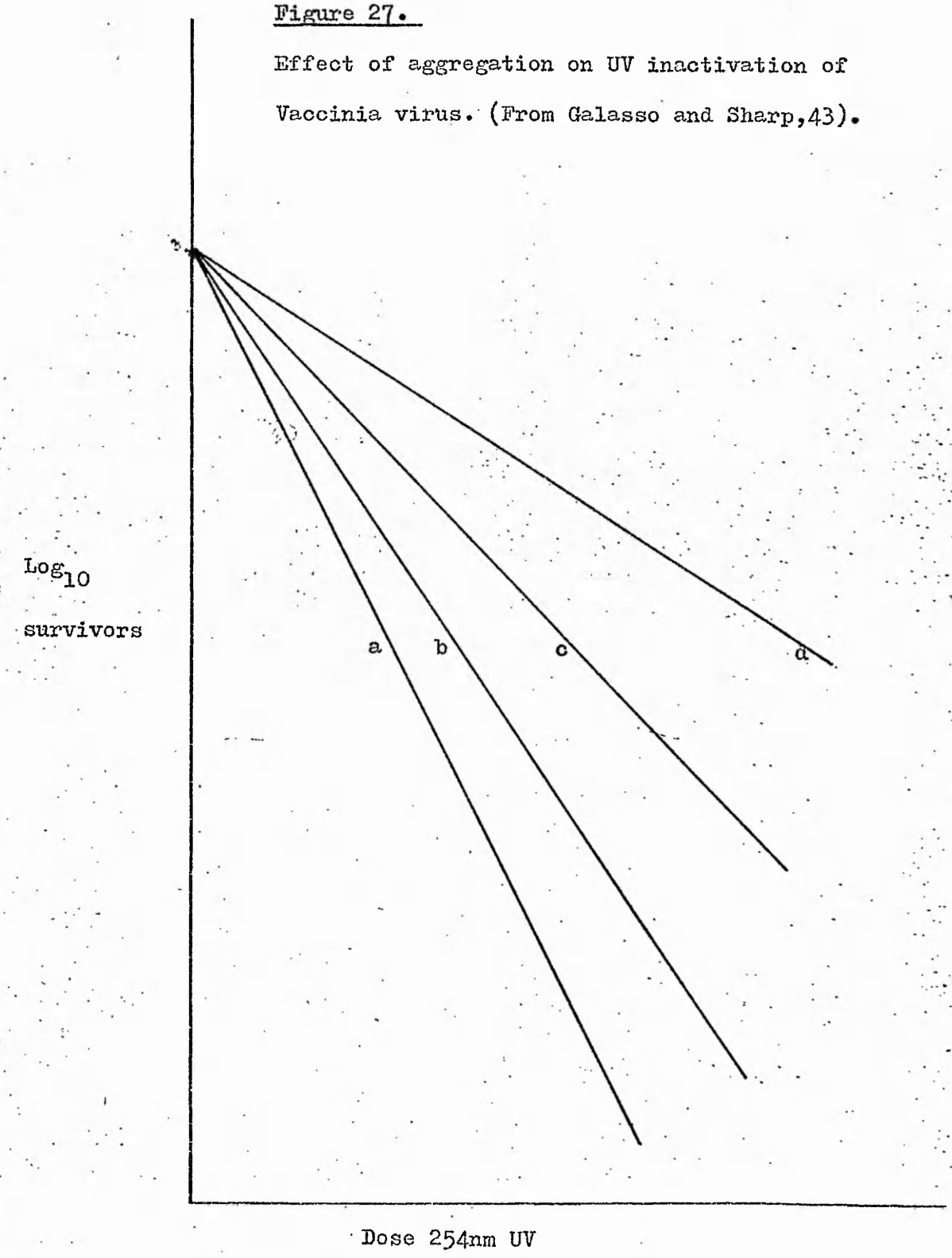

a un-aggregated virus

b,c,d, increasing aggregation of virus

of two experiments in which pH was used as a de-aggregant.

Table 16.	Effect of pH as a De-aggregant.	
Titre	30 min pH 4.0	4 hr pH 4.0
7.7×10^{10}	7.8×10^{10}	7.76×10^{8}
8.5×10^{10}	8.3×10^{10}	8.1×10^{8}

These results are also shown in Figure 28. Although acid conditions probably de-aggregated viruses, they also inactivated them, titres dropping 100 fold in 4 hours. It can be seen that there is a lag in inactivation. What might have happened is that inactivation occured at a constant rate, but at first de-aggregation increased the number of particles, so that a lag in inactivation was the overall result.

If the exponential part of the pH inactivation curve is extrapolated back to the ordinate, an extrapolation number of two is obtained, which is in agreement with the average number of aggregates shown later in results.

b) Sonic Vibration De-aggregation.

Several authors have described the use of ultra-sonic vibration to disrupt the aggregates (35,43). MS2 was sonicated three times at maximum amplitude for twenty second bursts. Table 17 and Figure 29 shows the results of this treatment. There was a slight rise in titre followed by a rapid loss of activity. It does not appear that inacti vation occured at a constant rate,against the rise in titre due to the aggregates dispersing, a lag in inactivation for the first few seconds was then followed by a rapid inactivation. It would be interesting to follow inactivation by sonication on de-aggregated viruses to look at the kinetics of the process. Inactivation by sonic vibration might not just be due to disruption of the particle

Figure 28.

The Effect of pH on the De-aggregation of MS2.

(Table 16 shows more results)

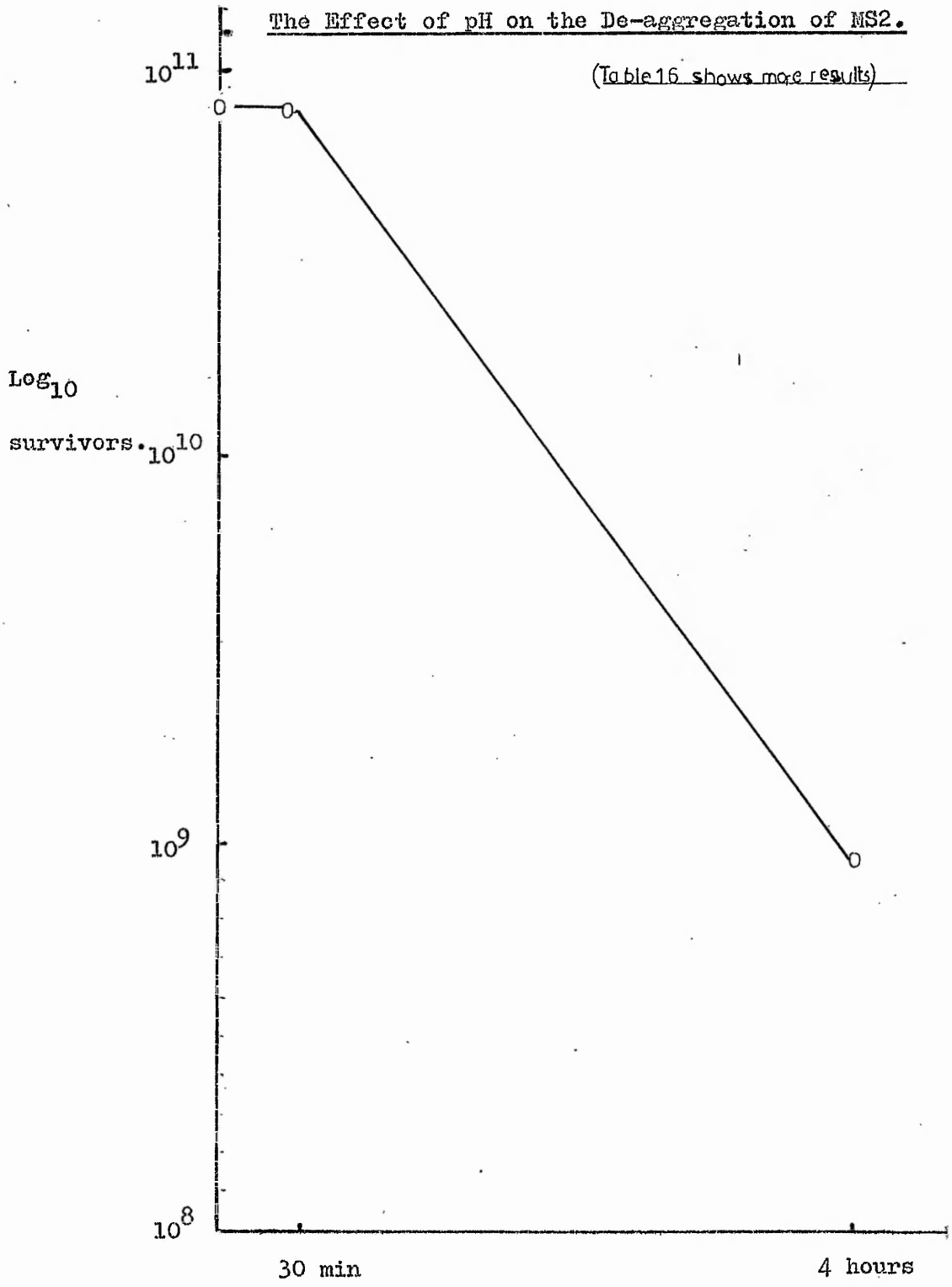

Figure 29.

The Effect of Sonication on the De-aggregation of MS2.

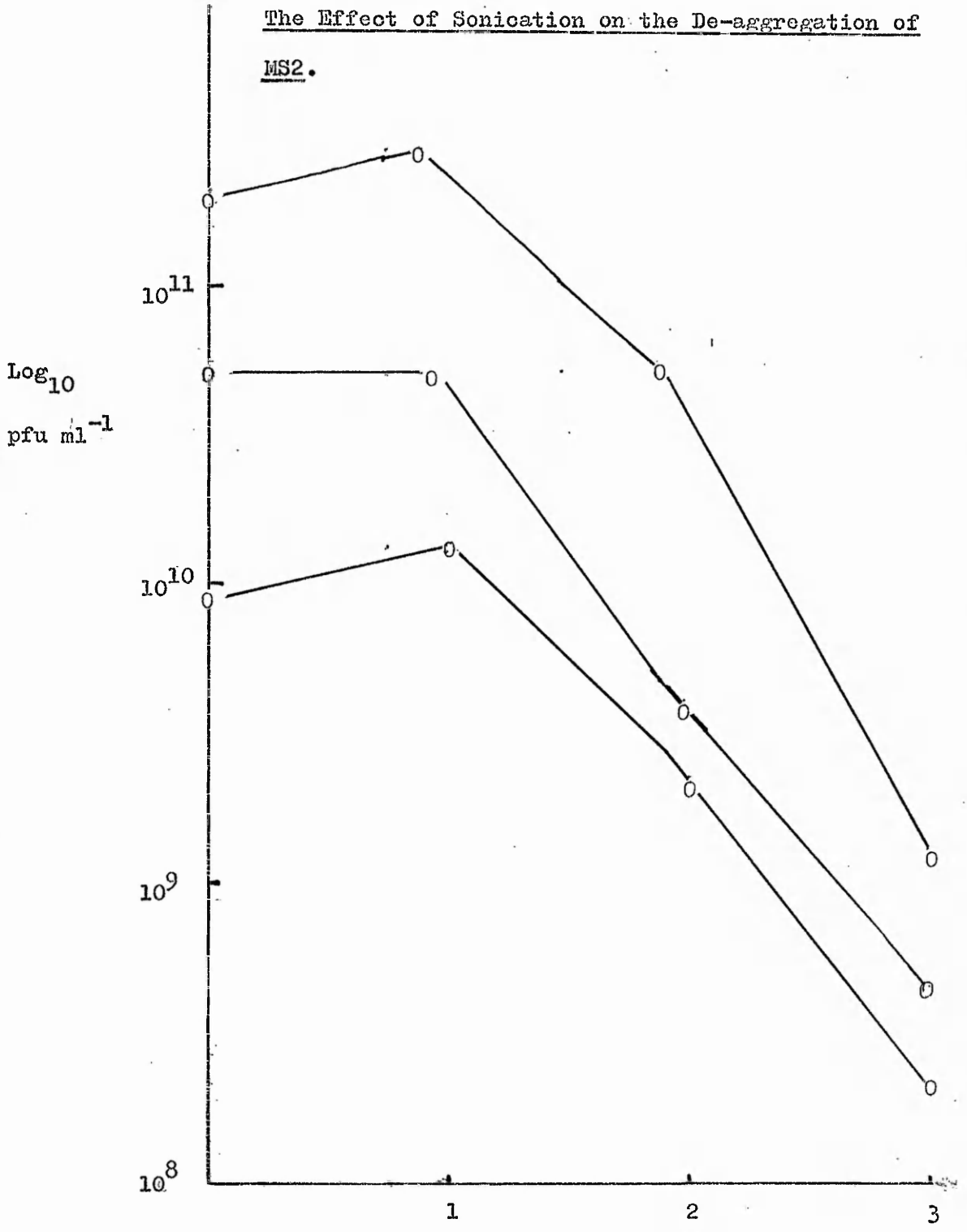

Table 17.	Effect of Sonic Vibration as a De-aggregant.		
No.	1st sonication	2nd	3rd.
9.2×10^9	1.3×10^{10}	3×10^9	2×10^8
6.5×10^{10}	6.2×10^{10}	3.5×10^9	4.6×10^8
2.1×10^{11}	3.7×10^{11}	4.7×10^{10}	1.3×10^9

but also due to a rise in heat, causing inactivation.

c) De-aggregation by Dilution.

An observation by Hawkes (personal communication, 126) that a suspension of MS2 inoculated into a large volume of tap water gave a higher titre than expected indicated that dilution could de-aggregate viruses. To test this observation, viruses were diluted into:-

i. 1/10 distilled water.

ii. 1/100 distilled water.

iii. 1/1000 distilled water.

iv. 1/1000 nutrient broth.

v. 1/1000 phosphate buffered saline.

Table 18 below shows the results of overnight dilution into these solutions at $4^{o}C$.

Table 18.	Dilution De-aggregation, Effect of Different Diluents.				
No.	i	ii	iii	iv	v
3.4^{10}	4.1^9	7.14^8	5.5^7	3.5^7	3.35^7
			(upper index figures are powers of 10)		
Degree of de-aggregation.					
	1.2	2.1	1.6	0	0

Dilution 1/10 into distilled water did not give as good a dissociation as into 1/100 distilled water. Dilution into 1/1000 distilled water

did not give as good a rise in titre as 1/100 dilution, over two days the titre had dropped to 2.1×10^6, which showed a rapid inactivation, while the 1/100 dilution remained stable. Dilution into nutient broth or saline did not result in any de-aggregation. It was concluded that it is not reduction of the virus numbers per ml that de-aggregates, but rather the reduction in the salts necessary for stable aggregation. Other work by Hawkes (to reported elsewhere) has shown that the salts involved are probably divalent cations. Table 19, below shows the results of further dilution de-aggregation experiments, 1/100 into distilled water.

Table 19. Effect of Dilution 1/100 into Distilled Water on Aggregates of MS2.

No.	Dilution at 4°C.	x 100 (correction for dilution)	Fraction rise.
1.0×10^9	1.8×10^7	1.8×10^9	x 1.8
3.4×10^{10}	7.1×10^8	7.1×10^{10}	x 2.1
2.8×10^{10}	4.8×10^8	4.8×10^{10}	x 1.7
4.5×10^{11}	1.0×10^{10}	1.0×10^{12}	x 2.2
6.7×10^8	1.0×10^7	1.0×10^9	x 1.5
2.1×10^{12}	6.5×10^{10}	6.5×10^{12}	x 3.1

The average rise in titre is about x 2.

Aggregates of viruses should show a multi hit type of curve, a shoulder while there is a lag in inactivation followed by exponential inactivation. If the exponential is extrapolated back to the ordinate, an extrapolation number is obtained which gives the mean number of aggregates. When the 1×10^9 pfu ml^{-1} lysate of MS2 (from above) was irradiated as an aggregated suspension, an inact-

vation curve was obtained, as reproduced in figure 30, A shoulder in the curve is seen, and when the straight line inactivation curve is extrapolated back to the ordinate, an extrapolation number of 0.25 is obtained, which is equivalent to 1.78×10^9. This is in good agreement with the dilution de-aggregation figure of a rise of 1.8 x.

The rate of inactivation was the same as the rate of inactivation of the de-aggregated suspension, irradiated as a control. Since the rates were the same, it indicates that aggregative multiplicity re-activation is not occuring in this virus, as a more resistant slope might be expected from the aggregated suspension, as in Galasso and Sharps'results.

Electron microscopic examination of virus suspensions were carried out to determine the type and frequency of aggregations. Three types of aggregation were observed:-

i) Attachment of viruses to pili. Depending on the length of the pili, up to 200 particles were counted. (Bacteriophages inject RNA into the pilus on contact and thus appear empty. It is not therefore possible to distinguish between a particle that was empty of RNA before it attached or had ejected after it attached). Electron micrographs 1 and 2 show MS2 particles attached to sex pili.

ii) Aggregates attached to debris. Electron micrograph 1 shows a group of five particles attached to cell debris.

iii) Viruses attached to one another. Electron micrographs 1,3,4 and 5 show viruses and virus particles attached to one another. Close examination of the micrographs reveal links between the viruses and between the viruses and the pilus. Electron micrograph 6 shows these structures most clearly, but there is no mention of such a structure in the literature.

Electron Micrograph 1.

MS2 bacteriophage of E.coli. attached to F+ pilus. Negatively stained with 2% phosphotungstate, pH 7.0. x 273,000 magnification.

The micrograph shows three viruses linked together (above the pilus), particles attached to the F+ pilus and to particles attached to the pilus and six particles attached to debris (below the pilus and on the right of the micrograph.

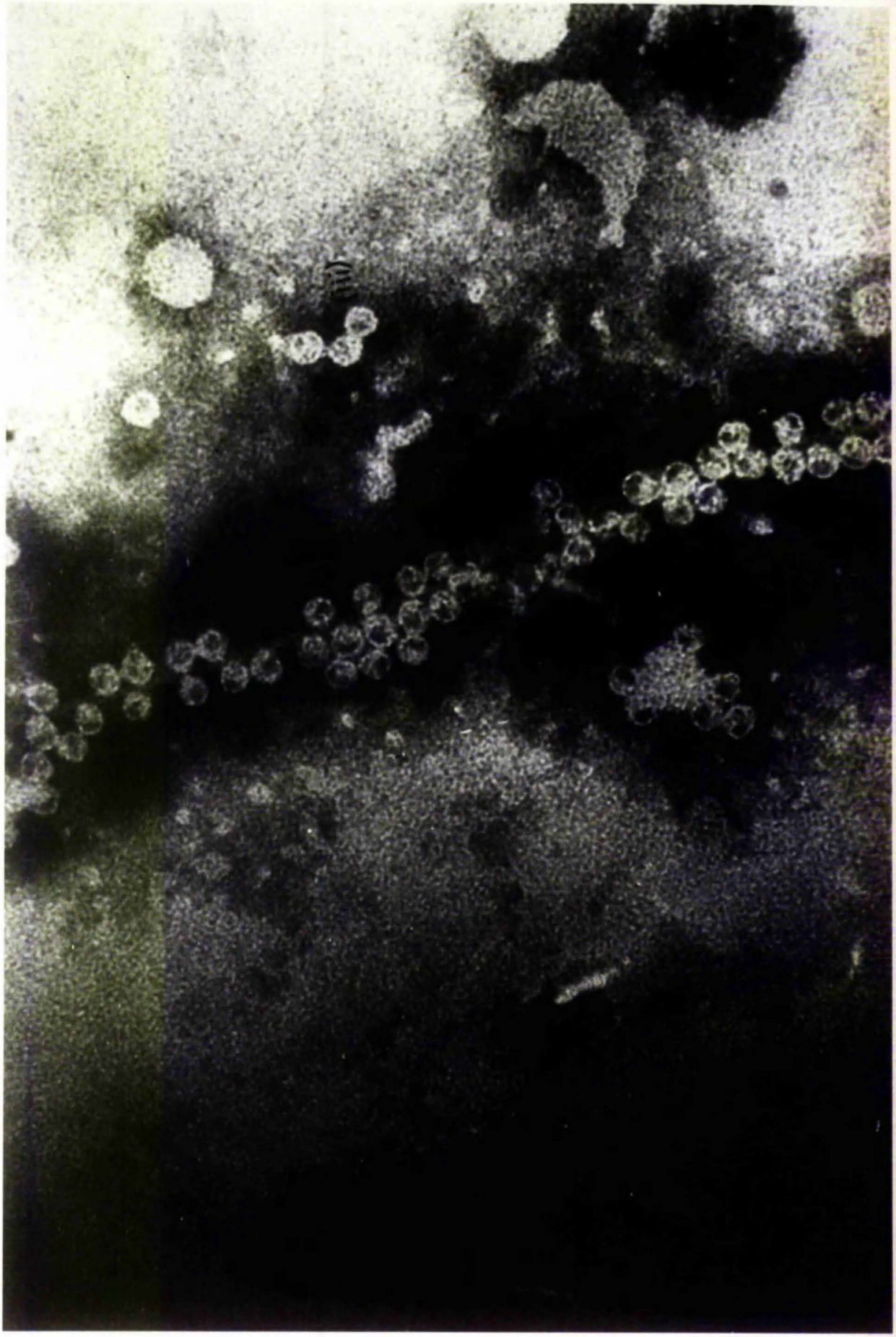

Electron Micrograph 2.

Bacteriophage MS2 of E.coli.attached to the F+ pilus. Negatively stained with 2% phosphotungstate, pH 7.0.

The micrograph shows empty capsids attached to the pilus and to other, pilus attached capsids.

A bacterial flagellum, much thicker than the pilus is seen lying from the top left down to the centre. A thinner pilus at the bottom left is thought to be an ordinary pilus because no male specific bacteriophage are attached to it.

x 273,000 magnification.

Electon micrographs 3,4 and 5 are to be found attached to the inside back cover of this thesis.

They show MS2 bacteriophage, purified by polyethylene glycol, sedimented in an ultracentrifuge and dialysed against buffer.

Stained with 2% phosphotungstate at pH 7.0. x 364,000 magnification.

The electron micrographs show aggregated particles of two, three four and five viruses.

ELECTRON MICROGRAPH 3.

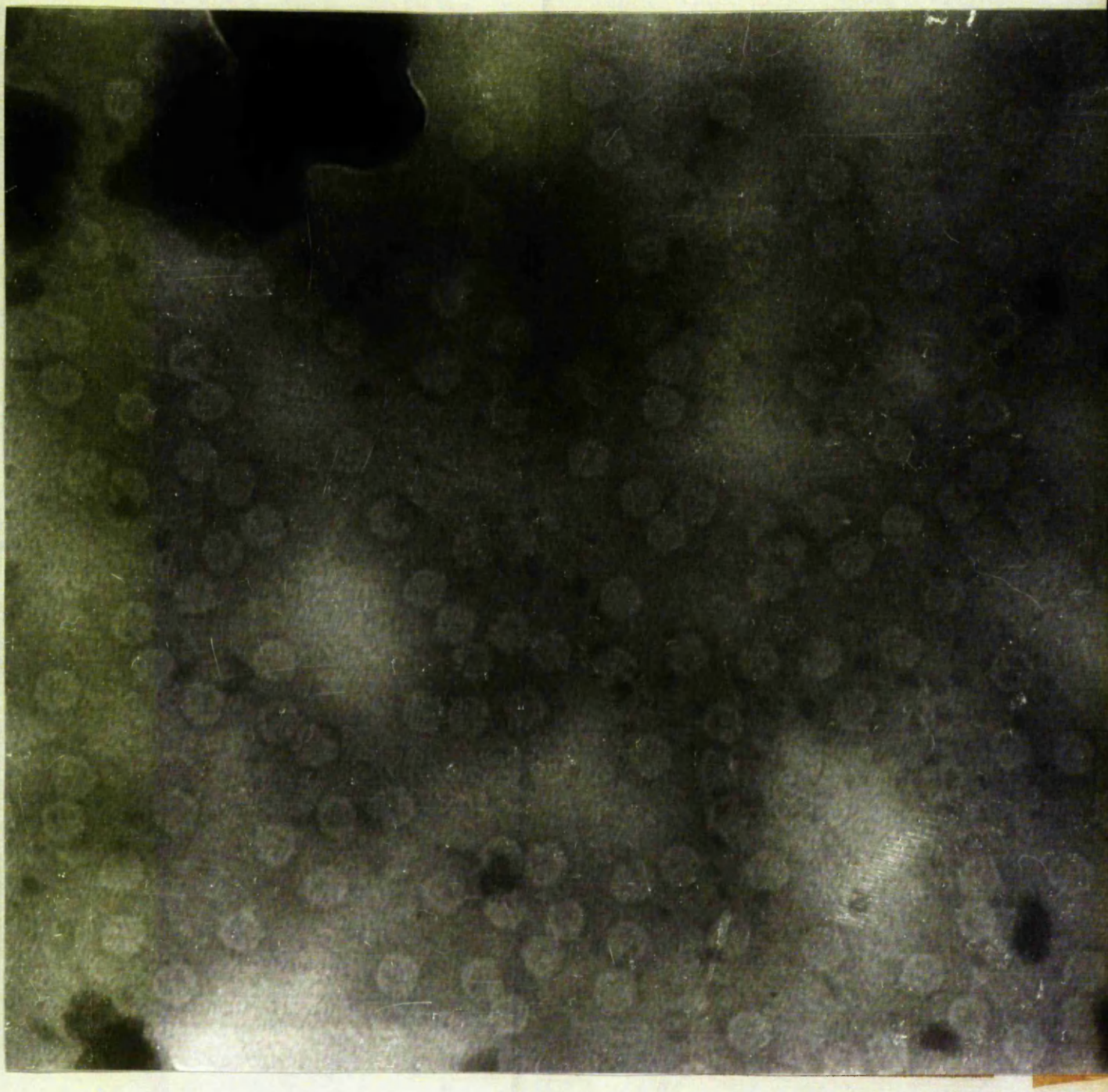

MS2, negatively stained with 2% phosphotungstate x 364,000, showing aggregates.

ELECTRON MICROGRAPH 4.

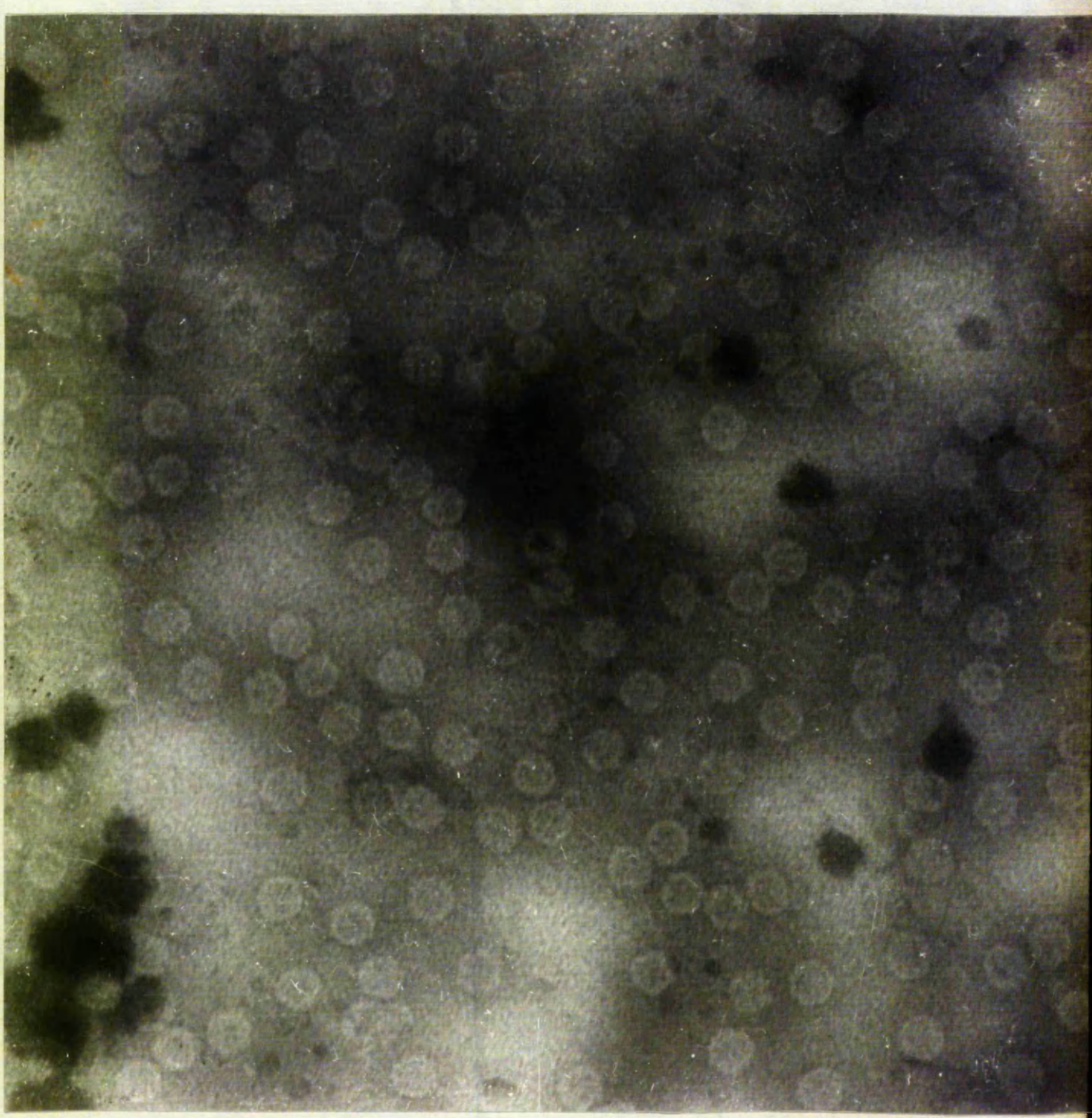

MS2, negatively stained with 2% phosphotungstate

x 364,000. Showing aggregation.

EM 4

ELECTRON MICROGRAPH 5.

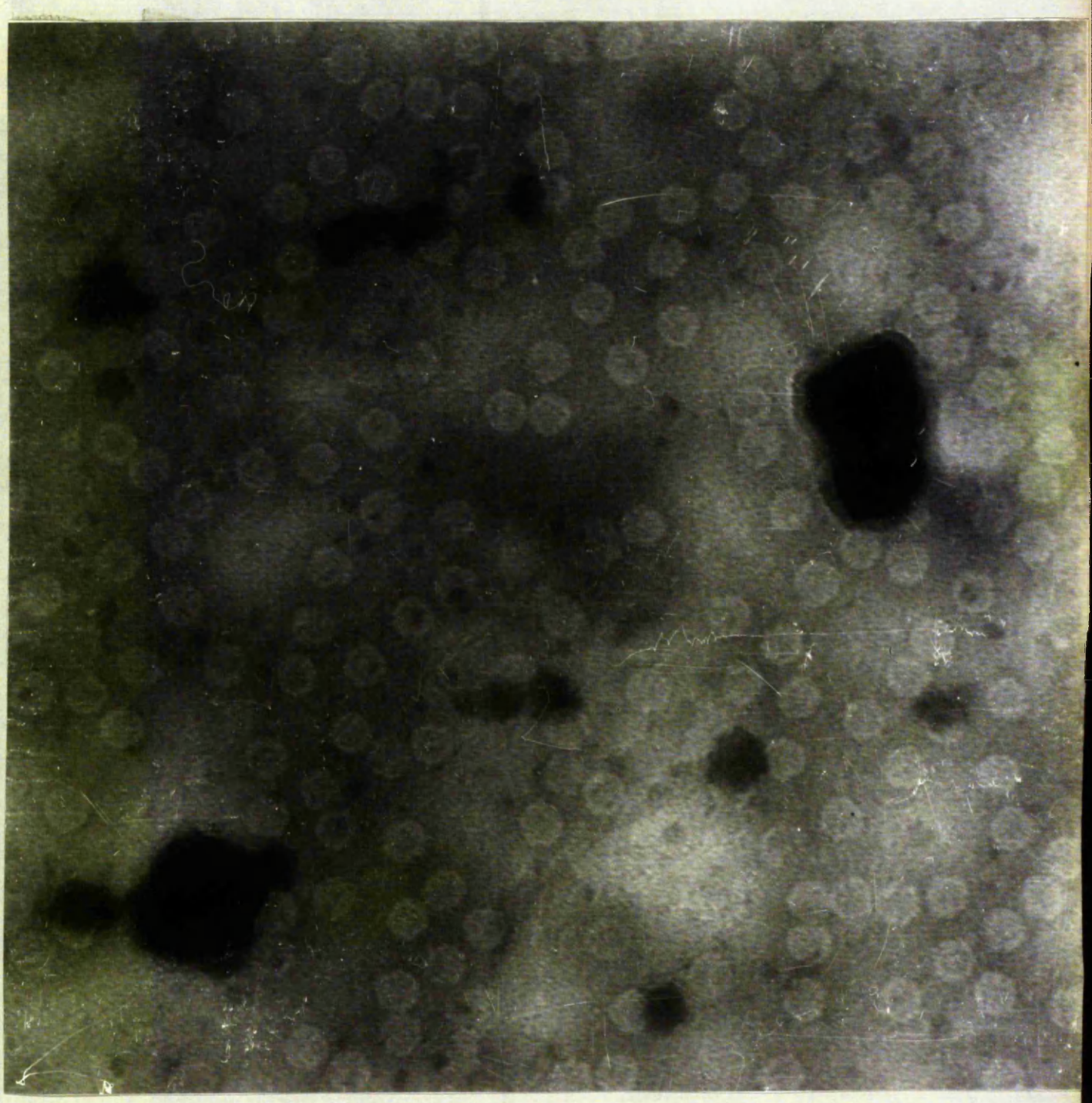

MS2, negatively stained with 2% phosphotungstate, x 364,000. Showing aggregation.

Electron Migrograph 6.

Bacteriophage MS2 attached to the F+ pilus of E.coli.
Negatively stained with 2% phosphotungstate, pH 7.0.
x 1,091,000 magnification.

This micrograph shows structures between the particle and the pilus at the point of attachment.

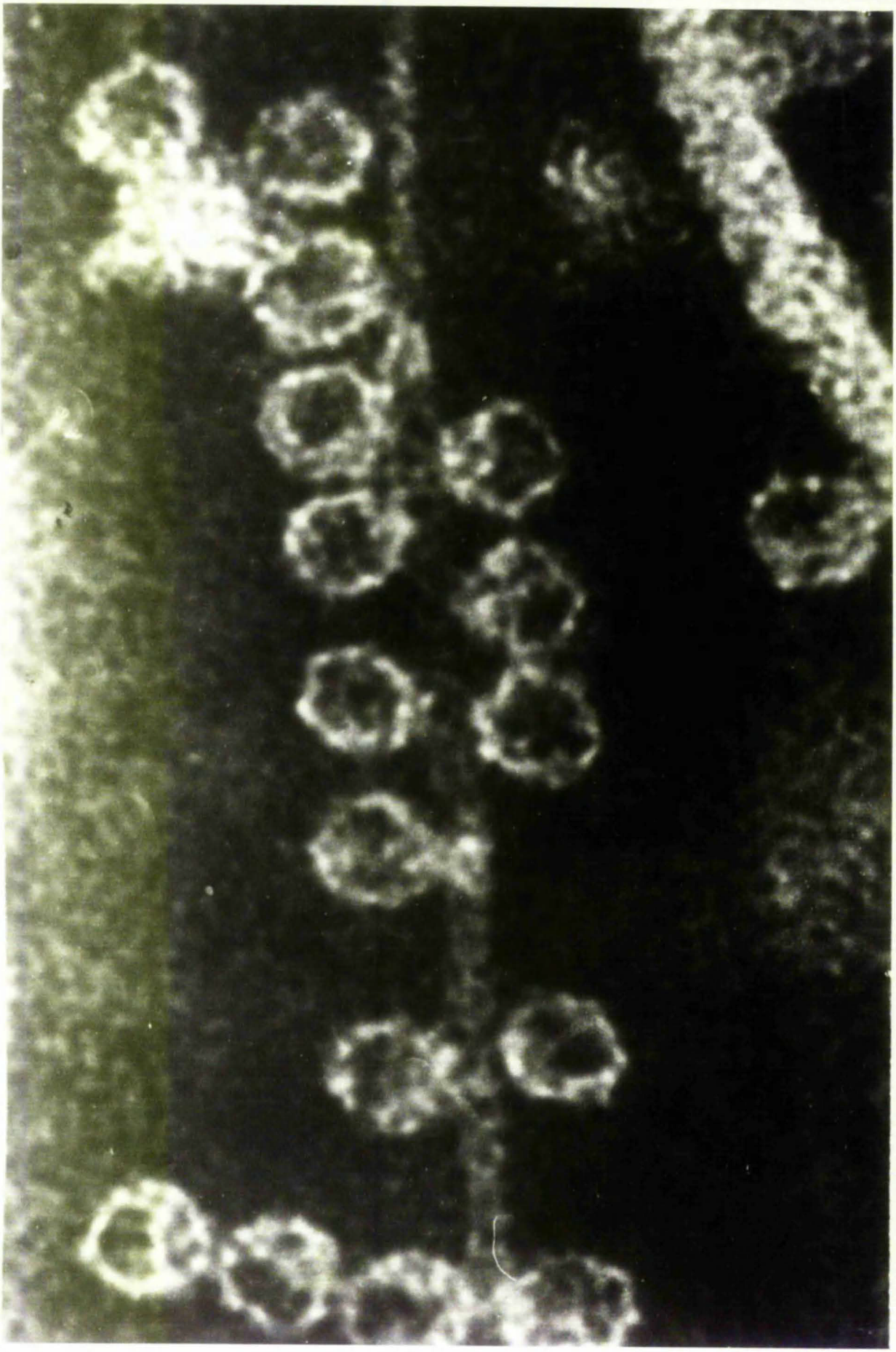

Figure 30.

Inactivation of Aggregated MS2 by 254nm UV.

(100 ergs mm^{-2} sec^{-1})

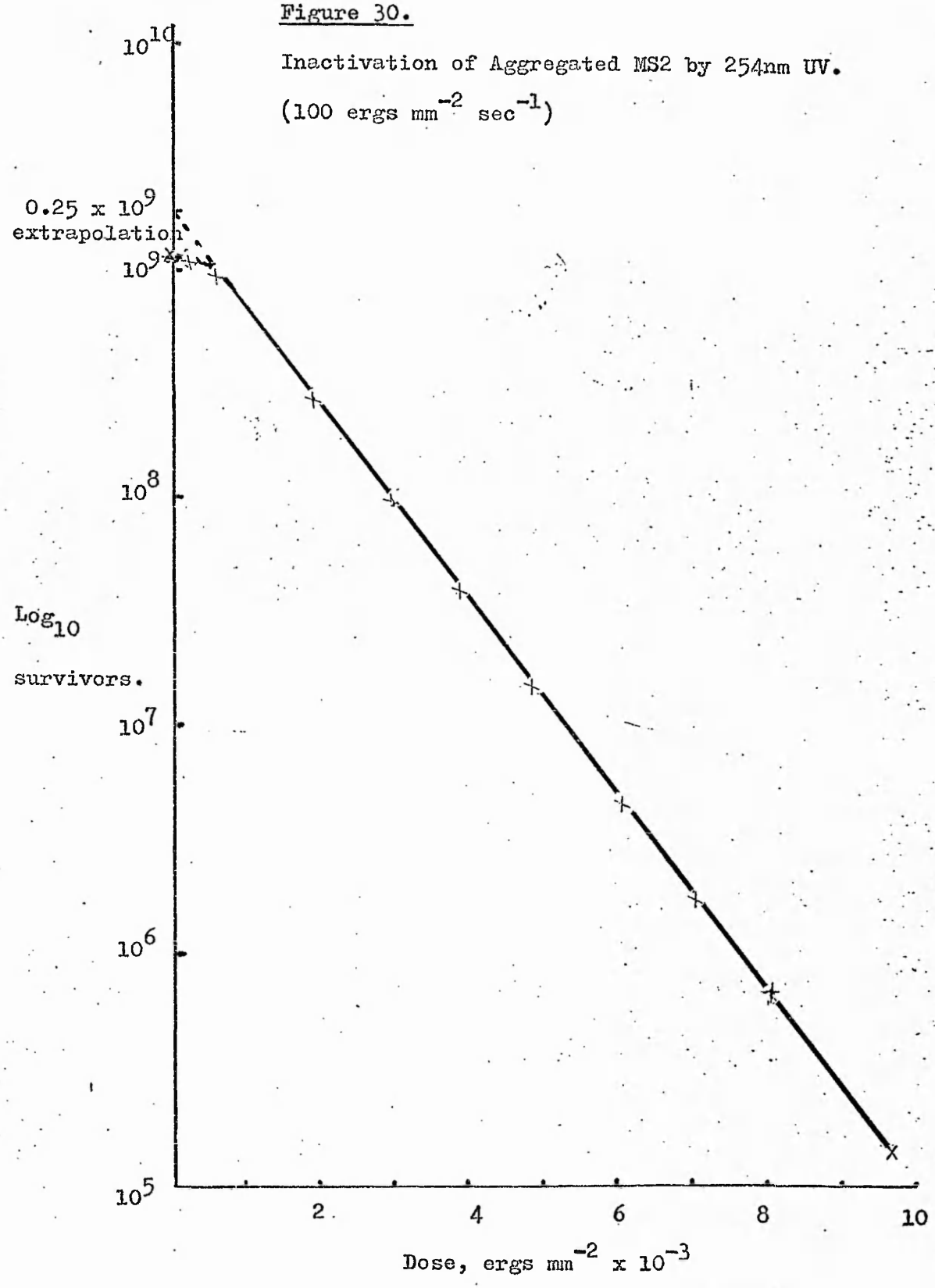

The distribution of aggregates was also studied. A lysate of aggregated MS2 with a titre of 2.3×10^{12} was used in the study. This suspension was irradiated with UV to get an inactivation curve (shown in figure 31). The straight line was extrapolated back to $\log_{10}$ 12.66, which is 4.5×10^{12}. The original titre was 12.36 $\log_{10}$, and therefore this indicates an aggregation of an average of 1.95 x. Dilution de-aggregation of the suspension gave a titre of 4.4×10^{10}, indicating an average aggregation of 1.9 x. Electron microscopic examination of the suspension was undertaken and the results shown in Table 20, below.

Table 20. Distribution of Aggregates in Lysate of MS2.

	No. particles	No. pfu
Single viruses	822	822
Attached to debris	30	7
Pilus attached	22	1
Linked	618	128
Totals	1492	958

There is a total of 1492 particles, but only 958 plaque forming units, if aggregates do form plaques. If these aggregates were dis-associated then there would be a rise of $\frac{1492}{958} = 1.55$ times. If aggregates do not form plaques then the rise would be $\frac{1492}{822} = 1.8$ times. If we assume that pilus linked and debris attached cannot form plaques or dis-associate then $\frac{1440}{822} = 1.75$ times. It is clear that linked viruses are the main mode of aggregation. Aggregates of two were the main type of aggregate with aggregates of three, four and five (see E.M.s 3,4 and 5, these photographs show a similar distribution of aggregation described above) occur. The best fit of de-aggregation is to assume that aggregates do not

Figure 31.

Inactivation of Aggregated MS2 by 254nm UV.

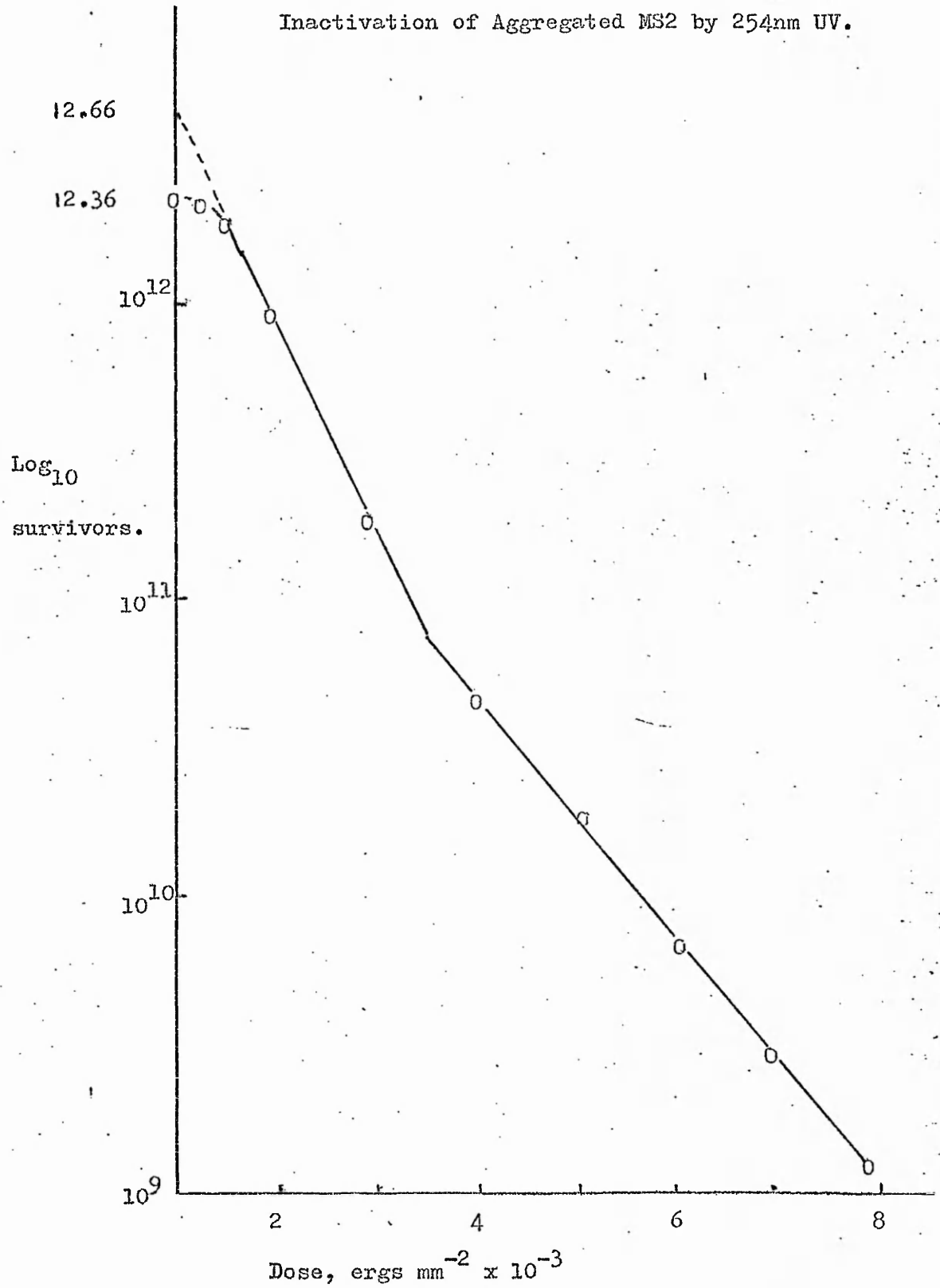

form plaques, but if this is so it is hard to explain why a shoulder occurs during inactivation. It might be that the aggregate is connected by the attachment site. In support of this are electron micrographs six and three.

It was assumed for the electron microscope studies that a capsid containing RNA was a potential plaque forming unit, but as shown on page 22, not all RNA containing particles can infect and form plaques. 80% of the particles are non-infectious and do not absorb efficiently to F+ pili, Class II particles. It is likely that these particles do not form aggregates, or if they do, not as many as Class I particles. Class III particles, which lack the A protein are assumed not to form aggregates at all. Investigation of the aggregation properties of the different type of particle should be carried out to resolve this issue.

It is concluded, never-the-less, that dilution de-aggregation is a good method for achieving dispersal of bacteriophage MS2, as no detectable inactivation occurs and the optical density of the suspension is lowered to a point where absorbance is not an important factor,in the system used, in the amount of UV needed to inactivate viruses.

C. Biphasic Inactivation of MS2.

During the course of the previous experiments it was noticed that some stocks of MS2 did not follow a true exponential decrease in numbers (shown by a straight line when the log of survivors is plotted against the integral dose). After 90% to 99% inactivation more UV was needed to achieve the same rate of inactivation. Figure 32 shows the results of an inactivation showing this phenomenon. Figure 31, from the previous section on aggregation also shows this biphasic curve and this result with de-aggregated viruses shows that it is not an artefact of aggregation. Figure thirty shows only one rate of inactivation, which is the same rate as the more resistant one shown in figure 32.

The literature gives several reasons for biphasic resistance, artifacts of the irradiation system, photoreactivation, multiplicity reactivation are amongst these.

a) Multiplicity reactivation.

It was first thought that multiplicity reactivation was causing biphasic resistance. It has been noted that poliovirus will undergo multiplicity reactivation at a very low probability (129), and although other work has not found any evidence for reactivation to occur in MS2 (130), it was thought worthwhile to investigate MR as a cause of resistance.

Multiplicity of infection is inherent in the system of assay. During inactivation less and less dilution of the virus suspension was required to adjust the pfu ml^{-1} to 30-300 plaques per plate and consequently increasing numbers of virus particles were added to the host with increasing dilutions. (For instance; in a suspension of 3×10^{12} pfu ml^{-1}, a dilution of 10^{-10} is carried out so that 30

Figure 32.

Inactivation of MS2 by 254nm UV Showing Biphasic Resistance.

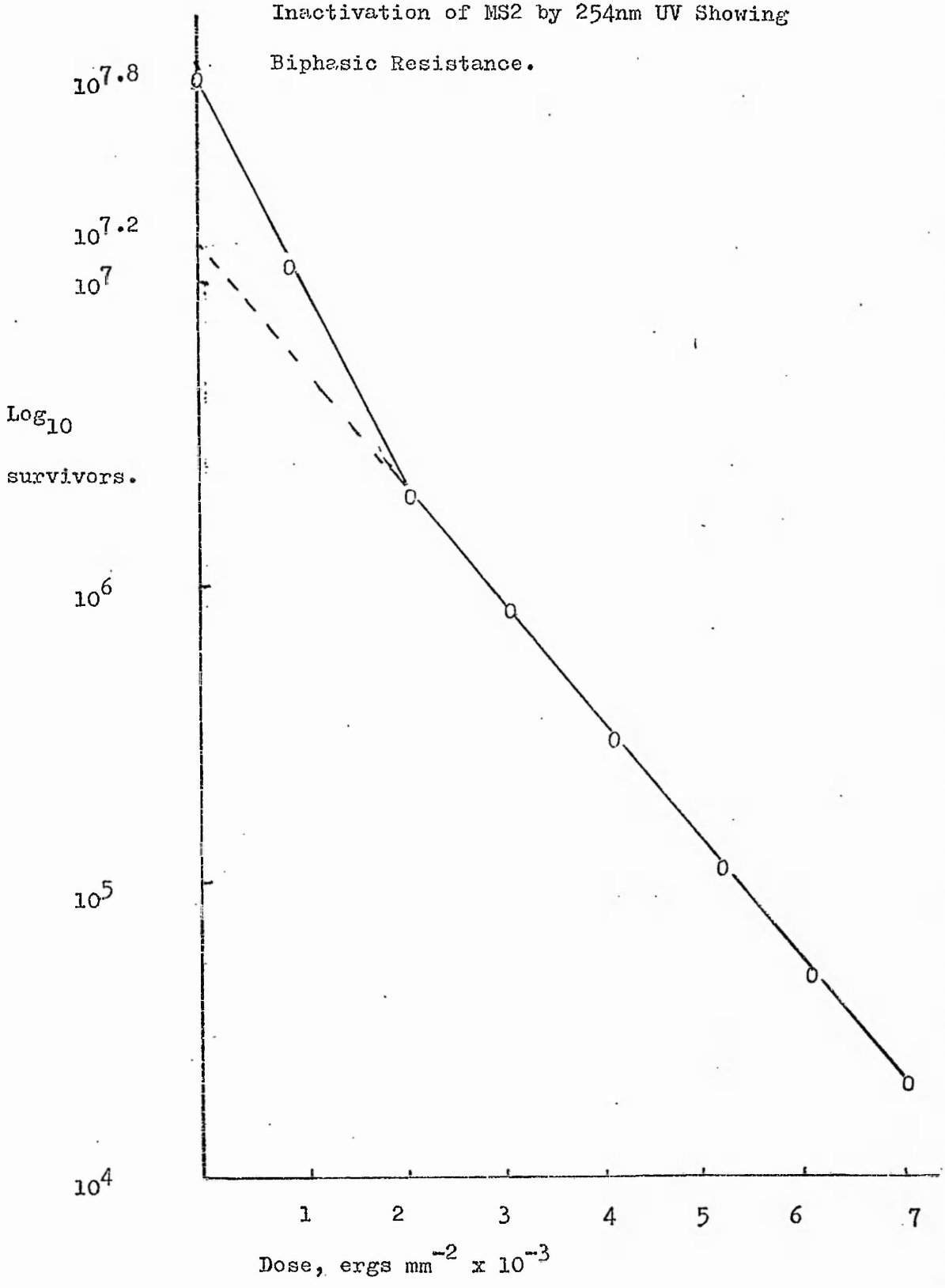

pfu per plate and 30 particles are added to the host, which on average contains 1 x 10^7 bacteria. After the population has been inactivated down to 300 pfu ml^{-1}, no dilution is needed to give 30 pfu per plate (0.1 ml samples are plated out) but 3 x 10^{12} particles are still in suspension and are added to the host. This means that there are about 10^4 phage added per bacterium- which might lead to multiplicity reactivation).

In an ordinary lysate, even if it is fresh, more particles are produced than viable virus (see introduction) so it might be possible that these particles can contribute to multiplicity of infection. It is not easy to assess the proportion of these particles and it is therefore difficult to ascertain when multiplicity of infeation is likely to occur. If the amount of host in the assay system were reduced ten or one hundred fold, then multiplicity of infection would occur much sooner in the assay, and MR, if it occurs, would appear as a resistant inactivation rate much earlier during inactivation.

Figure 33 shows the results of an experiment where the host has been diluted 1/100 in nutient broth to increase the multiplicity of infection. Virus dilutions were incubated for 15 minutes at 10°C to allow for absorption of particles to the pili and then added to soft agar and normal strength host for a normal assay. (This assumes that all the particles in the virus dilution were attached to the pili within the absorption period).

The ratios of virus to host were calculated for each dilution and also for a normal host strength control. Figure 33 shows no difference between high multiplicity and ordinary multiplicity, biphasic inactivation occuring at the same level. Although two experiments were performed only one curve is shown because of the

Figure 33.

Inactivation of MS2 by 254nm UV at High Particle/Host Ratios and Normal Particle/Host Ratios.

X High multiplicity

0 Low multiplicity

Numbers give particle: host ratio. Underlined figures are the high multiplicity ratios.

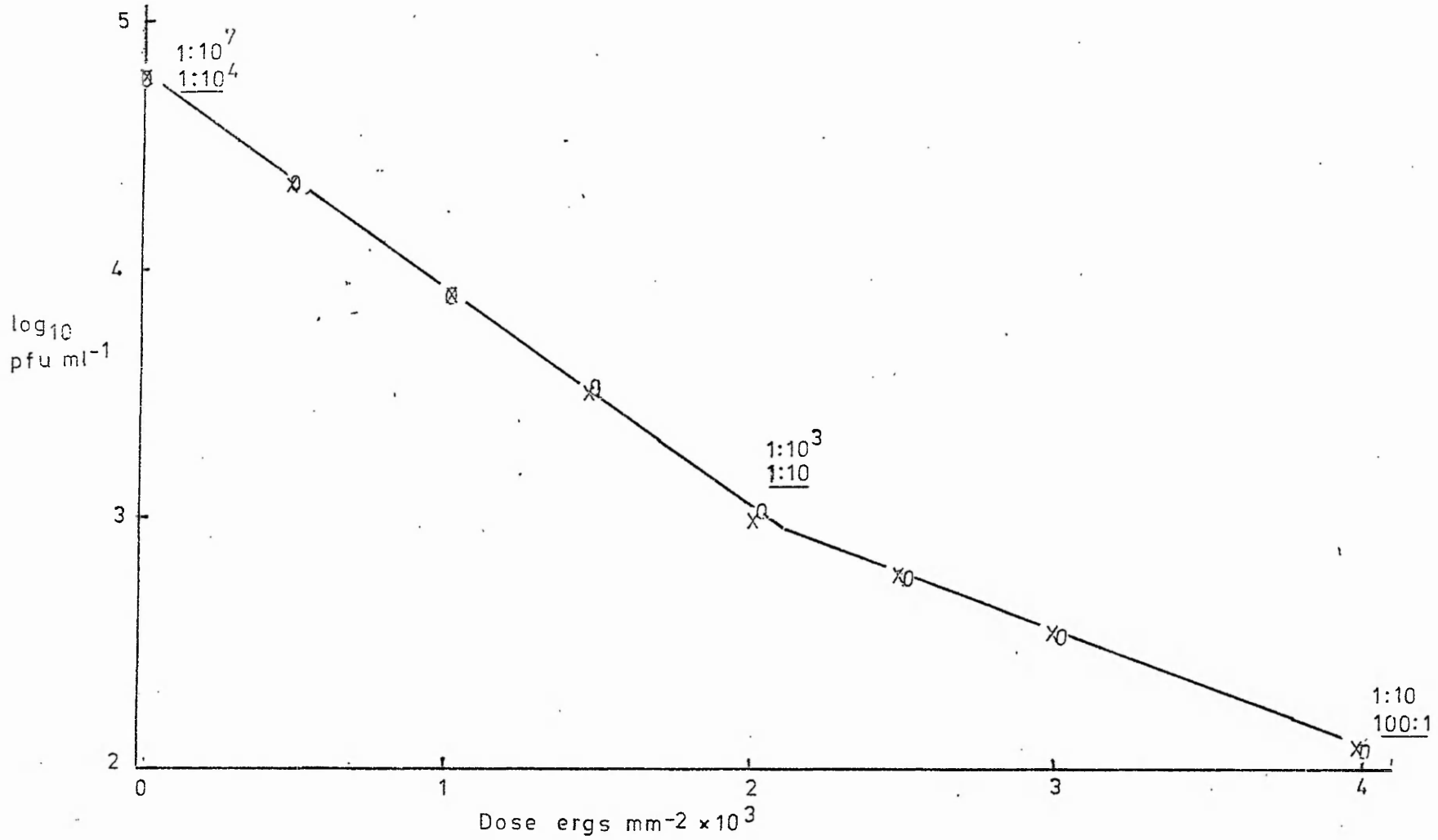
5
4
3
2
log10 pfu ml-1
1:10^7
1:10^4
1:10^3
1:10
1:10
100:1
0
1
2
3
4
Dose ergs mm-2 x10^3

good replication between the control and the high multiplicity experiment.

Other authors have described the biphasic phenomenon in MS2 and in other viruses (131,132,133,134,135) and have described a variety of reasons for this effect. These were investigated in turn.

b) Accuracy of observations.

If the results of inactivation show wide variation, it is not possible to distinguish statistically between a straight line and a curve. This is inherent in some techniques, such as the assay of poliovirus, where there is such wide variation of data, especially when low numbers of survivors are assayed that curve recognition is difficult. Statistical models currently available, such as linear regression analysis, only test for fit to a straight line and thus may be inappropiate to apply to a curve. In the conduct of experi - ments sample intervals should be chosen that are close together, so that any deviation from a straight line can be recognised, and dilutions should be performed so that good agreement is achieved between replicates. Figure 34 shows the results of two inactivation experiments, one with only five intervals, which can at best be interpreted as a curve, and the other with fifty intervals, which can easily be seen to comprise two straight lines, one more resistant than the other. There is at present no statistical model that will test fitness to such a biphasic curve, but it is obvious that the phenomenon under investigation is not an artifact of data variability.

c) Attachment to Vessel Walls.

Rauth (134) suggested that the biphasic curve was due to absorption of viruses onto the walls of his irradiation vessel (a cuvette) which in his system took them out of the path of the irr-

Figure 34.

Effect of Sample Interval on Curve Interpretation. Inactivation of MS2 by 254nm UV.

I = range of sample variation.

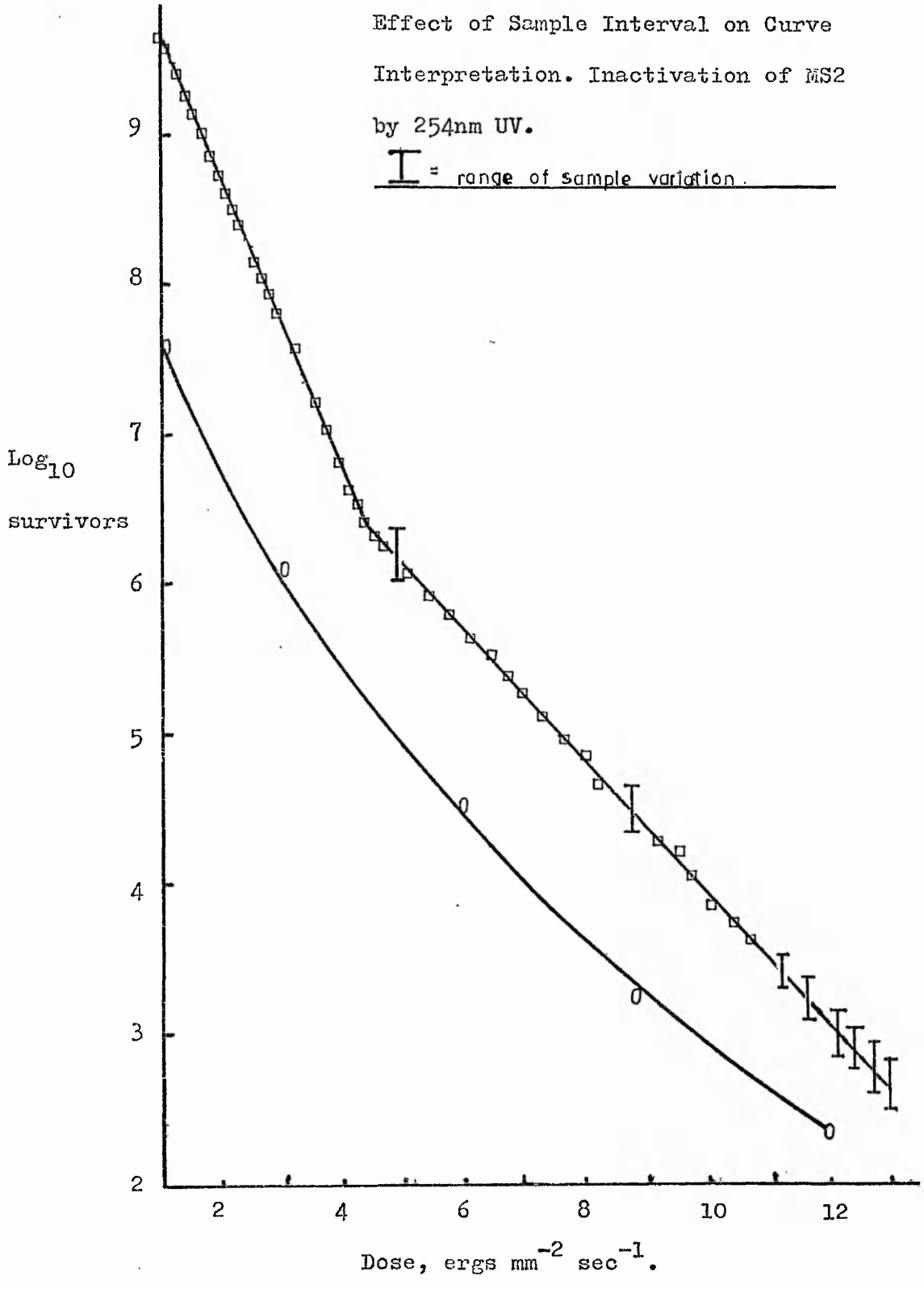

adiation. Later release, he sumised, gave rise to active virus in the suspension, which gave the appearance of being resistant. In the present studies the beam of UV was much wider than the shallow dish holding the virus suspension, so no particles were excluded, absorbed or not. However attachment to the walls might confer some type of resistance by stabilising the particle. It was reasoned that if a much greater proportion of UV inactivated viruses were added to a virus suspension than the active particles in it, these would compete for attachment to the vessel walls and thus prevent the active particles from being protected. Figure 32 shows that the resistant population is about 22% of the total population (7.63×10^7 and 1.5×10^7 are the relative figures for the sensitive and resistant population respectively) and therefore adding x1000 times dead viruses than live should compete for attachment to the walls.

A suspension of 1×10^{10} pfu ml^{-1} MS2 were irradiated with UV until no survivors were detected by plaque assay. To this was then added a suspension of 3.4×10^6 pfu ml^{-1} MS2, giving a suspension containing 5×10^9 inactive and 1.7×10^6 pfu ml^{-1}. When these were irradiated no difference was found in the inactivation rates of this suspension compared to that of a 50:50 dilution of the 3.4×10^6 pfu ml^{-1} suspension. Figure 35 shows the results of this experiment.

If attachment of 22% of the population were taking place, a 22% drop in titre should be noted when the suspension was added to the vessel. No such drop in titre was ever noted:- the original number of pfu ml^{-1} was always found by assaying the stock bottle and the suspension in the irradiation dish before exposure to UV.

It is concluded that there was not enough absorption to the vessel walls, if it did occur, to affect the inactivation of the

Figure 35.

Inactivation of MS2 by 254nm UV in the Presence of Inactivated Virus.

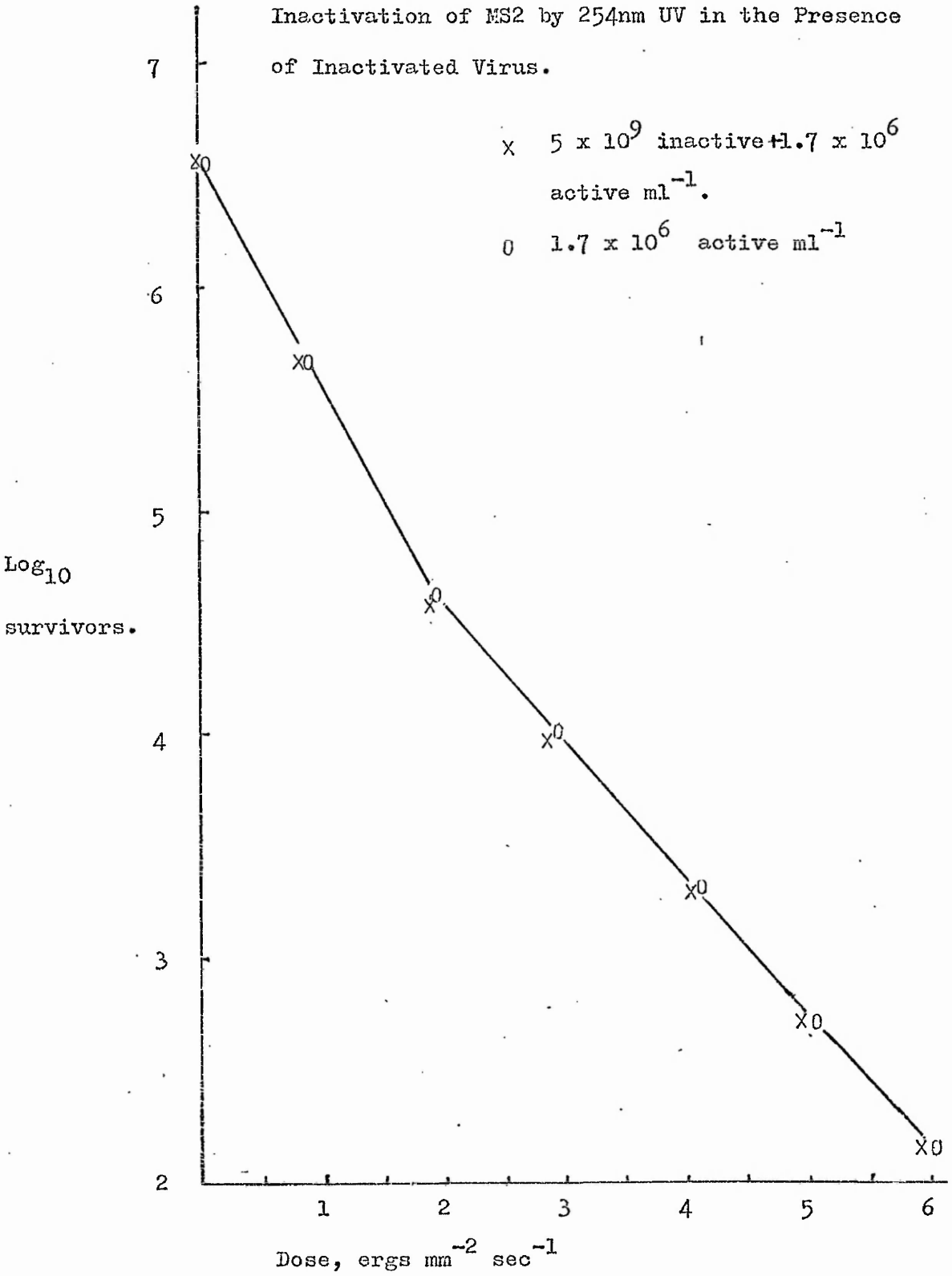

viruses.

d) Effect of Shielding.

The possibility of dead viruses absorbing UV and thus shielding active particles left in suspension is ruled out by the experiment above and shown in Figure 35. The suspension of 5×10^9 particles did not shield the 1.7×10^6 pfu ml^{-1}. The experiments investigating the effect of depth of suspension liquid also showed that absorption was not a factor in the experimental system used.

An experiment was conducted to investigate the level of absorbance that would shield the viruses. Figure 36 shows the results of adding 50% calf serum (O.D. 254nm 30 (calculated)), 5% calf serum (O.D. 254nm 3.0, measured) and a normal suspension (O.D. 254nm 0.3). It is seen that there is no significant difference between the inactivation rates of the 0.3 O.D. and 3.0 O.D. suspension, but the O.D. 30 suspension was twice as resistant.

It is concluded that absorbance and shielding do not affect the inactivation rates of viruses in the experimental system used.

e) Photoreversal.

Fidy and Karkzag (136) in their investigation of the two compartment curve, produced a mathematical model of a two compartment inactivation which fits the observed results. They suggested that there was a reversal of the inactivated state which might be caused by photoreversal:- the splitting of the uracil dimers that are thought to cause inactivation.

It was reasoned that irradiation of MS2 at 265nm (the peak wavelength for inactivation), where presumably dimers are formed maximally in vivo (dimers are formed maximally in vitro at 280nm) would yield a sharp inactivation rate. If these same viruses were

Figure 36.

Effect of Absorbance on the Inactivation Rate of MS2 by 254nm UV.

□ O.D. 254nm 30

● O.D. 254nm 3

X O.D. 254nm 0.3

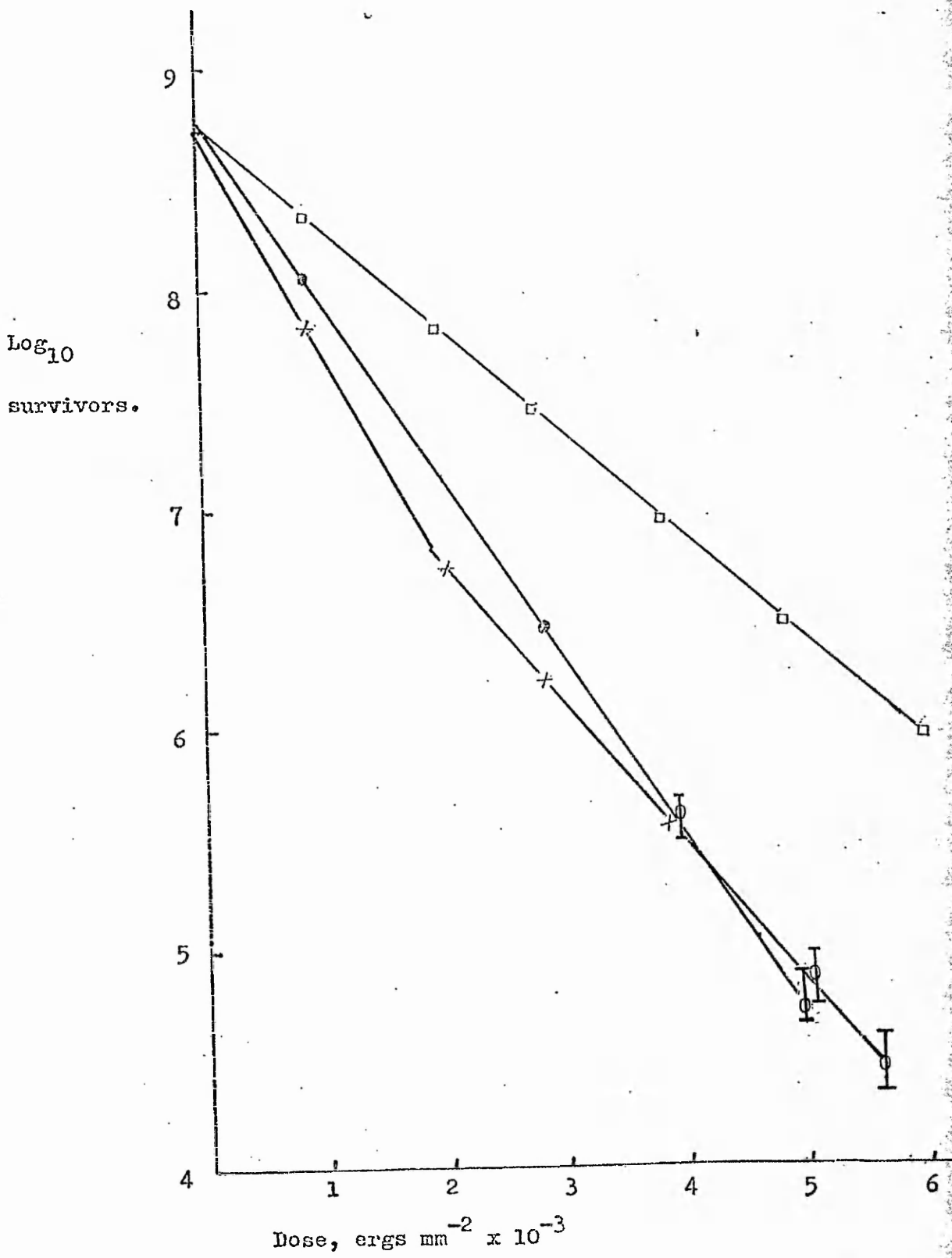
9
8
7
6
5
4
Log10 survivors.
1
2
3
4
5
6
Dose, ergs mm-2 x 10-3

then irradiated with 240nm photons the continuing slope should be much less and less than a normal slope for 240nm as the photons will be reversing dimers not split by 265nm photons.

The monochromator was first used to confirm the minimum and maximum wavelengths of inactivation reported by Rauth (134).

i) Inactivation of MS2 by 222-300nm UV.

MS2 was inactivated by a range of wavelengths emitted from the monochromator. The cross sectional area of inactivation was calculated for each wavelength from the D37, determined from the slope of the inactivation curves. Table 21 shows the D37 values computed from the slopes of the inactivation curves at different wavelengths (Figure 37 shows these slopes, all the figures have been re-calculated to bring the origins to the same point. The D37 is shown as a straight line.)

Table 21. The Inactivation of MS2 by Different Wavelengths of UV.

Wavelength nm	ergs photon^{-1}	D37 (ergs mm^{-2})	ϕ
222.5	8.9×10^{12}	1,100	3.0×10^{-14} mm
238.7	8.35	4,000	4.8×10^{-14}
248.3	8.0	1,000	2.0×10^{-14}
253.7	7.73	720	1.1×10^{-14}
265.2	7.5	625	9.0×10^{-13}
280.4	7.1	1,550	5.0×10^{-14}
289.4	6.87	5,150	7.5×10^{-14}
296.7	6.7	6,370	9.5×10^{-14}

The D37 represents the energy required to hit, on average, every particle and to inactivate it. The number of photons required to

Figure 37.

Inactivation of MS2 by Different Wavelengths of UV.

MS2 was inactivated by the UV output from the monochromator. The source was the 250w mercury discharge lamp. The inactivation rates have been recalculated to begin at a common origin.

Key.

a) 265.2nm

b) 253.7nm

c) 248.3nm

d) 222.5nm

e) 238.7nm

f) 280.4nm

g) 289.4nm

h) 296.7

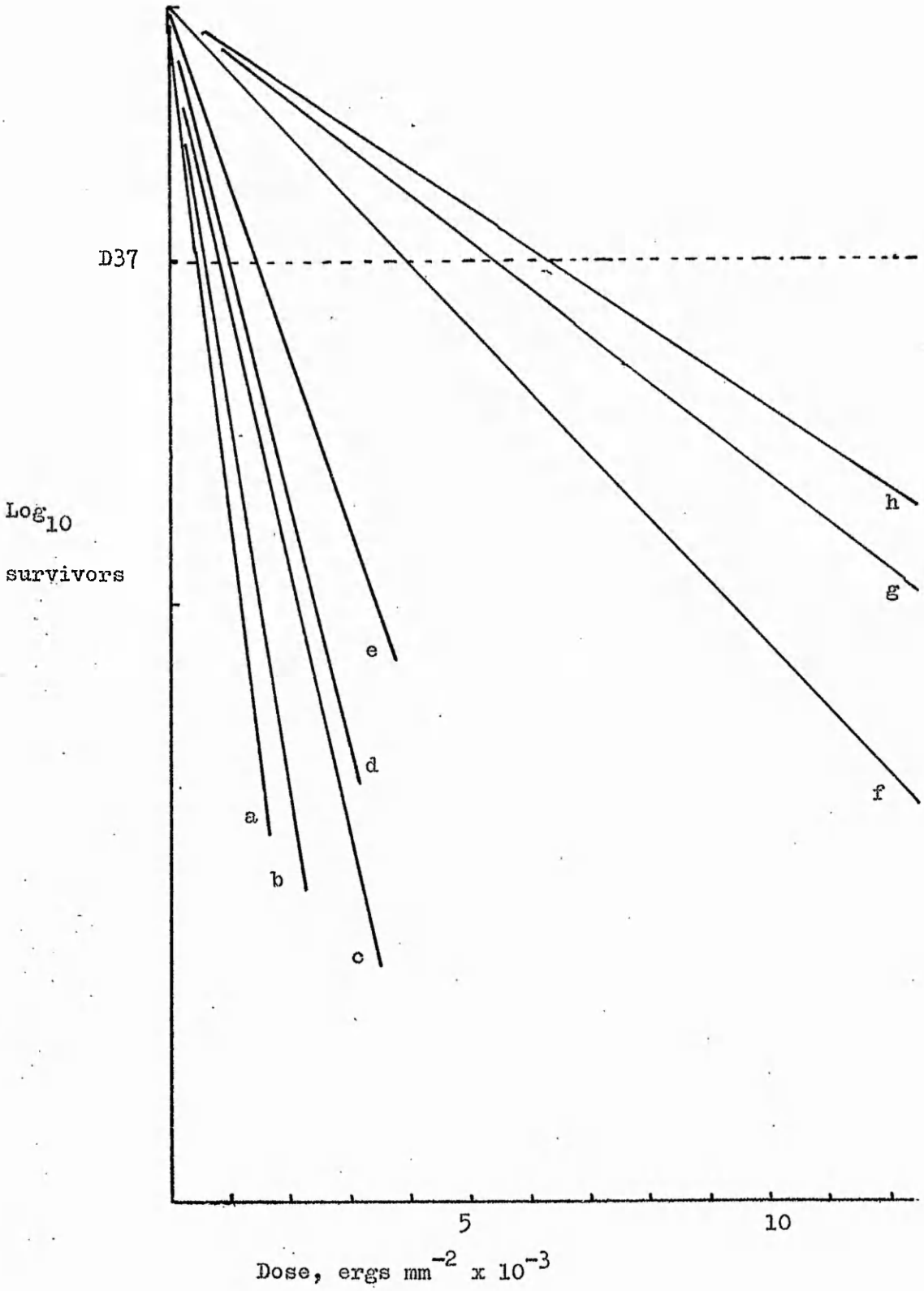
D37
Log10
survivors
a
b
c
d
e
f
g
h
5
10
Dose, ergs mm-2 x 10-3

achieve this energy per mm^2 gives the area of cross section of inactivation when expressed as a reciprocal, ϕ.

Figure 38 shows the cross sectional areas for each wavelength. This confirms that 255-275nm photons are the most efficient for inactivation and that 230-240nm photons the least active. These results are in almost complete agreement with those published by Rauth (134) for this virus.

The peak of inactivation occuring around 260nm means either that this is the wavelength where dimers are formed maximally in vivo or that other photoproducts are more important in causing inactivation. 238nm is the shortest wavelength that causes least inactivation, and efficiency of inactivation rises again so that at 222.5nm viruses are being inactivated as efficiently as at 255nm. Other workers have suggested that protein absorption might be the reason for death in this region (35,33,137).

Kleczkowski (36) has found no evidence for pyrimidine dimer formation at 220nm, and Goddard et al (37) have found that protein subunits are bound to the viral RNA, approximately one subunit per lethal hit. Shore and Pardee (139) have shown that there is no transfer of UV energy absorbed by either the RNA or the protein to the other macromolecule. It has not yet been demonstrated whether the protein absorbs UV and reacts with the RNA or if the RNA absorbs the UV and reacts with the protein. The structure of TMV (RNA helically wound inside the protein subunits) is very different to the structure of RNA bacteriophages and enteroviruses, the RNA is in much closer contact with the structural proteins. It is therefore hard to speculate on the nature of the photoproducts causing death at 200nm. It would appear from the fact that the inactivation curves are of the

Figure 38.

Cross Sectional Area of Inactivation of MS2 at Different Wavelengths.

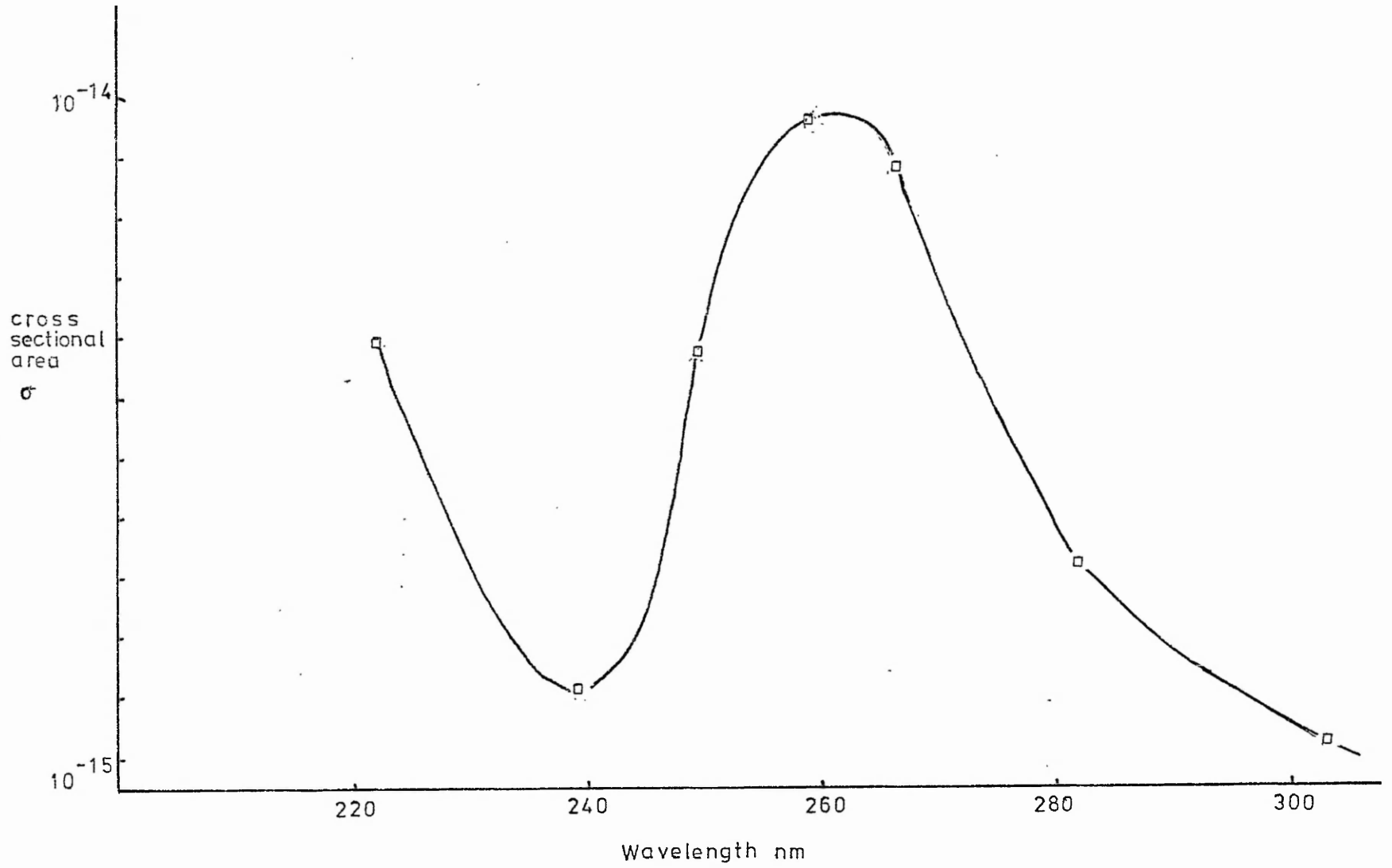
10^{-14}
cross sectional area
σ
10^{-15}
220
240
260
280
300
Wavelength nm

'one hit' type that the RNA is involved in some way.

Sime and Bedson (35) have suggested a role for protein in the inactivation of Vaccinia and bacteriophage T2 at 270-280nm. Since nucleic acids absorb twenty times as much UV (on a per weight basis) as protein, and viruses in general contain about three times as much protein as nucleic acid, it would seem that absorption by the nucleic acid is more important at this wavelength. Interaction with protein components to produce inactivation cannot be ruled out however.

ii) Inactivation of MS2 by tandem irradiation at two wavelengths.

If photoreversal of dimers were causing a reactivation, and thus the biphasic inactivation, the exposure to 265nm photons would cause maximum production of dimers while subsequent exposure to 240nm photons should split them and give less inactivation than would be expected. Figure 39 shows the results of inactivating MS2 down to 5% survival with 265nm UV and the subsequent inactivation with 240nm photons. Also shown in Figure 39 are the normal inactivation rate for 240nm irradiation and the expected inactivation rate if reactivation were occuring. It can be seen that the 240nm inactivation subsequent to the 265nm irradiation is no different to the normal slope. It is therefore concluded that photoreversal is not a significant feature of MS2 irradiations and that the biphasic curve is not a consequence of photoreversal.

f) Selection of Resistant Strains.

None of the explanations offered in the literature for the existance of the biphasic curve seemed to fit the observations and it also appeared that it was not an artifact of the experimental system.

Although the viruses had been selected from single plaques it

Figure 39.

Tandem Irradiation of MS2 by : 1. 265.2nm UV

2. 238.7nm UV

Key.

✕———✕ experimental results

a - - - - - theoretical result if there were no photoreversal

b —— —— theoretical result if photoreversal occured at a constant rate

c ——·——· theoretical result if photoreversal occured, reversing dimer formation at a rate faster than their being formed.

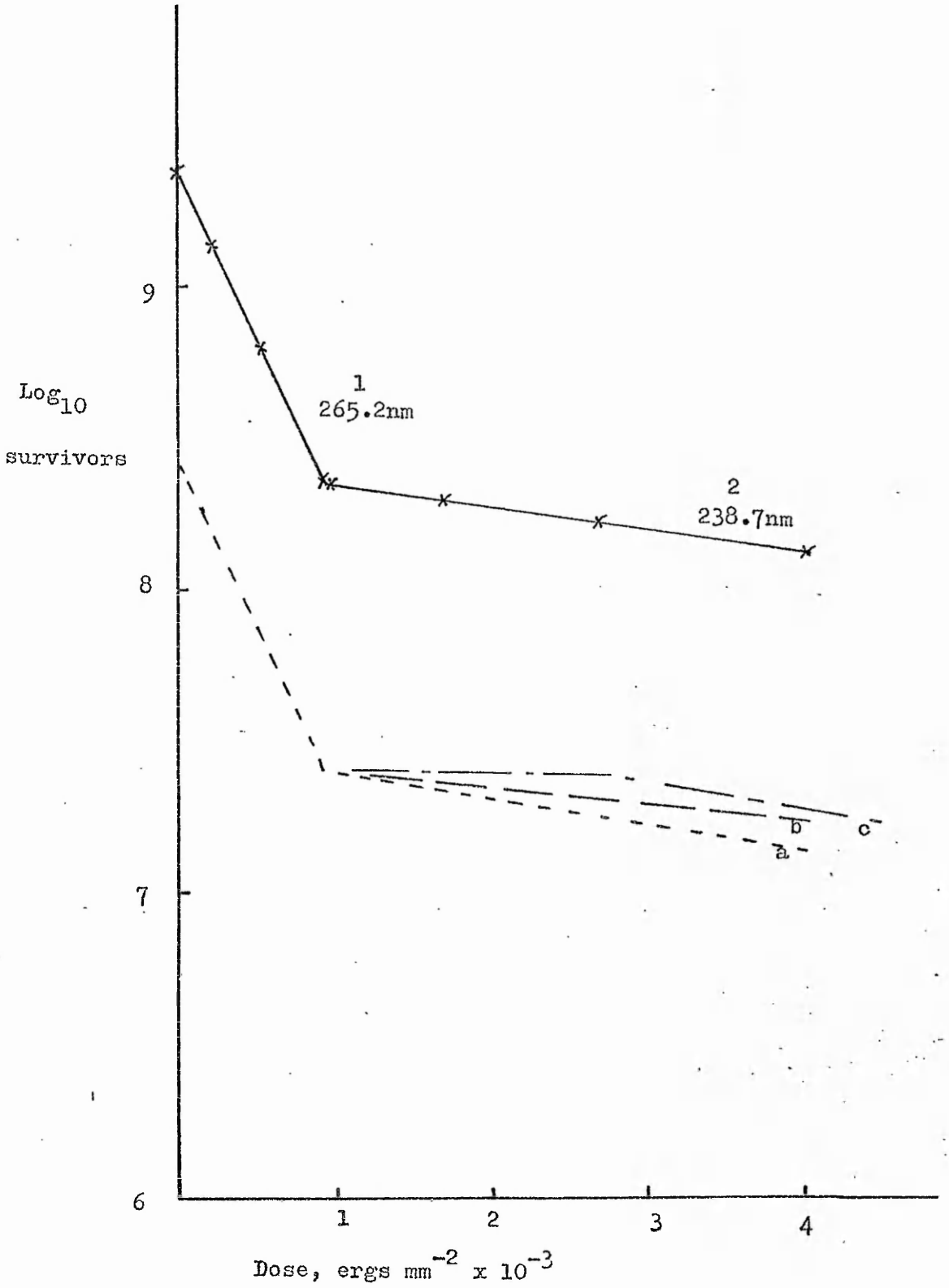
9
8
7
6
Log10
survivors
1
265.2nm
2
238.7nm
a
b
c
1
2
3
4
Dose, ergs mm-2 x 10-3

might be genetically unstable for UV resistance (throwing up a high proportion of UV resistant) and that selection of resistant strains might be possible from survivors or that some sensitive strains might be selected from a fresh lysate.

Selecting a plaque from a fresh lysate should give a 10:1 chance of selecting a sensitive, as they compose about 90% of the population. Conversely the selection of a plaque from a suspension that had been irradiated down to 0.00001% survival should result in a 1,000:1 chance of selecting a resistant strain, the sensitive viruses having been reduced to 0.001% of the remaining survivors.

Accordingly, twenty plaques from a fresh culture and twenty from an irradiated suspension were selected and tested for UV sensitivity. Of these forty strains, only one, S17, showed any difference to the normal biphasic curve. Figure 40 shows the results of this inactivation, a biphasic curve still exists, but there is a greater proportion of the population sensitive, approximately 99.9%. Plaques selected from S17 had a normal proportion of the population sensitive, as also shown in Figure 40.

It is clear that there is no direct relationship between resistance and genetic inheritance. The selection of a more sensitive strain than usual shows that there is some genetic factor involved but the RNA in each UV resistant type does not confer the possession of characters that produce that type, progeny being a mixture of the two types of resistance.

It is likely that either the S17 population was the result of some enviromental factor (host, growth temperature, media etc) or the result of a gene that controls the proportions of the particle.

Some experiments previously conducted (e.g. the target curve

Figure 40.

Inactivation of Two Clones of MS2, Selected for UV Sensitivity, by 254nm UV.

S17 and S17.1 (a lysate grown from a plaque formed from a plating out of S17) were irradiated by UV at 100 ergs mm^{-2} sec^{-1}.

Key.

0 S17

□ S17.1

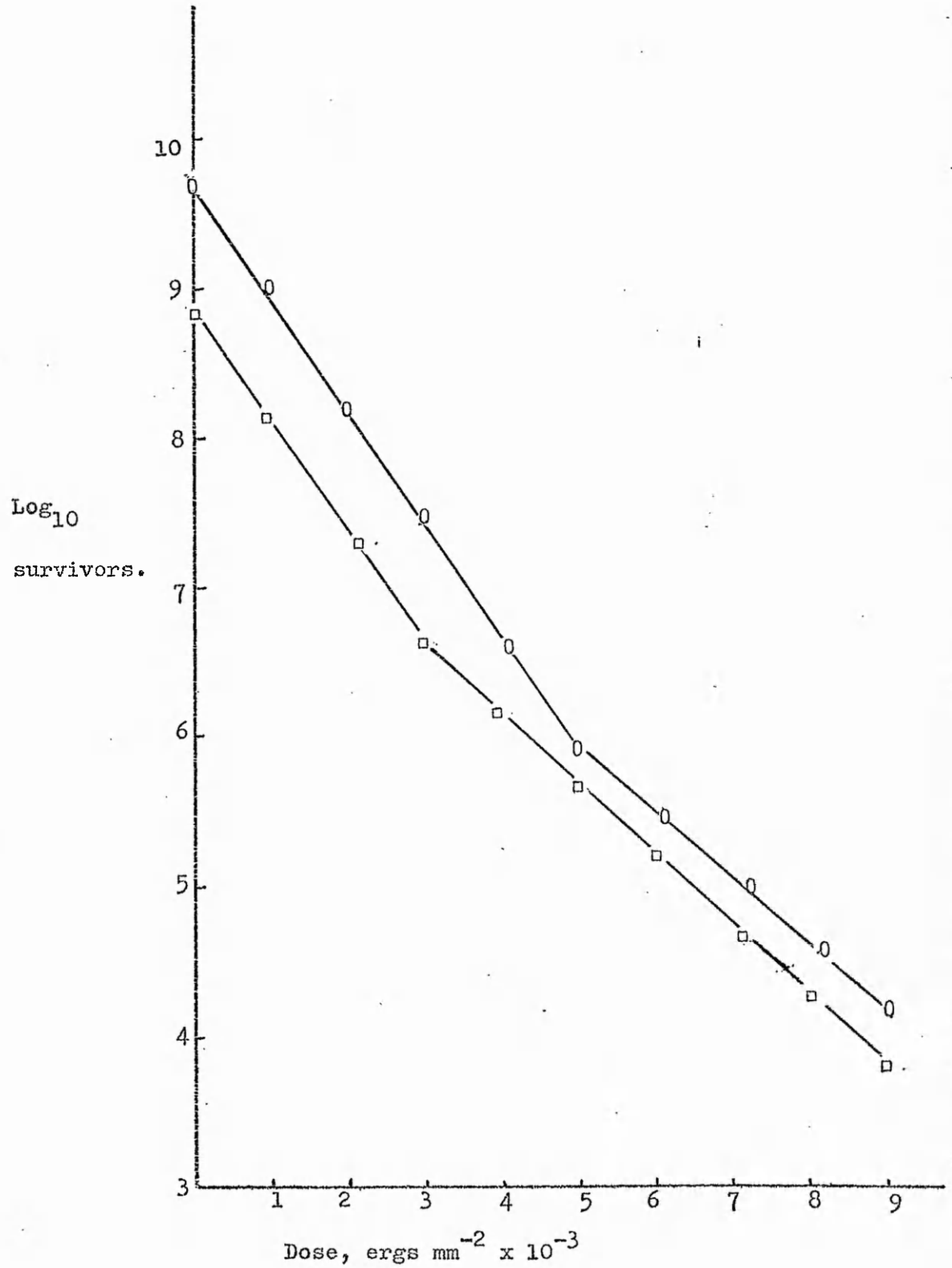
Log10 survivors.
10
9
8
7
6
5
4
3
1
2
3
4
5
6
7
8
9
Dose, ergs mm-2 x 10-3

experiment shown in Figure 30) did not have a two compartment curve, there being a true exponential decrease. Upon re-examination it was realised that the slope consisted of a resistant slope only, the sensitive viruses not being present. A chance observation made on a lysate of bacteriophage left out at room temperature overnight showed that the sensitive proportion of the virus population had disappeared. Figure 41 shows the inactivation rates of this lysate both before and after 12 hours at 20°C. It is interesting that none of the resistant viruses were inactivated by this treatment. The lysate used for the target curve experiment shown in Figure 30 had probably lost all the sensitive viruses and that particular experiment must only refer to resistant phage.

g) X-Ray Inactivation of MS2.

The two types of MS2, sensitive and resistant are not genetically different as any one 'type of particle gives rise to both types of virus. The viruses are also sensitive and resistant to other agents, as the inactivation of the sensitives overnight has shown.

MS2 produces many different types of particle during the course of an infection and it was thought that perhaps there was some structural difference between the two forms. UV is assumed to inactivate by causing dimers (53) in single stranded RNA viruses. X-rays inactivate by a different mechanism, mainly by nucleic acid chain breaks and chain linkages. X-rays are also absorbed equally by protein and nucleic acids alike, although it is the damage to nucleic a acids that account for the inactivation. If the two forms of MS2 were resistant and sensitive to X-rays too, then this must reflect a difference between the nucleic acids and the two types of particle.

Figure 41.

UV Inactivation of MS2 Treated at 20°C for 12 Hours.

Key.

X Lysate before treatment

0 Lysate after 12 hours at 20°C

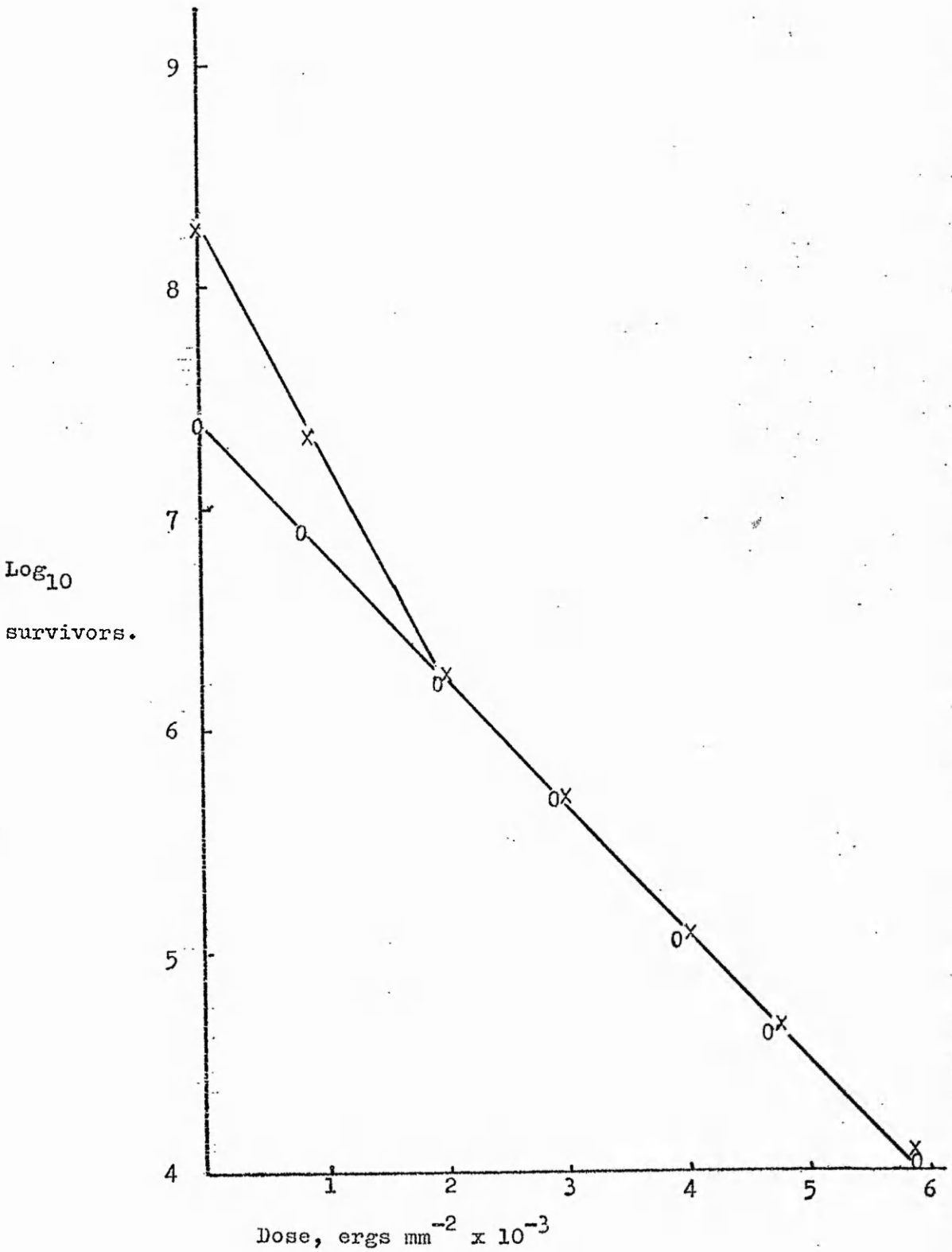
9
8
7
6
5
4
1
2
3
4
5
6
Log10
survivors.
Dose, ergs mm-2 x 10-3

i) Calibration of X-ray source.

10 ml of X-ray actinometer (see methods) were exposed to X-rays for 10 and 20 minutes. The absorbance at 305nm was measured and the concentration of ferric ions deduced from the calibration curve. (The calibration curve of 0.1 uM g^{-1} to 1 uM g^{-1} Fe^{3+} is shown in Figure 42).

10 min O.D. 0.28 = 0.24 uM Fe^{3+} g^{-1}

20 min O.D. 0.6 = 0.5 uM Fe^{3+} g^{-1}

Since 1 uM Fe^{3+} g^{-1} = 6.2×10^4 rads, then

0.24 uM Fe^{3+} g^{-1} = 1.488×10^4 rads in 10 minutes

0.5 uM Fe^{3+} g^{-1} = 3.1×10^4 rads in 20 minutes

Therefore the output of the X-ray machine is 1.5 kilorads min^{-1}

ii) Inactivation of 'Resistant' and 'Sensitive' MS2 by X-Rays.

Resistant MS2, made by overnight inactivation of the sensitive strain, and the S17 clone of MS2 were exposed to X-rays. Figure 43 shows the results of this inactivation. The UV res virus, which shows only one inactivation rate with UV, shows a marked two phase inactivation with X-rays. The S17 clone also shows a two phase inactivation. The first phase of the res virus, however, is more resistant than the first phase of the S17 clone. The second phase of the res strain is also more resistant than the second phase of S17. Therefore res is more resistant to X-radiation than the sens component. The second phase of S17 is more resistant than the first phase of res. This argues that the second phase of inactivation probably has nothing to do with different types of virus particle, but is an artifact of the experimental system. X-rays can inactivate directly or through the mediary of free radicals produced in the suspension. A free radical supressor was investigated to see if

Figure 42.

Calibration Curve for X-Ray Inactivation.

Optical Density at 305nm against uM Fe^{3+}.

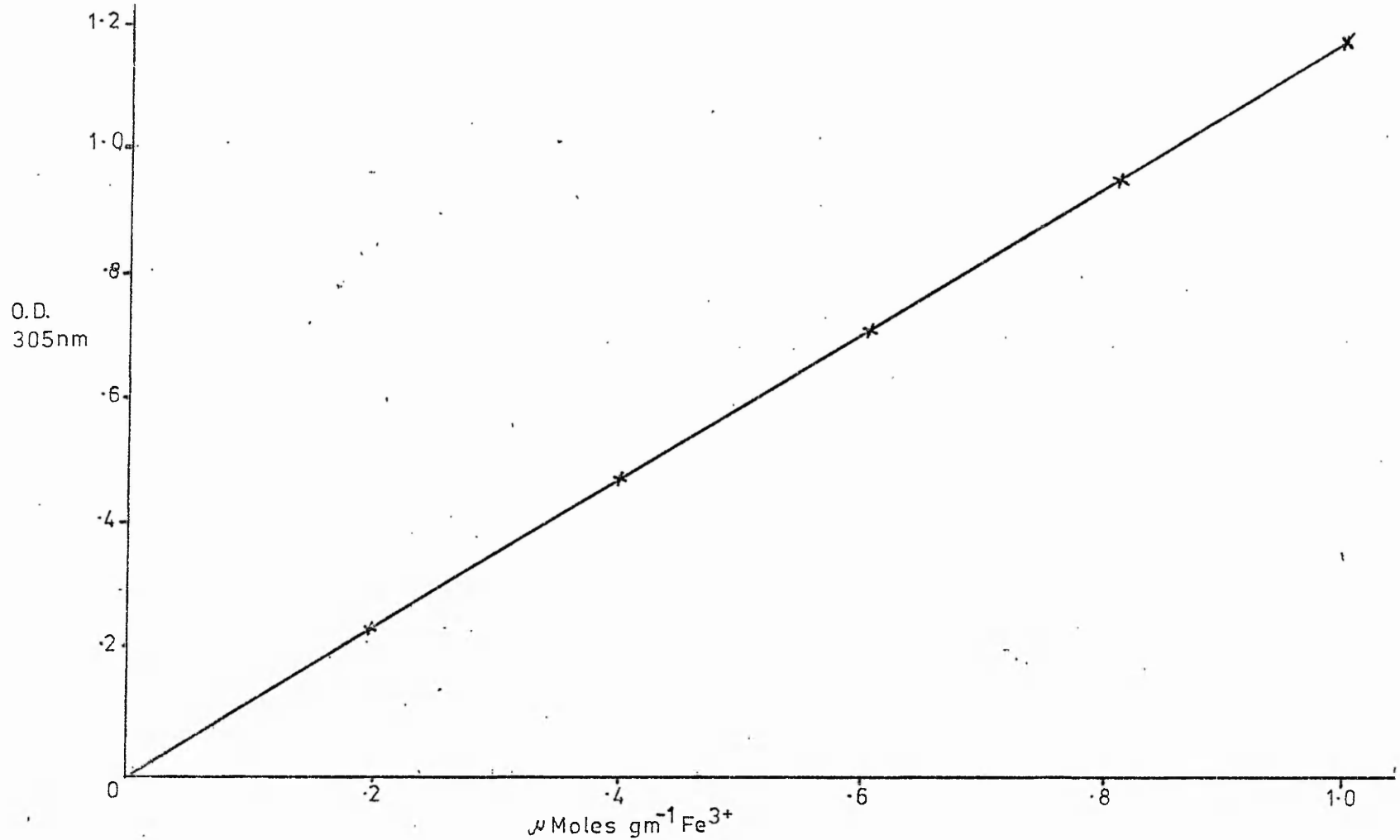
1·2
1·0
·8
·6
·4
·2
0
O.D.
305nm
·2
·4
·6
·8
1·0
μ Moles gm⁻¹ Fe³⁺

Figure 43.

X-Ray Inactivation of Resistant and Sensitive Components of MS2.

Key.

O Resistant, made by overnight exposure to 20°C.

X Sensitive, clone S17, high proportion of sensitive virus.

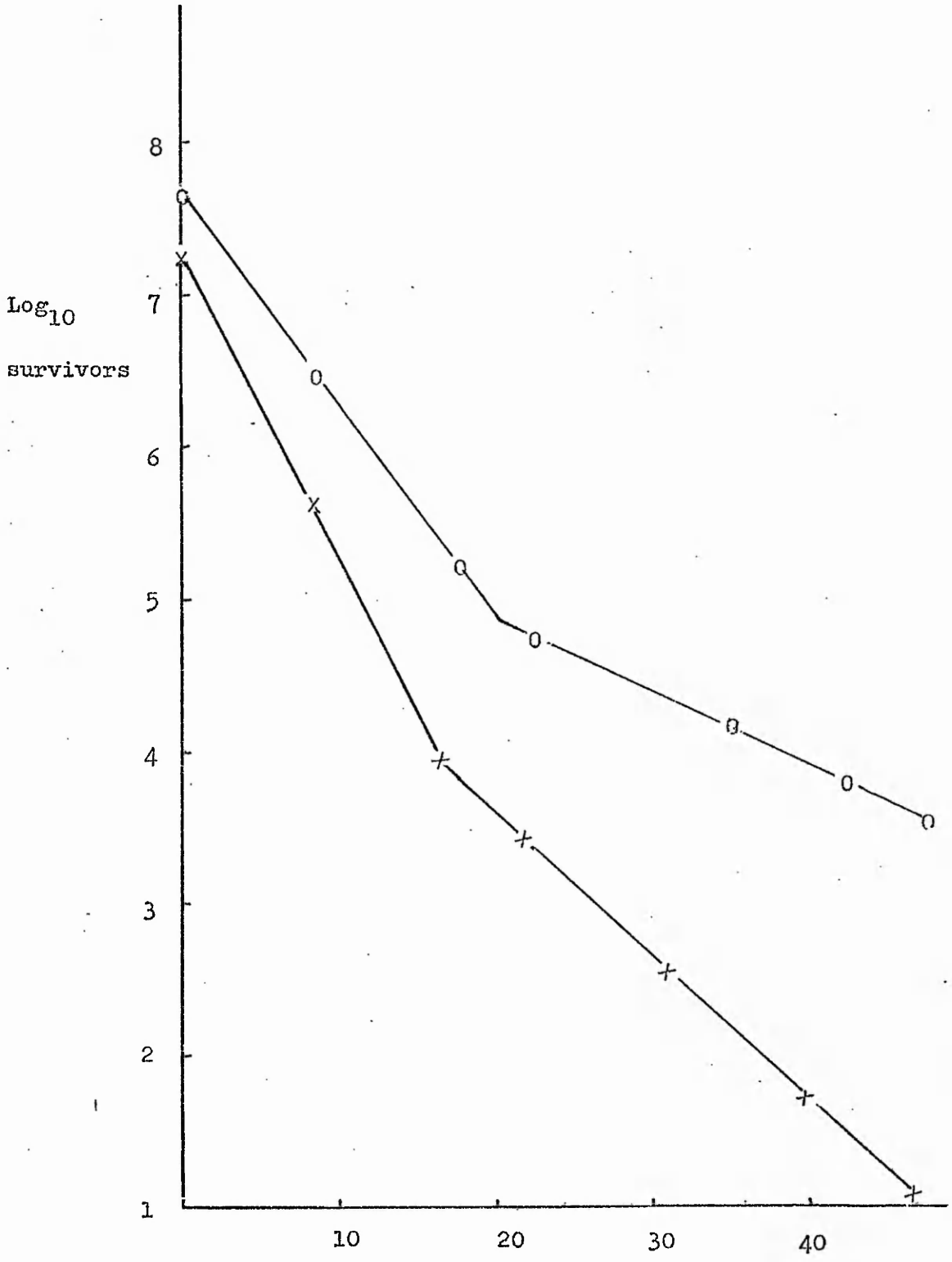
Log10
survivors
8
7
6
5
4
3
2
1
10
20
30
40
kilorads X Irradiation.

this would reduce the two rate inactivation to a single rate, but the mercapto ethanol used as the suppressor was found to inactivate the viruses quite rapidly.

Some viruses, such as rasberry ringspot virus, contain more than one copy of the virus genome (140), further, RRV, a nepovirus, produces three different particles, one with one molecule of RNA (M.W. 1.4×10^6), one with a 1.4×10^6 M.W. RNA and an RNA of 2.4×10^6 and a third type with two 1.4×10^6 M.W. RNA (140,141). The possession of more than one copy of a genome would affect the response to UV. However there has been no suggestion of there being any variability of the number of genomes in MS2 or that the individual ones vary in molecular weight.

It is clear from the UV data and the X-ray data that there is a physical difference between the two particles, the target area to both X-rays and UV is different and since UV and X-rays inactivate the RNA in different ways, this physical difference must lie within the RNA. If the RNA is the same in both particles, one possibility is that the secondary or tertiary structure of the RNA is in some way different.

h) Heat Inactivation of MS2.

Bacteriophage left overnight at 20°C lost the UV sens proportion of their populations (Figure 41). Inactivation of MS2 under more controlled conditions was carried out to see if different temperatures would produce selective inactivation of MS2. Heat inactivation was undertaken at 37°C, 45°C, 60°C and 20°C. All the inactivations were carried out with 1/100 dilutions of lysate in distilled water. Inactivation at 37°C took 10 hours to reach 99% inactivation (shown in Figure 44a), at 45°C, 5 hours (Figure 44b),

Figure 44a.

Inactivation of MS2 at 37°C.

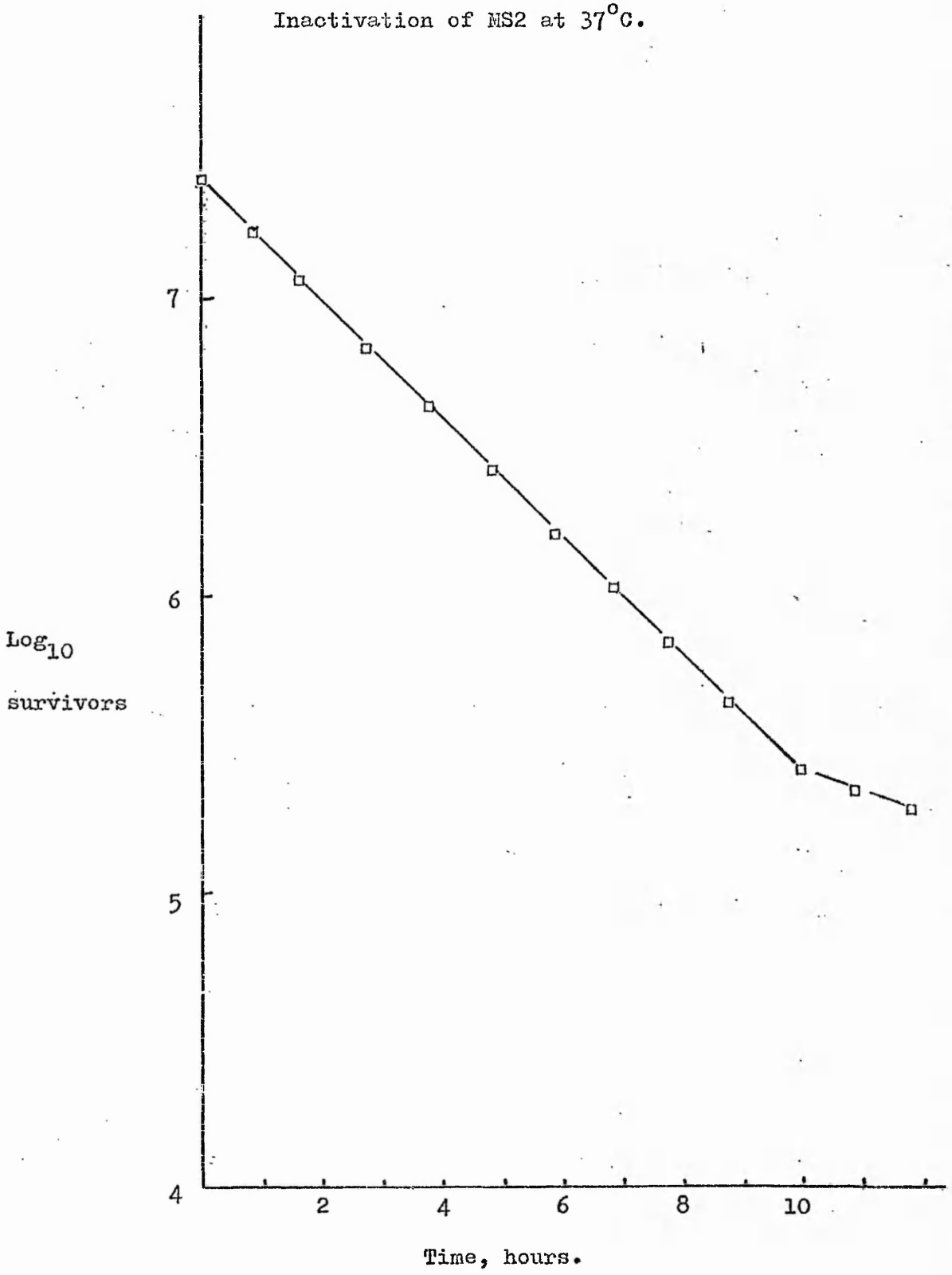

Figure 44b.

Inactivation of MS2 at 45°C.

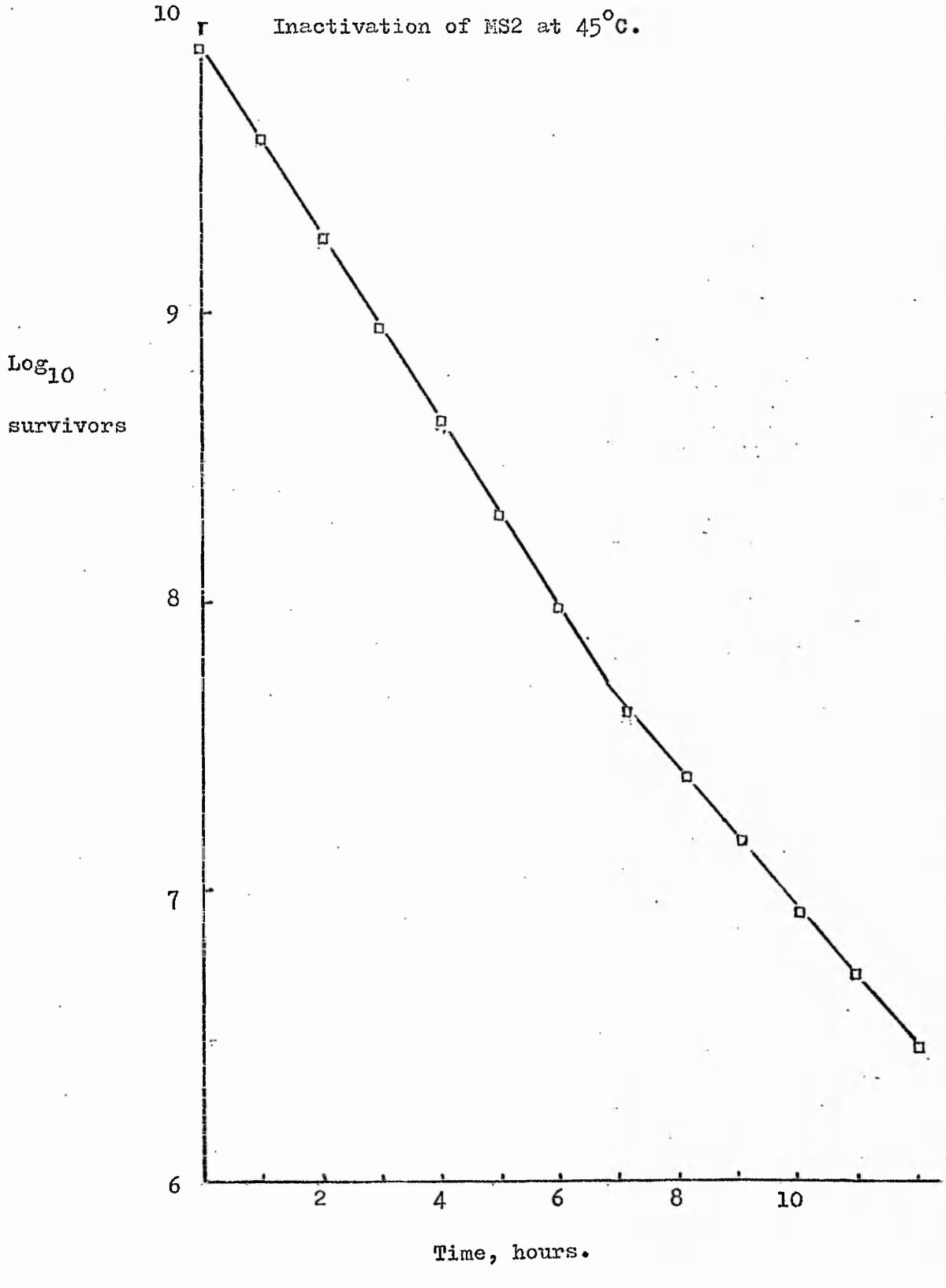

Figure 44c.

Inactivation of MS2 at 60°C

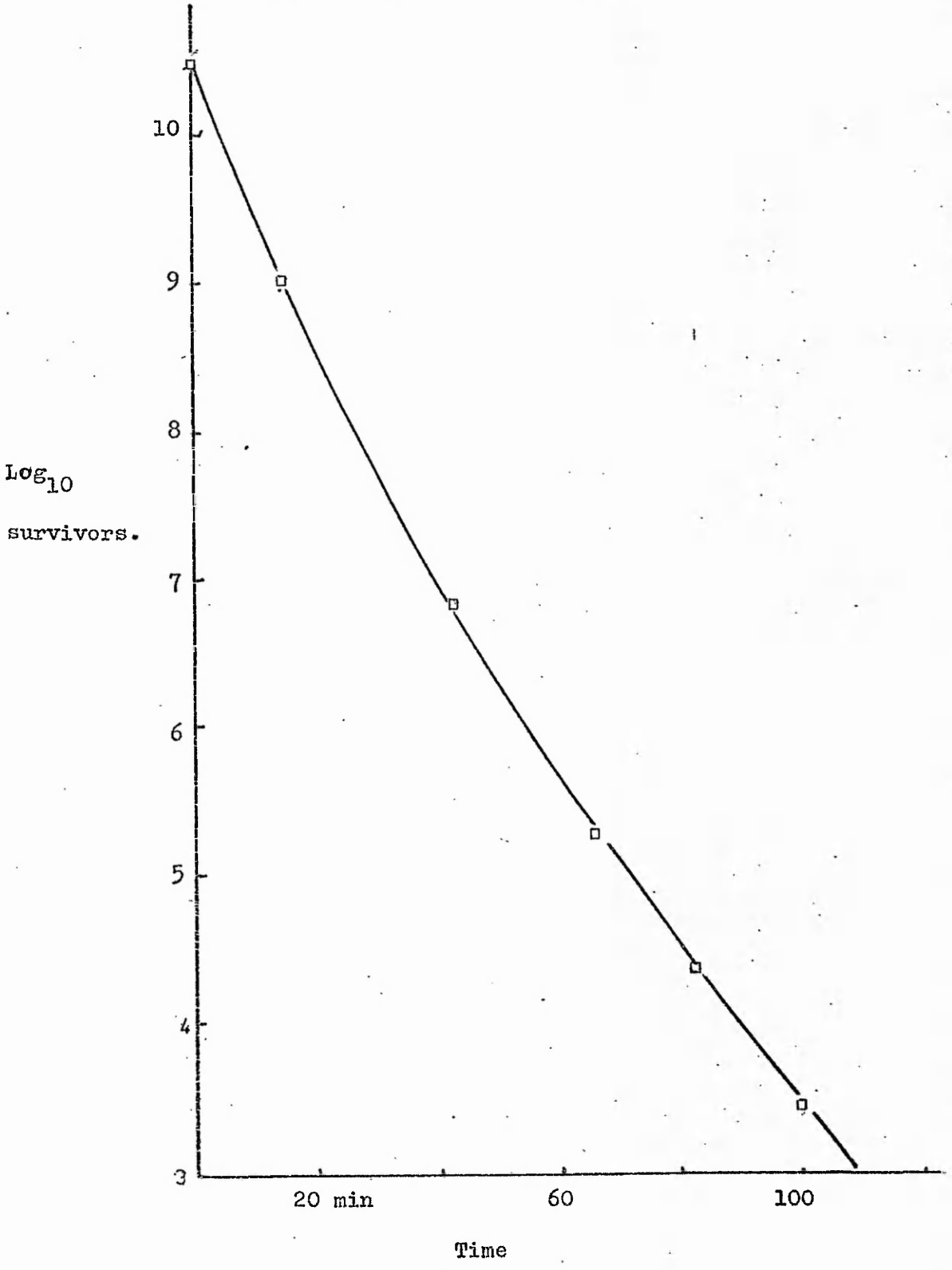

and at 60°C, 30 minutes. Although a sensitive/resistant difference can just about be seen in all the inactivations, the ratio between the slopes is different at each temperature, there being hardly any difference between sens and res at 60°C. At 20°C there is an initial overnight drop down to the res component, which is then stable for a few days, gradually dropping in titre, about 90% a week, as shown in Figure 44d.

Thus it is clear that MS2 produces two types of particles, sensitive and resistant to UV, heat and X-rays, that differ in some physical way. This difference is not inherited (although the proportions of sens to res might be genetically controlled).

The presence of extra genetic material in one would give a greater cross sectional area and lead to sensitivity. The D37 (254nm) of sens at 720 ergs mm^{-2} is 1.5 x less that of res at 1,100 ergs mm^{-2}. To account for the difference in sensitivities by this model would call for sens to have about 1.5 x the genome of res. The work of Fiers et al (1,2,3,) and others who have determined the M.W. of the virus (142) would have noticed a discrepancy of this magnitude.

One possibility to account for the difference between the two types of sensitivity would be a difference in the structure of the RNA within the capsid. If one RNA molecule were wrapped tightly, it was reasoned, this molecule might interact more with itself and thus experience more lethal photoproducts than a molecule less tightly wrapped. UV products produced in a 'tight' genome might be more likely to cause cross-links, dimers and other lethal effects. Conversely, a loose genome might be more susceptable to free radicals produced in the water during irradiation.

Assuming that packing was different between the two components,

Figure 44d.

Inactivation of MS2 at 20°C.

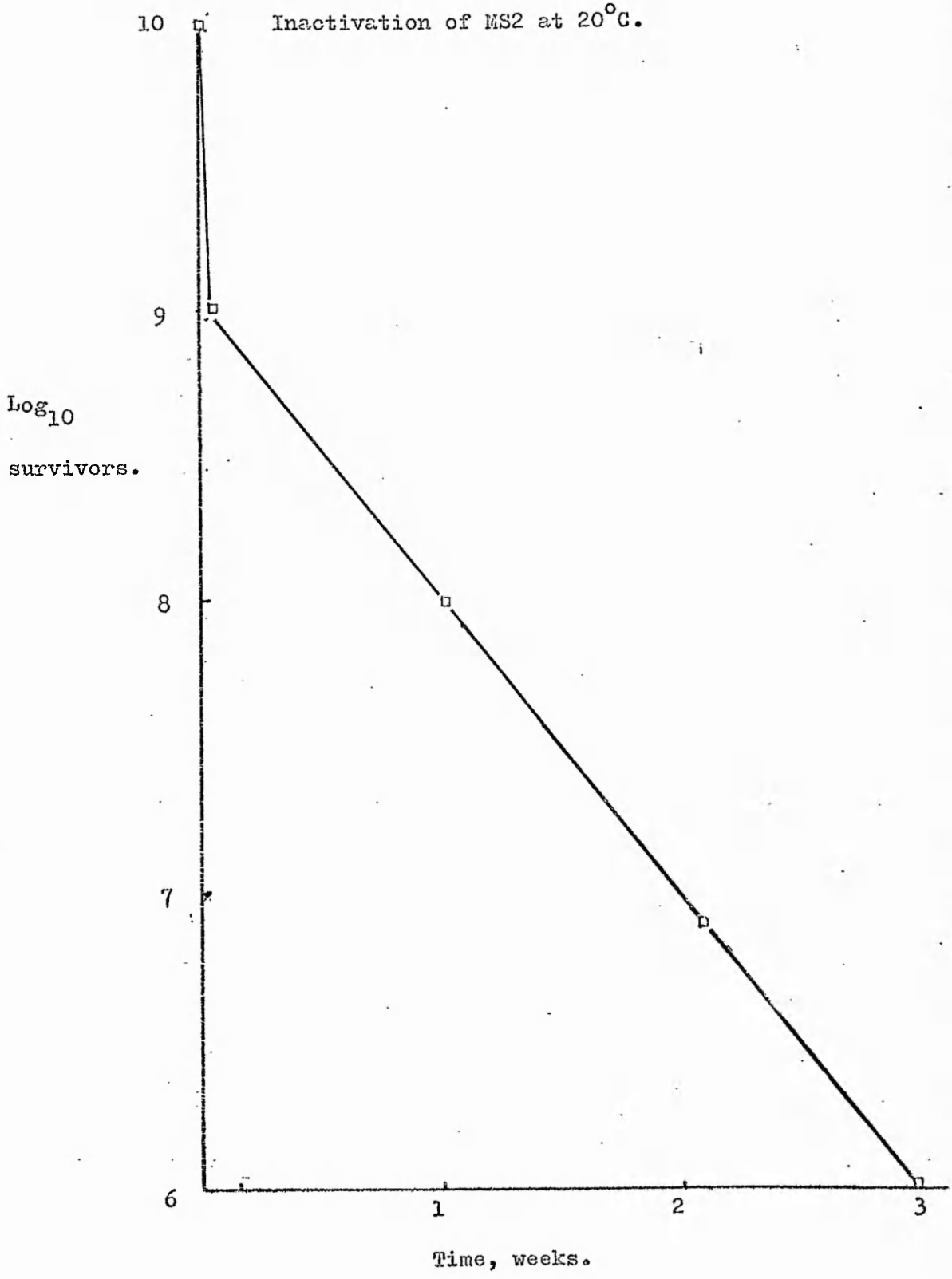

it was wondered if other physical propeties of the particle had changed in consequence, for instance the surface charge and the density. It was thought that a density difference might be shown if the RNA were structured into tight and loose, and if this were so, then the two density forms reported by Rohrmann and Kreuger (83) might be the two physical forms of sens and res.

i) UV Inactivation of the H and L forms of MS2.

Rohrmann and Kreuger named the heavy and light density forms of MS2 H and L. They separated MS2 on a 55% w/v caesium chloride density gradient and characterised the particles (see introduction).

Figure 45 shows the pfu ml^{-1} of fractions from a 55% $CsCl_2$ gradient. As reported by Rohrmann and Kreuger, two infectious fractions, one with a density of 1.46 g cm^{-3} and the other with a density of 1.44 g cm^{-3} were obtained. The lighter form was a white opalescent ring while the dense form was a pale yellow colour.

Figure 46a shows the results of irradiating a 1/1000 dilution of the pooled $CsCl_2$ peaks of infection in distilled water. The H and L fractions show different rates of inactivation, H being more sensitive than L. These rates are not the same rates as the sens and res rates of the original virus stock, H being more resistant than sens and L being more sens than res.

When the fractions from the $CsCl_2$ gradient were dialysed against 0.1 M Tris and diluted 1/100 in distilled water, the UV inactivation rates of H and L (shown in Figure 46b) showed the same inactivation rates as sens and res, H being sens, L being res.

The two density forms are therefore the physical forms of the sens and res components of the virus population.

The $CsCl_2$, it is surmised, had penetrated the particles and in

Figure 45.

Separation of MS2 by Caesium Chloride Density Gradient Centrifugation.

Pfus ml^{-1} against fraction number.

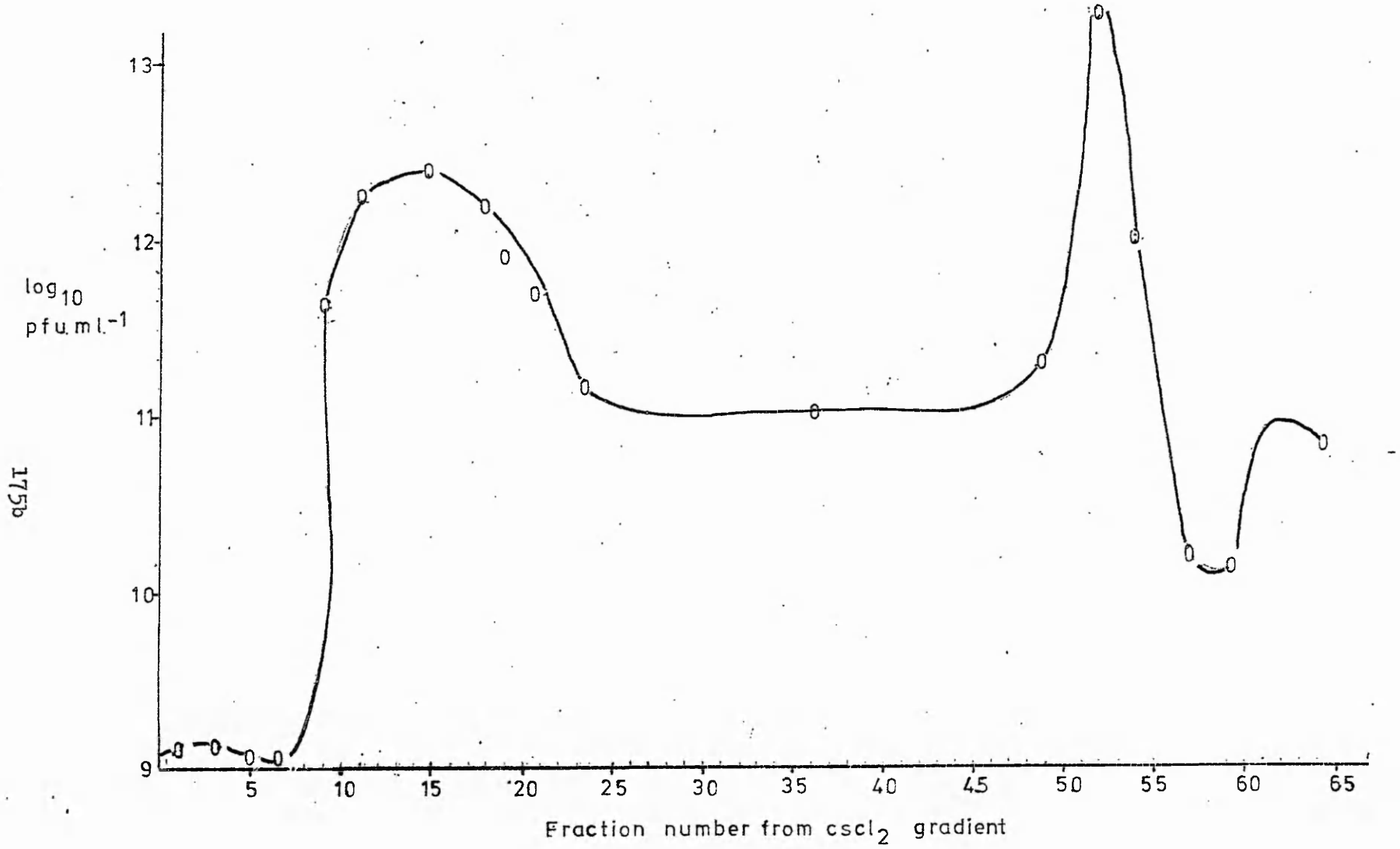
13
12
11
10
9
log10 pfu.ml.-1
175b
5
10
15
20
25
30
35
40
45
50
55
60
65
Fraction number from cscl2 gradient

Figure 46a.

Inactivation of H and L forms of MS2 by 254nm UV 1/1000 dilution of $CsCl_2$ fractions in distilled water.

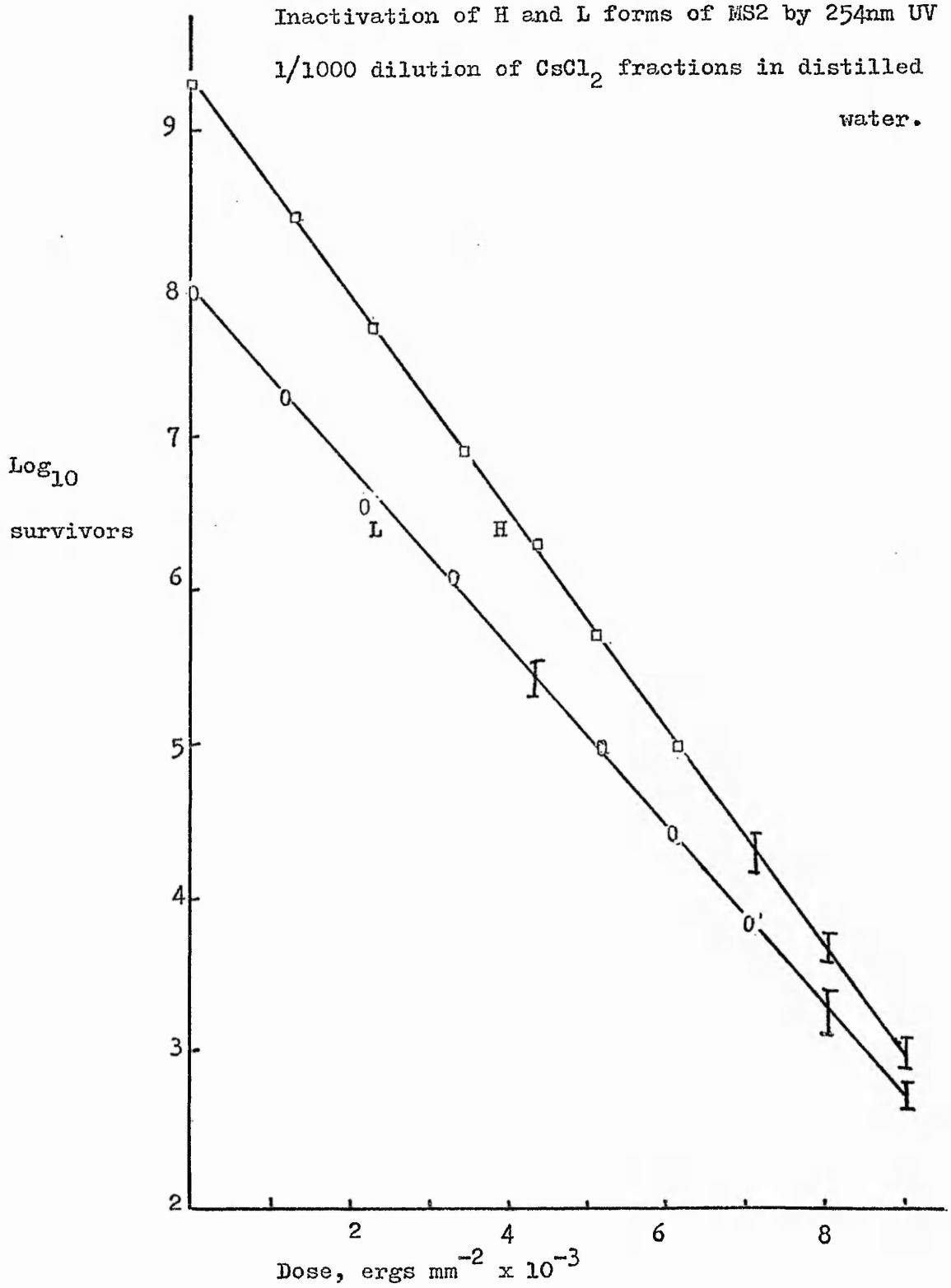

Figure 46b.

Inactivation of H and L Forms of MS2 by 254nm UV. 1/100 dilution of dialysed fractions in distilled water.

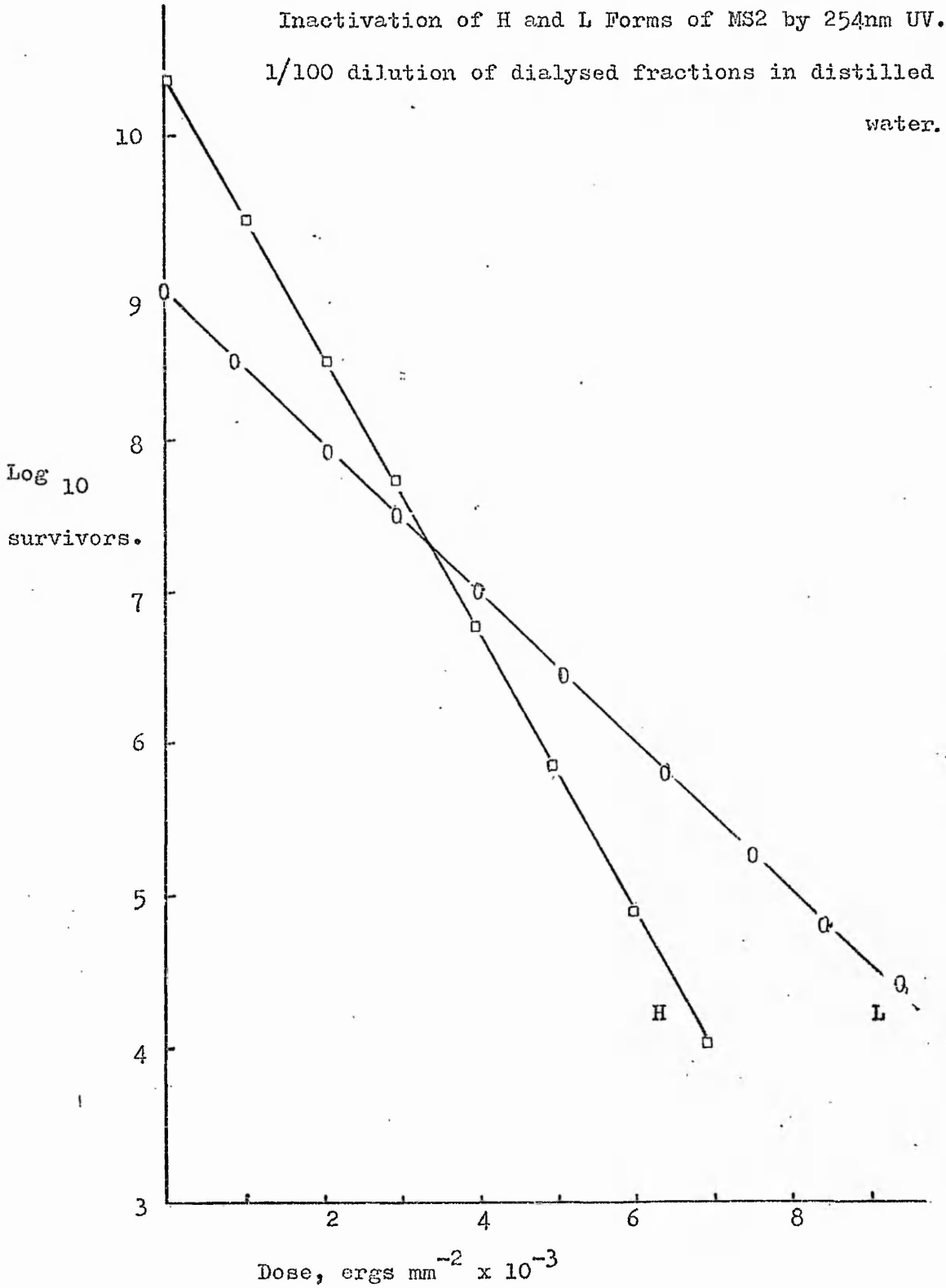

some way affected the resistance, perhaps by stabilising the RNA.

Rohrmann and Kreuger investigated other properties of these particles and showed that the sedimentation rates were the same. Each had the same amount of RNA A protein and were equally sensitive to ribonuclease. The two particles were shown to be identical serologically, measured by neutralisation and by immunodiffusion techniques. The discovery that these forms have different sensitivities is the first indication that these particles are different in some fundemental way.

j) Separation of Two Iso-Electric Forms of MS2.

It was thought that if the genomes of MS2 could be either loose or tightly packed, not only would there be a density difference but there might be surface changes as well. The charge on the surface of virus particles has been measured by gel electrophoresis and by free flowing electrophoresis systems (104,143).

Irwin (personal communication, 122) had determined the iso-electric point of MS2 and had found slight evidence for two populations with different iso-electric points. The major peak was at pH 7.0 and there was a slight peak at pH 4.0. It is known that low pH inactivates MS2 and that acrylamide gels are toxic. It was therefore decided to run lysates and the H and L fractions in agarose gels for electrophoresis at $4^{o}C$ for as short a time as possible.

Figure 47 shows that when the H fraction was run on the gel, only one fraction was found, a peak at pH 4.0 (the pH gradient is also shown on the graph). Figure 48 shows that the L fraction has only one iso-electric point at pH 6.8. The lysate, containing H and L forms has two iso-electric peaks, a major one at pH 4.0 and a minor one at pH 7.0. The H and L forms therefore consist of only one type of iso-

Figure 47.

Electrophoresis of the H Fraction of MS2.

pH gradient shown as a straight line.

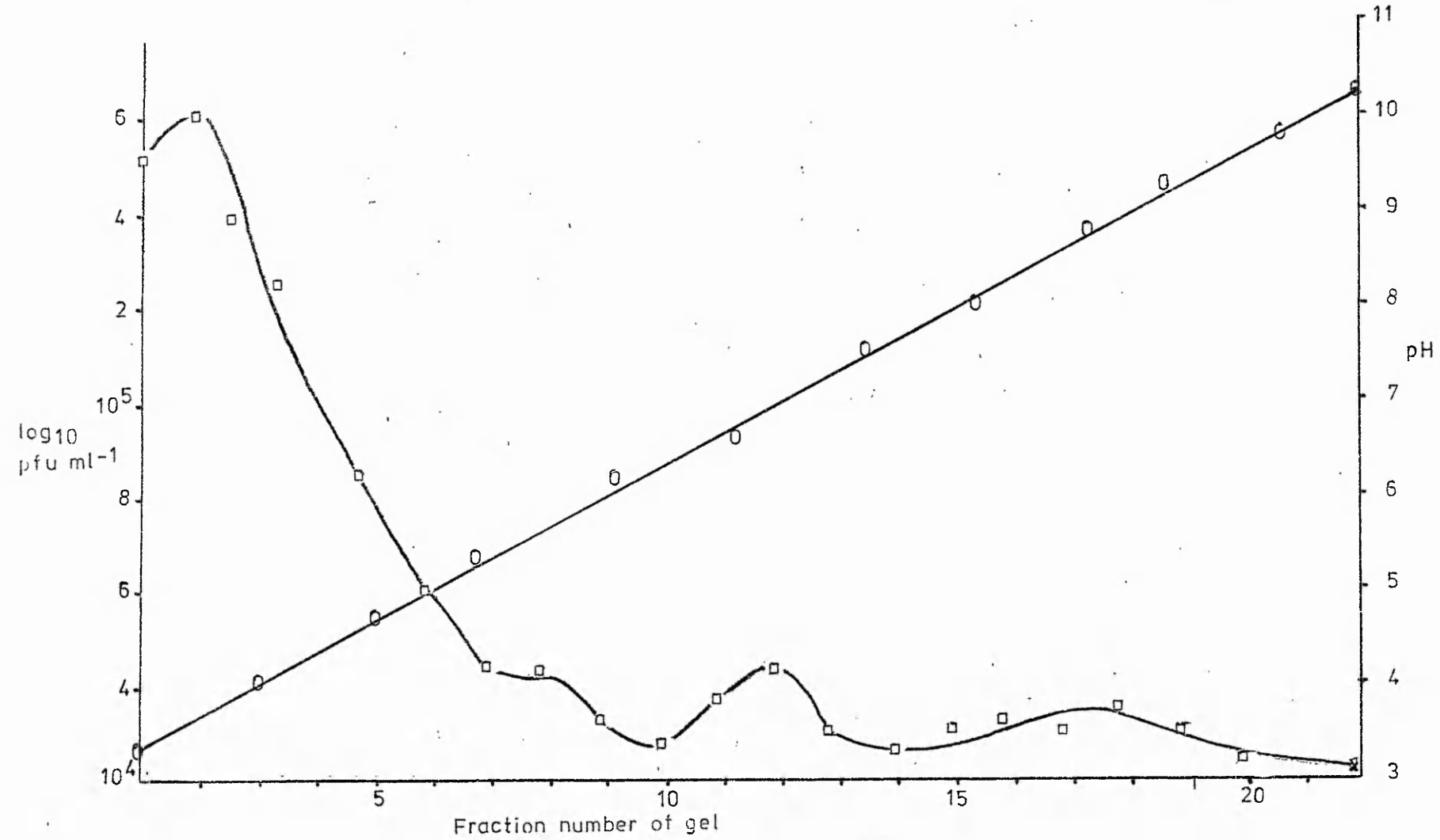
log10 pfu ml-1
pH
Fraction number of gel
6
4
2
10^5
8
6
4
10^4
11
10
9
8
7
6
5
4
3
5
10
15
20

Figure 48.

Electrophoresis of the L Fraction of MS2.

pH gradient shown as a straight line.

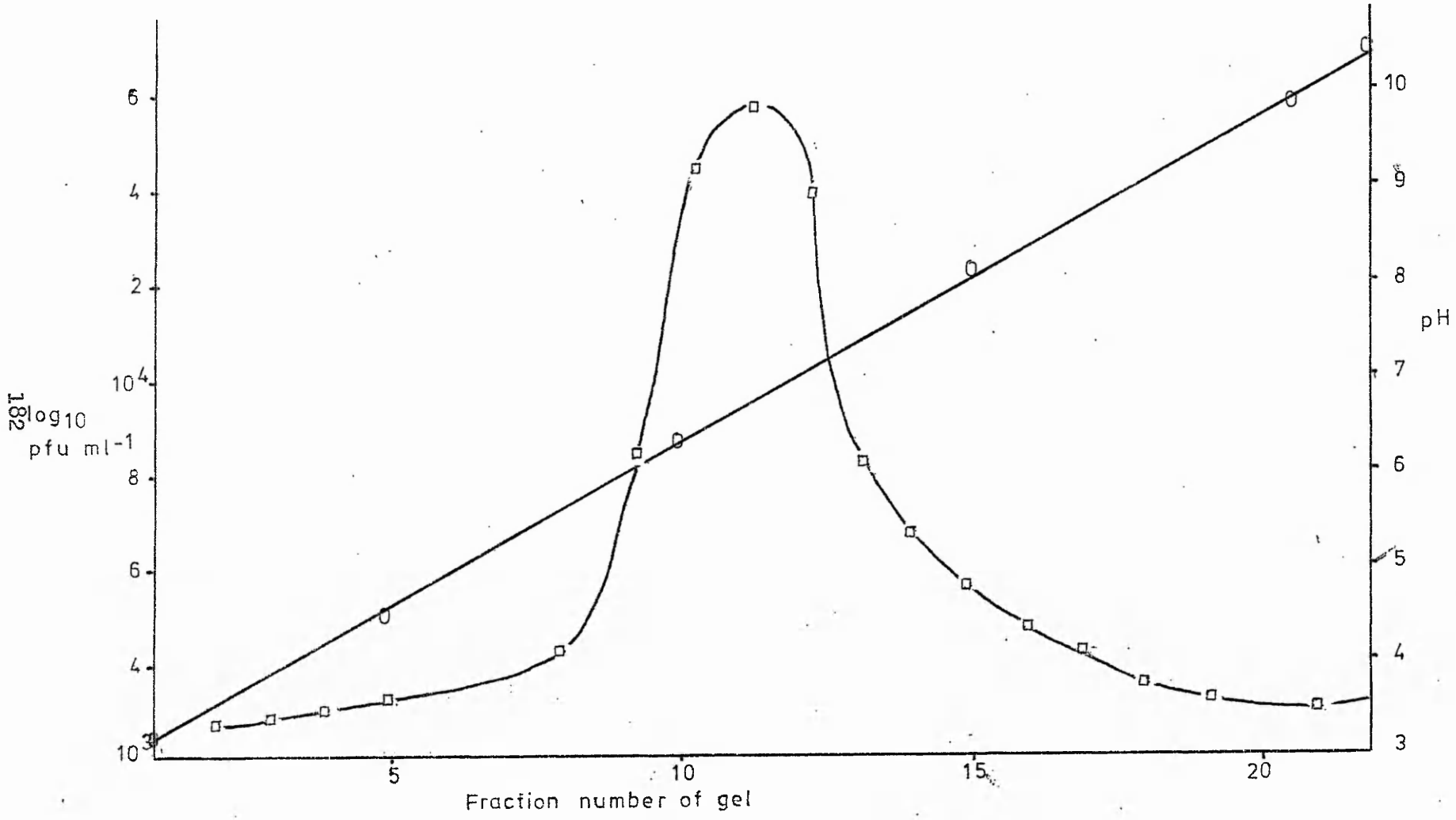
182 log10 pfu ml-1
6
4
2
10^4
8
6
4
10^3
5
10
15
20
Fraction number of gel
10
9
8
7
6
5
4
3
pH

Figure 49.

Electrophoresis of Lysate of MS2.

pH gradient shown as a straight line.

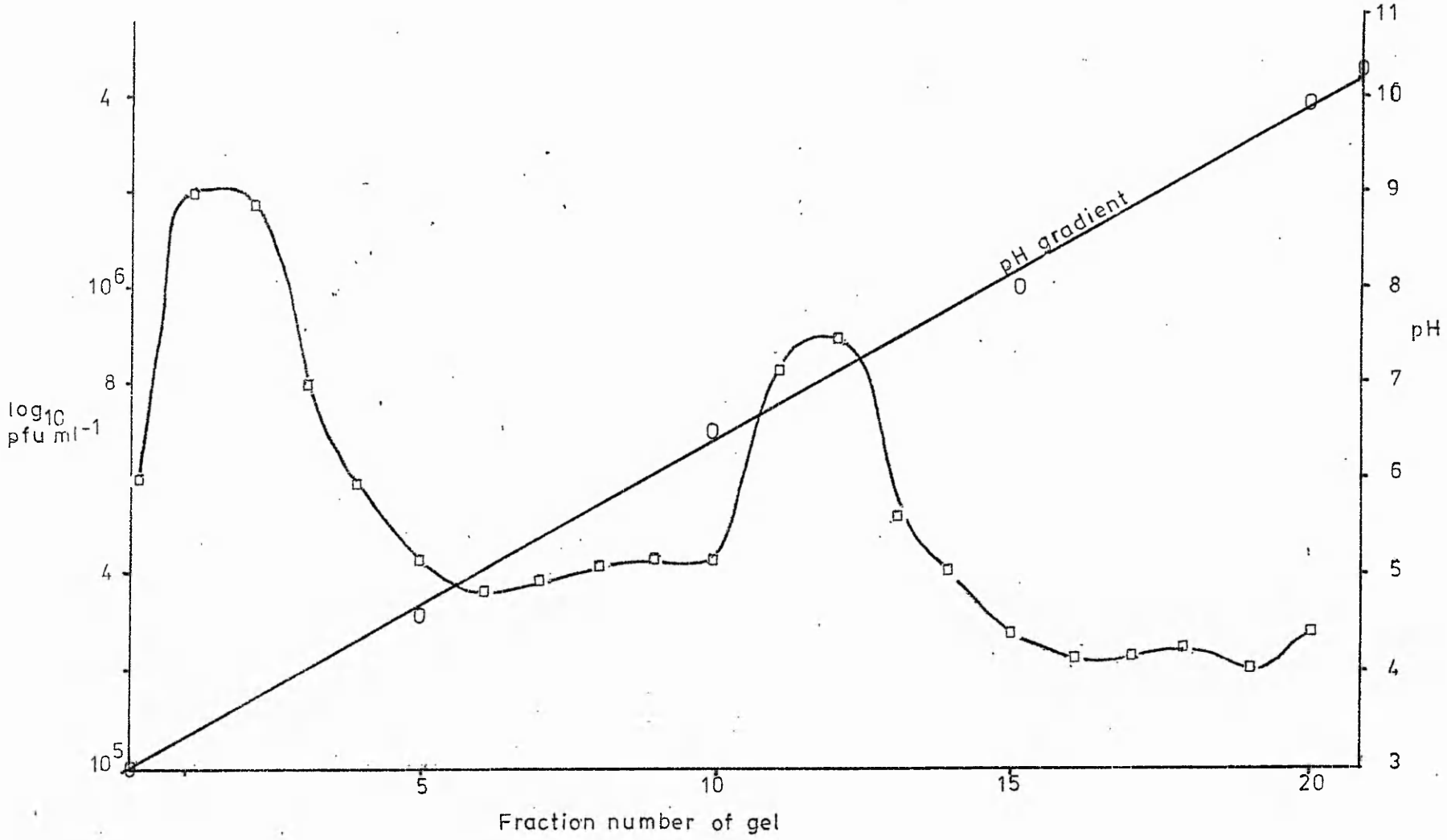
log10 pfu ml-1
4
10^6
8
4
10^5
pH gradient
pH
11
10
9
8
7
6
5
4
3
5
10
15
20
Fraction number of gel

electric point. When the separated particles were inactivated by UV, the pH 4 form was UV sensitive and the pH 7 form, the minor population, was shown to be UV res. Figure 50 shows the results of this inactivation on the separated viruses.

MS2 therefore consists of two types of particle of differing density and iso-electric point and each particle having a different resistance to UV, X-rays and heat.

These findings might be interpretable in connection with the model propsosed by Matthew and Cole (84) for RNA phage structure. They proposed that the coat protein has basic amino acids on the inside and acidic ones on the outside. Normally the virus is acidic (see Figure 9) but if the capsid were stretched the basic amino acids could affect the overall charge. This could account for the pH 4.0 (acidic form) and the pH 7.0 (basic amino acids neutralising the acidic ones) form. Stretching the capsid would also affect density but not the sedimentation velocity. Since the RNA is affected in the expanded virus, it may be that either the RNA has caused a change to the capsid or that a change to the capsid has affected the RNA. Matthew and Coles' model of bacteriophage structure and the results of Budowsky et al (63, see introduction) argue that there is a close relationship between the RNA and coat protein.

Budowski et al investigated the photoproducts formed by UV irradiation of MS2 and found evidence for RNA-protein links at 254nm. They suggested that these cross links accounted for about half of the inactivation. It is possible that a loose genome, not in contact with the coat protein would not form many of these links and thus be more resistant than a form that had close contact with the coat protein. This might be tested for by assaying for RNA-protein photo-

Figure 50.

Inactivation of Iso-Electric Forms of MS2.

Separated pH 4.0 form and pH 7.0 form at 254nm.

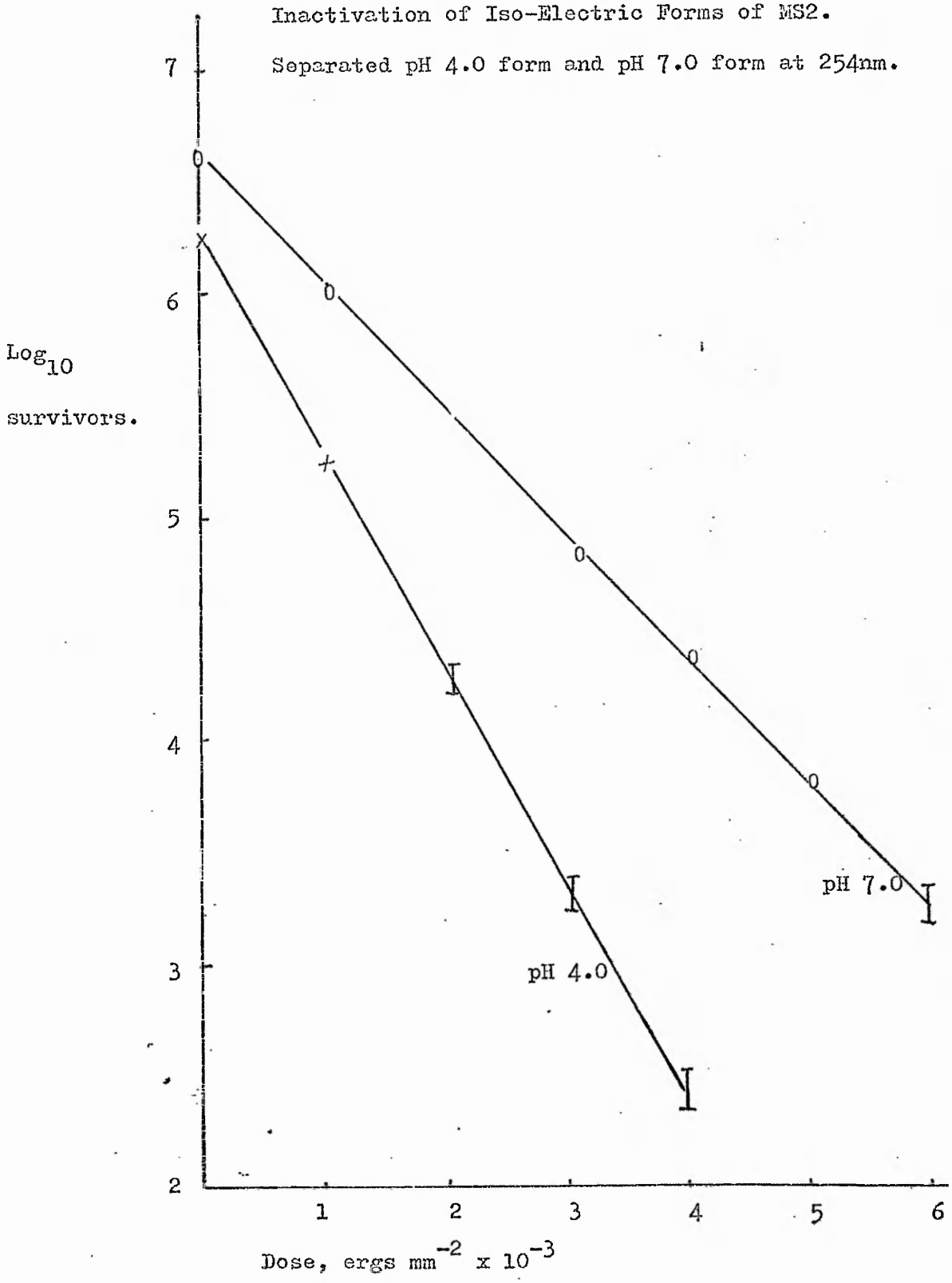

products in H and L forms after irradiation. More RNA-protein links should be formed in H than L viruses.

Why these two forms occur is not clear, A protein mutations are known to affect capsid structure (79), it might be possible that a certain percentage of A proteins are changed in some way, either by read through of the A protein cistron, as in QB coat protein, or by host modification, as in Broad Bean True Mosaic Virus, where host factors are known to affect the structure of the virus (144). BBTMV has three electrophoretic forms, and the host can influence the predominance of one form over another. Capsid proteins might also be changed by the host or by read through, although antigenic changes would be expected if that were so.

Differences in the amount of water contained in each particle might cause different resistances. A loose particle could contain more water than a tight particle which would create more hydration products in the looser particle, and these are known to be less lethal than other photoproducts. This might be tested by using heavy water as a suspendant, less hydration products would be expected in the virus because of the isotope effect (more energy is needed to make a heavier isotope react with the other molecules). If the particles became more resistant, this would show that water was an important intermediary in the photochemical damage of the nucleic acid. This theory does not explain the difference between the heat sensitivities of the two types however.

Fiers et al (1,2,3) have suggested a secondary structure for MS2 RNA based on their primary structure and chemical evidence. They propose that at least 80% of the bases are paired, but there is conflicting evidence over this point (see introduction). It might be

possible that there are two secondary structures of the RNA, tight and loose. If this did occur, then the two types should show different numbers and types of photoproducts, not necessarily lethal ones, which could be analysed (53,63,88). Another method would be to irradiate the viruses with 20,000 ergs mm^{-2} UV to cross link the RNA, extract it and analyse which areas of the RNA are most drastically affected, any difference in structure would appear as different digestion products.

k) Inactivation of expanded particles of MS2.

Verbraeken and Fiers (81) noticed that expanded particles of phage (measured by sedimentation velocity) could be made by heating in a salt solution and that the particles could be made more compact again (though not back to the original sedimentation value). Evidence showed that this change involved the RNA molecule in some way. MS2 was therefore heated at $48^{o}C$ in 0.15 M NaCl for twenty minutes to see if expansion had affected UV resistance. Figure 51 shows the results of a normal lysate (sens and res) irradiated with UV after this treatment. Also shown on this figure are the results of re-compacting the particles (by diluting 1/10 in distilled water and then increasing the salt concentration to 0.15 M NaCl again).

Expansion had no effect on either component but re-contraction (from 50s - 65s) changed res to sens. It is as if the res form was slightly unstable and was changed into a more energetically stable form.

It is therefore suggested that the UV resistant form of virus (the L form) is an alternative structural form brought about by either an alternative structure of the RNA, which causes the capsid to expand, or an alternative structure of the capsid, which causes an alteration to the RNA. The resistant form is probably less inter-

Figure 51.

The Inactivation of Expanded and Re-Contracted Particles by 254nm UV.

Key.

- 0 MS2 heated in 0.15 M NaCl at 48°C for twenty minutes. Expanded to 45s.
- □ MS2 (Expanded) in 0.015 M NaCl
- X Untreated MS2 diluted 1/10 in 0.015 M NaCl.
- ▲ Re-contracted MS2, expanded phage in 0.15 M NaCl was diluted 1/10 in distilled water and re-suspended in 0.15 m NaCl

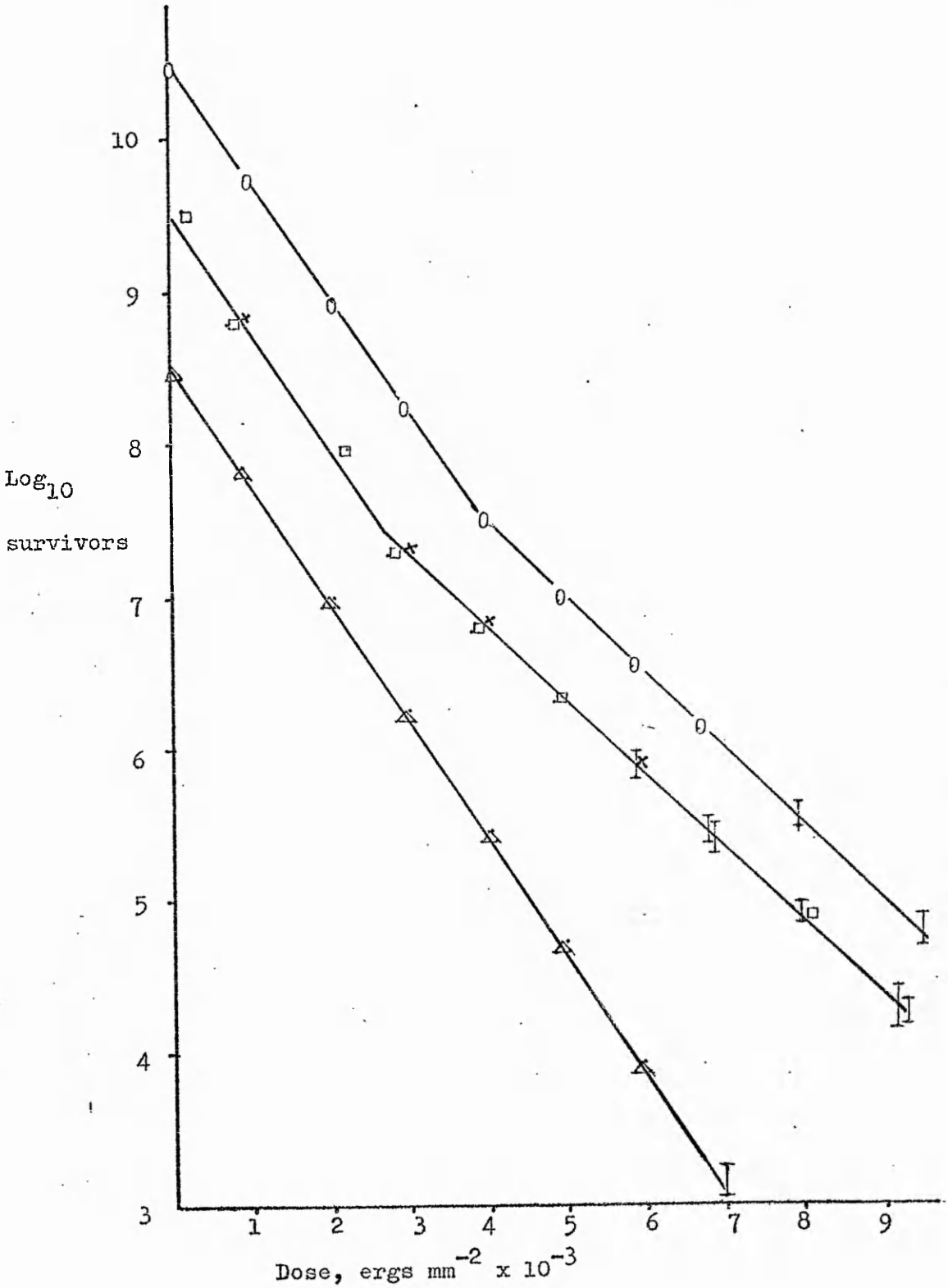
Log10 survivors
10
9
8
7
6
5
4
3
1
2
3
4
5
6
7
8
9
Dose, ergs mm-2 x 10-3

active with the coat protein. It is interesting to speculate on the chemical interactions of the main type of virus structure being more sensitive than the less common form.

Verbraeken and Fiers (81) made no mention of heavy and dense particles in their studies on the expansion of R17, so it is assumed that the results refer to the sensitive, heavy form. It would be interesting to see if the light form were affected in the same way by the expansion conditions. The light form, in being changed to sens by expansion and contraction, is obviously affected in some way. It would be interesting to see if it's density had changed with its UV sensitivity. Rohrmann and Kreuger report that the light form has an identical sedimentation velocity to the heavy, but that the light form is about $\frac{1}{5}$ as infectious as the heavy. Verbraeken and Fiers report that the expanded particle is about one third to a half as infectious. It is clear that the interaction of the RNA with the protein and the infectious process is little understood.

Inactivation of Bacteriophage QB by Ultra Violet Light.

QB is a single stranded male specific RNA bacteriophage slightly larger than MS2 (M.W. QB RNA 1.3 x 10^6, M.W. MS2 RNA 1.1 x 10^6). It also differes slightly in the structure of the capsid, where small amounts of read through protein, larger than the normal coat protein are present in small amounts in the normal capsid without interfering with function.

This virus was investigated to see if the sensitivity to UV was similar to MS2 and if two compartment curves could be observed. T.Vickers (118, personal communication) noticed two density forms of QB during a caesium chloride density gradient separation. The densities were much closer than in MS2, the lighter band being about 4 mm higher than the heavy, main band, but no measurements were made of the density.

A lysate of QB and a control suspension of MS2 were irradiated with 254nm UV. Figure 52 shows the results of this experiment and shows that there is no difference in the sensitivity of the virus to UV compared with MS2 (indicating a similar inactivation cross section) and that a two component curve is present, strong evidence for a similar sens-res phenomenon to MS2. The res component has a similar inactivation rate to the res component of MS2.

These results suggest that the resistance phenomenon might be common to other single stranded RNA male specific bacteriophages of E.coli, more related to MS2 than QB. It is therefore predicted that all male specific single stranded RNA bacteriophages have two density forms, two electophoretic forms and are similar in biological properties to the sens and res forms of MS2.

Figure 52.

Inactivation of Bacteriophages QB and MS2 by 254nm UV.

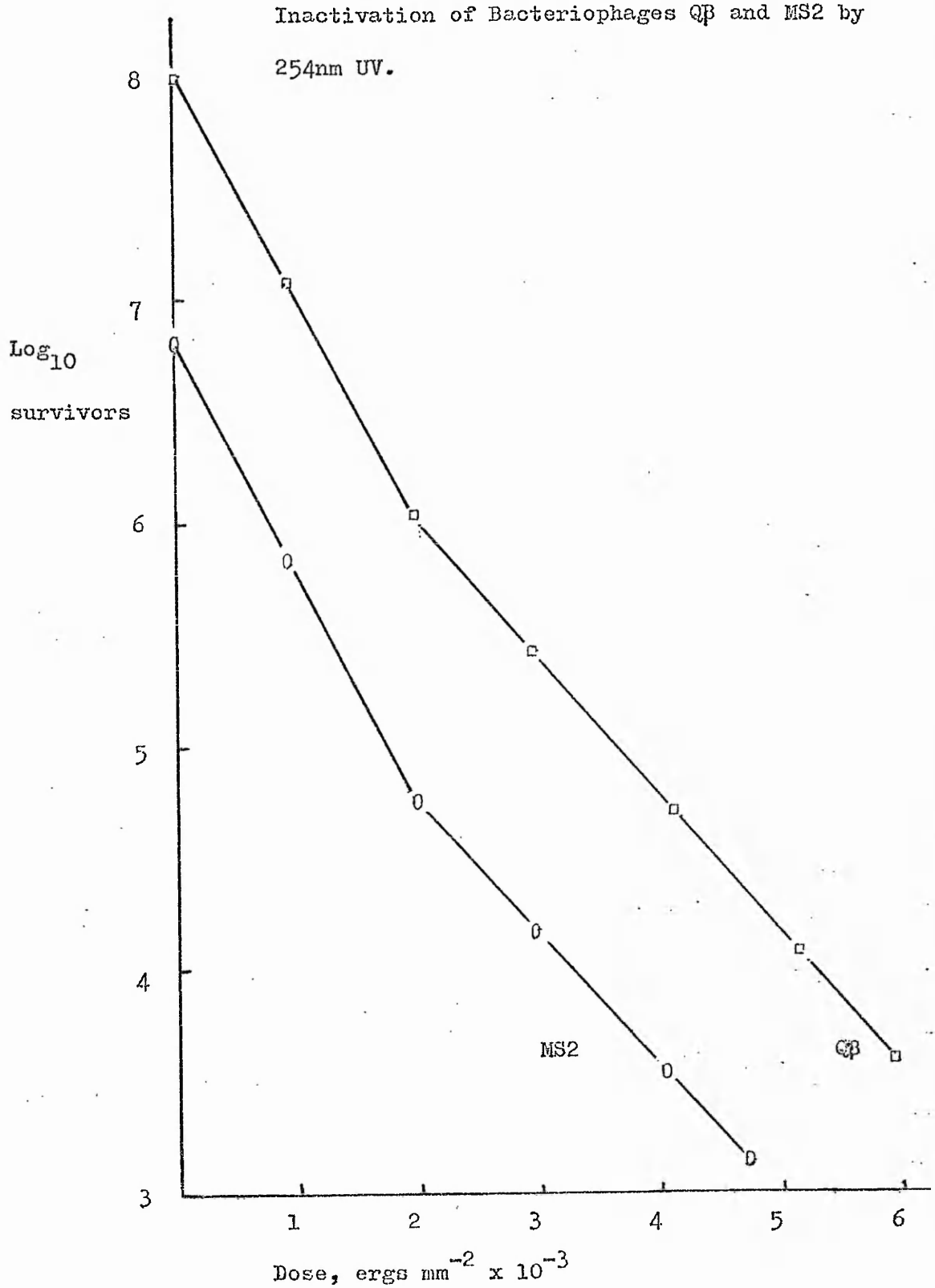

The Inactivation of Poliovirus Type 1 by Ultraviolet Light.

Poliovirus is another single stranded RNA virus, but with a much greater particle weight (8.4×10^6). There is much evidence for two structural forms similar to those found in MS2. Mandel (104), characterising Polio 1 by electrophoresis, found that there were two particles with different iso-electric points, one at pH 4.5 and another at pH 7.0. Heat treatment, antibody neutralisation and adsorption elution changed the pH 7.0 form into the pH 4.5 form. Heavy UV irradiation also had this effect.

Matossian and Garabedian (146) found that poliovirus showed biphasic resistance to sea-water inactivation. Rowlands et al (108) discovered that several vertebrate enteroviruses (all the ones they looked at, personal communication) had two density forms. Yamaguchi Koll et al (106) also found two density forms of poliovirus.

Taylor et al (145) in their studies of the UV inactivation of poliovirus showed data that could be interpreted as two component inactivation, but the data was too scattered to be accurate.

The inactivation of poliovirus by UV was therefore studied to see if two component inactivation took place, taking care over the reproducibility of the results in order to give an unequivical answer. Poliovirus was first de-aggregated by dilution de-aggregation.

a) Dilution De-aggregation of Poliovirus Type 1.

Poliovirus lysates were diluted 1/100 into distilled water to de-aggregate them, to see if this method was as successful as with MS2. Table 22 shows the results of the dilution de-aggregation 1:100 into distilled water of several lysates of poliovirus 1. It is interesting to note that a rise in titre of a similar order to MS2 is seen- about 1.5 x.

Table 22.	Dilution De-aggregation of Polio 1.	
No	overnight 1/100 distilled water	Fraction rise.
2.3×10^6	3.7×10^4	x 1.6
5.6×10^7	8.4×10^5	x 1.5
2.0×10^8	2.8×10^8	x 1.4

Inactivation of de-aggregated viruses by UV did not show any lag in inactivation, indicating that aggregation, if it was still present did not affect the inactivation rate of the virus (see Figure 53).

b) UV Inactivation of Poliovirus.

Poliovirus, concentrated by the polyethylene glycol two phase purification and concentration method (see methods), sedimented in the ultra centrifuge and the resultant suspension diluted 1/100 into distilled water, was irradiated by 254nm UV. Figure 53 shows the results of this inactivation and the figure clearly shows a two phase inactivation. The D37 of the sensitive phase is 410 ergs mm^{-2} while that of the resistant phase is 680 ergs mm^{-2}, about 1.65 x the resistance of the sensitive phase. This value is about the same proportion as the res to sens in MS2. Polio is about 1.75 x as sensitive to UV as MS2, which is not too different from the ratio of the M.W. of the viruses, about 2 x.

It is interesting to review the inactivation data from the literature in the light of this evidence of two populations. If the sensitive population had died, or was much reduced, the rates for inactivation would be biased towards the resistant rate. This probably accounts for the wide variation in the reported inactivation rates reported in the literature (see introduction).

The resistant population on this experiment is about 2% of the

Figure 53.

Inactivation of Poliovirus Type 1 by 254nm UV.

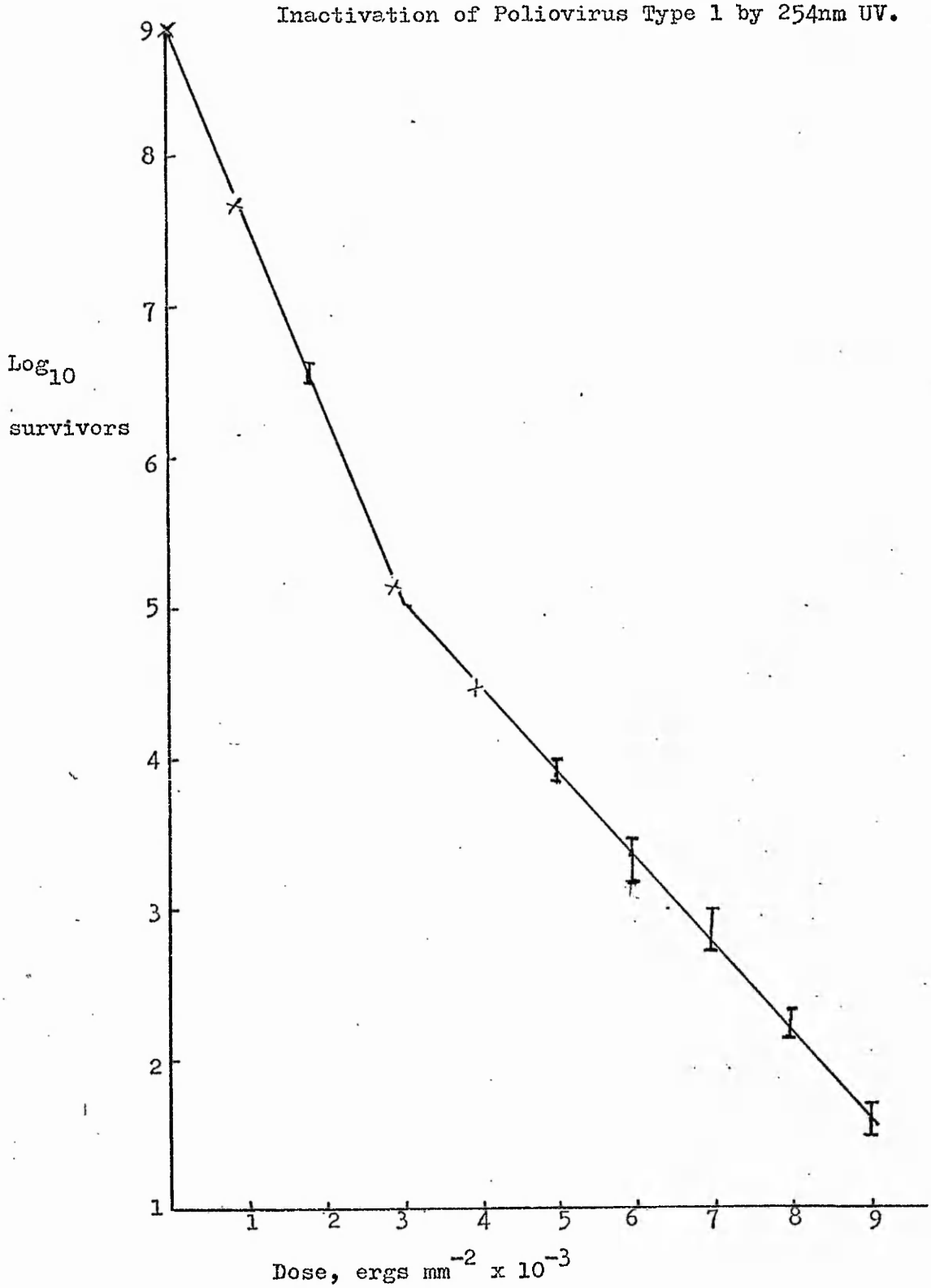

total population, much lower than the 22% (best proportion, as higher proportions might be the result of sens dying off) of MS2. It might be that a much lower proportion of res is made in polio, or that the sens is more stable than sens of MS2.

Density gradient separation of the two forms was undertaken to see if the light and heavy forms were different in their sensitivity to UV, as had been the case for MS2.

c) Density Gradient Separation of Polio 1.

Figure 54 shows the results of the $CsCl_2$ density gradient separation of polio 1, two peaks of infectivity showing clearly. Unfortunately the activity of the material recovered was too low to perform accurate experiments, more material was needed to start with. The heavier peak is the minor component of the population, and comprises about 1%.

Yamaguchi-Koll et al suggested that the heavy component was a more open structure than the light component with the result that $CsCl_2$ penetrates the particle making it more dense. In their electron microscope study of the heavy form of poliovirus, Boublik and Drzeniek (147) also interpret the heavy form as having a different, more open form of structure, easily penetrated by the caesium chloride and making it more dense than the 'Light' more compact structure. If this were so then the heavy component probably corresponds to the L form of MS2 and should be UV resistant. The heavy form of polio was also less infective than the light form, again a similarity with the L form of MS2.

If poliovirus has the same type of structure as MS2, several points may be predicted:-

1. The heavy component should be UV, heat and X-ray resistant

Figure 54.

Separation of Two Components of Poliovirus by Caesium Chloride Density Gradient Centrifugation.

Titre of plaque forming units against fraction number.

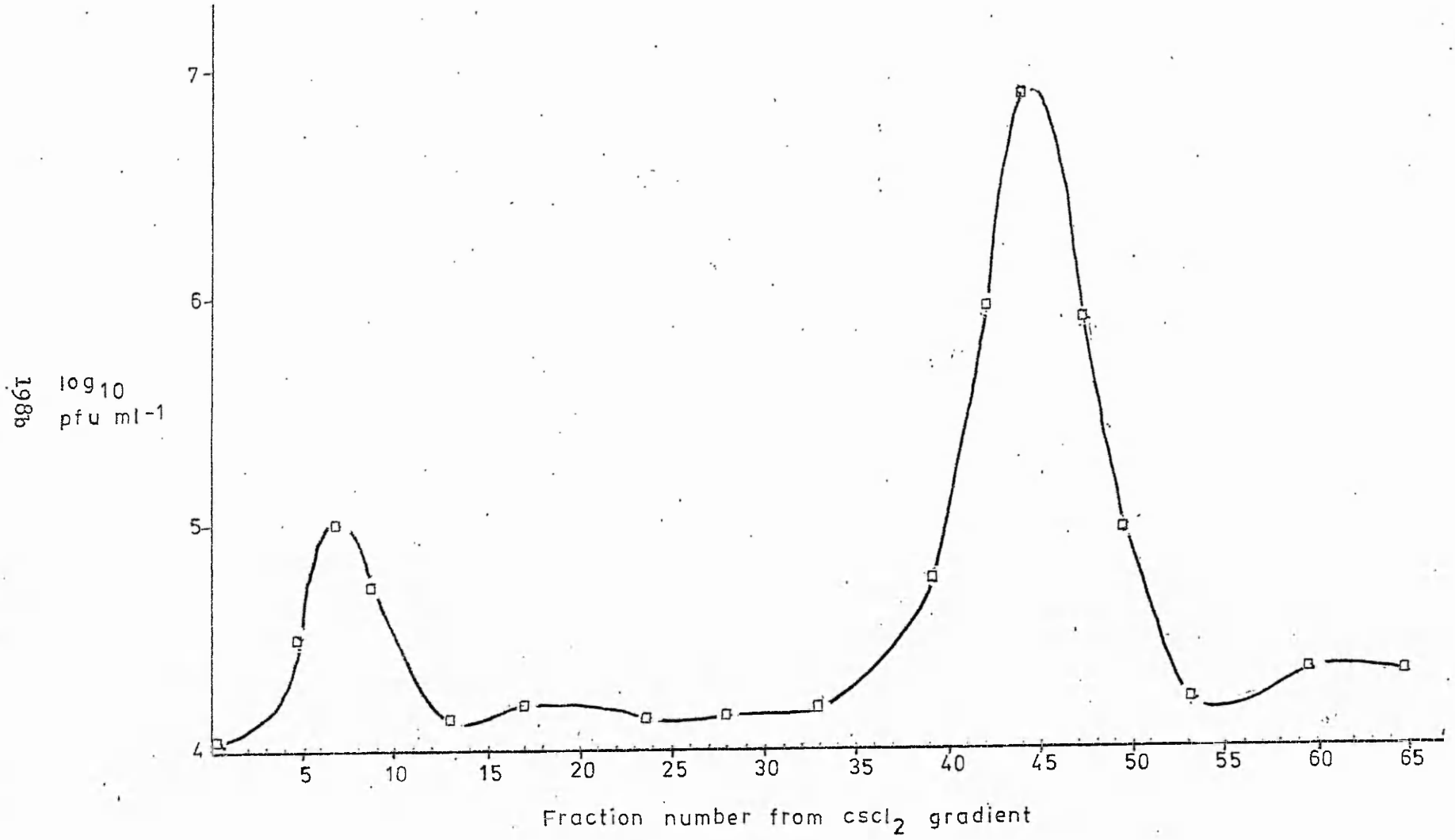
7
6
5
4
$\log_{10}$ pfu ml^{-1}
5
10
15
20
25
30
35
40
45
50
55
60
65
Fraction number from $CsCl_2$ gradient

and have an iso-electric point of 7.0.

2. The light component should be UV, heat and X-ray sensitive and have an iso-electric point of pH 4.5.

Considering the available evidence it would appear that picorna viruses and RNA bacteriophages have an RNA that interacts with the coat protein in two ways, which leads to different sensitivities to UV, heat and X-rays.

Hawkes (126, personal communication) has also found two compartment inactivation of MS2 by heavy metals , and Irwin (122) two compartment inactivation by quaternary ammonium surfactants. Cameron (148), Ross et al (149) and Bochstahler (150) have also noticed a two compartment inactivation rate in the UV inactivation of Herpes virus. Zavadova et al (151) have also noticed two compartment inactivation of pseudorabies virus. It would be very interesting to discover how many viruses show two compartment inactivation and if it is a reflection of alternative structural forms rather than host cell reactivation or other feature.

Ross et al and Cameron have described a small plaque effect, where, after UV inactivation, smaller plaques are found being produced by the survivors. Since resistant component of MS2 and the heavy form of polio are less infective than the major component, it might be that smaller plaques are a result of less infective virus infecting the cells. (In view of the different surface properties of the two types, infectivity might be lessened by less favourable attachment to the host. The virus would take longer to become attached and therefore the progeny, although of mixed infectivity would be a few bursts behind a more infectious particle. The plaque might be smaller as a result). A small plaque effect was looked for

in MS2, but not seen. Many factors affect the size of plaques in this system, such as state of the host, dryness of the plate, how quickly the plate dries out, making this a difficult feature to investigate.

While it is difficult to speculate on the exact reason for the presence of two types of particle, whether it be RNA or protein, it is not difficult to speculate on the advantage to the virus in having two types of particle.

A virus has to cope with two enviroments, that of the host where it has to replicate and infect while the host is available, and that of the external enviroment into which it must pass in order to contact a new host. The sensitive structure has evolved to be as infectious as possible in the hosts enviroment (the intestines) while the resistant structure can cope with adverse conditions and thus maximise its chances of contacting a new host. Selective pressures have perhaps evolved a structure that can meet both demands by providing alternative forms.

Conclusions.

The two compartment inactivation of MS2 by Ultra Violet light is caused by the presence of two structural forms of the virus. The UV sensitive form has a density of 1.46 g cm^{-3} and the UV resistant form a density of 1.44 g cm^{-3}. The iso-electric points of these two forms are also different, sens being pH 4.0 and res being pH 7.0. Other inactivating agents, such as heat and X-rays also inactivate these forms at different rates.

QB and poliovirus show a similar phenomenon of two compartment inactivation, two density forms and two iso-electric points.

De-aggregation, necessary for the investigation of inactivation rates was shown to be effectively achieved by dilution 1:100 of the lysate into distilled water.

Summary.

A review of the literature shows that there is variation in the published rates of inactivation for many viruses by UV.

UV equipment was constructed to investigate several aspects of inactivation of viruses by UV. A Bausch and Lomb monochromator in conjunction with a 250 watt mercury discharge lamp driven at 750 watts gave an output of 1.6 ergs mm^{-2} sec^{-1} at 253.7nm, as measured by actinometry. A surface steriliser at 253.7nm had an output of up to 175 ergs mm^{-2} sec^{-1}. A British Rail UV steriliser was calibrated and had an output of 165 ergs mm^{-2} sec^{-1} at a flow rate of 1.4 l min^{-1} and was judged to give a satisfactory treatment at 6 l min^{-1} flow.

MS2 and poliovirus were concentrated by a polyethylene glycol two phase system and purified by caesium chloride density gradient separation.

Inactivation of MS2, Qβ and poliovirus with 253.7nm UV gave a biphasic inactivation rate. The D37 of the sensitive population of MS2 and Qβ was 720 ergs mm^{-2}, while that of the resistant population was 1,100 ergs mm^{-2}. The D37 of the sensitive polioviruses was 410 ergs mm^{-2} and that of the resistant, 680 ergs mm^{-2}.

The phenomenon of biphasic inactivation was investigated and multiplicity reactivation, photoreversal, variabilty of data, shielding and attachment of viruses to vessel walls were all investigated and found not to explain the data. The two populations, sens and res, were not genetically distinct. X-radiation showed that sens had a greater cross sectional area of inactivation than res. Sens was also more sensitive to heat.

Two densities of MS2 were isolated that had the same UV sensitivities as sens and res. Sens had a density of 1.46 g cc^{-3} and res a density of 1.44 g cc^{-3}. The two populations also had different iso-

electric points, sens at pH 4.0 and res at pH 7.0.

Resistant MS2, expanded at 45°C in 0.15 M NaCl and re-contracted was converted to sensitive UV resistance.

Qβ and poliovirus were also shown to have two densities, two iso-electric points and two phase inactivation.

It is postulated that MS2 has two structures, one in which the RNA is tightly bound and is in stable contact with the coat - the sens form, and one in which the RNA is loosely bound and stretches the capsid - the res form.

References.

1. Min Jou W., G.Haegeman, M.Ysebaert and W.Fiers. Nature 1972 237 82-88.
2. Fiers W., R.Contreras, F.Duerinck, H.Haegeman, J.Merregaert, W.Min Jou, A.Raeymakers, G.Volkaert, M.Ysebaert, J.Van de Kerckhove, F.Nolf and M.Van Montagu. Nature 1975 256 273-278.
3. Fiers W., R.Contreras, F.Duerinck, G.Haegeman, D.Iserentant, J.Merregaert, W.Min Jou, F.Molemans, A.Raeymakers, A.Van den Borghe, G.Volkaert and M.Ysebaert. Nature 1976 260 500-507.
4. Poynter S.F., J.S.Slade and H.H.Jones. Water Treatment and Examination 1973 22 (3) 194-209.
5. Melnick J.L., J.Emmons, E.M.Opton and J.H.Coffey. Am.J.Hyg. 1954 59 185-195.
6. Berg G. Transmission of Viruses by the Water Route. Interscience, New York 1967.
7. Melnick J.L. In G.Berg, Transmission of Viruses by the Water Route. Interscience, New York 1967.
8. Chang S.L. Bull. Wld Hlth Org. 1968 38 401-414.
9. Poduska R.A. and Hershey. J.Wat. Pollut. Control Fed. 1972 44 (5) 738-745.
10. Swain R.H.A. Medical Microbiology. 11th E & S, 1970. Livingstone Edinburgh and London.
11. Bush A.F. and J.D.Isherwood. J.sanit. Engng Div. Am. Soc. civ. Engrs 1966 February. 99-107.
12. Jepson J.D. Seven-Trent Water Authority. Personal communication.
13. Hill W.F., F.E.Hamblet, W.H.Benton and E.W.Akin. Appl. Micro. 1970 19 (5) 805-812.
14. Hill W.F., F.E.Hamblet and E.W.Akin. Appl. Micro. 1967 15 (3) 533-536.

15. Kelly C.B. Am. J.publ. Hlth. 1961 51 1670-1680.

16. Vadjic A.H. Ontario Water Resources Commission. Divisional Research Paper no. 2015. 1969.

17. Gilcreas W. and C.Delalla. J. New Engl Wat. Wks. Ass. 1953 67 130-136.

18. Luckiesh M. and L.L.Holladay. General Electric Review. April 1944 45-50.

19. Huff C.B., B.S.Smith, W.D.Boring and N.A.Clarke. U.S. Publ. Hlth. Rep. 1965 80 695-705.

20. Taylor A.R., W.W.Kay, I.W.McLean, F.Oppenhiemer and F.D.Stimpert. J. Immun. 1957 78 45-55.

21. Schmidt B., M.Inge and W.Thiele. Z.f. Hyg. Bd. 1954 139 505-515.

22. Jepson J.D. Water Treatment and Examination. 1973 22 (3) 175-193.

23. Summer W. Process Biochem. 1975 (Nov) 43-46.

24. Hoather R.C. J. Instn Wat. Engrs 1955 9 (2) 191-207.

25. Kleczkowski A. In Methods in Virology. Ed. K. Maramorosch and H.Koprowski. Vol. 4 94-140. Acad. Press 1967.

26. Hiatt C.W. Nature 1961 189 678.

27. Morowitz H.J. Science 1950 3 229-230.

28. Hollaender A. and J.W.Oliphant. J.Bact. 1944 48 447-454.

29. Gates F.L. J. exp. Med. 1934 60 179-188.

30. Winkler U., H.E.Johns and E.Kellenberger. Virology 1962 18 434-358.

31. Duggar B.M. and A.Hollaender. J.Bact. 1933 27 219-256.

32. Rivers T.M. and F.L.Gates. J.exp. Med. 1928 47 45-49.

33. Rauth A.M. Biophys. J. 1965 5 257-273.

34. Franklin R.M., M.Friedman and R.B.Setlow. Archs Biochem. Biophys. 1953 44 259-264.

35. Sime E.H. and H.S.Bedson. J.gen Virol. 1973 18 55-60.

36. Kleczkowski A. Photochem. Photobiol. 1963 2 497-501.

37. Goddard J., D.Streeter, C.Weber and M.P.Gordon. Photochem. Photobiol. 1966 5 213-222.

38. Baker S.L. and P.R.Peacock. Br. Jour. exp. Path. 1926 7 310-316.

39. Fogh J. Proc. Soc. exp Biol.and Med. 1955 89 464-465.

40. Baptist J.E. and R.H.Haynes. Photochem. Photobiol. 1972 16 459-464.

41. Karczag A., G.Y.Ronto and I.Tarjan. Acta Biochem. et Biophys. Acad. Sci. Hung. 1972 7 (2) 173-177.

42. Abel P. Virology 1962 16 347-348.

43. Galasso G.J. and D.G.Sharp. J.Bact. 1965 90 (4) 1138-1142.

44. Setlow R.B. and J.K.Setlow. Proc. Natl. Acad. Sci. U.S.A. 1962 48 1250-1257.

45. Tamm I. and D.J.Fluke. J.Bact. 1950 59 449-461.

46. Yarus M. and R.L.Sinsheimer. Biophys. J. 1967 7 267-278.

47. Finsen N.R. Comptes Rendus 1903 136 1596-1598.

48. Ricks H.C., J.R.Cortelyou, T.D.Labecki, M.A.McWhinnie, F.J.Underwood, J.E.Semrad and G.R.Reeves. Am. J. publ. Hlth. 1955 45 1275-1282.

49. Hiatt C.W. Bact. Rev. 1961 28 (2) 150-163.

50 Kleczkowski A. In Methods in Virology Ed. K.Maramorosch and H.Koprowski. Vol 4. Ch. 3. Academic Press 1968.

51. Jagger J. Introduction to Research in Ultraviolet Photobiology. Prentice-Hall, New Jersey, 1967.

52. Setlow R.B. In Mammalian Cytogenetics and Related Problems in Radiobiology. 291-307. Pergamon Press, Long Island City, N.Y. 1964.

53. Miller R.L. and P.G.W.Plageman. J.Virol 1974 13 (3) 729-739.

55. Shore V.G. and A.B.Pardee. Arch. Biochem. Biophys. 1956 62 355-368.

56. Yarus M. and R.C.Sinsheimer. Biophys. J. 1967 7 267-278.

57. Setlow J.K.In Current Topics in Radiation Research. Ed. M.Ebart and A.Howard. Vol. 2. 195-248. North-Holland Publ. Co. 1966.

58. Mayo M.A., B.D.Harrison, A.F.Murant and H.Barker. J.gen. Virol. 1973 19 155-159.

59. Franke B. and D.S.Ray. J.Virol. 1972 9 (6) 1027-1032.

60. Howard-Flanders. Personal communication.

61. Wicker R. and J.Coppey. Int. J. cancer 1972 9 (3) 626-631.

62. Roizman B.,M.M.Mayer and P.R.Roane. J.Immun. 1959 82 19-25.

63. Budowski E.I., N.A.Simukova, M.F.Turchinsky, I.V.Boni and Y.M. Skobler. Nucleic Acids Research 1976 3 (1) 261-276.

64. Fenner F. Br. med. J. 1962 (July 21st) 135-142.

65. Howard-Flanders. Personal communication.

66. Crawford E.M. and R.F.Gestland. Virology 1964 22 165-170.

67. Weber K. and W.Konisberg. J.biol. Chem. 1967 242 3563.

68. Wittman-Leobold B. and H.G.Wittman. Mol. Gen. Genet. 1967 100 358-364.

69. Lin J.Y., C.M.Tsung and H.Fraenkel-Conrat. J.Mol. Biol. 1967 24 1-7.

70. Vandekerckhove J., H.Franq and M.Van Montagu. Arch. Inern. Physiol. Biochim. 1969 77 175.

71. Nishihara T., Y.Nozu and Y.Okada. J.Biochem. (Japan) 1970 67 403.

72. Maita T. and W.Konisberg. J.biol. Chem. 1971 246 5003.

73. Loeb T. and N.D.Zinder. Proc. Natl.Acad. Sci. U.S.A. 1961 47 282-287.

74. Overby L.R., G.H.Barlow, R.H.Doi, M.Jacob and S.Spiegelman. J.Bact. 1966 91 442-446.

75. Zipper P., O.Kratky, R.Herrman and T.Hohn. Eur.J.Biochem. 1971 18 1-10.

76. Fischbach F.A., P.M.Harrison and J.W.Anderegy. J.Mol. Biol. 1965 13 638.

77. Horiuchi K. In RNA Phages. Ed. N.D.Zinder. Ch. 2. Cold Spring Harbor Laboratory 1975.

78. Lodish H.F. Progress in Biophysics and Molecular Biology. 1968 18 285-312.

79. Krahn P.M., R.J.O'Callaghan and W.Parenchych. Virology 1972 47 628-637.

80. Reynolds S. and W.Parenchych. Can. J. Microbiol. 1976 22 1647-1653.

81. Verbraeken E. and W.Fiers. Virology 1972 50 690-700.

82. Jacobsen A.B. Proc. Natl. Acad. Sci. U.S.A. 1976 73 307-311.

83. Rohrmann G.F. and R.G.Kreuger. J.Virol. 1970 6 (3) 269-279.

84. Matthews K.S. and R.D.Cole. J.Mol. Biol. 1972 65 1.

85. Knolle P. and T.Hohn. In RNA Phages. Ed. N.D.Zinder. Cold Spring Harbor Laboratory 1975.

86. Horiuchi K. I RNA Phages. Ed. N.D.Zinder. Cold Spring Harbor Laboratory 1975.

87. Thomas G.J., B.Prescott, P.E.McDonald-Ordzie and K.A.Hartman. J.Mol.Biol. 1976 102 103-124.

88. Cerutti P.A., N.Miller, M.G.Pleiss, J.F.Remsen and W.J.Ramsey. Proc. Natl. Acad. Sci. U.S.A. 1969 64 731-738.

89. Lodish H.F. and N.D.Zinder. J.Mol. Biol. 1966 19 333.

90. Robertson H.D. In RNA Phages. Ed. N.D.Zinder. Cold Spring Harbor Laboratory 1975.

91. Lodish H.F. J.Mol.Biol. 1970 50 689.

92. Philips B.A. and D.F.Summers. Virology 1968 36 48.

93. Scraba D.C. and J.S.Colter. PAABS Revista 1974 3 (2) 401-408.

94. Summers D.F., J.V.Maizel and J.E.Darnell. Proc.Natl.Acad.Sci. U.S.A. 1965 54 505.

95. Butterworth B.E., C.Hall, C.M.Stoltzfus and R.R.Rueckert. Proc.Natl.Acad.Sci. U.S.A. 1971 68 3083.

96. Butterworth B.E. and R.R.Rueckert. Virology 1972 50 535.

97. Lundquist R.E., J.Meyer and J.V.Maizel. Abstcts. Ann. Meet. Am. Soc. Microbiol. 1976 76 250.

98. Beckman L.D., L.A.Caliguiri and L.S.Lilly. Abstcts. Ann. Meet Am. Soc. Microbiol. 1976 76 250.

99. Philipson L., S.T.Beatrice and R.C.Crowell. Virology 1973 54 69.

100. Johnston M.D. and S.J.Martin. J.gen. Virol. 1976 30 317-328.

101. Breindl M. Virology 1971 46 962-964.

102. Su R.T. and M.W.Taylor. J.gen.Virol. 1976 30 317-328.

103. Baltimore D. In From Molecules to Man- Perspectives in Virology. VII. Ed. M.Pollard. Academic Press 1971.

104. Mandel B. Virology 1971 41 554-568.

105. Le Bouvier G.L. Lancet 1955 269 1013-1016.

106. Yamaguchi-Koll U., K.J.Weigers and R.Drzeniek. J.gen.Virol. 1975 26 307-319.

107. Boublik M. and R.Drzeniek. J.gen.Virol. 1976 31 447-449.

108. Rowlands D.J., M.W.Shirley, D.V.Sangar and F.Brown. J.gen.Virol. 1975 29 223-234.

109. Yogo Y. and E.Wimmer. Proc.Natl.Acad.Sci. U.S.A. 1972 69 1877.

110. Lee Y.F., A.Nomoto and E.Wimmer. Fed. Proc. 1976 35 (7) 1297.

111. Eliceiri G.L. and M.S.Sayavedra. Fed. Proc. 1976 35 (7) 1297.

112. Bishop J.M., N.Quintrell and G.Koch. J.Mol.Biol. 1967 24 125-128.

113. Jagger J. In Introduction to Reseaerch in Ultraviolet Photobiology. 137. Prentice-Hall, New Jersey 1967.

114. Duncan J.F. Isotopes in Chemistry. Oxford Univ. Press 1968.

115. Hatchard C.G. and C.A.Parker. Roy.Soc. (London), Proc., 1956 A235 518-536.

116. Loeb T. and N.D.Zinder. Proc.Natl.Acad.Sci. U.S.A. 1961 47 282.

117. Strauss J.H. and R.L.Sinsheimer. Eur.J.Biochem 1970 17 63-67.

118. Vickers T.G. Ph.D. Thesis. University of Bristol 1967.

119. Carlile W. Ph.D. Thesis. Trent Polytechnic 1975.

120. Albertson P-A. In Methods in Virology. Ed. K.Maramorosch and H.Kowprowski. Vol. 2 Ch 10 . Academic Press 1967.

121. Irwin R. Ph.D. Thesis. Trent Polytechnic 1977.

122. Awdeh Z.L., A.R.Williamson and B.A.Askonas. Nature 1968 219 66.

123. Puck T.T., A.Garen and J.Cline. J.exp. Med. 1951 93 65-88.

124. Dulbecco R. and M.Vogt. Ann. New York Acad. Sci. 1955 61 790-800.

125. Cooper P.D. In Methods in Virology. Ed. K.Maramorosch and H. Kowprowski. Vol. 3. 244-311. Academic Press 1967.

126. Hawkes M. Ph.D.Thesis. Trent Polytechnic 1977.

127. Chatfield R. British Rail Area Science Laboratory, Crewe. Personal Communication.

128. Guy M.D. Ph.D. Thesis. Trent Polytechnic 1974.

129. Fenner F. Br. Med. J. 1962 (July 21st) 135-142.

130. Horiuchi K. In RNA Phages. Ed. N.D.Zinder. Ch. 2. Cold Spring Harbor Laboratory 1975.

131. Zavadova Z. and J.Zavada. Acta. Virol. 1968 12 507-514.

132. Bochstahler L.E. and Lytte C.D. Biochem. Biophys. Res. Comm. 1970 41 184-189.

133. Ross L.J.N., P.Wildy and K.R.Cameron. Virology 1971 45 (3) 808-812.

134. Rauth A.M. Biophys.J. 1965 5 257-273.

135. Fidy J. and A.Karczag. Acta Biochim. Biophys. Acad. Sci. Hung. 1974 9 115-120.

136. Karczag A., G.Y.Ronto and I.Tarjan. Acta Biochim. Biophys. Acad. Sci. Hung. 1972 7 (2) 173-177.

137. Winkler U., H.E.Johns and E.Kellenberger. Virology 1962 18 343-358.

139. Shore V.G. and A.B.Pardee. Arch. Biochem. Biophys. 1956 62 355-368.

140. Mayo M.A. and J.I.Cooper. J.gen.Virol. 1973 18 281-289.

141. Murant A.F., M.A.Mayo, B.D.Harrison and R.A.Goold. J.gen.Virol. 1972 16 327-338.

142. Overby L.R., G.H.Barlow, R.H.Doi, M.Jacob and S.Speigleman.

143. R.Irwin. Virology Unit, Trent Polytechnic. Personal communication.

144. Blevings S. and R.Stace-Smith. J.gen.Virol. 1976 31 199-216.

145. Taylor A.R., W.W.Kay, I.W.McLean, F.Oppenhiemer and F.D.Stimpert. J.Immun. 1957 78 45-55.

146. Matossian A.M. and G.A.Garabedian. Am.J. Epidem. 1967 85 1-8.

147. Boublik M. and R.Drzeniek. J.gen.Virol. 1976 18 51-54.

148. Cameron K.R. J.gen.Virol. 1973 18 51-54.

149. Ross L.J.N., K.R.Cameron and P.Wildy. J.gen.Virol. 1972 16 299-311.

150. Bochstahler L.E. and C.D.Lytte. Biochem. Biophys. Res. Comm. 1970 41 184-189.

151. Zavadova Z. and J.Zavada. Acta Virol. 1968 12 507-514.

152. Ziola B.R. and D.G.Scraba. Virology 1976 71 111-121.

153. Huang A.S. and D.Baltimore. Nature 1970 226 325-327.

154. Norman A. Virology 1960 10 384-387.

155. Osborn M., A.M.Weiner and K.Weber. Eur. J. Biochem. 1970 17 63-67.